FLOCCULATION STUDIES IN PAPERMAKING

PhD Thesis

ELISABETE SIMÕES ANTUNES

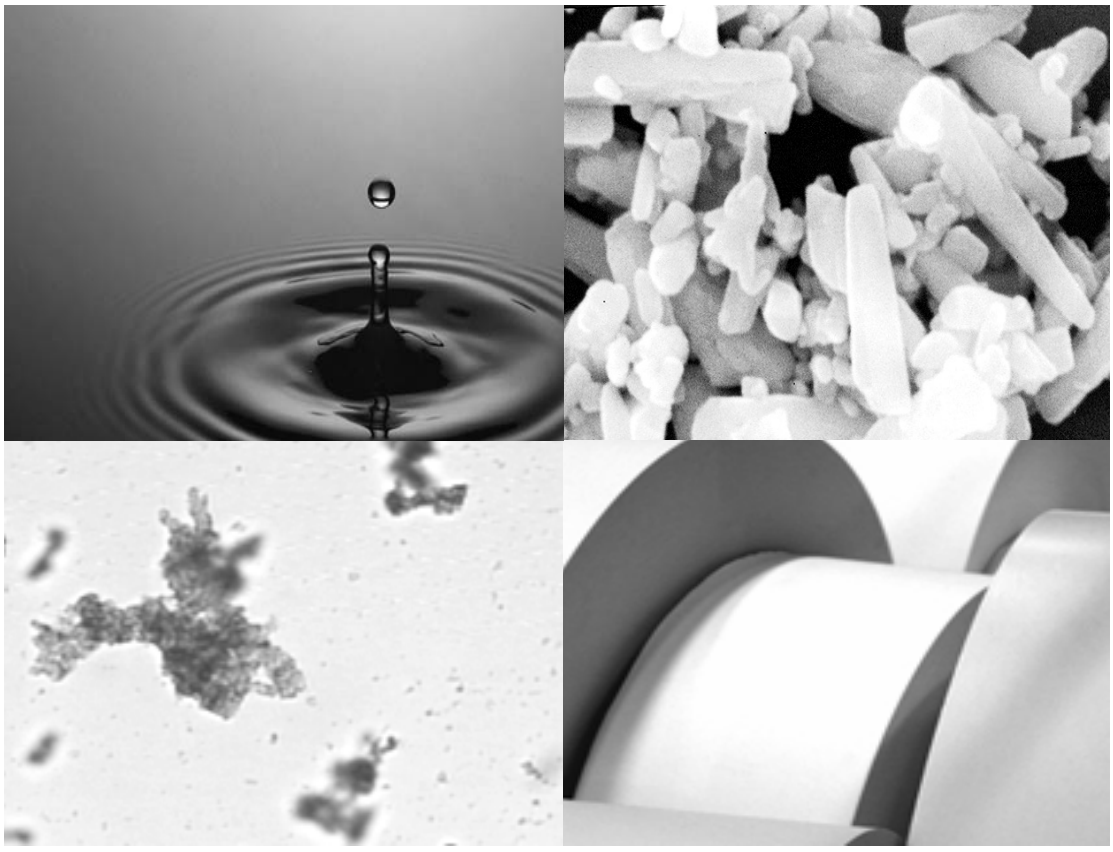

2009

UNIVERSITY OF COIMBRA
FACULTY OF SCIENCES AND TECHNOLOGY
CHEMICAL ENGINEERING DEPARTMENT

· U C ·

FLOCCULATION STUDIES IN PAPERMAKING

A dissertation submitted to the
University of Coimbra

in fulfilment of the requirements for the degree of

Doctor of Philosophy

by

Elisabete Simões Antunes

University of Coimbra
Chemical Engineering Department
2009

To my parents, Jaime and Benilde and my sister, Célia

ACKNOWLEDGEMENTS

I would like to thank those that helped me to make this thesis possible. First of all, I would like to express my gratitude to my supervisors.

To Professor Graça Rasteiro for all the help, guidance and support during the realization of the research work and especially for encouraging me and believing in me since the day that I became one of her students.

To Professor Carlos Negro for his advice and especially, for his support and help during my stay in Madrid.

I am also thankful to Prof. Fernando Garcia and to Dr. Paulo Ferreira for their assistance whenever necessary since the beginning of this work and for their comments that made valuable inputs to this work.

Then, I would like to acknowledge the collaboration of the Aqua+Tech Specialities, S.A., Switzerland, for providing flocculants samples with a special thank to Doctor David Hunkeler for his constant interest in my work.

I also wish to thank the Paper and Forest Research Institute RAIZ (Portugal) that had kindly provided the Dynamic Drainage Analyser and the Labgran of the "Instituto Pedro Nunes" (Portugal) that allowed using the microscope for image analysis.

I would like to thank the European Project "Novel Device to Study Pulp Suspensions Behaviour in order to Move towards Zero Energy Losses in Papermaking", (COOP-CT-2004/513117) and the "Fundação para a Ciência e Tecnologia" (Portugal) (POPH-QREN funding program) for the financial support.

My acknowledgments go also to people from the Chemical Engineering Department of the Complutense University of Madrid, especially to Professor Angeles Blanco and to Dr. Elena Fuente for all the help, comments and support.

Finally, my sincere thank to my parents and my sister for all their support and encouragement over the years and to João for his patience and support, without which none of this would be possible.

CONTENTS

ABSTRACT

The flocculation process induced by polymeric additives has been studied extensively and is well reported in the literature. However, from the point of view of the papermaking process, still few studies relate flocculation behaviour and flocs characteristics with retention, drainage and sheet formation under various process conditions and for different retention aid systems. This correlation is of great importance in order to understand, predict and optimize retention and drainage performance and thus, sheet formation and quality.

In this study, a strategy that allows obtaining information about flocculation kinetics, flocs characteristics, flocs resistance and reflocculation capacity in a single test and in turbulent conditions was developed. The light diffraction scattering technique (LDS) was used to monitor the flocculation process due to its advanced capabilities that allow one to extract information on both the particle size distribution and the fractal dimension of the flocs.

Monitorization of the flocculation of precipitated calcium carbonate particles with new cationic polyacrylamides allowed assessing how the polymer characteristics, namely the charge density and the degree of branching affect flocculation, flocs characteristics, flocs resistance and reflocculation capacity in distilled and in industrial water.

It was shown that the optimum flocculant dosage decreases and flocs produced are smaller, denser and more resistant as the polymer charge density increases. However, independently of the charge density, the flocs strength decreases as the flocs size increases. Furthermore, when flocculation takes place by bridging, flocs restructuring occurs during flocculation. When branched polymers are used, flocculation is slower and the flocs produced are larger and have a more open structure when comparing with linear polymers. Reflocculation is very small or practically inexistent for all the polymers studied with the exception of the linear polymer of high charge density that produces flocs that partially reflocculate. The structure of the reflocculated flocs is more compact than before flocs break up and more open as the charge density decreases. The use, simultaneously, of a microparticle retention aid improved significantly the reflocculation process and, in this case, the reflocculated flocs have a more open structure than reflocculated flocs without microparticles. However, the action of the microparticles is reduced as the charge density of the polymer decreases and as the degree of branching of the polymer increases.

The high cationic content of the industrial water enhances the flocculation kinetics. Nevertheless, the optimum flocculant dosage becomes higher in industrial water than in distilled water. Flocculation kinetics and flocs characteristics are less affected by the cationic content of the water when highly branched polymers are used.

The effect of the degree of polymer branching on retention and drainage performance of flocculated kraft pulp fibre suspensions containing precipitated calcium carbonate (PCC) was investigated in the dynamic drainage analyser (DDA) and the results have been correlated with flocs properties obtained by LDS. The results show that polymers of medium charge density are more adequate to be used as retention aids. The results also demonstrate that it is possible to correlate the flocculation process evaluated by LDS with the flocculant's performance in the drainage test.

The effects of the chemical flocculation on the rheological behaviour of the pulp suspension have been studied correlating flocculation data obtained by LDS with the rheological behaviour obtained with the rotational viscometer developed by UCM. It was

shown that the choice of the flocculants is important for reducing the power consumption in papermaking. Flocculants with high charge density and without branches seem to be those that more reduce the resistance of the pulp suspension to shearing.

As a whole, LDS and DDA results have shown that medium charge density highly branched polymers can be promising additives for papermaking. They offer good retention and drainage with low flocculant dosage and with relatively fast flocculation kinetics due to the formation of small flocs with an open structure, mainly at the secondary aggregates level. Furthermore, highly branched polymers are less affected by the water cationic content in all the flocculation stages (flocculation and break up) leading to similar flocs properties independently of the suspending medium.

A population balance model for the flocculation of PCC particles with polyelectrolytes of very high molecular weight and medium charge density is presented. The model describes successfully the flocculation kinetics of both linear and branched polymers. Correlations of the optimized parameters (maximum collision efficiency, kinetic parameter for flocs restructuring and parameter for fragmentation rate) with flocculation data show well the effects of flocculant concentration, flocs structure and polymer structure on these parameters as well as on the flocculation kinetics and flocs restructuring.

RESUMO

O processo de floculação induzido por aditivos poliméricos tem sido extensivamente estudado e divulgado na literatura. Contudo, do ponto de vista do processo de fabrico do papel, ainda poucos estudos relacionam a cinética da floculação e as características dos flocos com a retenção, drenagem e formação da folha sob diferentes condições processuais e para diferentes agentes de retenção. Esta correlação é de grande importância para perceber, prever e optimizar o desempenho da retenção e da drenagem e por conseguinte a formação e a qualidade da folha.

Neste estudo foi desenvolvida uma estratégia que permite obter informação sobre a cinética da floculação, as características e a resistência dos flocos e a capacidade de refloculação num único teste e em condições turbulentas. A técnica de espectroscopia de difracção de luz (LDS) foi usada para monitorizar o processo de floculação devido às suas capacidades avançadas que permitem extrair informação sobre a distribuição granulométrica dos flocos mas também sobre a sua dimensão fractal.

A monitorização da floculação de partículas de carbonato de cálcio precipitado com novas poliacrilamidas catiónicas permitiu perceber como as características do polímero, nomeadamente a sua densidade de carga e o seu grau de ramificação afectam a floculação, bem como as características e a resistência dos flocos e a capacidade de refloculação em água destilada e industrial.

Demonstrou-se que a dosagem óptima de floculante diminui e os flocos produzidos são mais pequenos, mais densos e mais resistentes com o aumento da densidade de carga do polímero. Contudo, independentemente da densidade de carga, a resistência dos flocos diminui com o aumento do tamanho dos flocos. Além disso, quando o processo de floculação ocorre por formação de pontes, existe reestruturação dos flocos durante a floculação. A floculação é mais lenta e os flocos produzidos são maiores e mais abertos quando se usam polímeros ramificados. A refloculação é baixa ou praticamente inexistente para todos os polímeros estudados excepto para o polímero linear de alta densidade de carga que produz flocos que refloculam parcialmente. A estrutura dos flocos refloculados é mais compacta do que antes da quebra e mais aberta com a diminuição da densidade de carga. O uso simultâneo de micropartículas com o agente de retenção melhora significativamente o processo de refloculação e, neste caso, os flocos refloculados são mais abertos que os flocos refloculados sem micropartículas. Contudo, a acção das micropartículas baixa com a diminuição da densidade de carga e com o aumento do grau de ramificação do polímero.

O elevado conteúdo catiónico da água industrial promove a cinética de floculação. Todavia, a dosagem óptima de floculante torna-se elevada em água industrial. A cinética de floculação e as características dos flocos são menos afectados pela cationicidade da água quando se usam polímeros ramificados.

O efeito do grau de ramificação do polímero no desempenho da retenção e da drenagem de suspensões floculadas de fibra de pasta kraft contendo carbonato de cálcio precipitado (PCC) foi investigado no “dynamic drainage analyser” (DDA). Os resultados foram correlacionados com as propriedades dos flocos obtidas por LDS. Os resultados mostram que os polímeros de média densidade de carga são mais adequados para serem usados como agentes de retenção. Os resultados demonstram também que é possível correlacionar o processo de floculação avaliado por LDS com o desempenho do floculante no teste de drenagem.

O efeito da floculação química na reologia das suspensões de fibra de pasta kraft foi avaliado correlacionando os dados de floculação de LDS com o comportamento reológico obtido no viscosímetro rotacional desenvolvido pela UCM. Mostrou-se que a escolha do floculante é importante para reduzir o consumo energético no fabrico do papel. Os floculantes de elevada densidade de carga e lineares são aqueles que mais reduzem a resistência da suspensão de pasta á velocidade de corte.

No geral, os resultados de LDS e DDA mostraram que os polímeros altamente ramificados de média densidade de carga podem ser aditivos promissores para a indústria do papel. Estes polímeros oferecem uma retenção e uma drenagem eficaz com baixa dosagem de floculante e com uma cinética de floculação relativamente rápida devido á formação de flocos pequenos com uma estrutura aberta, essencialmente ao nível dos agregados secundários. Além disso, os polímeros altamente ramificados são menos afectados pelo conteúdo catiónico da água em qualquer das etapas do processo de floculação (floculação e quebra) originando propriedades dos flocos similares independentemente do meio.

Propôs-se um modelo baseado num balanço de população para a descrição da floculação das partículas de PCC com polielectrólitos de alto peso molecular e de média densidade de carga. O modelo descreve com sucesso a cinética de floculação com os polímeros lineares e ramificados. As correlações dos parâmetros óptimos do modelo (eficiência de colisão máxima, parâmetro cinético para a reestruturação dos flocos e parâmetro para a velocidade de fragmentação) com os dados experimentais da floculação mostram bem os efeitos da concentração de floculante, da estrutura dos flocos e da estrutura do polímero, nestes parâmetros, bem como na cinética de floculação e na reestruturação dos flocos.

RÉSUMÉ

Le procédé de la floculation induit par des additifs polymériques a été considérablement étudié et divulgué dans la littérature. Toutefois, du point de vue de la fabrication du papier, encore peu d'études établissent un lien entre le comportement de la floculation et les caractéristiques des flocons avec la rétention, le drainage et la formation de la feuille sous différentes conditions processuelles et pour différents systèmes d'aide à la rétention. Cette corrélation est de très grande importance afin de comprendre, prévoir et optimiser la performance de la rétention et du drainage et donc la formation et la qualité de la feuille de papier.

Dans cette étude, une stratégie, qui permet d'obtenir des informations sur la cinétique de la floculation, les caractéristiques des flocons, leur résistance et leur capacité de refloculation en un simple teste et dans des conditions turbulentes, a été établie. La technique de spectroscopie de diffraction de la lumière (LDS) a été utilisée pour suivre le procédé de la floculation grâce à ses capacités avancées qui permettent d'extraire des informations á la fois sur la distribution granulométrique des flocons et sur leur dimension fractale.

Le suivi de la floculation de particules de carbonate de calcium précipité avec de nouvelles polyacrylamides cationiques a permis d'évaluer comment les caractéristiques du polymère, à savoir la densité de charge et le degré de ramification, affectent la floculation, les caractéristiques des flocons, leur résistance et leur capacité de refloculation en eau distillée et industrielle.

On a démontré que le dosage optimum de floculant diminue et les flocons produits sont plus petits et plus résistants quand la densité de charge du polymère augmente. Cependant, indépendamment de la densité de charge, la résistance des flocons diminue avec l'augmentation de la taille des flocons. Par ailleurs, quand la floculation a lieu par pontage, il y a une réorganisation des flocons pendant la floculation. Quand les polymères ramifiés sont utilisés, la floculation est plus lente et les flocons produits sont plus larges et ont une structure plus ouverte que les flocons produits avec les polymères linéaires. La refloculation est très faible ou pratiquement inexistante avec tous les floculants étudiés sauf pour le polymère linéaire de très haute densité de charge qui partiellement reflocule. La structure des flocons refloculés est plus compacte que celle des flocons avant leur rupture et plus ouverte à mesure que la densité de charge diminue. L'utilisation simultanée de microparticules avec l'agent de rétention améliore significativement la refloculation et, dans ce cas, les flocons refloculés ont une structure plus ouverte que ceux refloculés sans les microparticules. Cependant, l'action des microparticules baisse avec la diminution de la densité de charge et l'augmentation du degré de ramification du polymère.

La haute teneur en cations de l'eau industrielle favorise la cinétique de la floculation. Le dosage optimum de floculant devient néanmoins plus élevé en eau industrielle. La cinétique de la floculation et les caractéristiques des flocons sont moins affectées par la teneur en cations de l'eau quand les polymères très ramifiés sont utilisés.

L'effet du degré de ramification du polymère sur la performance de la rétention et du drainage d'une suspension de pâte kraft fibreuse contenant du carbonate de calcium précipité (PCC) a été évalué avec le "dynamic drainage analyser" (DDA). Les résultats ont été corrélés avec les propriétés des flocons obtenues avec le LDS. Les résultats montrent aussi que les polymères de densité de charge moyenne sont plus adaptés pour être utilisés

comme agents de rétention. De plus, le procédé de la floculation évalué par LDS peut être corrélé avec la performance du floculant obtenu par le teste de drainage.

Les effets de la floculation chimique sur la rhéologie de la suspension de pâte fibreuse ont été étudiés en corrélant les données de la floculation obtenues par LDS avec la rhéologie obtenue avec le viscosimètre rotatif développé par UCM. Il a été démontré que le choix du floculant est important afin de réduire la consommation énergétique de la fabrication du papier. Les floculants de densité de charge élevée et sans ramifications semblent être ceux qui réduisent le plus la résistance de la suspension fibreuse à la vitesse de cisaillement.

Dans l'ensemble, les résultats de LDS et de DDA ont montré que les polymères très ramifiés de densité de charge moyenne peuvent être des additifs prometteurs pour l'industrie papetière. Ils offrent une rétention et un drainage efficaces avec un bas dosage de floculant et une cinétique de floculation relativement rapide grâce à la formation de petits flocons de structure ouverte, essentiellement au niveau des agrégats secondaires. De plus, les polymères très ramifiés sont moins affectés par la teneur cationique de l'eau au niveau de toutes les étapes du procédé de la floculation (floculation et rupture) ce qui origine des flocons de propriétés similaires indépendamment du milieu.

Un modèle de balance de population pour la floculation des particules de PCC avec des polyelectrolytes de poids moléculaire très élevé et de densité de charge moyenne est présenté. Le modèle décrit avec succès la cinétique de la floculation aussi bien pour les polymères linéaires que pour ceux ramifiés. Les corrélations entre les paramètres optimisés (efficience de collision maximale, paramètre cinétique pour la réorganisation des flocons et paramètre pour la vitesse de fragmentation) et les données expérimentales de la floculation montrent bien les effets de la concentration de floculant, de la structure des flocons et de la structure du polymère, sur ces paramètres, bien comme sur la cinétique de la floculation et la réorganisation des flocons.

LIST OF FIGURES

LIST OF TABLES

NOMENCLATURE

B fitting parameter for fragmentation rate

C collision efficiency factor for $t=0$

d_F mass fractal dimension

$d_{F,max}$ maximum mass fractal dimension

D fitting parameter for $d\alpha/dt$

$d[4,3]$ volume mean size (μm)

d_{p10} particle size for which 10 % of the material has a size lower or equal to this value (μm)

d_{p90} particle size for which 90 % of the material has a size equal or higher to this value (μm)

d_{p50} median particle size (μm).

d_0 characteristic diameter for the class i=0

D_i characteristic diameter of the class i (cm)

G average shear rate (s^{-1})

k_c constant ≈ 1

k_B Boltzmann constant (J/K)

m consistency index

n behaviour index

N number of primary particles in an aggregate

N_i number concentration of flocs containing 2^{i-1} particles (#/cm^3)

R_c effective capture radius (cm)

r_0 primary particle radius (cm)

R_g radius of gyration (nm)

st_{error} standard error

SE scattering exponent

S_i fragmentation rate of flocs in i interval (s^{-1})

t time (s)

T absolute temperature (K)

V_0 volume of primary particle (cm^3)

v_i volume of flocs in i interval

x,y fitting parameters for α_{ij}

Greek letters

α_{ij} collision efficiency between aggregates in *i* and *j* intervals

α_{max} maximum collision efficiency

β_{ij} collision frequency between aggregates in *i* and *j* intervals (cm^3/s)

Γ_{ij} Breakage distribution function

ε average energy dissipation rate (m^2/s^3)

ε_{bi} critical energy dissipation rate (m^2/s^3)

γ fitting parameter for dd_F/dt

μ fluid viscosity (Pa.s)

τ shear stress (N/m^2)

θ fraction of surface coverage

ν fluid kinematic viscosity (m^2/s)

ζ zeta potential (mV)

Abbreviations

AFM	atomic force microscope
AKD	alkyl ketene dimmer
ASA	alkenyl succinic anhydride
CFS	canadian standard freeness
CSLM	confocal scanning laser microscopy
C-PAM	cationic polyacrylamide
DCS	dissolved and colloidal susbstances
DDA	dynamic drainage analyser
DDJ	dynamic drainage jar
FBRM	focus beam reflectance microscopy
G/W	Gess/Weyerhauser
LDS	laser diffraction spectroscopy
MBDT	moving belt drainage tester
PBE	population balance equations

PCC	precipitated calcium carbonate
PEI	polyethyleneimine
PAM	polyacrylamide
PAE	polyamideamine epichlorohydrine
PFR	phenol formaldehyde resin
poly-DADMAC	poly-diallyldimethylammonium chloride
PEO	polyethyleneoxide
SALLS	small-angle laser light scattering
SR	Schopper-Riegler

CHAPTER 1 – LITERATURE REVIEW

1.1 – OVERVIEW OF THE WET-END CHEMISTRY IN PAPERMAKING

A paper machine is usually divided into six sections: headbox, forming, press, drying and surface treatment sections and reel. Figure 1.1 shows a schematic representation of a Fourdrinier paper machine where the sections referred above can be identified. The wet-end part of the machine consists of the headbox, the forming or wire section and the press section where the wet sheets are formed and in which water is present. In the drying and surface treatment sections, that are also named dry-end part, the wet sheets formed in the wet-end stage are dried and various surface treatments are applied to the paper (Fardim, 2002).

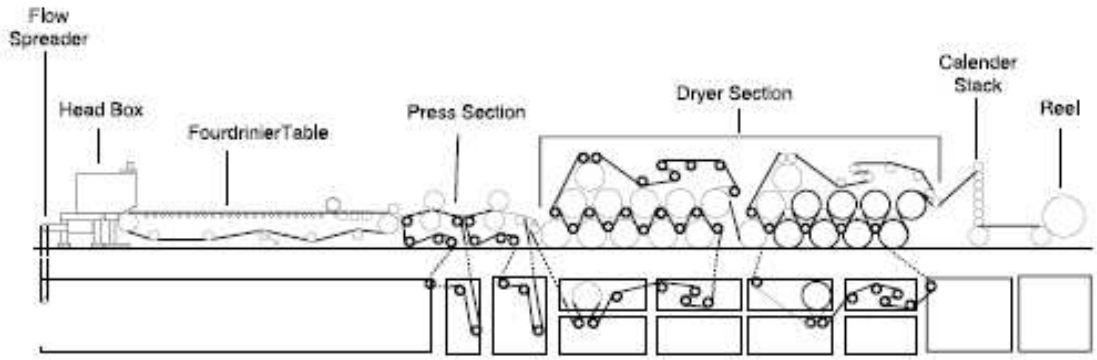

Figure 1. 1. Schematics of a Fourdrinier paper machine (US EPA, 2002).

Briefly, the papermaking process consists of the sheet formation starting with a dilute suspension containing cellulosic fibres, fillers and additives (Roberts, 1991; Smook, 1992; Blanco *et al.*, 1995). Papermaking additives can be categorized either as process additives or as functional additives. Process additives are materials that improve the operation of the paper machine, such as retention and drainage aids, biocides, dispersants and defoamers. Functional additives are materials that enhance or alter specific properties of the paper product, such as fillers, sizing agents, dyes, optical brighteners, and wet- and

dry- strength additives. Process additives are added at the wet-end of the paper machine whereas functional additives may be added internally or to the surface of the sheet (Kirk *et al.*, 1998). Trends observed in papermaking follow, in general, the evolution of the chemical additives. Initially, paper was usually made in an acidic environment due to the use of rosin and aluminium sulphate for sizing. However, since 1970s the acidic systems moved away rapidly towards neutral and even alkaline systems. The use of an alkaline system reduces corrosion, allows high filler addition and energy savings associated with the easier drying of filled paper. This change has had a profound effect on the whole wet-end chemistry (Roberts, 1991). For example, the use of rosin and sulphate aluminium in acidic systems as sizing agents were replaced by alkenyl succinic anhydrides (ASA) and alkyl ketene dimmers (AKD) which operate more effectively at high pH. Trends observed in papermaking, such as increase of machine speed, increased used of fillers and increased use of recycled paper, resulted in the growth in the use of retention aids. Initially, cationic, neutral and anionic polymers are used either singly or in combination but they are rapidly replaced by cationic polyelectrolytes such as polyacrylamides and polyethyleneimines and subsequently in combination with colloidal silica (Roberts, 1991).

The pulp suspension goes from the headbox to the wire section where a significant amount of water is removed (see Figure 1.1). The drainage is improved by the application of vacuum in the wire section. In this way, the suspension consistency that was initially around 0.2 to 1.5% in the headbox increases to 18 to 23% at the end of forming section. In the press section, the suspension consistency reaches 33 to 50%. After the dry-end stage, the sheet has a consistency of approximately 92 to 96% (Blanco, 1994).

The paper structure is mainly determined in the wet-end section. Therefore, after this stage it is very difficult to modify the sheet characteristics. Indeed, in the wet-end stage many physico-chemical phenomena take place between fibres, fines, fillers and additives which are related with the desired paper characteristics (Blanco *et al.*, 1995; Fardim, 2002). Flocculation is the most important phenomena of the wet-end stage since it affects process efficiency (e.g. retention, drainage and runnability) and the quality of the final product (e.g. formation, strength and porosity) (Eklund and Lindström, 1991; Unbehend, 1992).

The flocculation process consists in the formation of flocs of fibres, fines, fillers and additives which compose the furnish suspension. Flocculation of fibres is done by a mechanical entanglement between fibres, and thus, fibres can be easily retained in the wire (Blanco *et al.*, 1995). However, since the holes in the wire are larger than the fine particles,

significant mechanical retention of the small particles on the wire can not be achieved (Allen, 1985; Luukko and Paulapuro, 1999; Norell *et al.*, 1999; Stén, 1999; Pruden, 2005). Additionally, the unflocculated fine fraction of the stock suspension can increase drainage resistance (Allen, 1985; Luukko and Paulapuro, 1999; Pruden, 2005). In fact, some authors (Britt *et al.*, 1986; Wildfong *et al.*, 2000a, 2000b; Hubbe, 2002; Paradis *et al.* 2002) have described that the unattached fine particles, which can move freely through the web during dewatering, have a high tendency to block the channels through which the water is able to flow as described in Figure 1.2. In this way, retention of fines and fillers has to be achieved chemically by chemical additives as in Figure 1.2.

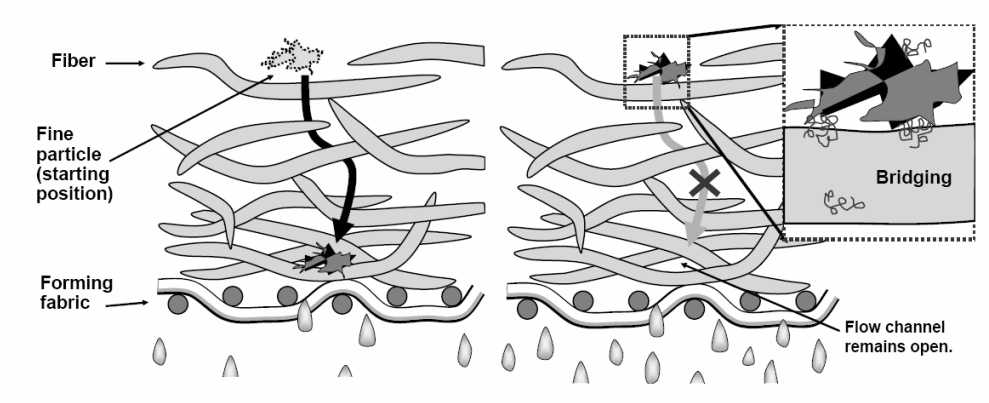

Figure 1. 2. Schematic effect of the choke-point mechanism and proposed effect of bridging bonds by polyelectrolytes on reducing choke-point mechanism (Hubbe and Heitmann, 2007).

Studies on the wet-end chemistry have established different retention/flocculation mechanisms. These mechanisms, that will be described later in section 1.2.1, depend on several factors, namely on flocculants' characteristics and dosage, pH, temperature, water conductivity, fines and fillers characteristics and machine conditions such as residence time and shear forces (Eklund and Lindström, 1991; Litchfield, 1994; Norell *et al.*, 1999). The flocculation evaluation is of great importance to control the wet-end stage because retention and drainage performance and the final quality of the product depend on the flocculation degree and on the flocs characteristics (Blanco, 1994; Blanco *et al.*, 2005; Cadotte *et al.*, 2007).

Moreover, nowadays, the optimal wet-end control is becoming more and more important because most of the strategies adopted by papermakers to maintain their competitiveness will have an influence on wet-end. The increase of the speed of paper machines and the tendency to increase white water recirculation are examples of measures

adopted in order to increase productivity and reduce costs (Blanco *et al.* 2002; Nurmi *et al.*, 2004). On the one hand, the high turbulence in high speed machines, leading to increased productivity, stress the importance of the kinetics, flocs structure and strength, and the reflocculation ability (Norell *et al.*, 1999). Indeed, these characteristics are now important for the efficiency of the retention systems because the time allowed for interaction is in the order of seconds to milliseconds (Norell *et al.*, 1999) and because flocs properties depend a lot on shear forces (Spicer *et al.*, 1998; Blanco *et al.*, 2005; Jarvis *et al.*, 2005). On the other hand, the improvement of environmental performance by reducing water consumption will increase the amount of dissolved and colloidal material present in the process water (Hulkko and Deng, 1999; Nurmi *et al.*, 2004; Cadotte *et al.*, 2007). These contaminants will affect the retention aids systems, and thus, may change flocculation kinetics and flocs properties. Since these modifications in the paper machine affect the performance of the wet-end chemistry, it is essential to further understand the flocculation mechanisms and the resulting flocs properties, especially from the point of view of how they may change over time depending on the process conditions in order to increase productivity and reduce costs, but still maintaining quality product.

The main objective of the optimal control of the wet-end stage is to improve the performance of the retention and drainage additives without damaging sheet formation, in order to have the best retention and dewatering performance and a sheet with a good formation, printing and optical properties.

1.2. – RETENTION AND DRAINAGE IN PAPERMAKING

1.2.1 – CHEMICAL ASPECTS OF RETENTION

The basis for a more fundamental understanding of the performances of retention and drainage additives in papermaking is supplied by chemical interactions. In fact, flocculation in the furnish can be caused by basic types of interactions such as electrostatic interactions, hydrogen bonding, hydrophobic and steric interactions.

When two phases are in contact (e.g. solid-liquid), the dissolved ions associated with the liquid phase are redistributed into the system in a structured way to form the

electrical double layer, around the particle, where a potential difference arises across the solid-liquid interface as represented in Figure 1.3 (Eklund and Lindström, 1991).

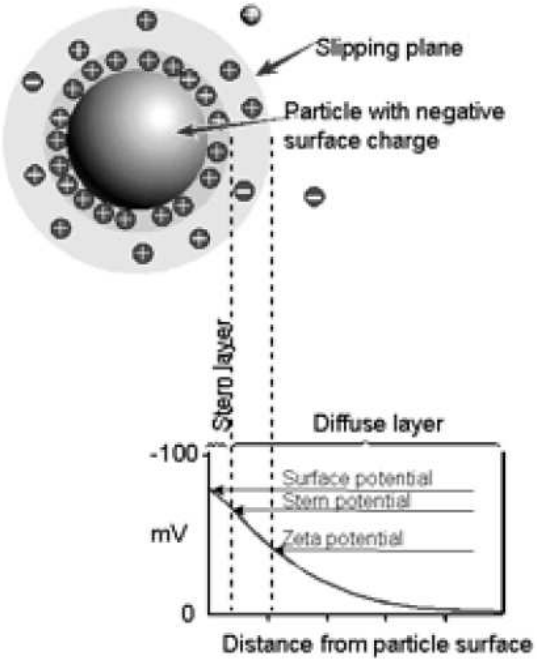

Figure 1. 3. Schematic representation of a negatively charged particle in a suspension.

In the double layer the surface, Stern and zeta potentials can be identified. However, since the surface and stern potentials are not known for many colloidal systems, electrical properties of the particles are indirectly determined by the measurement of the zeta potential that represents in this way the magnitude and the sign of the charged particles (Norell *et al.*, 1999).

A system is considered stable if aggregation does not occur. The stability of colloidal systems due to electrostatic interactions is described by the DLVO theory developed by Derjaguin and Landau (1969) and Verwey and Overbeek (1948) which states that the interaction between two particles is the sum of the attractive and the repulsive forces (Hiemenz and Rajagopalan, 1997). Figure 1.4 shows the total energy interaction curve resulting of the attraction and repulsion potentials as a function of the distance between two charged particles. When two charged particles approach each other, there is an electrostatic repulsion due to the similar charges of the particles but, at the same time, there is an intrinsic attraction due to van der Waals forces.

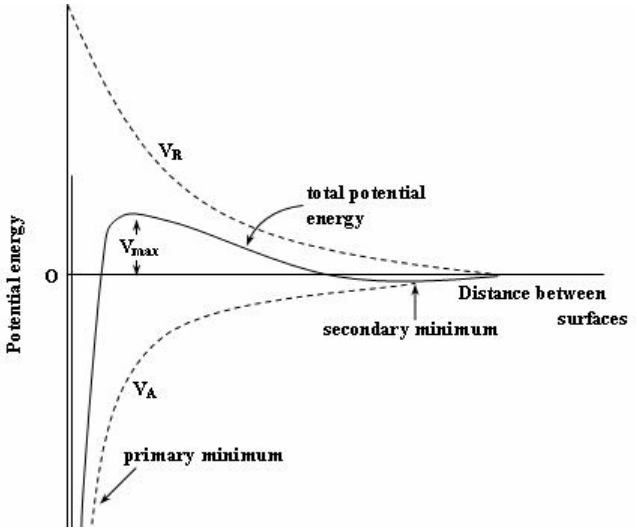

Figure 1. 4. Total interaction energy showing curve showing attractive van der Waals and repulsive potentials.

The steric stabilization is also a mechanism for the stabilization of colloidal particles. Steric stability occurs when polymer chains adsorb at the particle surface. The polymer chains extend beyond the electrical double layer avoiding particles to approach each other, and thus, reducing the effect of van der Waals forces (Blanco, 1994).

Aggregation occurs if the particles in the system are destabilized. One way to achieve aggregation is to diminish the repulsion forces by adding ions in order to reduce the electrical double layer thickness or reduce the electrokinetic potential causing the coagulation of the particles. Another way is to use polymeric additives that form bonds between the particles, and thus, causes flocculation of the system (Blanco, 1994).

Since a papermaking furnish has got many negatively charged surfaces (fibres, fines and fillers), there is a high negative surface potential of the system resulting in a high affinity of adsorption for cationic additives that can cause system destabilization (Norell *et al.*, 1999). Improvement of fines and fillers retention in the wet-end section of the paper machine is thus achieved through the use of retention aid systems that act by several flocculation mechanisms. In the case of papermaking, flocculation mechanisms can also be called retention mechanism.

1.2.2 – FLOCCULATION MECHANISMS

Based on the chemical interactions described before, the destabilization of a suspension or the aggregation of the particles can occur by coagulation or by flocculation. During aggregation, various processes take place simultaneously: adsorption of the polymer molecules at the particles surface; re-arrangement (or reconformation) of the adsorbed polymeric chains; collisions between destabilized particles to form new aggregates and break-up of the aggregates (Gregory, 1985; Berlin and Kislenko, 1995; Biggs *et al.*, 2000). The importance and the kinetics of each process depend on the flocculant characteristics (structure, molecular weight, charge density and concentration); on the characteristics of the suspended particles (size and charge density); on the characteristics of the suspending medium (pH, conductivity and ionic charge); on the contact time and turbulence intensity, among others (Berlin and Kislenko, 1995; Berlin *et al.*, 1997; Bremmel *et al.*, 1998; Blanco *et al.*, 2002).

Many studies allowed establishing that, depending on the retention aids systems used, aggregation of the particles can occur by charge neutralization, patching, bridging or complex flocculation mechanism (Eklund and Lindström, 1991; Cadotte *et al.*, 2007). This section discusses the aforementioned retention mechanisms showing how they operate.

1.2.2.1 – Charge neutralization

Charge neutralization is a coagulation mechanism since aggregation occurs due to the reduction of the repulsive forces between particles. The addition of an electrolyte salt or very low molecular weight polyelectrolyte compresses the electrical double layer enough so that repulsion between particles is diminished and van der Waals attractive forces can induce coagulation between particles of the same electrostatic charge. The optimal dosage corresponds to reaching the isoelectrical point. Beyond that the particles are redispersed. Polyvalent cations, polyethyleneimine (PEI), poly-diallyldimethylammonium chloride (poly-DADMAC), polyamines and polyamideamine epichlorohydrine (PAE) are common retention aids that act based on charge neutralization mechanism (Norell *et al.*, 1999; Cadotte *et al.*, 2007).

1.2.2.2 – Patch model

The patch model is also based on an electrostatic mechanism but is different from the charge neutralization theory. It is based on the formation of cationic sites or "patches" of the cationic polyelectrolyte on the anionic fibre or filler surfaces as Figure 1.5 shows. The polymer is absorbed in cationic patches on the negative surface of the particle. Flocculation will then take place by electrostatic forces between the oppositely charged sites on the particles.

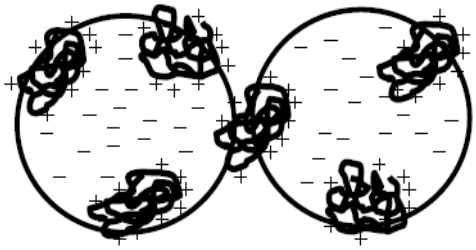

Figure 1. 5. Schematic of the patching mechanism (Scott, 1996).

The degree of attraction depends on the charge density and on the surface coverage by the polymer. Polyelectrolytes of low and medium molecular weight ($<10^6$) and of high charge density are necessary for the patching mechanism to occur. Polyethyleneimine, polyacrylamide (PAM) of low molecular weight and polyamines are examples of retention aids following this mechanism (Cadotte *et al.*, 2007).

A surface coverage of about 50% or less gives optimum flocculation (Eklund and Lindström, 1991). However, in this case, the patches must be thicker than the electrostatic double layer. If not, the polymer adsorbed only allows neutralizing the system.

Flocs formed via patch model, also called "soft flocs", are sensitive to shearing, i.e., aggregates break-up easily. Nevertheless, when the turbulence decreases, the particles partially reflocculate (Spicer *et al.*, 1998; Blanco *et al.*, 2002) (see section 1.2.3).

1.2.2.3 – Bridging

Flocculation of particles induced by polyelectrolytes of very high molecular weight ($>10^6$) occurs by the bridging mechanism. This mechanism was firstly proposed by studies carried out by La Mer and Healy (1963). These authors also referred that a maximum in the flocculation rate takes place when the polymer surface coverage is 50%.

The polymer adsorbs on the particle surface in such a way that tails and loops are extended far beyond the surface. In some cases, trains can also be found as in Figure 1.6 that illustrates an example of the polymer conformation at the particle surface. In this way, the particle can interact with other particles creating bridges between particles, and thus, allowing aggregation as described in Figure 1.7.

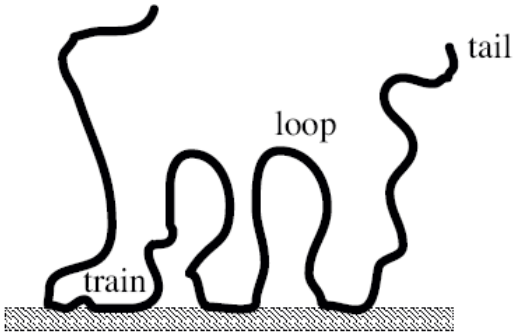

Figure 1. 6. Schematic of adsorbed polymer chain with trains, tails and loops.

Fleer and Scheutjens (1993) described the bridging mechanism as the result of three consecutive steps: polymer adsorption, bridging and depletion.

The configuration of the polymer at the particle surface and, thus the polymer thickness and the bridging performance, depends on the polymer characteristics (Bremmel *et al.*, 1998; Blanco *et al.*, 2005). The suspending medium characteristics also influence the bridging flocculation since many studies have shown that they affect the retention aid performance (Hulkko and Deng, 1999; Stemme *et al.*, 1999; Nyström *et al.*, 2004) (see section 1.2.3).

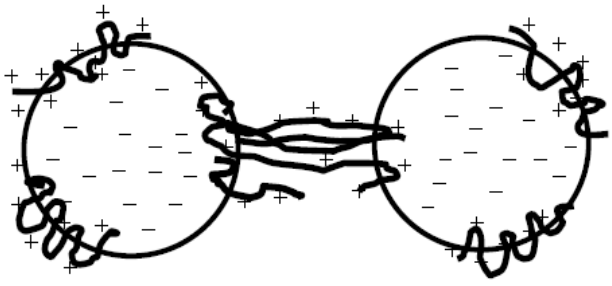

Figure 1. 7. Schematic of the bridging mechanism. (Scott, 1996).

Very high molecular weight polyacrylamides or poly(ethylene oxides) are examples of retention aids widely studied and used for flocculation by bridging mechanism (Cadotte *et al.*, 2007).

Additionally, aggregates formed by bridging mechanism are relatively strong. Although, if shearing is too high, the flocs, also called "hard flocs", will break-up originating polymer degradation. When the shear forces decrease thereafter the possibility of reflocculation by bridging is low and reflocculation takes place rather through the patch mechanism (Norell *et al.*, 1999; Blanco *et al.*, 2005) (see section 1.2.3).

1.2.2.4 – Complex flocculation

More recently, studies about new retentions aids systems are being conducted in order to improve retention and drainage. These retention aids systems exhibit a more complex flocculation mechanism than those described before. We can distinguish the dual polymer flocculation, the microparticle flocculation and the network flocculation mechanisms.

A dual polymer system is a combination of a cationic polymer (alum, polyethyleneimine, poly-DADMAC or cationic starch) with an anionic polymer (anionic polyacrylamide). The cationic polymer, which is usually added first, flocculates the anionic particles. The anionic polymer is then added in order to reflocculate, by a bridging mechanism, flocs that were broken up during a shear stage (Yu and Somasundaran, 1993; Fan *et al.*, 2000). Some studies have shown that a dual polymer systems improve dewaterability and flocs strength and exhibit higher reflocculation capacity than the single systems (Lee and Liu, 2001; Yoon and Deng, 2004).

The microparticle system is a type of dual system in which highly anionic submicron particles (montmorillonite or colloidal silica) are used along with a cationic polymer such as polyacrylamide or starch. The cationic flocculant is generally added first causing particles' aggregation. Then, the flocs formed are broken during a shear stage and the microparticles are added afterwards to induce reflocculation of the system. The reflocculated flocs formed are smaller and denser than the original ones as described in Figure 1.8 (Swerin *et al.*, 1993; Asselman and Garnier, 2001; Brouillette *et al.*, 2005). The advantages of the microparticle system are numerous and well reported in literature.

Swerin *et al.* (1993, 1996a) demonstrated the reflocculation capacity of microparticle systems significantly improve fines and filler retention induced by cationic polyacrylamides. In the same way, other authors have demonstrated that these systems improve simultaneously retention and drainage without overflocculation (formation of large flocs) which can damage sheet formation (Miyanishi and Shigeru, 1997).

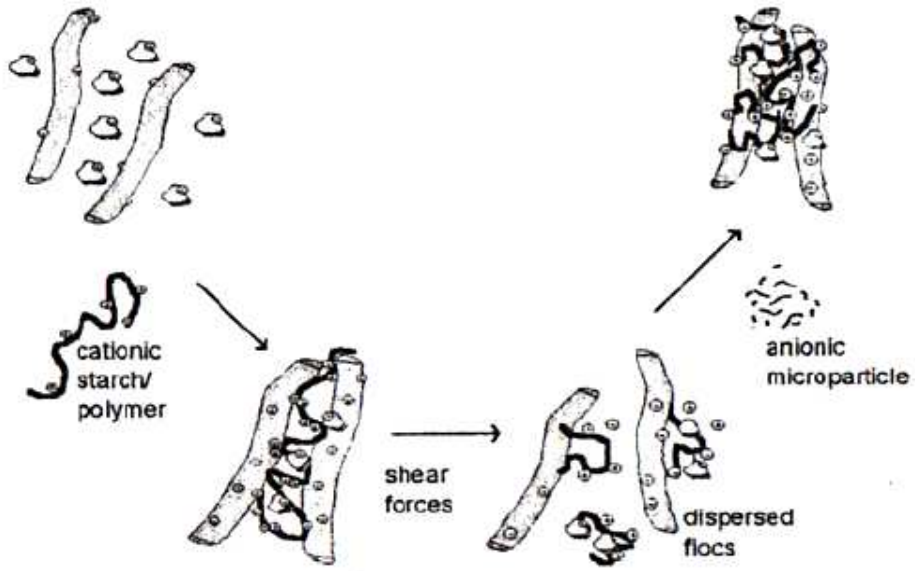

Figure 1. 8. Schematic representation of a complex flocculation with microparticles (Norell *et al.*, 1999).

The network flocculation happens when a polyethyleneoxide (PEO) is used in association with a phenolic resin. When used alone, PEO does not adsorb on calcium carbonate or bleached Kraft fibres. Therefore, it is necessary to use another compound that makes the interaction possible. The compounds normally used have aromatic cycles as in the phenol formaldehyde resin (PFR) (Lindström and Glad-Nordmark, 1984). Since the polymer is able to form hydrogen bonds with other electron acceptor compounds, it has been proposed that the flocculation mechanism is based on the formation of non-soluble complexes between PEO and PFR (Lindström and Glad-Nordmark, 1984; Negro *et al.*, 2005). However, several other theories have been proposed by many authors to describe the flocculation mechanism induced by this retention aid system. Lindström and Glad-Nordmark (1984) believe that the PEO and the phenolic resin form a transient and unstable network which encloses the fillers and fines particles. More recently, van de Ven and

Alince (1996a) proposed that flocculation occurs by association-induced bridges, i.e., the complex formed by the PEO and the phenolic resin forms bridges between the particles promoting their aggregation. Studies carried out by Xiao *et al.* (1996), have also proposed a complex bridging model to explain the retention mechanism. This model has been confirmed by Negro *et al.* (2005) that additionally proved that the complex produces a fast flocculation of the suspension forming unstable flocs, i.e., flocs that reflocculate easily upon shearing decrease.

1.2.3 – FACTORS THAT INFLUENCE RETENTION MECHANISMS

As described in the section 1.2.1, there are varied and complex factors affecting the wet-end chemistry that have to be controlled in order to obtain a good final product quality. In this section, some of these factors that influence the retention mechanisms, and thus, the flocs properties, will be discussed in more details: polymer charge density, polymer concentration, polymer structure, shear forces and electrolytes and anionic trash in the suspending medium.

1.2.3.1 – Polymer charge density

The charge density of the polyelectrolyte determines its conformation when adsorbed on the particle surface, and, therefore, the predominant flocculation mechanism (Bremmel *et al.*, 1998; Blanco *et al.*, 2005). In general, if molecular weight is high and charge density is low the polymer adsorbs on the particle surface in such a way that tails and loops are extended far beyond the surface and can interact with other particles – in this case the flocculation process is dominated by bridging bonds (Biggs *et al.*, 2000; Blanco *et al.*, 2002) (see section 1.2.2.3). Additionally, the conformation of the adsorbed polymer depends on its cationicity: at low cationicity only tails and loops are found and, as the cationicity increases, trains can also be found (Figure 1.6 in the previous section). As a consequence, when the charge density is high, the bridging capability is reduced because there is a tendency for the polymer chains to adopt a flatter conformation on the particle surface, which results in the formation of cationic patches that attract the polymer free surfaces of other particles (Swerin *et al.*, 1997; Blanco *et al.*, 2002). In this case, the adsorption rate becomes slower and the polymer reaches the final conformation earlier, i.e., the conformation rate becomes faster as the cationic charge of the polymer increases.

1.2.3.2 – Polymer concentration

The concentration of the flocculant is also a key parameter, since the rate of adsorption depends on the amount of polymer adsorbed per unit area of the particle surface. Tadros (2005) proposed the "diffusion-controlled adsorption kinetics model", stating that adsorption dominates when the surface concentration of polymer is lower than the equilibrium concentration, whereas desorption is the ruling phenomena when the surface concentration is higher than the equilibrium concentration. La Mer and Healy (1963) have shown that when flocculation occurs by the bridging mechanism, the equilibrium concentration was reached when the polymer surface coverage is 50%. Moreover, the flocculant concentration also affects the conformation rate: polymers re-arrangement is relatively fast at low surface concentration but rather slowly on crowded surfaces, since neighbouring molecules interfere with the re-arrangement (van de Ven and Alince, 1996b; Biggs *et al.*, 2000).

Flocculant overdosage is a problem that can occur in papermaking since it is difficult to control the optimal flocculant dosage in real time. This excess of flocculant represents not only an increase of the costs but also affects the flocculation process and the flocs properties. Blanco and co-workers (2005) presented a study about the effect of C-PAM (cationic polyacrylamide) overdosage on PCC (precipitated calcium carbonate) flocculation kinetics and flocs properties and they concluded that the excess of flocculant originates an increase of the repulsive forces between particles, which besides contributing to the decrease of the flocculation rate, does also inhibit the reflocculation of the particles. However, a moderate excess improves strength and stability of the flocs.

1.2.3.3 – Polymer structure

As referred in the section 1.2.2, not only the charge density of the polymer affects the flocculation mechanism. In fact, the conformation of the polymer at the particle surface also depends on its molecular weight. When the polymer molecular weight is low, the polymer adsorbs at the particle surface in a flat conformation allowing aggregation by the patching mechanism. When the polymer molecular weight is very high, the polymer adsorbs in a more extended configuration allowing the formation of bridges between

particles. In this case, the configuration and the thickness of the adsorbed polymer layer at the particles surface depend on the charge density and on the concentration of the polymer.

The polymer branching is also a parameter that describes the polymer structure. Since the thickness of the adsorbed polymer layer at the particle surface depends on the tails and loops formed, the polymer structure affects also the flocculation performance. Few studies have been performed to analyse the polymer conformation at the particle surface when branched polymers are used. Nicke and co-workers (1992) have demonstrated the use of a novel branched copolymer from diallyldimethyl-ammonium chloride (DADMAC) and approximately 1.5% by weight of triallylmethylammonium chloride, as an attractive flocculant for the paper industry. In the same way, Shin and co-workers (1997a) compared the flocculation of ground calcium carbonate induced by highly branched cationic polyacrylamides of low molecular weight and low cationic charge with conventional linear polyacrylamides of high molecular weight. They concluded that the highly branched polymer produces small flocs with great shear resistance and, when associated with microparticles, the flocs size increases. Additionally, the highly branched polymer seems to be a potential retention aid in complex microparticulate retention systems. The addition of microparticles to the deflocculated suspension improves significantly the reflocculation capacity. Afterwards, the same authors have studied the potential of the highly branched polymer as a retention aid for microparticulate systems by performing retention tests (Shin *et al.*, 1997b). The results have shown that the branched polymer exhibits better retention efficiency than the linear polyelectrolytes. Handsheets formation tests also allowed the authors to conclude that when the highly branched polymer is used in conjunction with microparticle system, it produces sheets with good formation even if the amount of filler in the sheet is higher. Indeed, the strength properties of handsheets usually decrease with an increase in filler retention. Nevertheless, they sustain that this type of polymer is promising as a papermaking retention aid where small flocs, resistant to shear and with high retention properties are required to have simultaneously high retention and good formation.

More recently, Brouillette *et al.* (2004, 2005) have also studied the performance of branched C-PAM of high molecular weight in conjunction with a microparticle system on retention, drainage and sheet formation but under high turbulence conditions. As in earlier studies, they found that this retention aid system improves filler retention as compared with the conventional ones. Nevertheless, this improvement is particularly significant as the turbulence level increases. Despite the filler retention of all polymers decreasing with the

increase of the turbulence level (Brouillette *et al.*, 2005), the branched polymers are less affected by the shearing, and thus, give the best efficiency. The same happens with the drainage time which increases with the turbulence level increase for all the polymers, but giving the best results for the branched polymers. In addition, the polymer dosage required to obtain a good retention decreases with the increase of the shearing for the branched polymer, just as opposed to what was observed for the linear one. This polymer dosage reduction could result in savings in chemical costs. The branching did not affect sheet formation which was good with both the linear and the branched flocculants. As a general conclusion, branched polymers are expected to exhibit better performance on faster paper machines, where a high turbulence level is generated, than the traditional linear flocculants.

1.2.3.4 – Shear forces

As mentioned in the section 1.1, high speed paper machines are used in modern papermaking in order to be more competitive. Therefore, the need to develop retention aid systems that are able to produce stronger flocs is of crucial importance because the flocs properties (size, structure and strength) have a great impact on the wet-end performance. Studies have to be performed in two ways, since in the paper machine headbox, where flocculation occurs, a very high turbulence level is induced, while in the forming section this turbulence decreases significantly. Under the high shear conditions in the headbox the initial flocs are usually broken up, but the suspension partially reflocculates when the shear forces decrease in the forming zone (Yoon and Deng, 2004). However, both the flocculation process and the dynamics and degree of the reflocculation process depend on the polymer characteristics. In fact, initial floc properties, mainly size and structure, which are conditioned by the course of aggregation, play a crucial role in the reflocculation stage (Hermawan *et al.*, 2003). Hence, since the final reflocculation stage determines the performance of the wet-end section, it is fundamental to understand both the flocculation and reflocculation processes.

In the flocculation process, shearing is an important key parameter. In reality, in addition to destabilization, mixing is essential to promote flocculation since polymer molecules have to collide with the fine particles in order to be adsorbed, and the polymer-coated particles have also to collide with each other (Gregory, 1985). Therefore, as the shearing increases, the collision frequency between particles increases resulting in a higher

flocculation rate (Norell *et al.*, 1999). However, as the flocs become larger further growth is restricted by the applied shear that erodes or breaks down the flocs, depending on their size (Parker *et al.*, 1972; Spicer and Pratsinis, 1996a; Thomas *et al.*, 1999). In fact, the shearing forces that tend to disrupt the flocs become larger as their size increases and this reduces the collision efficiency of the particles. Therefore, there is a limiting size for flocs growth, determined by the balance between aggregation and breakage (Gregory, 1985; Spicer *et al.*, 1998; Yukselen and Gregory; 2004). In general, the rupture of a floc is classified as either "surface erosion" or "large-scale fragmentation". Erosion is the separation of small particles from the floc surface, whereas fragmentation refers to the break up of flocs into pieces of smaller and comparable size. Theoretical models in the literature have considered particle erosion as resulting from shearing stresses on the floc surface, while fragmentation is thought to be caused by pressure gradients across the entire body (Figure 1.9) (Yeung and Pelton, 1996; Jarvis *et al.*, 2005).

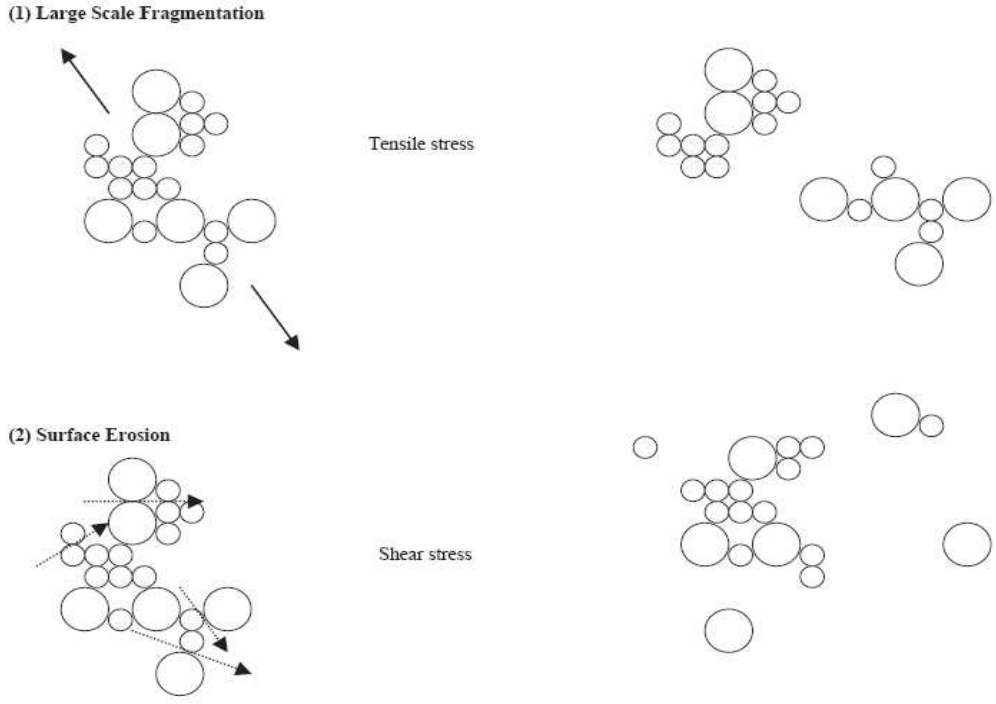

Figure 1. 9. Proposed mechanisms for the flocs breakage under different shear conditions (Jarvis *et al.*,2005).

Flocs break-up for a given shear condition also depends on the flocs strength that is directly related to flocs structure, and thus, to the floc formation process dependent on the polymer characteristics (Jarvis *et al.*, 2005). Many authors (Parker *et al.*, 1972, Tang *et al.*, 2001) found that the mechanical strength of the floc depends on both the interparticle

forces and on how the particles are packed within the aggregate. The stronger the bonding forces between the particles the higher the floc strength. Similarly, the more compact the floc structure is, the higher the number of interparticle bonds, and thus, stronger flocs are obtained (Hermawan *et al.*, 2003; Jarvis *et al.*, 2005).

Subsequently, the limiting size of the aggregates depends on both the applied shear rate and the strength of the flocs. Parker *et al.* (1972) suggested an empirical expression to correlate the maximum floc size with the shear rate and the floc strength (Equation 1.1).

$$d = CG^{-\gamma} \tag{1.1}$$

where d is the floc diameter, C is the floc strength coefficient, G is the average velocity gradient and γ is an exponent related to the stable floc size. This equation that takes into account the effect of the shear rate on the flocculation process is used on the population balance models that will be described later in Chapter 6.

Many studies have shown that, when polyelectrolytes are used to induce aggregation of a suspension, the flocs strength and the reflocculation capacity depend on the predominant flocculation process as referred previously (Swerin *et al.*, 1997; Spicer *et al.*, 1998; Biggs *et al.*, 2000; Blanco *et al.*, 2005). In fact, flocs formed using polyelectrolytes are reformed after being broken up but do not regain their original size and structure except if neutralisation is the main flocculation mechanism (Spicer *et al.*, 1998; Blanco *et al.*, 2002). This is due, for example, to the detachment of polymer chains from particles resulting in polymer degradation and/or reconformation. Thus, the original bonds are not able to reform to their previous extent reducing the efficiency of aggregation between fragments of flocs. Since flocs break up occurs at the weakest point in the floc structure, this results normally in more compact aggregates, though smaller than the initial flocs. That is, when the flocs reform partially, the new structure is compacted to denser forms by shear-induced reorganization (Spicer *et al.*, 1998).

Moreover, “hard flocs” are stronger than “soft flocs” but the stronger the flocs initially are the more difficult is reflocculation when the aggregate breaks (Norell *et al.*, 1999). In fact, when the shear force increases the tails and loops of high molecular weight polymers are broken and, therefore, when the shear force decreases thereafter the possibility of reflocculation by bridging decreases and reflocculation takes place rather through the patch mechanism (Norell *et al.*, 1999; Blanco *et al.*, 2005). When patching is

the aggregation mechanism, the effect of shear forces on the polymer degradation is lower but if the polymer is re-conformed within the diffuse layer the interactions with other particles will decrease. Hence, reflocculation, though easier, may be also lower than the original flocculation degree (Blanco *et al.*, 2002).

In papermaking, it is essential to produce flocs resistant to the high shear forces present in the paper machine, because too small flocs can reduce the retention of fines and filler particles and the dewatering ability. To reduce the effect of shear on flocs size, microparticle retention systems have been widely used in papermaking since the microparticles help reflocculation of the suspension. These effects were shown by Brouillette and co-workers (2005).

1.2.3.5 – Electrolytes and anionic trash in the suspending medium

One of the current trends in papermaking is to reduce the water consumption. However, the increase of the closure of the process water circuits results in a significant increase of inorganic salts in the water. Many studies demonstrated that the presence of electrolytes can affect the performance of the retention aid, and thus, the wet-end performance (Shubin and Linse, 1997; Hulkko and Deng, 1999; Stemme *et al.*, 1999; Stoll and Chodanowski, 2002; Solberg and Wågberg, 2003; Nyström *et al.*, 2004). For example, Hulkko and Deng (1999) found that single C-PAM systems and microparticle retention aids systems were significantly affected by the increase of electrolyte concentration due to the salting-out effect. The presence of dissolved salts generally leads to the decrease in the solubility of organic compounds and this process is known as salting out effect. Studies performed by Stemme and co-workers (1999) have also indicated that the increase of the ionic strength affects the performance of the microparticle retention aids systems. More recently, Stoll and Chodanowski (2002) have shown the influence of the ionic concentration on the polymer chain stiffness and of the ionic concentration on polymer adsorption by using Monte Carlo simulations. They found that better adsorption of the polymer was promoted by decreasing the chain stiffness or by decreasing the ionic concentration. High concentrations of dissolved inorganic compounds may affect the conformation of the polymer chain due to the salting-out effect thus reducing the polymer's bridging capability as shown in Figure 1.10 (Hulkko and Deng, 1999). Consequently, these changes in polymer conformation result in alterations on the flocs characteristics and on the flocculation kinetics. Additionally, it was observed that the

impurities of the water (anionic trash) affect the surface charge of the Precipitated Calcium Carbonate (PCC). These impurities can adsorb onto the PCC surface that becomes more negative, and thus, a higher amount of polymer is necessary to neutralize those charges. (Vanerek *et al.*, 2000).

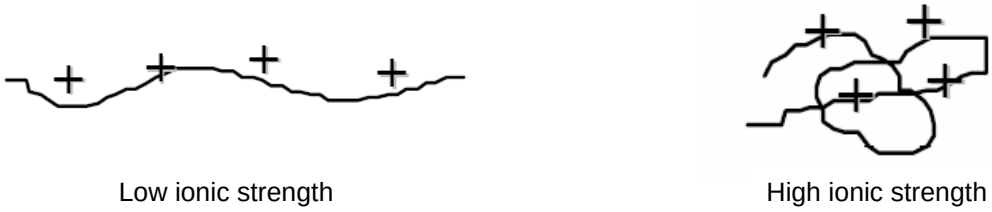

Figure 1. 10. Polymer chain conformation as a function of the ionic concentration.

1.2.4 – DRAINAGE MECHANISMS

If the retention performance is of great importance for the wet-end efficiency, removal of water is also a key parameter to achieve the desired paper properties, increasing productivity and reducing costs.

Water is removed from the fibre suspension, and later from the fibre web, in three basic sections of a paper machine: in the forming, in the press and in the drying sections. In the forming and wet pressing sections, water is removed mechanically, whereas in the drying section it is removed by evaporation.

Most of the free water in a paper web can be removed in the forming and in the press sections (see Figure 1.1). The remaining water is understood to be held in very small capillary spaces either within fibres or between them. Such water can be removed only in the dryer section (Scott, 1996).

Two major mechanisms for dewatering in the paper machine can be identified: thickening and filtration (Parker, 1972). Filtration occurs when the suspension is at such a low concentration that the fibres and other suspended components are free to move independently of each other. The result is a suspension of constant consistency over a fibre web of increasing thickness as the filtration progresses. Filtration tends to form a fibre web in which the fibres are significantly in the plane of the sheet, as if formed in infinitely thin layers. Filtration dewatering is also characterized by a sheet which is relatively consistent. Thickening occurs when the fibres and other suspended solids are somewhat immobilized in a network, such that they do not behave independently during dewatering. Thickening

tends to form a sheet with some fibres oriented out of plane, or even perpendicular to the plane of the web. Since the fibres are in the form of a network, the sheet may appear less homogeneous. In practise, the drainage mechanism is a combination of the filtration and thickening mechanisms in a high speed of the paper machine (Smook, 1992). The sheet forming process is a balance between oriented shear and turbulence patterns. Parker (1972) proposed that both oriented shear and turbulence play significant roles during drainage of the wet web. Turbulence will prevent the development of a dense, relatively impermeable web of fibres adjacent to the forming fabric, thus keeping the sheet open for drainage. Oriented shear is expected to influence the network structure by dispersing the fibres in the direction of the major force (Figure 1.11).

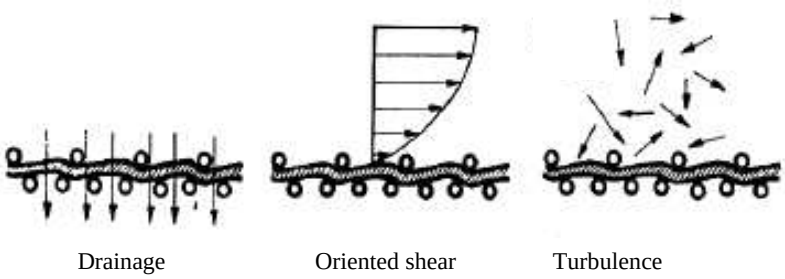

Figure 1. 11. Flow patterns on the wire of a paper machine (Smook, 1992).

Since in the majority of the paper machines the wire section is divided into two zones, the forming zone and the suction zone, two types of dewatering can be identified. Dewatering in the forming zone occurs by thickening, filtration or both, depending on the paper machine type (Norell *et al.*, 1999). Whereas in the suction zone, where a vacuum-assisted dewatering occurs, the vacuum forces air to compress the sheet and to remove water. Unbehend (1992) showed that dewatering in the vacuum-assisted zone was governed by compression. The subsequent densification of the wet web is the major mechanism of water removal, since a denser web has less space for free water.

As described previously for retention, flocculation affects also the drainage performance. In fact, Unbehend (1992) showed that there are many similarities between the two processes, and thus, improvements in retention usually result in improvements in drainage. Flocculation influences drainage by the retention of fines and colloidal substances at the fibre surfaces and by increasing the free volume for water removal. However, a high degree of flocculation, resulting in large flocs, reduces drainage because it is difficult to remove the interstitial water from the very large flocs. When a vacuum-

assisted dewatering occurs, the use of polyelectrolytes can cause less vacuum-zone drainage due to an increase in the porosity of the sheet or bad formation as a result of increased fines retention (Scott, 1996). Water is quickly replaced by air when air is able to leak through channels of low basis weight areas of the wet web.

In papermaking, the choice of the retention aids systems has to be made with caution since they have to simultaneously increase retention of raw materials and decrease drainage time without damaging sheet formation.

1.2.5 – RETENTION AND DRAINAGE MEASUREMENT DEVICES

1.2.5.1 – Direct methods

A number of devices have been developed for laboratory retention and drainage studies in the past few decades. Some types allow simultaneously determination of the drainage rate and of the sheet properties. Some of the existing methods to evaluate retention and drainage will be described below.

The Canadian Standard Freeness (CFS) test and Schopper-Riegler (SR) test are the most common methods for the determination of freeness. Freeness is relative to the ease of water flow from a fibre suspension. These tests are used to measure the drainage time of a specific volume of water from a given quantity of pulp suspension. The disadvantage of using a freeness tester has been that the test is very sensitive to the quantity of fines in the wet mat. Furthermore, since tests are carried out without stirring, the web tends to have high resistance to flow, compared to dewatering rates observed in paper machines (Krogerus, 1999; Hubbe, 2003). With the CFS test, freeness is reported as mL of free water drained while with SR test, it is reported as degrees.

The Britt jar or the dynamic drainage jar (DDJ) was introduced in 1973 and remains one of the most widely used tests for screening of retention aids. It allows to measure in an excellent and easy way the retention of fine fibres and fillers under real dynamic conditions. Figure 1.12 is a schematic representation of a DDJ. Moreover, the DDJ has been also used to evaluate drainage by measuring the drained volume during a fixed time (Krogerus, 1999; Hubbe 2003).

Because in paper machines vacuum is also used in some sections to promote the release of water, some laboratory devices have been developed, where dewatering of a sample of pre-agitated papermaking furnish over a forming screen is carried out using

vacuum to withdraw the filtrate through the screen. The Moving Belt Drainage Tester (MBDT), the Gess/Weyerhauser (G/W) system and the Dynamic Drainage Analyser (DDA) are examples of dynamic drainage apparatus.

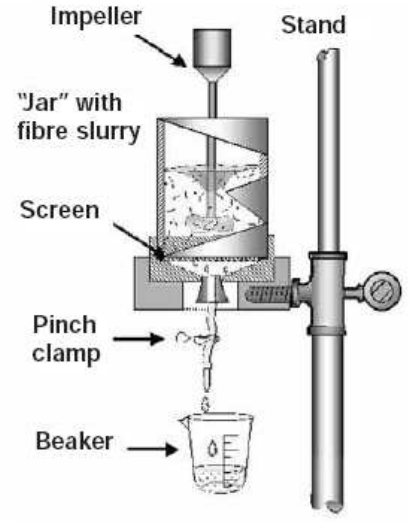

Figure 1. 12. Schematic representation of a Dynamic Drainage Jar (Hubbe, 2003).

The MBDT, introduced in 1992 by Räisänen, Paulapuro and Karrila (1995), simulates drainage and pulsation on the wire. The vacuum profile and pulsation frequency are adjustable to real paper machine conditions. The white water can be constantly removed and analysed qualitatively and quantitatively. First pass retention or wire retention can be determined while a sheet for structure analysis is being formed. The authors concluded that at a higher pulse frequency the retention was poorer.

The G/W system introduced in 1983 is mainly used to determine the drainage rate under a constant volumetric rate of pumping of the vacuum pump. The change in the vacuum applied to a furnish as it drains on a screen is measured as a function of time. This gives a drainage curve that is characteristic of the furnish, i.e., with four zones as shown in Figure 1.13: “web forming” from start to point A, “compacting zone” from point A to point B, “free water removal” from point B to point C and “pressing zone” from point C to the end (Trepanier, 1992). Point A is related with the “wet line” whereas the point B is associated with the “dry line”.

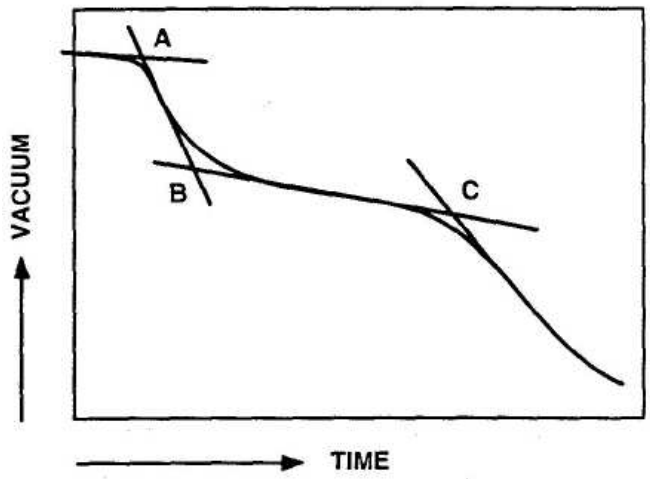

Figure 1. 13. Typical G/W drainage curve (Trepanier, 1992).

The DDA, introduced by Forsberg and Bengtsson in 1990, was built to measure drainage but can simultaneously give information about retention and wet sheet permeability for the same sample (DDA manual, 2001). It consists of a drainage unit and a microprocessor that controls the vacuum, the shear and the chemical addition during the test. Figure 1.14 is a schematic representation of a DDA.

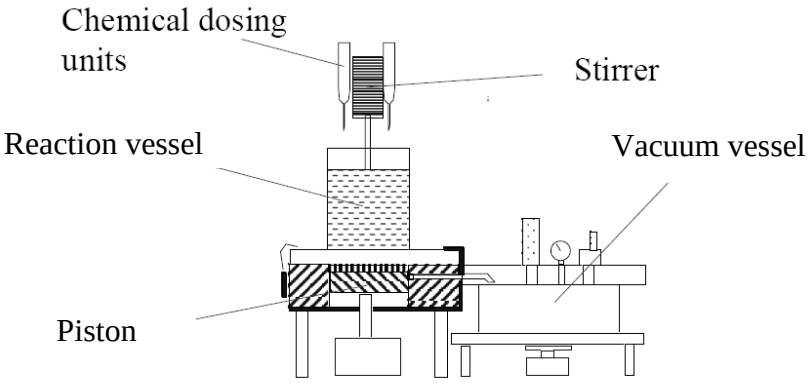

Figure 1. 14. Schematic illustration of a DDA (The DDA manual, 2001).

During the experiment the volumetric rate of pumping of the vacuum pump is maintained constant, the vacuum and the time are recorded and stored by the microprocessor. Similar to the G/W system, a drainage curve can be obtained with the DDA. Figure 1.15 illustrates a typical drainage curve obtained with the DDA. The sharp drop in vacuum starting at zero time is associated with the initial rapid flow of white water

through the forming wire, i.e., free drainage through the screen. It seems likely that point "A" in the curve is related to the point where the wire has effectively become covered with a layer of pulp. The rise in vacuum, going from point "A" to point "B" appears to coincide with the build-up of the fibre mat. Point "B" is associated with the "dry line", just before the breakthrough of air. The vacuum at the right-hand limit of the curve (point "C") can be used as a measure of the permeability of the wet sheet to air.

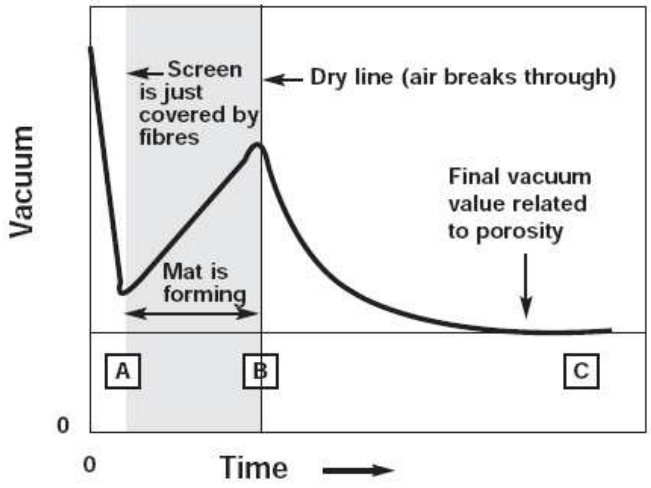

Figure 1. 15. Typical vacuum curve obtained with the DDA (Hubbe, 2003).

The air permeability expressed in pressure units (bars) is related to the sheet porosity. Forsberg and Bengtsson (1990) showed that a more porous sheet gives a higher drainage rate. Moreover, the sheet permeability is an indication of the degree of flocculation of the formed wet web. A low permeability, i.e., low porosity, indicates an undesirable high degree of flocculation, resulting in large flocs that would not easily allow the release of interstitial water. This type of floc would not easily dewater in the press and drying sections of a paper machine. A high degree of flocculation could also result in poor formation. Good formation is necessary to obtain a uniform distribution of ink and coating but also, to prevent breaks on fast paper machine. As a result, a lower drainage time in combination with higher sheet permeability is the desired response to have good dewaterability without bad formation.

The wet sheet formed can also be used to determine fines and filler retention by conventional analytical methods as gravimetric methods or calcinations, and/or submitted to further analysis to evaluate sheet properties for example the formation index, the brightness or the resistance.

1.2.5.2 – Indirect methods

However, to control and better predict the wet-end stage, it is necessary to know and understand how chemical additives act during the flocculation process. Indeed, as mentioned before, both retention and drainage performance depend mainly on the flocculation kinetics, flocculant dosage and aggregates properties. Since measurement of retention and drainage does not give information about flocculation behaviour and flocs properties others methods have been developed.

Firstly, methods such as titration, zeta potential determination and turbidity, were used to determine the optimum flocculant dosage. Optimum flocculant dosage by titration and zeta potential determination is based on the DLVO theory which relates the optimum flocculant dosage to the zero zeta potential ("isoelectric point"). This theory is valid when flocculation occurs by charge neutralization but does not fit when medium or high molecular weight polymers are used and the bridging or patching mechanisms dominate (Blanco *et al.*, 1996; Bremmel *et al.*, 1998; Claesson *et al.*, 2005; Negro *et al.*, 2005). Consequently, the methods based on electrokinetic parameters or polyelectrolytes titration should be used with great caution.

Nevertheless, zeta potential is an important parameter in flocculation studies. On the one hand, the decrease in this parameter corresponds to a decay of the surface charge during the flocculation process as a result of the transition from the bridging to the charge neutralization mechanism and it is an indication of polymer conformation (Koethe and Scott, 1993; Miyanishi, 1995; Yan and Deng, 2000; Hubbe, 2004). On the other hand, many authors used this parameter to evaluate the effect, for example, of flocculant concentration, pH and ionic strength on the particle surface charge (Vanerek *et al.*, 2000; Yan and Deng, 2000; Blanco *et al.*, 2005) which is of course related with flocculation kinetics.

Turbidity is also used to determine the flocculation ability. The presence of colloidal substances is evaluated by measuring the white water turbidity (Krogerus, 1999; Yan and Deng, 2000). Another traditional technique to assess the performance of flocculants is based on settling tests in the absence of turbulence, monitored by different means, which can supply indirect information on flocs average size and structure namely the mass fractal dimension (Glover *et al.*, 2000; Liao *et al.*, 2005; Heath *et al.*, 2006a) for the conditions prevailing in a sedimentation system. However, these traditional methods

that were used to investigate flocculation mechanisms of colloidal particles were mostly based on the evaluation of final stage of the flocculation process that is the flocs characteristics at the end of flocculation.

In this way, more recent studies have been focused on flocculation monitoring to evaluate flocculation kinetics and flocs structure. Laser, dynamic light scattering and static light scattering techniques are examples of methods applied to monitor the flocs size evolution in the aggregation process.

Blanco (1994) was the first to use a non-imaging scanning microscope as an alternative method to optimize flocculation dosage, based on monitoring the growth of the particle aggregates during flocculation: the mean floc size increases when polymer is added, but when the total added dosage is higher than the optimum no more aggregation takes place and the mean size can even decrease due to steric stabilization and/or electrostatic repulsion (Blanco *et al.*, 1994, 1996). To measure the particle size of the aggregates, a focused beam reflectance measuring probe (FBRM) was used to get information about the average chord of the aggregates. The weight of each size class is determined by the number of counts. Afterwards, other authors have published different applications of this technique namely to study flocculation mechanisms of retention aid systems, flocs resistance and reflocculation (Alfano *et al.*, 1999; Lumpe *et al.*, 2001; Blanco *et al.*, 2002).

Recently, static light scattering techniques, such as small-angle laser light scattering (SALLS) has been extensively employed in acquiring information on the aggregates structure in terms of the mass fractal dimension (Spicer *et al.*, 1998; Biggs *et al.*, 2000; Glover *et al.*, 2000; Stone *et al.*, 2002; Bushell, 2005; Liao *et al.*, 2005) in friendly and fast way. Other studies have also shown that SALLS (also called laser diffraction spectroscopy-LDS) is a useful technique to monitor the dynamics of flocculation and to evaluate the influence of the flocculant characteristics and dosage (Rasteiro *et al.*, 2007). LDS not only allows the determination of the aggregate mean size and size distribution, but gives also the mass fractal dimension of the flocs as a function of time (Biggs *et al.*, 2000; Bushell; 2005; Liao *et al.*, 2005; Rasteiro *et al.*, 2007).

In addition, the traditional technique of image analysis can also be used to determine the floc size and the floc structure by calculating the fractal number (Bushell *et al.*, 2002; Chakraborti *et al.*, 2003; Liao *et al.*, 2005).

Since the strength of the aggregates is related with the aggregate structure, some authors have studied flocculation mechanisms and flocs strength using AFM (atomic force

microscope) that gives directly the interaction force between the particle surface and the polyelectrolytes (Bremmel *et al.*, 1998; Claesson *et al.*, 2005). Bremmel and co-workers (1998) showed that these measurements allow to describe the conformation of the polymer at the particle surface, and thus, to identify the flocculation mechanisms.

Glover *et al.* (2000), Bushell *et al.* (2002) and Liao *et al.* (2005) estimated and compared the mass fractal dimension of the aggregates by various methods: settling, image analysis, 3D imaging technique using confocal scanning laser microscope, light scattering and light obscuration. They suggested that for rapid on-line analysis of aggregate structure the light scattering technique should be the preferred method for process monitoring. In fact, the other techniques present sampling difficulties besides being, in general, quite time consuming.

The FBRM, LDS and image analysis techniques will be discussed in more detail in section 1.3.

1.3 – FLOCCULATION EVALUATION

As seen in the previous section, most of the methods used to understand flocculation mechanisms, and thus, to control the wet-end stage, are based on measurements of the particles and aggregates properties. Therefore, this section will describe common aggregates properties used to evaluate the flocculation performance, and thus, the wet-end efficiency. Moreover, some techniques that measure these properties will be addressed.

1.3.1 – AGGREGATES PROPERTIES

1.3.1.1 – Size distribution

Particles are three-dimensional objects for which three parameters are required in order to provide a complete description. Consequently, it is not possible to describe a particle using a single number that can be associated to the particle size. Therefore, most sizing methods assume that the material being measured is spherical since a sphere is the only shape that can be described solely by its diameter. This approximation is useful because it simplifies the way for the particle size distributions to be represented, although, this means that different sizing techniques can produce different results when measuring non-spherical particles. Figure 1.16 reports the spherical equivalent diameters measured using different techniques depending on the physical property measured. The choice of the spherical equivalent diameter will be dependent on what is most relevant for a given process (surface, volume, etc.) (Kippax, 2005).

The size distributions can be expressed based on the number, volume, mass or surface area and are generally plotted as the fractional distribution or cumulative distribution versus the size intervals. The size distribution is usually described by statistical parameters such as the mean, the median, the mode, d_{10} and d_{90}.

The median or d_{50} is the value of the particle size which divides the population into exactly two equal parts, i.e., 50% of the particles are larger and 50% are smaller than the median.

The mode is the most common value of the frequency distribution, i.e., the highest point of the frequency curve.

d_{10} represents the value of the particle size for which 10% of the material has a size lower than or equal to this value while d_{90} is the value of size for which 90% of the material has a size lower than or equal to this value.

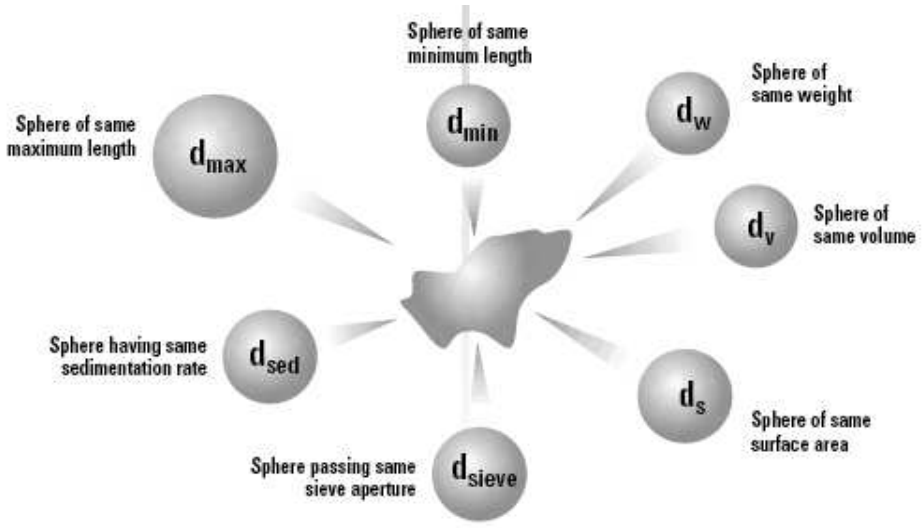

Figure 1. 16. Equivalent sphere representation for an irregularly shaped particle (Rawle, 2000).

The mean is the weighted arithmetic average of the particle sizes. However, depending on the particle physical property that is measured, several means can be calculated. In fact, as seen, the diameter can be based on the number, surface area, volume, mass, etc. that will depend on the sizing technique used. Hence, it is possible to distinguish among others, the arithmetic mean diameters weighted by number, *d[1,0]*, by surface area, *d[3,2]* (Sauter mean diameter) and by volume, *d[4,3]*. Moreover, the mean has also to take into consideration the property being measured, this meaning that the mean diameter can be calculated based for instance on an average of the sample volume, sample sedimentation velocity or sample cross section area, which will lead to different expressions for the particle size distribution mean. Equation 1.2 is the general expression to calculate the particle size distribution mean (Rawle, 2000; Allen, 1990).

$$d[p,q] = \left[\frac{\sum f_c d_c^{\,p}}{\sum f_c d_c^{\,q}} \right]^{\frac{1}{p-q}} \quad with\ p \neq q \tag{1.2}$$

f_c is the percentage of particles in the c^{th} size class (d_c) and q refers to the order of distribution while (p-q) represents the order of the property being measured.

Scattering techniques generally generate a mean size from a mass or volume size distribution, while (p-q) is usually considered to be either 1 or 2.

1.3.1.2 - Structure

Aggregate structure is of great interest in papermaking. Indeed, we have shown that flocs strength and flocs density, which are related with the flocs structure, are parameters that determine the retention and the dewatering ability (section 1.2.3 and section 1.2.4).

The fractal concept, that was introduced in 1982 by Mandelbrot, has been widely used for the quantitative characterization of aggregate structure. The mass fractal dimension, d_F, provides a mean of expressing the degree to which primary particles fill the space within the nominal volume occupied by an aggregate and is, therefore, a convenient parameter to characterize the density of the flocs (Chakraborti *et al.*, 2003). Aggregates of colloidal particles have been shown to be fractal in nature (Glover *et al.*, 2000). For any mass fractal aggregate, the mass, $m(R)$, of the aggregate is directly proportional to its radius, R, raised to a power equal to d_F, according to Equation 1.3.

$$m(R) \propto R^{d_F} \tag{1.3}$$

Furthermore, the fractal dimension can be used to characterize changes in aggregate mass density, $\rho(R)$, through Equation 1.4.

$$\rho(R) \propto R^{d_F - 3} \tag{1.4}$$

This relationship implies that as the floc size (R) increases, the floc density is in fact decreasing. Hence, a large floc will have a lower density than a smaller floc with similar structure. Therefore, the mass fractal dimension gives a good indication of the structural compactness of the aggregate, with $1<d_F<3$ in the three-dimensional Euclidean space. Small fractal dimension values indicate very spread out, tenuous and stringy structures while larger values indicate structures mechanically stronger and quite dense (Bushell, 2005).

Many techniques exist to determine the mass fractal dimension of aggregates of fine particles. One of the most common techniques is the light scattering technique (Teixeira, 1988; Bushell *et al.*, 2002). In any light scattering study, the scattered intensity is measured as a function of the magnitude of the scattering wave vector, *q*. *q* is given by Equation 1.5.

$$q = \frac{4\pi n_0}{\lambda_0}\sin(\theta/2) \tag{1.5}$$

In this equation, n_0 is the refractive index of the dispersing medium, θ is the scattering angle and λ_0 is the incident light wavelength *in vacuo*.

It has been shown that for a mass fractal aggregate that satisfies the conditions for the Rayleigh-Gans-Debye (RGD) theory Equation 1.6 can be used to correlate the scattered light intensity (*I*) with the scattering wave vector (*q*). The RGD theory is most appropriate for small aggregates of sub-micron spherical particles with relatively low refractive index (Farias *et al.*, 1996).

$$I(q) \propto S(q)P(q) \tag{1.6}$$

The form factor *P(q)* describes the scattered intensity function from a single primary particle, and the structure factor *S(q)* describes the additional scattered intensity due to the spatial correlation between particles in the aggregate (Bushell *et al.*, 2002). *P(q)* is effectively constant at small values of *q* (large particles), while *S(q)* is effectively constant at large values of *q* (small particles), so that the overall variation in intensity at small *q* values is entirely due to aggregate structural effects, while the overall variation at large *q* values is that of the primary particles (Bushell *et al.*, 2002).

Therefore, Equation 1.7 is classically used to determine the mass fractal dimension from the negative slope of the linear region of the log-log plot of *I* vs *q* (Figure 1.17).

$$I(q) \propto q^{-d_F} \tag{1.7}$$

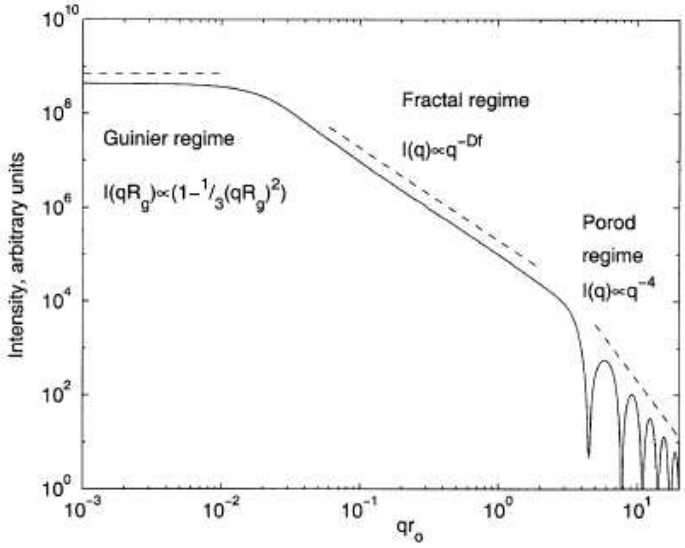

Figure 1. 17. Scattering diagram for aggregates of monodisperse spherical particles showing the Guinier, fractal and Porod scattering regimes (Bushell *et al.*, 2002).

This q^{-d_F} dependence on the scattered intensity is valid within limits of length scales much larger than the primary particles and much smaller than the floc as described in Equation 1.8. This regime is recognized as the fractal regime.

$$\frac{1}{R_{aggregate}} << q << \frac{1}{R_{particle}} \tag{1.8}$$

Nevertheless, this technique of evaluating floc structures based on their fractal dimension should be employed with caution, since many aggregates do not exhibit fractal characteristics, and the applicability of RGD theory is limited (Farias *et al.*, 1996). The slope in the fractal regime should be constant throughout the length of an aggregate when its structure shows a fractal-scaling behaviour, as usually found in colloidal flocs formed in the absence of shear (Lin *et al.*, 1990). However, restructuring may occur when the flocs are exposed to shear, resulting in a more compact structure. Restructuring would take place at the larger length scales first, since the floc strength decreases while the hydrodynamic forces experienced by aggregates are higher as the size increases (Parker *et al.*, 1972; Lin *et al.*, 1990). Consequently, the slope of a restructured aggregate will be higher at low *q* (large length scale) compared to that at high *q*, as observed in Figure 1.18 (Lin *et al.*, 1990). In other words, the structure as a uniform mass scaling with aggregate length scale

is not observed. However, information regarding the large scale floc structures can still be acquired, while the configurations at small length scales usually remain intact. The slope of scattering patterns at low q (large length scale) is therefore referred to as the scattering exponent (*SE*), on account of both the restructuring effects and the uncertainty involved in using the RGD approximation. The scattering exponent should still provide an indication about the compactness of the aggregates (Selomulya *et al.*, 2002) and is usually higher than d_F (Liao *et al.*, 2005). In addition, Biggs *et al.* (2000) indicate that scattering patterns at small length scale refer to the scattered light from primary aggregates whereas at large length scale correspond to the scattered light from secondary aggregates that resulted from the aggregation of the primary ones.

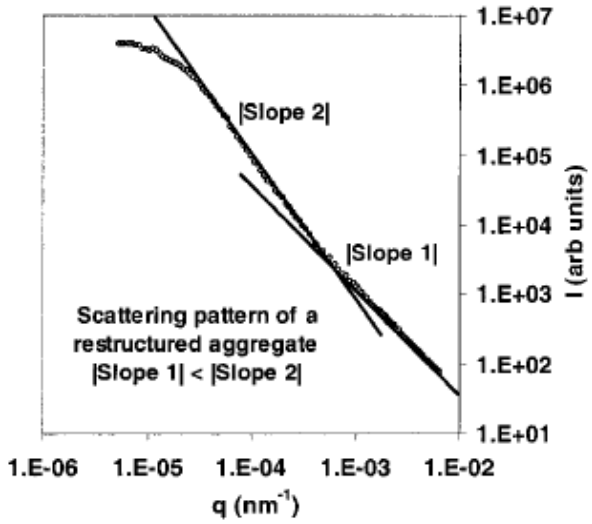

Figure 1. 18. Scattering diagram of a restructured aggregate (Selomulya *et al.*, 2002).

1.3.2 – MEASUREMENT OF AGGREGATE PROPERTIES

1.3.2.1 – Image analysis

Imaging is probably one of the oldest particle characterisation techniques and one of the most versatile. In fact, it not only measures aggregates size but gives also information about particle morphology by direct imaging of the aggregates, whereas other techniques measure size and structure, in a direct way, on basis of some existing theories. Images of aggregates have been obtained from various instruments including transmission electron microscopes, optical microscopes and *in situ* microscopes. The *in situ* microscope is preferred to determine flocs morphology since sampling and sample preparation for

microscopic examination can modify the aggregates structures. To quantify the fractal dimension of the aggregate from 2D images, analysis procedures such as box counting, sand box and mass-radius methods are used with the aid of image processing software (Bushell *et al.*, 2002).

Bushell and co-workers (2002) reported that image analysis works best with particles that are large and of high contrast, forming structures of low fractal dimensionality. The existing methods to obtain fractal information from images give results with reasonable confidence but there are difficulties associated with image processing and poor statistics due to the fact that it is a particle counting technique. However, a benefit should be credited to this technique since examination of aggregates on a one-by-one basis gives information about the variability of aggregate structure, something that is not observable from the light scattering techniques. Additionally, impurities can be excluded from the analysis eliminating, to a large extent, the problem that light scattering has with dust contamination.

Confocal scanning laser microscopy (CSLM) is the only technique that can avoid the problem of projecting a three-dimensional structure onto a plane. With this 3D imaging technique the fractal dimension is easily determined by any of the techniques applicable to 2D images. However, in practise, CLSM is limited by relatively low resolution because of its optical technology. Problems associated with multiple scattering also exist (Bushell *et al.*, 2002).

1.3.2.2 – Non-scanning laser microscopy

Recently, the number of optical techniques available to monitor the flocculation behaviour and dynamics in papermaking has been expanded by employing non-imaging scanning laser microscopy also called focused beam reflectance microscopy, FBRM. Figure 1.19 is an example of a Lasentec® FBRM.

The FBRM operates by scanning a highly focused laser beam at a fixed speed across particles in suspension. When the beam crosses a particle or an aggregate, some of the light is reflected back into the probe and transmitted to a photodiode detector. The temporal duration of the reflection from each particle or aggregate multiplied by the velocity of the scanning laser results in a characteristic measurement of the particle geometry known as the chord length. Thousands of chord length measurements are collected per second, producing a histogram in which the number of the observed counts is

sorted in several chord length bins over the range 0.5 to 1000 or 2000 μm. From the data, total counts, counts in specific size regions (population), mean chord length, and other statistical parameters can be easily calculated and analysed through the FBRM software (Blanco *et al.*, 2002).

Studies showed that this technique is well suited to investigate flocculation mechanisms of retention aids systems, optimize flocculant dosage and evaluate flocs strength and reflocculation capacity (Alfano *et al.*, 1999; Blanco *et al.*, 2002).

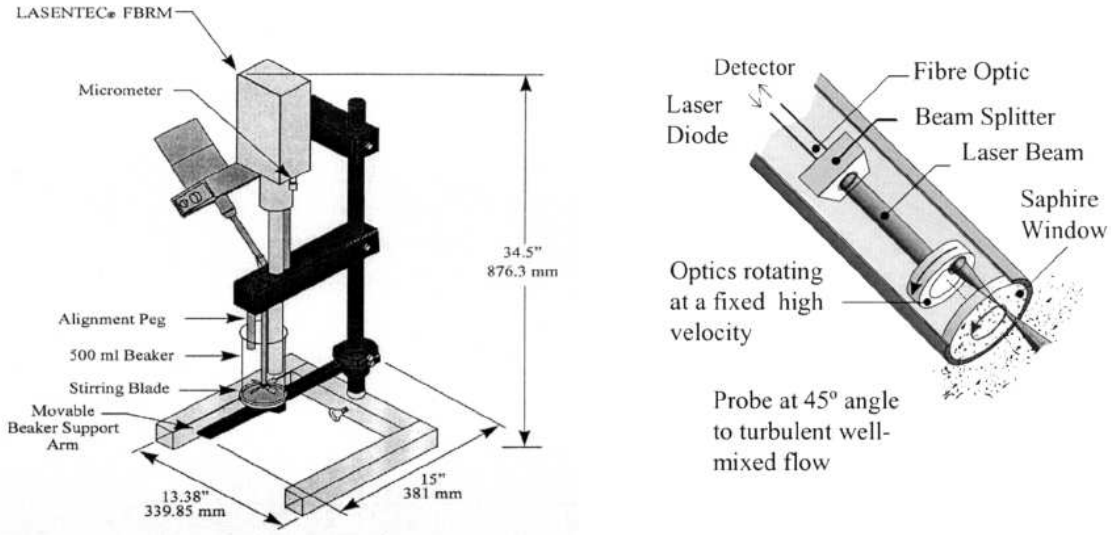

Figure 1. 19. Schematic illustration of the M500LF FBRM (Blanco *et al.*, 2002).

1.3.2.3 – Light scattering

Light scattering relies on the fact that particles interfering with a laser beam will scatter light at an angle that is directly related to their size. As particle size decreases, the observed scattering angle increases logarithmically. Scattering intensity is also dependent on particle size, diminishing with particle volume. Therefore large particles scatter light at narrow angles with high intensity, whereas small particles scatter at wider angles but with low intensity (ISO 13320-1, 1999).

There is a range of instruments based on the light scattering that use this property to determine particle size. A typical system (see Figure 1.20) consists of a laser, to provide a source of coherent, intense light of fixed wavelength; a series of detectors to measure the light pattern produced over a wide range of angles; and some kind of sample presentation system to ensure that the material under test passes through the laser beam as a

homogeneous stream of particles in a known and reproducible state of dispersion. The wavelength of light used for the measurements is also important, with smaller wavelengths (e.g., blue light sources) providing improved sensitivity to sub-micron particles.

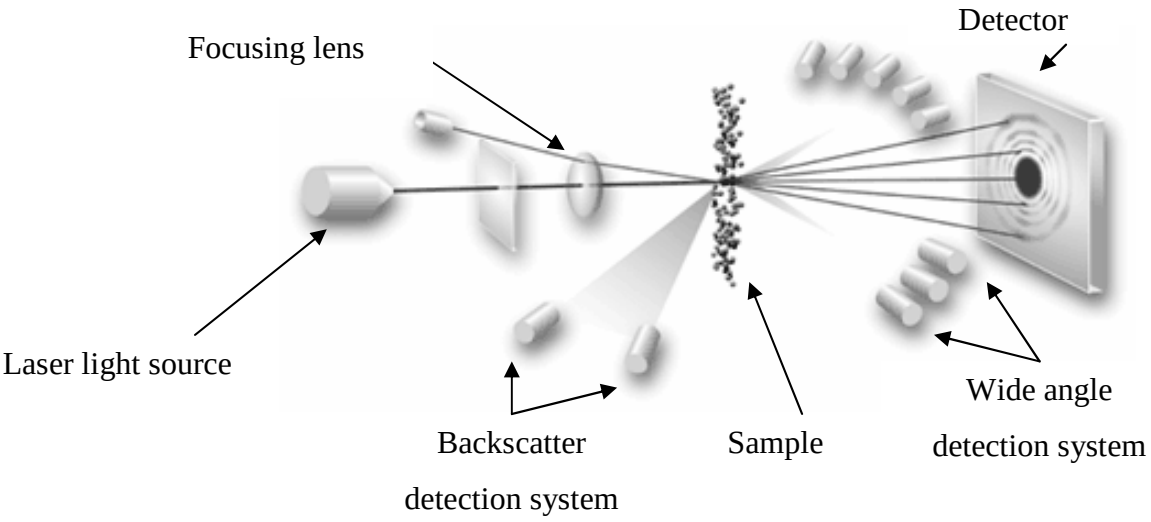

Figure 1. 20. Schematic representation of a light scattering technique.

In laser diffraction equipment, particle size distributions are calculated by comparing the scattering pattern of a material with an appropriate optical model. Traditionally, two different models are used: the Fraunhofer approximation and the Mie Theory. The Fraunhofer approximation was used in early diffraction instruments. It assumes that the particles being measured are opaque and that the light scattering is only due to the interference of the laser beam with the contour of the particle. As a result, it is only applicable to large particles and will give an incorrect assessment of the fine particle fraction. The Mie Theory provides a more rigorous solution for the calculation of particle size distributions from light scattering data. It predicts scattering intensities for all the particles, small or large, transparent or opaque (De Boer *et al.*, 1987; ISO 13320-1, 1999). The Mie Theory takes into account primary scattering from the surface of the particle, with the intensity predicted by the refractive index difference between the particle and the dispersion medium. It also predicts the secondary scattering caused by light refraction within the particle – this is especially important for particles below 50 microns in diameter, as stated in the international standard for laser diffraction measurements (ISO 13320-1, 1999). As described in the previous section, light scattering techniques are a good tool to supply information on the aggregate structure based on the scattering pattern. However,

Bushell and co-workers (2002) alerted to the fact that the complicated theories of scattering, required to accurately predicting light scattering for particles of different sizes and optical properties, can render difficult the interpretation of the scattered intensity pattern.

Light scattering techniques can be either static or dynamic. In the case of static light scattering techniques particle size information is extracted from intensity characteristics of the scattering pattern at various angles. With dynamic light scattering, particle size is determined by correlating variations in light intensity with the Brownian motion of the particles. Values obtained by the latter technique vary widely depending on the concentration and condition of the sample, as well as on environmental factors. In the case of flocculation monitoring only static light scattering techniques are of interest.

1.4 – RHEOLOGICAL PROPERTIES OF FLOCCULATED SUSPENSIONS

Cellulosic fibres in suspension form three-dimensional networks that exhibit viscoelastic properties (Wahren, 1964; Kerekes *et al.*, 1985). This behaviour has practical implications in many stages of the papermaking process such as during pumping of fibre suspensions and the forming of paper (Swerin, 1998). Wahren (1964) was the first to study theoretically and experimentally the viscoelastic properties of fibre suspensions. He concluded that a three-dimensional network forms since fibres change their direction in turbulent shear and are constrained in a network structure as they try to regain their original shape. This mechanical flocculation depends on pulp consistency, fibre length, electrostatic charge of the fibre surface, hydrodynamic forces and ionic strength and pH of the suspending medium (Kerekes *et al.*, 1985).

However, during paper manufacture, chemical flocculants are added to flocculate fine fibres and fillers onto fibre surfaces, and thus, retain them in the web. This chemical flocculation is also a factor that affects the mechanical flocculation of the fibre suspension, and thus, the rheological behaviour of the whole suspension (Swerin, 1998). Therefore, it is of real interest to study flow behaviour of flocculated suspensions by chemical additives. Studies that have been performed until now suggest that the effect of chemical flocculation on rheological behaviour of pulp suspensions is not significant when the pulp consistency is high (3% or over) because the fibre network strength is already too high to be significantly enhanced by the flocculant (Swerin *et al.*, 1992). Nevertheless, it has been shown that the flocculation induced by cationic polymers in low consistency fibre suspensions increases the strength of the formed network (Li and Ödberg, 1996; Swerin, 1998).

As seen, the flocculation mechanism determines the properties of the flocs and therefore the rheological behaviour of the suspension. However, only few studies relate the flocculation mechanism with the rheological behaviour of the flocculated fibre suspension (Swerin, 1998; Negro *et al.*, 2006). Consequently, the flow behaviour of flocculated suspension is not clearly understood yet. One of the constraints to the study of the rheological behaviour of fibre suspension comes from the fact that the commercial equipment available is not adequate for the characterization of this type of suspensions, namely due to aggregation effects that prevail. In the work of Negro *et al.* (2006) a rheometer with a completely different geometry has been used, as will be described later.

All fluids for which the viscosity varies with shear rate are non-Newtonian fluids. This is the case for the pulp fibre suspensions. Within the non-Newtonian fluids several behaviours can be found. In the case of the pseudoplastic behaviour the apparent viscosity decreases with the increasing shear rate. Pseudoplastic fluids typically obey a power law model described by Equation 1.9 (Cheng and Heywood, 1984; Blanco, 1994).

$$\tau = m\,\gamma^{n} \tag{1.9}$$

τ is the shear stress, m is the consistency index, γ is the shear rate and n is the behaviour index.

In the case of the Bingham behaviour, a finite stress, called yield stress is required before continuous deformation occurs. After, the fluid exhibits a Newtonian behaviour. Bingham fluids behaviour is described the Equation 1.10 (Cheng and Heywood, 1984).

$$\tau = \tau_B + \mu_p \gamma \tag{1.10}$$

τ is the shear stress, τ_B is the Bingham yield stress, μ_p is the plastic viscosity and γ is the shear rate.

The model of Herschel-Bulkley takes into account both features exhibited by pseudoplastic and Bingham fluids and is described by Equation 1.11 (Cheng and Heywood, 1984).

$$\tau = \tau_y + m\gamma^{n} \tag{1.11}$$

τ is the shear stress, m is the consistency index, γ is the shear rate, n is the behaviour index and τ_y is the yield stress.

Some authors have used the Herschel-Bulkley model to describe the flow of fibre suspensions (Schuster and Friedrich, 1997; Servais and Manson, 1999; Servais *et al.*, 2002; Ventura *et al.*, 2007)

For the rheological characterisation of fibre suspensions, which will depend on the fibre type, consistency and effect of additives, a viscometer has to be used. Traditionally, rotating viscometers have been used. (Duffy and Titchener, 1975; Gullichsen and Härkönen, 1981; Chase *et al.*, 1989; Bennington *et al.*, 1990) However, as referred, normal

commercial viscometers do not provide enough mixing to maintain uniform fibre distribution, which cause the measurements to approach the viscosity of the pure water (Blanco *et al.*, 1995). Therefore, to study the rheological properties of the pulp suspensions it is necessary to use non-commercial viscometers (Chase *et al.*, 1989; Bennington *et al.*, 1991; Blanco *et al.*, 1995). One of these non-commercial viscometers was presented by Blanco and co-workers (1995). This rotational viscometer designed by UCM (Universidad Complutense of Madrid) maintains a uniform distribution in heterogeneous fibre suspensions and avoids the formation of a fibre plug between the measuring elements. Moreover, because it uses a large enough sample it is well suited for the characterization of industrial suspensions which sometimes present some heterogeneities. Figure 1.21 is a schematic representation of this rotational viscometer.

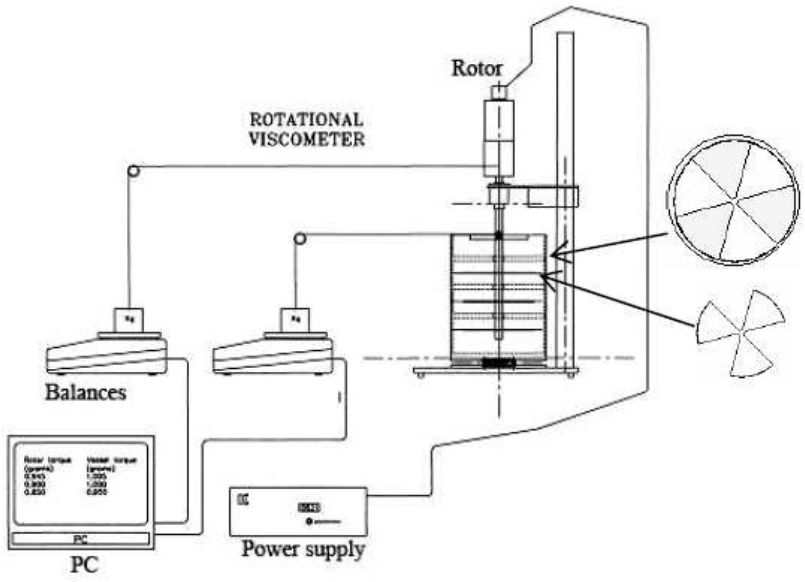

Figure 1. 21. Schematic illustration of the rotational viscometer developed by UCM (Negro *et al.*, 2006).

Negro and co-workers (2006), by using this rotational viscometer, demonstrated that low consistencies pulp suspensions of *Eucalyptus Globulus* (long fibres) show a pseudoplastic behaviour. For higher consistencies other authors (Hammarström, 2004; Ventura *et al.*, 2007) have found that the Herschel-Bulkley model described better the rheological behaviour of the suspension. Negro and co-workers (2006) were the firsts to study the effect of the flocculation mechanism on the rheological behaviour of pulp suspensions. They found that the flocculant addition decreases the shear stress and the consistency index of the pulp and increases considerably the flow behaviour index (*n*).

Therefore the pseudoplastic behaviour of the fibre suspension decreases and becomes closer to the Newtonian behaviour. They proved that the size of the flocs, their resistance and their reflocculation capacity were the main factors that affect the rheological behaviour index of the pulp.

1.5 – MODELLING OF FLOCCULATION PROCESSES

The characterisation and the control of the aggregates properties are of great importance since size, shape and structure of the flocs are related with the final quality of the product and with the process efficiency. As seen before, this is the case of the papermaking process where the flocs structure and size depend namely on flocculant concentration, polymer characteristics and mixing rate. Hence, it is necessary to monitor and manipulate adequately these parameters to control flocs size and structure during the flocculation process.

In this way, to understand, predict and control the aggregation process, quantitative models which are able to describe flocculation under various processing conditions need to be developed. The common modelling approach is based on population balance equations (PBE).

The mathematical modelling of flocculation usually makes use of the classic Smoluchowski approach (1917) that described the rate of irreversible aggregation between flocs containing *i* and *j* number particles, respectively, to form aggregates with *k* particles where $k=i+j$ (Equation 1.12).

$$\frac{dn_k}{dt} = \frac{1}{2}\sum_{i=1,\, j=k-1}^{i=k-1} \alpha_{ij}\beta_{ij}n_i n_j - n_k \sum_{i=1}^{i=\infty} \alpha_{ik}\beta_{ik}n_i \qquad (1.12)$$

n_i and n_j are number concentration, α_{ij} and β_{ij} are the collision efficiency and frequency respectively.

Since the solution of this equation is not immediate, Smoluchowski made a number of simplifying assumptions. He assumed that every collision is successful ($\alpha_{ij}=1$), the particles are of same size and both particles and aggregates are spherical in shape. In addition, binary collision between particles occurs due to laminar fluid motion and no flocs

breakage is considered (Thomas *et al.*, 1999). However, the analytical solution of this classical approach is significantly constrained by these assumptions and deviates from the real systems.

In this way, many authors proposed modifications to this equation and considerable progress has been made in using numerical techniques to model the growth of particles by aggregation (Thomas *et al.*, 1999). For instance, a sectional method, which divides the whole particle-size range of concern into a convenient number of size sections, has been developed to solve the coagulation kinetic equations for the time evolution of the size distribution (Hounslow *et al.*, 1988). Attempts also have been made to incorporate the breakage process into flocculation models. In the early work of Fair and Gemmell (1964), aggregate breakage was included in a simple numerical study of flocculation, and the authors demonstrated the important role of breakage in a flocculating system. In recent developments, the numerical approach has been further improved, using the sectional approximation in combination with simplified breakage functions to simulate particle flocculation, accounting for both aggregation and breakage (Cohen, 1992; Spicer and Pratsinis, 1996b; Kostoglou *et al.*, 1997). It has been demonstrated that the particle size distribution reaches a stable state in a batch flocculation system.

More recently, the effects of turbulent shear rate, flocculant dosage, primary particle size and solid fraction have been incorporated into PBEs that simultaneously account for aggregation and breakage (Heath *et al.*, 2006b). As stated by Thomas and co-workers (1999), the knowledge of the fractal dimension is useful to make flocculation modelling more applicable to real systems. In this way, some authors have introduced the fractal dimension into PBEs to model the shear-induced flocculation of porous aggregates (Serra and Casamitjana, 1998; Flesch *et al.*, 1999). However, these attempts have usually been conducted by assuming a constant structure for all flocs during the process. In fact, Selomulya and co-workers (2003) have shown that flocs structure changes considerably during flocculation. The flocs restructuring was incorporated into the PBEs by the fractal dimension (referred as the scattering exponent) variation during flocculation time (Equation 1.13). c_1, c_2 and c_3 are fitted parameters, d and d_0 are the floc and primary particle diameters respectively and $d_{F,max}$ is the maximum value of d_F observed.

$$\frac{d\,d_F}{dt} = \left[c_1 \left(\frac{d}{d_0} \right)^{c_2} + c_3 AB \right] \times \left(d_{F,\max} - d_F \right) \tag{1.13}$$

Moreover, since the collision efficiency decreases as the aggregate size increases, Kusters *et al.* (1997) proposed a model where the collision efficiency decreased exponentially with increasing dimensionless floc size as described in Equation 1.14. Its value approaches zero when the size ratio of the colliding aggregates is ≤ 0.1.

$$\alpha_{ij} = \left[\frac{\exp\left(-x\left(1 - \frac{i}{j} \right)^2 \right)}{(i \times j)^y} \right] \times \alpha_{\max} \qquad (1.14)$$

i and *j* indicate the size sections where colliding aggregates are located, α_{max} is the upper limit of α_{ij} ($0 \leq \alpha_{max} \leq 1$), *x* and *y* are fitting parameters. The collision efficiency estimated using $x=y=0.1$ and $\alpha_{max}=1$ is shown in Figure 1.22. As seen in Figure 1.22 α_{ij} values are higher for smaller flocs of similar size ($i \approx j$).

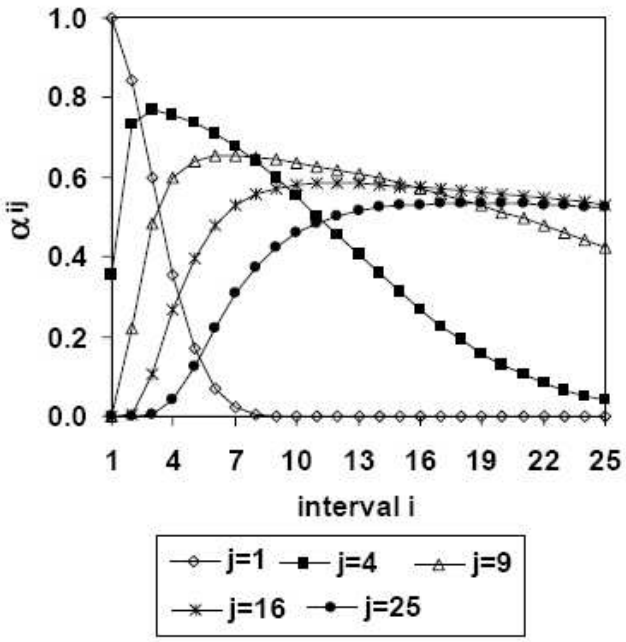

Figure 1. 22. Collision efficiency estimated with x=y=0.1 and $\alpha_{max}=1$ (Selomulya *et al.*, 2003)

Soos and co-workers (2006) used Selomulya *et al.* (2003) results but in this case, they considered that α_{max} is an adjustable parameter, since as observed experimentally,

α_{max} is lower than one. Furthermore, they used a more simplistic model to describe aggregate restructuring during flocculation, through the mass fractal dimension variation, that gives also good results. The change of fractal dimension with time is given by Equation 1.15 where γ is a time constant (Bonanomi *et al.*, 2004).

$$\frac{dd_F}{dt} = \gamma\left(d_{F,\max} - d_F\right) \tag{1.15}$$

Furthermore, the collision efficiency factor not only depends on the flocs size but also on the flocculant characteristics. Swerin and co-workers (1996b) have considered that the flocculation efficiency factor is proportional to the product of the fraction of the surface covered with adsorbed polymer on one particle and non-covered fraction on the second particle, as in Equation 1.16.

$$\alpha = \theta(1-\theta) \tag{1.16}$$

θ is the degree of surface coverage. In this work, the authors described three models for the collision efficiency determination depending on the flocculant used. When the flocculant acts by the bridging mechanism, the polymer layer thickness affects the collision efficiency. Hence, the collision efficiency factor is described by the bridging action related to coverage and by the layer extension that enhance collisions. The resulting collision efficiency factor for a flocculant that acts by bridging is given by Equation 1.17.

$$\alpha = 2\theta(1-\theta) + a\left(1-\exp(-b\theta)\right) \tag{1.17}$$

a and *b* are constants and can be determined experimentally from data for the hydrodynamic layer thickness of the flocculant on particles.

Heath and co-workers (2003, 2006b) have proposed another way to implement the decrease in the flocs size during flocculation into the model. They considered that the decrease in the flocs size is due to polymer degradation as a consequence of flocs break-up. In the first study (2003), this breakage irreversibility was introduced into the model by making the particle collision efficiency term decrease during flocculation time. In Equation 1.18, *C* is the initial collision efficiency and *D* is a parameter for the rate of decrease in the

collision efficiency with time. *C* and *D* are fitted parameters and should probably dependent on other variables like polymer concentration or polymer characteristics.

$$\alpha = Ce^{-t/D} \tag{1.18}$$

In the second study (2006), the polymer degradation was incorporated into the model by introducing Equation 1.19 in the breakage kernel. Θ is the degree of flocculant degradation in the range [0,1], ϕ is the solid volume fraction and ϕ_{eff} is the effective volume fraction that includes aggregate porosity. *a* is a constant that includes system properties.

$$\frac{d\Theta}{dt} = a\left(1-\Theta\left(\frac{\phi_{eff}}{\phi}\right)^{1/3}\right) \tag{1.19}$$

The discretized population balance equation proposed by Hounslow *et al.* (1988) and Spicer and Pratsinis (1996b) has been widely used to describe flocculation in terms of aggregation and breakage. The particle size interval was discretized doubling the particle or floc volume (v_i) after each interval ($v_{i+1}=2v_i$) which results in Equation 1.20.

$$\begin{aligned}\frac{dN_i}{dt} = &\sum_{j=1}^{i-2} 2^{j-i+1}\alpha_{i-1,j}\beta_{i-1,j}N_{i-1}N_j + \frac{1}{2}\alpha_{i-1,i-1}\beta_{i-1,i-1}N_{i-1}^2 \\ &- N_i\sum_{j=1}^{i-1} 2^{j-i}\alpha_{i,j}\beta_{i,j}N_j - N_i\sum_{j=i}^{\infty}\alpha_{i,j}\beta_{i,j}N_j - S_iN_i + \sum_{j=i}^{\infty}\Gamma_{i,j}S_jN_j\end{aligned} \tag{1.20}$$

N_i is the number concentration of flocs containing 2^{i-1} particles. In this case, N_1 is the number concentration of primary particles. The first two terms of Equation 1.20 describe the formation of flocs in the interval *i* resulting from the collisions of flocs from smaller size ranges. The third and fourth terms represent the loss of flocs in the interval *i* due to the aggregation of flocs from section *i* with those from other size intervals. The fifth term accounts for the loss of flocs in the interval *i* through its fragmentation, and the last term denotes the gain of flocs in section *i* by fragmentation of larger flocs. The parameters $\alpha_{i,j}$ and $\beta_{i,j}$ are the collision efficiency and frequency, respectively, between flocs in *i* and *j* sections. The parameter S_i is the fragmentation rate of flocs in the interval *i*, whereas $\Gamma_{i,j}$ is

the breakage distribution function for the break-up of flocs in the interval *j*, which generates fragments of sizes that fall in the interval *i*.

In chapter 6 the population balance model expressed by Equation 1.20, which will be used in this work in combination with Equation 1.15, will be described in more detail showing the relation with operating conditions and relevant physicochemical characteristics of the primary particles.

CHAPTER 2 – PROBLEM ANALYSIS AND OBJECTIVES

Many attempts have been made by papermaking industries to maintain their competitiveness. The main trend is to increase productivity and reduce costs without decreasing products quality and even try to improve it (Blanco *et al.* 2002; Nurmi *et al.*, 2004). Moreover, nowadays, in achieving these goals, the environmental impact has to be taken into account for the sustainability of the processes (Hulkko and Deng, 1999; Nurmi *et al.*, 2004; Cadotte *et al.*, 2007).

On the one hand, the increase of the productivity and the reduction of production costs are achieved by maximising the speed of the machine, which can originate an increase of breaks of the paper web (Nurmi *et al.*, 2004; Cadotte *et al.*, 2007). On the other hand, attempts to improve the environmental performance by reducing the water consumption will increase the amount of dissolved and colloidal materials present in the process water (Hulkko and Deng, 1999; Nurmi *et al.*, 2004). In addition to mill water closure, the increased use of the recycled fibres is another source of contamination of the furnish (Hulkko and Deng, 1999). These contaminants, that amplify production difficulties such as increased deposits, foaming, biological activity, corrosion, decreased retention and paper strength, will affect the performance of the wet-end stage, and thus, the final product quality (Hulkko and Deng, 1999; Nurmi *et al.*, 2004; Cadotte *et al.*, 2007). Consequently, to prevent the effect of the water closure and the increase of the paper machine speed, the addition of more efficient chemical additives are the main tools to improve the retention and the sheet properties, which increase the productivity and maintain a cleaner system (Nurmi *et al.* 2004). In addition, new additives are also introduced to improve the paper quality. These additives such as sizing agents, defoamers, dyes, retention and drainage aids and biocides, increase the complexity of the wet-end chemistry (Hulkko and Deng, 1999). Furthermore, additives that are not retained in the sheet will accumulate in the process water and may cause environmental problems.

Several problems associated to the trends observed in papermaking industries remain to be solved. A very important objective is the reduction of wet-end breaks and of the contaminants in the recycled water. One way to achieve that is by increasing the additives performance. Since breaks of the paper web can be due to the destabilisation of retention and drainage stages and, on the other hand, chemical additives have got a great

impact on the retention and drainage performance and, consequently, on the presence of contaminants on the recycled water and on the final product quality, a deeper knowledge of flocculated pulp suspensions behaviour is necessary. In fact, flocculation is the most important phenomena of the wet-end stage closely related to one of the most important strategic focuses of papermakers which is the optimal control of the wet-end stage. The optimization of the retention chemicals use requires further understanding of the flocculation mechanisms and how these mechanisms may change over the time, and also how they depend on the process conditions, the pulp characteristics and the polymeric system added.

The flocculation processes promoted by polymeric additives have been studied extensively and are well reported in the literature (Gregory, 1985; Swerin *et al.*, 1993; Berlin and Kislenko, 1995; van de Ven and Alince,1996a; Miyanishi and Shigeru, 1997; Bremmel *et al.*, 1998; Spicer *et al.*, 1998; Hulkko and Deng, 1999; Stemme *et al.*, 1999; Biggs *et al.*, 2000; Asselman and Garnier, 2001; Blanco *et al.*, 2002; Nyström *et al.*, 2004; Brouillette *et al.*, 2005; Negro *et al.*, 2005; Cadotte *et al.*, 2007). However, concerning the papermaking process, only few studies relate flocculation dynamics and flocs characteristics with retention, drainage and sheet formation under various process conditions and for different retention aids systems (Alfano *et al.*, 1999; Shin *et al.*, 1997a, 1997b; Dunham *et al.*, 2002; Fuente *et al.*, 2003; Cadotte *et al.*, 2007). For instance, Alfano and co-workers (1999) detected an inverse correlation of the scanning laser microscopy peak mean chord length with the DDJ filtrate turbidity. Dunham *et al.* (2002) performed flocculation measurements using FBRM to determine the relationship between cellulosic fibre aggregation and drainages rates in the DDA. Moreover, they evaluated the effect of the polyelectrolytes on the dissolved and colloidal substances (DCS) distribution and its impact on drainage rates. They concluded that the presence of DCS is detrimental on both flocculation and drainage with CPAM. However, the flocculation is improved if DADMAC was added to neutralize the DCS. The same was not observed with the drainage and the authors attributed this to the formation of some particulate complexes that effectively retard drainage. The correlation between flocs characteristics and retention, drainage and sheet formation is of great importance in order to understand, predict and optimize retention and drainage performance, and thus, sheet formation and quality.

Since flocculation mechanisms and flocs characteristics depend mainly on the polymer characteristics, the choice of the retention aids systems is an important key to achieve papermaking industry objectives in-line with the most recent trends. The main goal

of the use of retention aids is the aggregation of fines and additives to the larger fibres in order to maximize the retention of the particles into the paper sheet and simultaneously to maximize the drainage rate. The optimization of the wet-end stage leads to the decrease of contaminants in the water closure and to the increase of the paper machine speed. The kinetics, the flocs structure and strength and the reflocculation capacity are characteristics that describe the retention aid systems efficiency. These characteristics are important because of the high speed and turbulence verified in the paper machine. In fact, flocculation kinetics need to be fast because the time allowed for interaction is in the order of seconds to milliseconds (Norell *et al.*, 1999). On the other hand, the flocs produced need to be resistant and with a high reflocculation capacity due to the high turbulence observed in the paper machine (Norell *et al.*, 1999). Moreover, flocs properties are essential to improve the drainage. Flocs size cannot be too large because voluminous flocs are very difficult to dewater (Norell *et al.*, 1999). The flocculation reversibility is a prerequisite for good dewatering. Lindström *et al.* (1989) and Swerin *et al.* (1993) showed that the use of microparticles systems improves significantly the reflocculation that originates smaller and denser flocs. This contributes to increase retention and drainage efficiency. Furthermore, small and uniform flocs structures are essential to improve dewatering when vacuum dewatering is used (Scott, 1996).

Recently, some studies have shown that branched polyelectrolytes offer a promising alternative as papermaking retention aids. Indeed, Shin and co-workers (1997a, 1997b) have shown that branched polymers produce small flocs with great shear resistance and, when associated with microparticles, the reflocculation ability is improved. In addition, when compared with traditional linear polymers, the branched polymers lead to better retention efficiency, though the formed sheet properties are not affected by the increase of the filler content in the sheet. Other authors (Brouillette *et al.*, 2004, 2005) showed that the efficiency of the branched polymers increases with the increase of the turbulence level, i.e., the retention increases and drainage time decreases as the shearing increases. This property of the branched polymers could be useful on faster paper machines where high turbulence levels are encountered during paper formation. They also found that the use of branched polymers does not affect the sheet formation performance and that the required polymer dosage decreases as the shearing increases in comparison with the use of the traditional linear polymers. Hence, by using branched polymers it is possible to increase filler retention without affecting the final product quality and, simultaneously, to

save production costs and to decrease problems associated with the increase of contaminants on the process water.

Considering the information that already exists about the wet-end chemistry and the way that papermaking industry is evolving, there is a need to further understand flocculation mechanisms with branched polyelectrolytes under different processing conditions. Moreover, flocculation with branched polymers has to be correlated with retention, drainage and formation performance in order to predict and control the wet-end stage.

In addition, the study of the rheological flow behaviour of flocculated suspensions with chemical additives can be also interesting for optimising the power consumption in papermaking since the chemical flocculation affects the mechanical flocculation of the fibre suspension. The evaluation of the rheological properties of the pulp suspension is important because the flow behaviour has practical implications on the papermaking process, namely on the pumping of the pulp suspension and on the forming of paper (Swerin, 1998). However, only few studies consider the effect of the chemical flocculation on the flow behaviour of the pulp suspensions (Li and Ödberg, 1996; Swerin, 1998; Negro *et al.*, 2006) indicating the necessity of further investigations on this field

Finally, since flocculation behaviour is so important during the wet-end stage, affecting the retention and the drainage performance, it is most essential to be able to define, a priori, the operating conditions and the flocs characteristics that conduct to a desired performance. Hence, to understand, predict and control the flocculation process by polyelectrolytes, a quantitative model which is able to describe flocculation under various processing conditions, not restricted just to one type of additive, is of most importance. This model will constitute a valuable piece for the modelling of the wet-end of the paper machine.

Therefore, the main objectives of this thesis were:

- to develop a strategy that allows obtaining information about flocculation kinetics, flocs characteristics (size distribution and structure), flocs resistance and reflocculation capacity in a single test and in turbulent conditions.

- to assess how polyelectrolytes characteristics, namely the charge density and the degree of branching, affect flocculation dynamics, flocs characteristics, flocs resistance and reflocculation capacity.

- to evaluate the influence of the water characteristics on the flocculation, deflocculation and reflocculation processes, namely those promoted by branched polyelectrolytes.

- to investigate how microparticle retention aid systems can be used to improve the performance of the polymers, in particular of the branched polymers.

- to correlate information on the flocculation process and flocs characteristics (size and structure) with retention and drainage results in order to further understand and control the wet-end stage.

- to evaluate and understand the flow behaviour of flocculated suspensions and correlate rheological data with flocculation information.

- to implement a model that is able to describe the flocculation process and which can predict the aggregates' characteristics for fixed operating conditions or, on the other hand, determine the operating conditions that lead to a desired performance.

The thesis is divided in seven Chapters. Chapter 1 gives a first introduction to the subject of the thesis and chapter 2 states the main objectives. The remaining chapters, which start by presenting the methodology adopted, discuss the results obtained. Chapter 3 deals with the evaluation of flocculation when different retention aids systems are used in distilled and in industrial water. The retention and drainage evaluation is described in Chapter 4 whereas rheological data are presented in Chapter 5. Chapter 6 deals with the modelling of the flocculation process. Results in Chapters 4, 5 and 6 are correlated with results presented previously in Chapter 3. Finally, in Chapter 7, final conclusions and recommendations for future work are summarized.

CHAPTER 3 – FLOCCULATION EVALUATION

3.1 – INTRODUCTION

After a preliminary analysis of the techniques available to follow flocculation processes, it was decided, in the present study, to select the LDS technique to monitor flocculation. In fact, the results obtained prove that LDS possesses the capability to allow an integrated evaluation of flocculants performance, by supplying, simultaneously, information on flocs size distribution, average size and mass fractal dimension, in a continuous way, as time elapses, if the equipment is pre-programmed for continuous data acquisition. Moreover, flocculation can be processed in the equipment dispersion unit in controlled turbulent conditions that can simulate adequately what is happening in the process itself.

Because of the importance of filler retention in papermaking the flocculation of precipitated calcium carbonate (commonly used as filler in the papermaking process), under turbulent conditions, has been studied as the model of flocculation process. Results obtained in order to assess the flocculation mechanism of eight different high molecular weight cationic polyacrylamides (C-PAMs) with different charge density and degree of branching, are presented and discussed in this chapter.

In a first stage, the effects of the flocculant charge density, degree of branching and concentration on the flocs size and structure and on the flocculation process itself, including flocculation kinetics and mechanism, were investigated. Moreover, zeta potential measurements have been conducted as flocculation progressed. Optical microscopy with image analysis was also used, initially, to visualize the flocs shape, at the end of the flocculation process, in order to validate the results obtained by LDS.

Then, the use of the LDS technique was extended in order to evaluate the deflocculation and reflocculation processes, when flocs are submitted either to sonication with different frequencies (mechanical forces) or to an increase of the shear forces in the recirculation tubes of the test equipment (hydrodynamic shearing) by increasing the pump speed. An assessment of flocs resistance and reflocculation capacity was carried out for all

the C-PAMs tested to evaluate the influence of the polyelectrolyte characteristics on those parameters.

It is important to note that initially, during the first stage of adapting the LDS technique to monitor flocculation processes, flocculation, deflocculation and reflocculation were first performed with three of the C-PAMs studied (A1++, BHMW and E1+) for a solid concentration of 0.02% (w/w). These preliminary results have been discussed in two papers (Rasteiro *et al.*, 2008a, 2008b) and will not be presented here. Other preliminary results have also originated a third paper (Antunes *et al.*, 2008) where the effect of the PCC characteristics on the flocculation kinetics was evaluated.

After this initial stage the flocculation, deflocculation and reflocculation processes were investigated for a solid concentration of 0.05% (w/w) in order to approach the PCC suspension concentration to the one usually found in paper industry. A solid concentration of 0.05% (w/w) in the LDS technique corresponds to around 70% obscuration. This level of obscuration was relatively higher than the range normally used in the equipment to ensure a good signal quality (5%-20%). However, it is possible to increase the PCC concentration in the equipment because during the flocculation process the obscuration rapidly decreases due to the growth of aggregate size. In this case, 70% obscuration is the maximum value that guarantees that at the end of the flocculation process obscuration is kept within the range normally used in the equipment to analyse the sample.

Results have shown that flocculant properties affect in the same manner the flocculation, deflocculation and reflocculation processes for the two PCC concentrations tested. Since flocculants of medium charge density had shown more adequate behaviours to papermaking process (confirmed by Gray and Ritchie, 2006), the polymers of high charge density were abandoned (A1++ and BHMW). Attention was then focused on the six polymers of medium charge density and of low charge density (E1, E1+, E1++++, G1, G1+ and G1++++).

Afterwards, the effect of the water ionic content on flocculation, flocs resistance and reflocculation capacity was investigated. For that, tests were performed in industrial white water using the LDS technique and the same methodology was applied to evaluate flocculation in distilled water including zeta potential measurements. In addition, the effects of the polymer concentration and of the polymer branching are also discussed. In this case, results for industrial water are compared with those obtained in distilled water. These tests were conducted only with C-PAMs of medium charge density (E1, E1+ and E1++++) since, on the one hand, flocculation experiments in white water for polymers of

high charge density gave many problems of runnability in the LDS equipment and, on the other hand, the concentrations required for the low charge density polymers were too high.

Additionally, two of the C-PAMs of medium charge density and two of the C-PAMs of low charge density were used with complex microparticulate systems. Flocculation in distilled water was monitored using the LDS technique and after breaking up the flocs, by sonication or by increasing the pump speed, the microparticles (bentonite) were added. The reflocculation capacity of those systems was investigated.

Moreover, we have compared the ability of the LDS technique to monitor the flocculation process with the FBRM technique already described in the literature to monitor the flocculation of papermaking fillers. At the Universidad Complutense of Madrid, flocculation of PCC with both the E1s and G1s polymer series was performed in the FBRM equipment. Moreover, flocs resistance and reflocculation capacity of the flocs formed were investigated, as well as the reflocculation capacity of flocs produced with complex microparticulate systems. These results were, afterwards, compared with those obtained by the LDS technique.

3.2 – EXPERIMENTAL STRATEGY

3.2.1 – MATERIALS

3.2.1.1 – Precipitated Calcium Carbonate (PCC)

In order to perform the flocculation tests, a commercial scalenohedral PCC suspension was used in this study. Before use, the supplied original PCC particles were suspended in distilled water and the suspension stocked during several days as an attempt to remove most of the additives used in the PCC production, that are present at the particles' surface. Then, the water was removed and the PCC dried to obtain a dry powder. This procedure was required to obtain a stable PCC suspension that did not change during the tests. The PCC suspensions were prepared at 1 % (w/w) in distilled water and, in order to obtain a good dispersion of the particles, the suspensions were first magnetically stirred for 20 minutes and then submitted to sonication at 50 kHz during 15 minutes. The PCC suspensions were prepared daily.

After this treatment, the median size of the particles, as obtained by LDS, was approximately 0.5 μm and the suspension pH 7.5. The zeta potential of the particles was -30 mV in distilled water. Figure 3.1 shows the size distribution of the PCC particles.

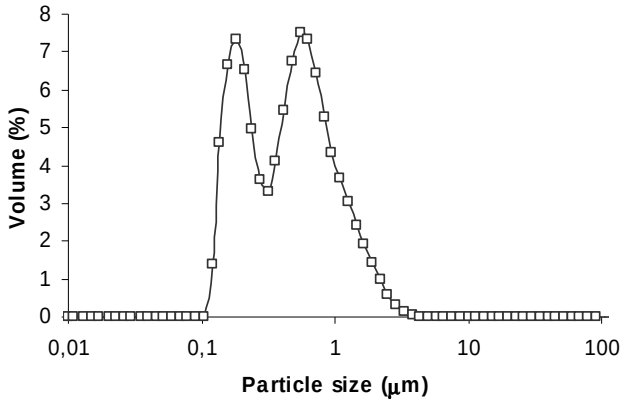

Figure 3. 1. Size distribution of the PCC particles.

3.2.1.2 – Flocculants

Eight new cationic polyacrylamide (C-PAM) emulsions of very high molecular weight, developed and supplied by AQUA+TECH, were used in this study. The main characteristics of the polyelectrolytes used are summarized in Table 3.1. The main difference between the polyelectrolytes tested is on charge density and degree of branching. The polymer content of the emulsions was approximately 40% (w/w). The cationic monomer in all the polymers is dimethylamino ethyl acrylate. Flocculant solutions were prepared with distilled water at 0.1% (w/w). In order to guarantee the effectiveness of the flocculants, the diluted solutions have to be prepared everyday.

Table 3. 1. Alpine-Floc™ properties.

Alpine-Floc™	Intrinsic Viscosity (mL/g)	Molecular weight (g/mol)	Charge density (%)	Number of Branches
G1	1200	4.6×10^6		Linear
G1+	1210	4.7×10^6	20	1
G1++++	1151	4.4×10^6		4
E1	2560	1.2×10^7		Linear
E1+	2720	1.3×10^7	50	1
E1++++	2515	1.2×10^7		4
BHMW	1720	7.2×10^6	80	Linear
A1++	1790	7.6×10^6	90	2

3.2.2 – FLOCCULATION MONITORING

3.2.2.1 – LDS technique

PCC flocculation was monitored by measuring the aggregates sizes by light diffraction scattering (LDS) using a Malvern Masterziser 2000 (Malvern Instruments) (see section 1.3.2.3). The PCC suspension was added to 700 mL of distilled water in the equipment dispersion unit until 70% obscuration (average PCC concentration around 0.05% (w/w)) and the tests were carried out setting the pump speed to 1400 rpm (312 s^{-1}). Obscuration was always kept above 5% to assure a good signal quality (Rasteiro *et al.*, 2007). Ideally, obscuration should be below 20%. However, as obscuration decreases during the flocculation test, due to floc growth, the tests are initiated with an obscuration of 70% to guarantee that, at the end of flocculation, obscuration is always higher than 5%.

Both flocculants were tested for a range of concentrations close to the optimum dosage. This optimum was previously determined following the methodology developed by Blanco and co-workers (1996). For that, the flocculant solution was progressively added to the PCC suspension as flocculation occurs. When the total added dosage is higher than the optimal one, no more aggregation takes place. Therefore, the mean aggregate size stops increasing and can even start decreasing due to steric stabilization or electrostatic repulsion. This test only gives an estimation of the optimum flocculant dosage range because the flocculant was added progressively during the test. It is, thus, necessary to found the effective optimum flocculant dosage. For that, flocculation tests where the

flocculant was added at once to the suspension were carried out for several flocculant dosages close to the optimum found by the test developed by Blanco and co-workers.

For each flocculation test, the particle size of PCC was always measured before adding the flocculant to the suspension. After that, a fixed predetermined amount of flocculant was added at once to the suspension and the flocs size distribution was measured every minute during 14 minutes, i.e., till the flocs size seemed to stabilize.

The mass fractal dimension of the flocs during the flocculation process and at the end of reflocculation was also computed offline from the scattering pattern used to determine particle size. The individual particles could be considered to follow the Rayleigh-Gans-Debye approximation (particles smaller than 1.0 μm and refractive index 1.572) (Liao *et al.*, 2005). Since secondary aggregates resulting from the aggregation of primary aggregates can be formed, the so called scattering exponent (Liao *et al.*, 2005), corresponding to the region of the larger scattering aggregates (lower diffraction angles), was also computed from the scattering pattern (see section 1.3.1.2).

The zeta potential (ζ) of the flocs was measured as well in the course of flocculation, using the Zetasizer NanoZS equipment (Malvern Instruments), at three moments: one minute after the addition of the flocculant, 7 minutes after the addition of the flocculant and at the end of flocculation (14 minutes).

Moreover, the distilled water conductivity was controlled between 5 and 8 μS/cm, since significant variations of this parameter strongly affect the flocculation process. The flocculation tests were repeated at least four times for each flocculant concentration.

For the optimal flocculant dosage, optical microscopy with image analysis (Olympus BH-2 microscope with analysSIS 2.11) was used to visualize the flocs shape, at the end of the flocculation process, in order to validate the results obtained by LDS. The mean flocs sizes were measured until 95% of confidence was reached.

3.2.2.2 – FBRM technique

Before performing flocculation tests, the optimum flocculant dosage was also determined using the Blanco's methodology (Blanco *et al.*, 1996) as described previously but, this time, in the FBRM M500LF manufactured by Lasentec (see section 1.3.2.2).

Flocculation tests were then performed for flocculant concentrations close to the optimum flocculant dosage. For that, 30 mL of the PCC suspension at 1 % was added to 120 mL of distilled water in the equipment beaker (average PCC concentration around

0.2% (w/w)). The stirring speed was set to 250 rpm. The flocculant was added at once after measuring the PCC particle size. Flocs sizes were measured every 10 seconds during 4 minutes.

3.2.3 – FLOCS RESISTANCE AND THEIR REFLOCCULATION CAPACITY

The floc resistance evaluation was performed using two different types of shear forces. The first approach was to submit the flocs to sonication at two different frequencies during 30 seconds: 10 kHz and 20 kHz. This mechanical shear force was directly applied to the suspension in the LDS dispersion unit, after flocculation. The second method involved the application of different hydrodynamic shear forces during one minute by increasing the recirculating peristaltic pump speed from 1400 rpm first to 1800 rpm and then to 2200 rpm, which corresponds to increasing the shear rate from 312 s^{-1} to 488 s^{-1} and to 708 s^{-1}, respectively. After both shearing tests, the shear force was restored to the initial value to allow the reflocculation process to take place, which was monitored during 5 minutes.

Moreover, the mass fractal dimension and the scattering exponent of the reflocculated flocs were calculated at the end of the reflocculation process.

3.2.4 – FLOCCULATION IN WHITE WATER

The industrial water used for this study is a white water from the industrial plant. The water was withdrawn from the factory always in the same conditions and for the same paper production to avoid significant variability of the water characteristics. Before use, biocide was added to the white water and the solids of the water were removed by microfiltration. The main quantifiable difference between the two waters is their ionic content and consequently, the value of the conductivity (see Table 3.2). The ionic content of the two waters was determined by Atomic Absorption Spectroscopy (AAS) and by ion chromatography. In addition, the industrial water can eventually contain other non-quantifiable materials such as colloidal materials.

The PCC suspension was prepared in the same manner as described in section 3.2.1.1 but, in this case, industrial water was used as dispersing medium. The zeta potential of the particles in white water was -37 mV.

Table 3. 2. Characterization of distilled and industrial waters.

	Ionic content (mg/g)								Conductivity	pH
Water	**Na^+**	**Ca^{2+}**	**Mg^{2+}**	**Al^{3+}**	**K^+**	**Cl^-**	**SO_4^{2-}**	**Br^-**	**(μS/cm)**	
Distilled	0.27	0.27	0.027	-	0.27	-	-	-	4-8	6.4
Industrial	87	23	5.4	0.18	2.9	62	17	3.8	569	7.7

The same methodology described in previous sections was adopted to monitor flocculation, deflocculation and reflocculation in industrial water using the LDS technique. However, flocs resistance was only evaluated submitting flocs to sonication at 20 kHz and to an increase of the pump speed from 1400 rpm to 2200 rpm.

3.2.5 – COMPLEX FLOCCULATION WITH A MICROPARTICLE SYSTEM

Flocculation tests were performed also with a microparticle systems composed by a polyelectrolyte and bentonite. The median size of the bentonite particles is 5.7 μm and the bentonite suspension was prepared at 2% (w/w) in distilled water. Bentonite was added to the PCC suspension in a concentration of 2.5 mg/g (mg bentonite/g PCC) (based on industrial plant information).

3.2.5.1 – LDS technique

When flocculation was monitored by the LDS technique, bentonite was added to the flocculated suspension after breaking up the flocs either by sonication or by increasing the pump speed as described in section 3.2.3.

Flocs were broken up after 30 seconds of the flocculation process and the bentonite was added after the initial shearing being restored. Reflocculation takes place, after that, during 15 minutes and was continuously monitored during that period.

Additionally, flocculation with the microparticulate system was also performed for flocs broken up at the end of the flocculation process (14 minutes). The bentonite was added after the initial shearing being restored. Reflocculation takes place, after that, during 7 minutes being continuously monitored during that period.

3.2.5.2 – FBRM technique

In this case, the flocs were broken up 30 seconds and 1 minute after the flocculant addition, during 1 minute and for two different stirring speeds (450 and 650 rpm). The bentonite was added at the same time as the initial stirring speed was restored. Reflocculation takes place, after that, during 3 minutes and was continuously monitored during that period.

The reflocculation process was also carried out without the bentonite addition to compare with the reflocculation process with microparticles.

3.3 – RESULTS AND DISCUSSION

3.3.1 – FLOCCULATION PROCESS

3.3.1.1 – Optimum flocculant dosage

Figures 3.2 to 3.4 show, for the eight flocculants studied, the d_{p10} and the median (d_{p50}) equivalent spherical diameters of the flocs as a function of the amount of polymer added to the PCC suspension (expressed in terms of mg of polymer/g of PCC). These tests enabled the selection of a range of flocculant concentrations for the subsequent experiments in the following section 3.3.1.2. Considering the maximum values in d_{p10} and d_{p50} curves, it was possible to define for each flocculant a range of concentration where the optimum flocculant dosage can be reached or can be close to. Depending on the flocculant, sometimes, there is a maximum for both d_{p50} and d_{p10} which are reached simultaneously. In other cases the d_{p50} reaches a plateau but the d_{p10} exhibits a clear maximum. In these situations the optimum is associated with the maximum in the d_{p10}. In fact, a decrease of the d_{p10} is an indication of the deflocculation of flocs that produces smaller flocs. Flocculants dosage ranges as determined by Blanco's methodology are summarized in Table 3.3. The effective optimum flocculant dosage corresponds to the optimum flocculant dosage determined by LDS when a fixed predetermined amount of flocculant was added at once to the suspension.

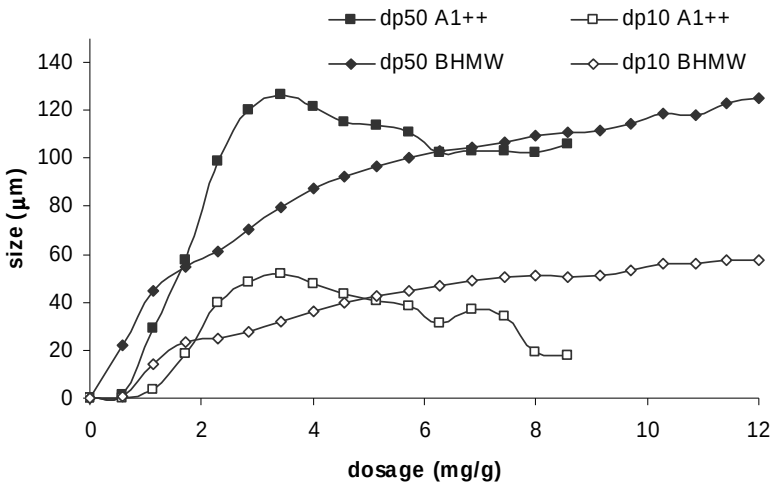

Figure 3. 2. Optimum flocculant dosage for A1++ and BHMW.

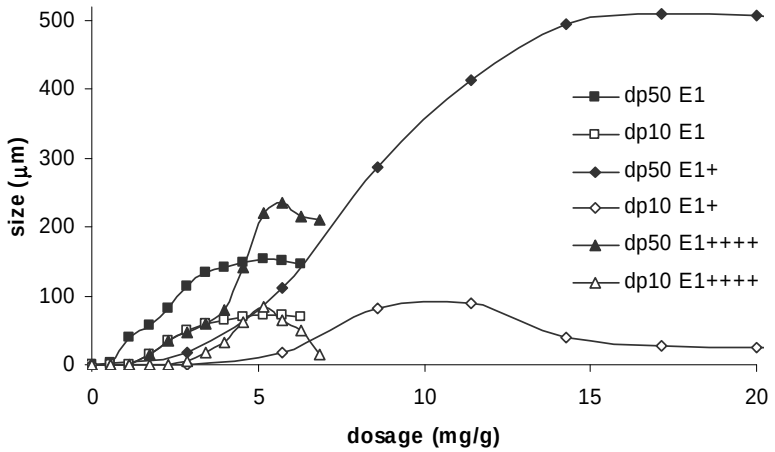

Figure 3. 3. Optimum flocculant dosage for E1, E1+ and E1++++.

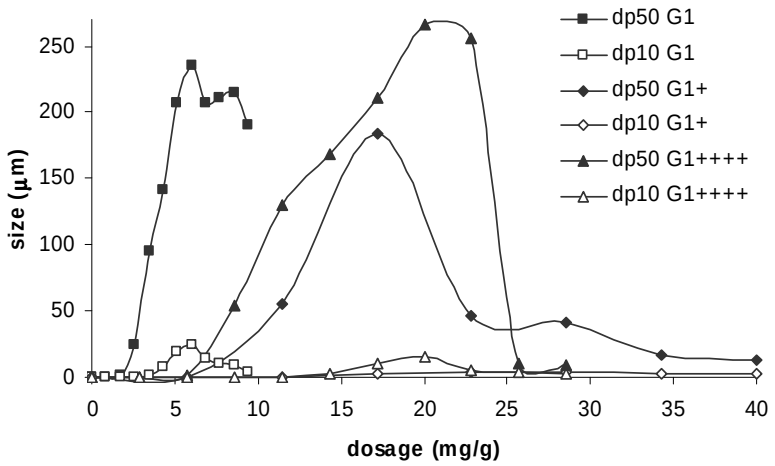

Figure 3. 4. Optimum flocculant dosage for G1, G1+ and G1++++.

Table 3. 3. Flocculant dosage range and effective optimum flocculant dosage.

	A1++	**BHMW**	**E1**	**E1+**	**E1++++**	**G1**	**G1+**	**G1++++**
Dosage range (mg/g)	3-5	6-10	4-6	10-16	4-7	4-7	15-20	20-25
Effective optimum dosage (mg/g)	4	6	4	12	8	10	30	30

From the results of Table 3.3, it can be seen that the optimum flocculant dosage will be dependent on the charge density and on the degree of branching of the polymer.

3.3.1.2 – Flocculant dosage effect

Considering the flocculant concentration ranges defined in the previous section, several flocculation tests were carried out to found the effective optimum flocculant dosage for each polyelectrolyte following the methodology described in section 3.2.2.1. The optimum flocculant dosage in this study was taken as the dosage that gives the largest flocs with fast flocculation kinetics. After defining the optimum flocculant dosage (Table 3.3), flocculation was monitored for this flocculant dosage and also for a lower and a higher flocculant concentration. However, for A1++ and BHMW, flocculation was only monitored for the optimum and for a higher flocculant dosage since, after preliminary studies in a PCC suspension with a concentration of 0.02% (w/w), it was concluded that these flocculants are not adequate to papermaking. Figures 3.5 to 3.12 illustrate the flocculation process carried out for the eight flocculants, in terms of the evolution of the floc median size with time, as a function of polymer concentration. In addition, the deflocculation and reflocculation processes are also presented since the LDS technique allows evaluating simultaneously, in a single test, the three processes. Flocs resistance and reflocculation will be discussed in sections 3.3.2 and 3.3.3.

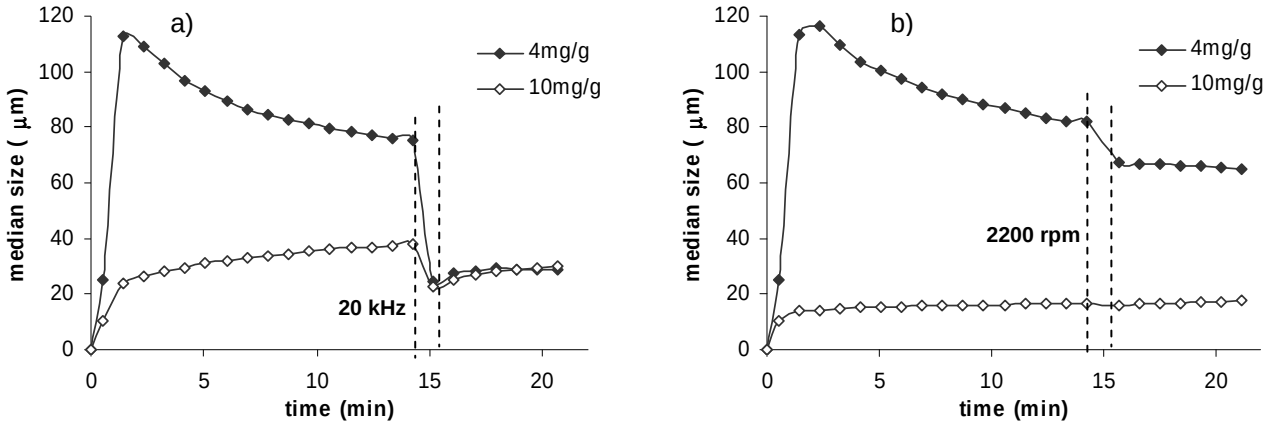

Figure 3. 5. Flocculation, deflocculation and reflocculation with A1++ when flocs are submitted to a) sonication at 20 kHz, b) increase of pump speed to 2200 rpm.

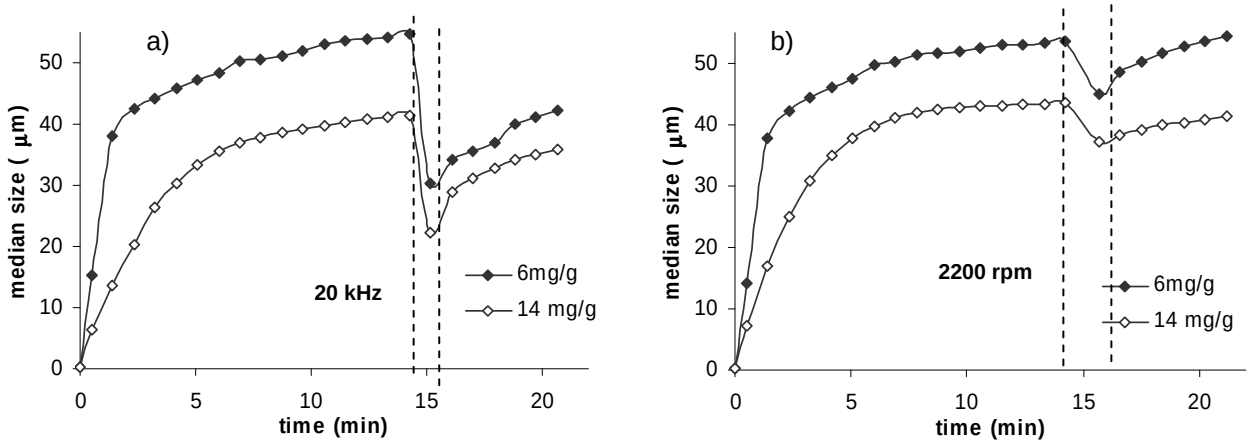

Figure 3. 6. Flocculation, deflocculation and reflocculation with BHMW when flocs are submitted to a) sonication at 20 kHz, b) increase of pump speed to 2200 rpm.

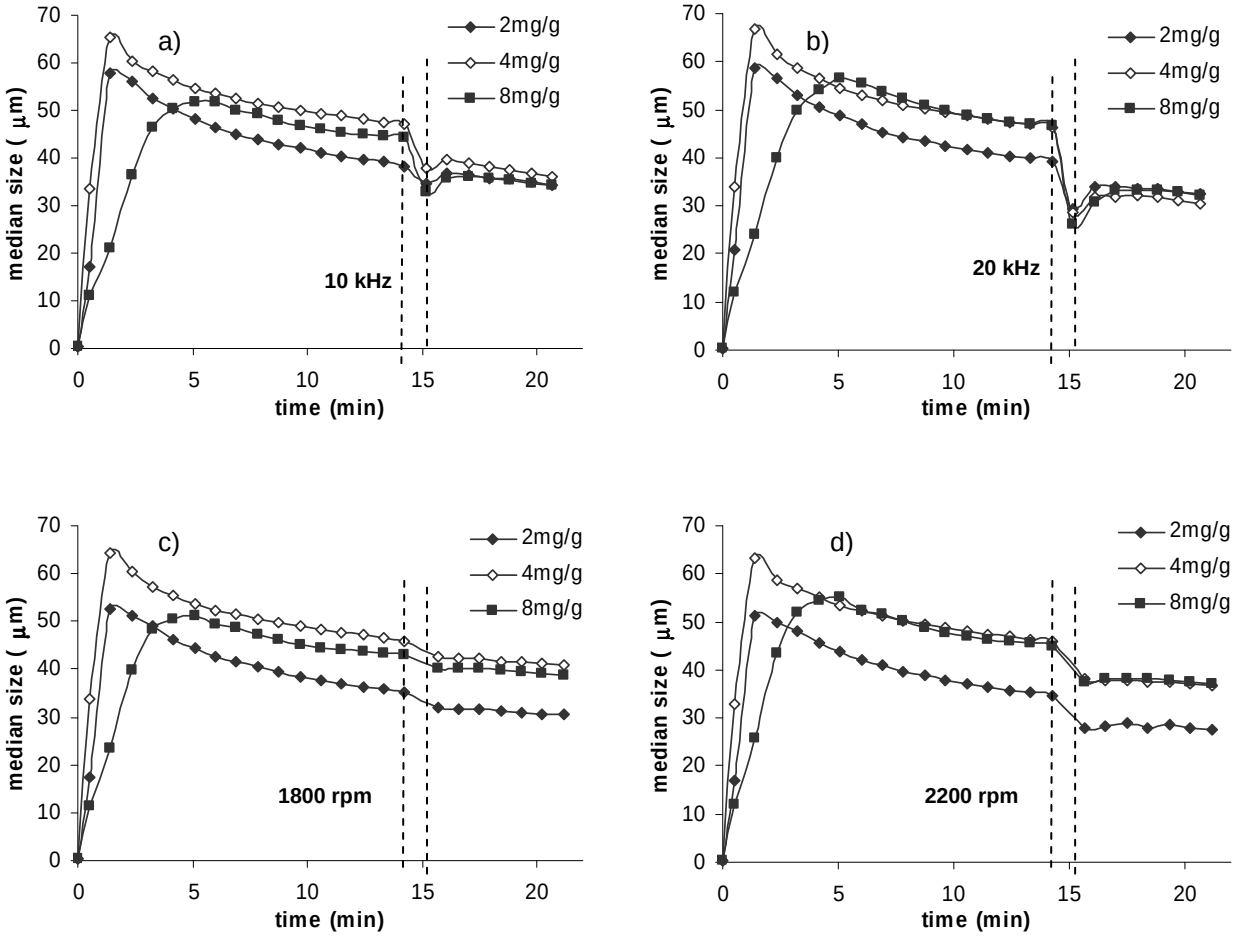

Figure 3. 7. Flocculation, deflocculation and reflocculation with E1 when flocs are submitted to sonication at a) 10 kHz, b) 20 kHz and increase of the pump speed to c) 1800 rpm, d) 2200 rpm.

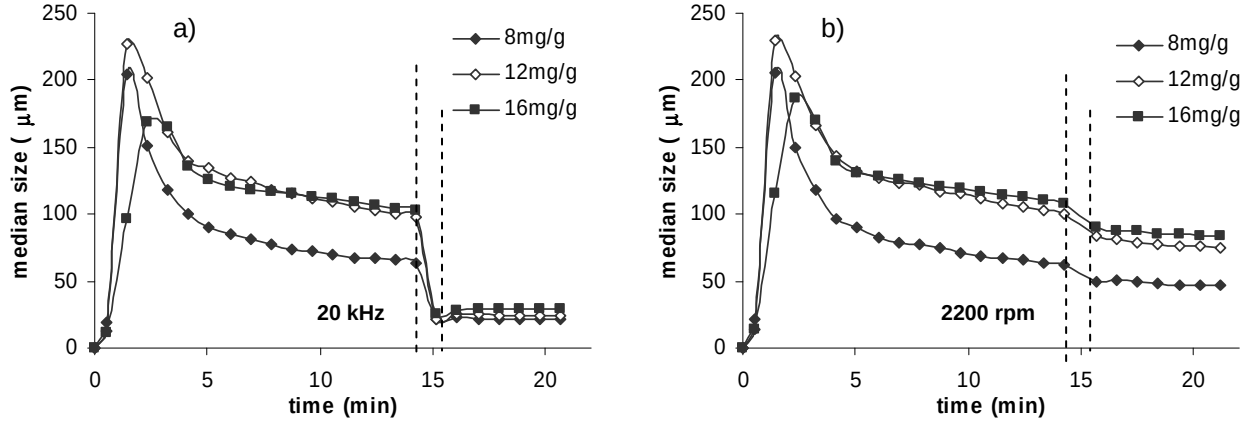

Figure 3. 8. Flocculation, deflocculation and reflocculation with E1+ when flocs are submitted to a) sonication at 20 kHz, b) increase of pump speed to 2200 rpm.

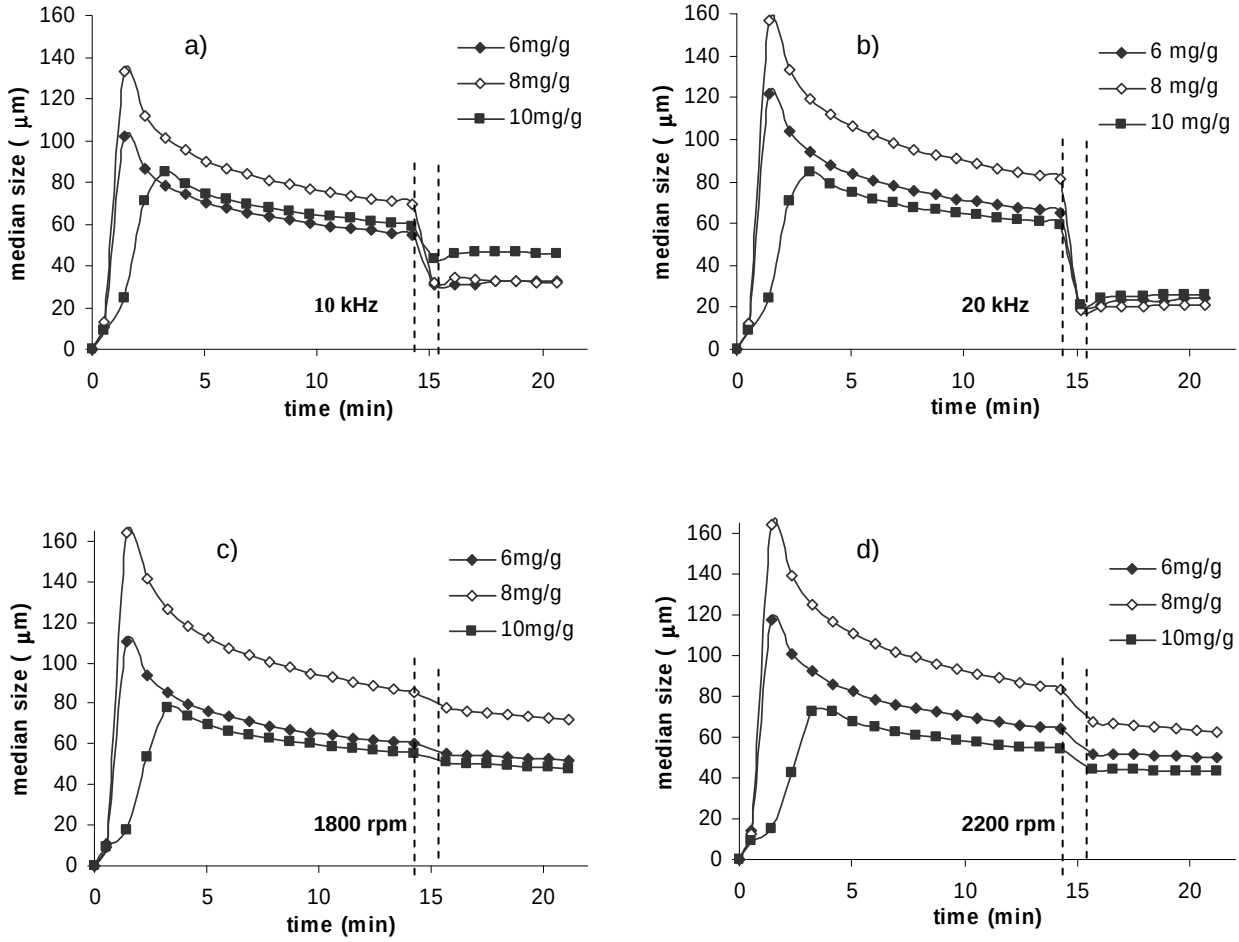

Figure 3. 9. Flocculation, deflocculation and reflocculation with E1++++ when flocs are submitted to sonication at a) 10 kHz, b) 20 kHz and increase of the pump speed to c) 1800 rpm, d) 2200 rpm.

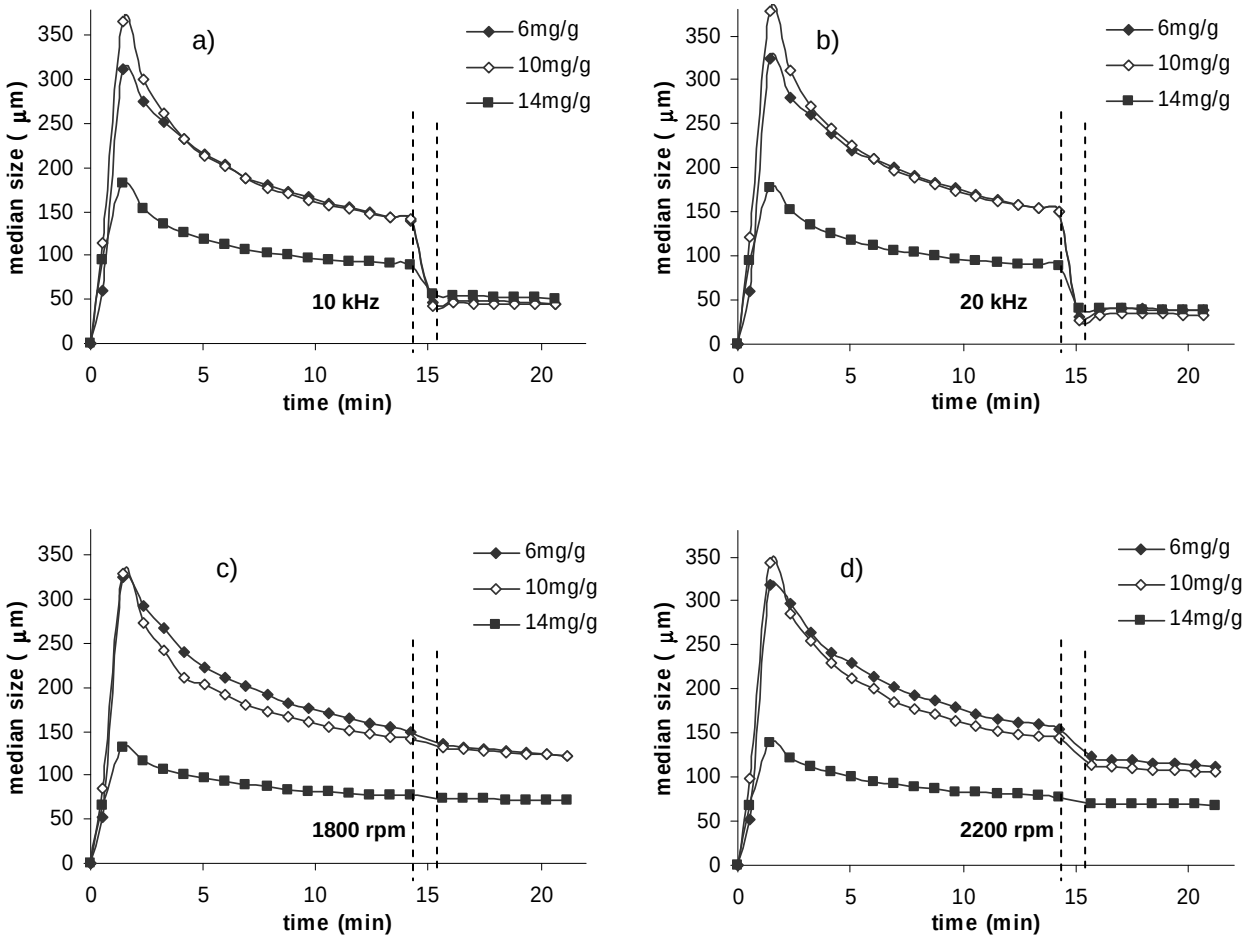

Figure 3. 10. Flocculation, deflocculation and reflocculation with G1 when flocs are submitted to sonication at a) 10 kHz, b) 20 kHz and increase of the pump speed to c) 1800 rpm, d) 2200 rpm.

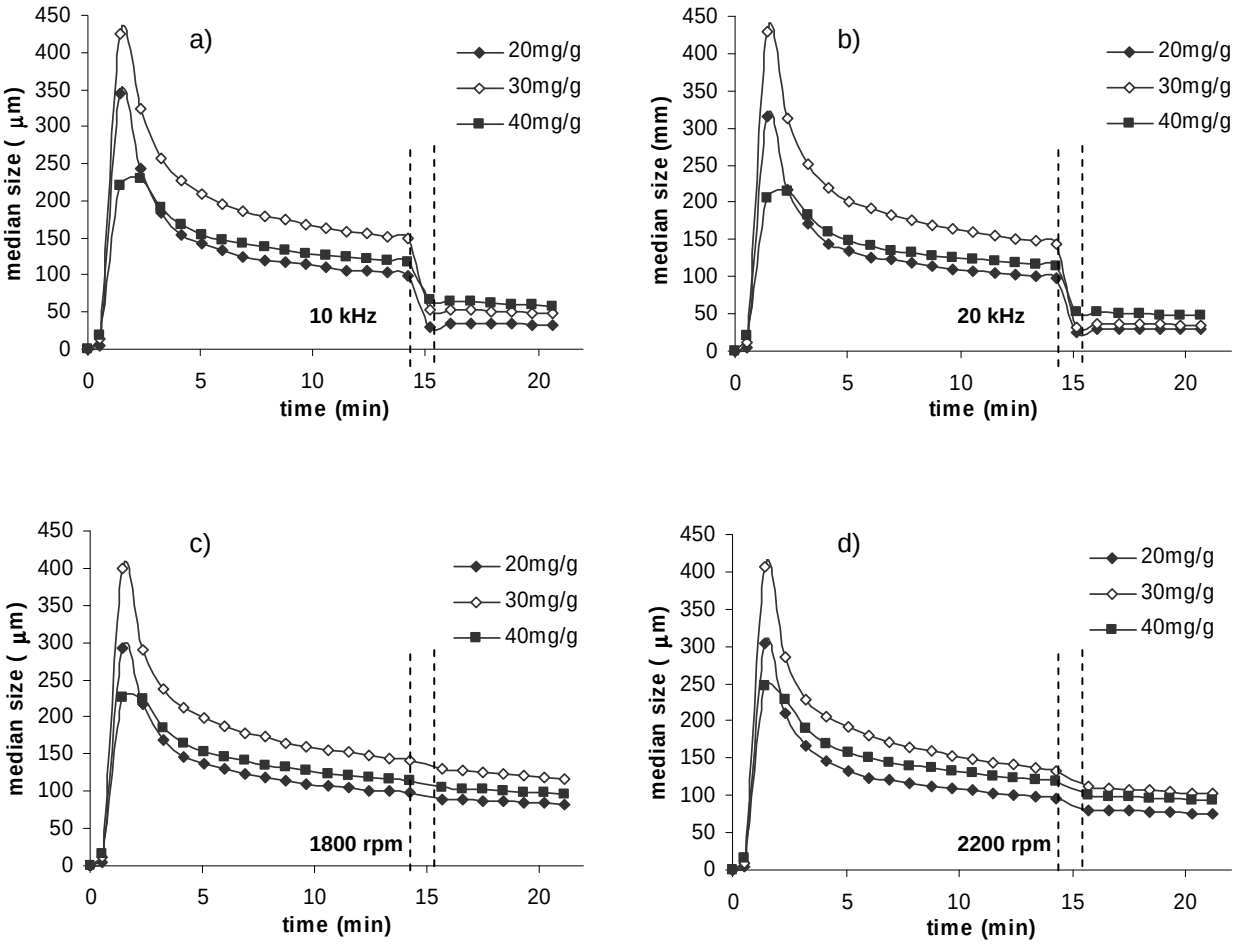

Figure 3. 11. Flocculation, deflocculation and reflocculation with G1+ when flocs are submitted to sonication at a) 10 kHz, b) 20 kHz and increase of the pump speed to c) 1800 rpm, d) 2200 rpm.

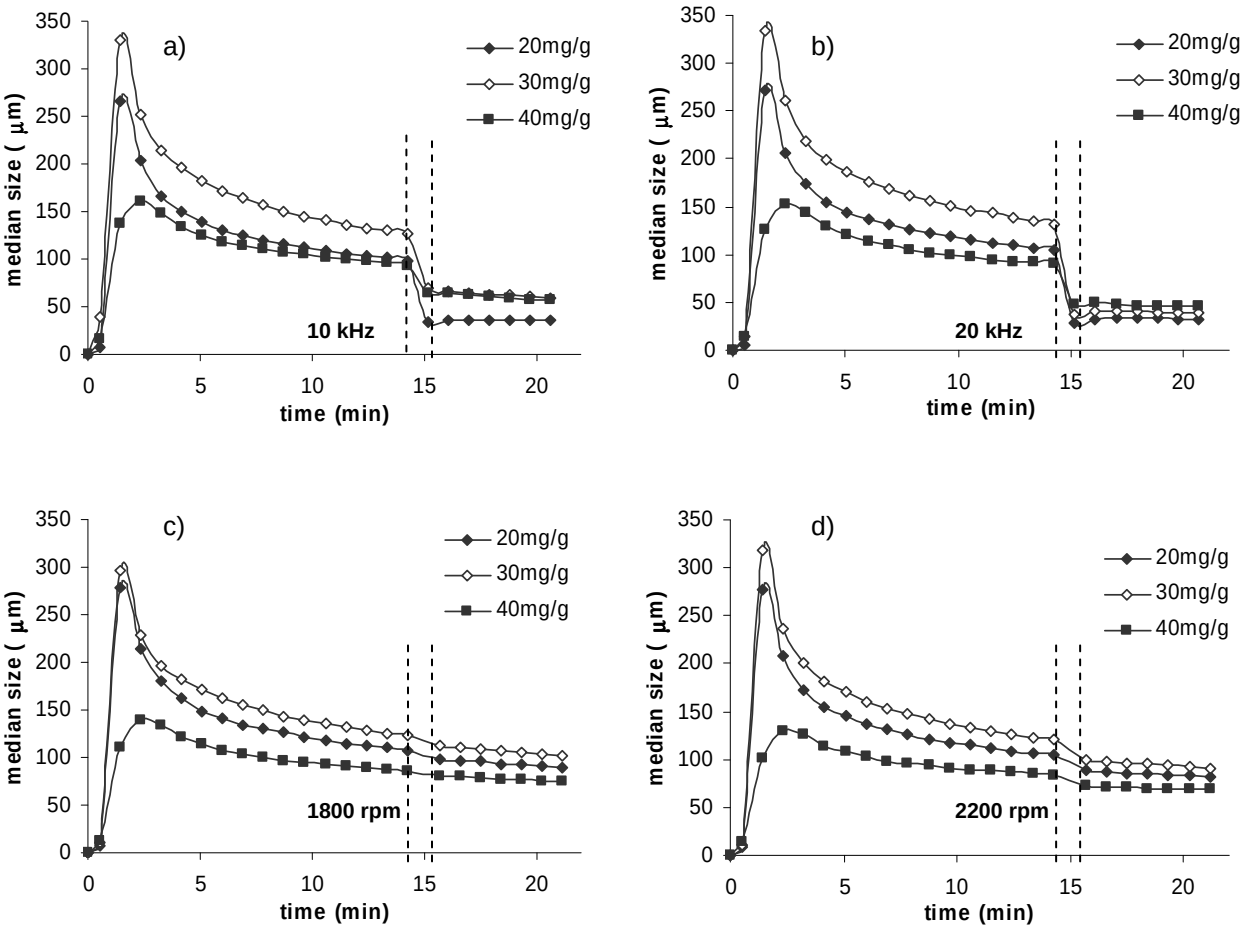

Figure 3. 12. Flocculation, deflocculation and reflocculation with G1++++ when flocs are submitted to sonication at a) 10 kHz, b) 20 kHz and increase of the pump speed to c) 1800 rpm, d) 2200 rpm.

As expected, flocculation rate decreases as the flocculant concentration increases, above the optimum, for all the polymers. Since the stirring speed is the same for all the tests, this decrease can be explained by the diffusion-controlled adsorption kinetics model, in such a way that the higher the amount of polymer, the lower the polymer adsorption rate on the particle surface (Tadros, 2005). Therefore, the equilibrium point is reached more rapidly when the flocculant concentration is lower and, as a consequence, the final flocs size is reached earlier. At high dosages, floc size increases very slowly due to the excess of polymer dosage that increases the repulsive forces between particles.

If the amount of flocculant added is lower than the optimum flocculant dosage the flocs sizes are smaller because the efficiency of the primary particles collisions is lower reducing the flocs size. When the polymer is in excess, flocs size is also smaller than at the

optimum flocculant dosage but, in this case, due to steric stabilization or electrostatic repulsion.

Moreover, the shapes of the kinetics curves observed in Figures 3.5 to 3.12 are different. In fact, the flocculation kinetics depend on the flocculants characteristics and this will be discussed in more details in the following sections. In the case of the medium and low charge density polymers the flocs size decreases after reaching a maximum due to polymer reconformation (see section 3.3.1.3) and the degree of polymer reconformation is also conditioned by the polymer concentration as will be referred later in the next section 3.3.1.3. Indeed, at high flocculant concentration, polymers re-arrange slowly on crowded surfaces because neighbouring molecules interfere with the re-arrangement (van de Ven and Alince, 1996b; Biggs *et al.,* 2000), and thus, the degree of polymer conformation is lower.

3.3.1.3 – Flocculant charge density effect

The flocculant charge density affects mainly the flocculation mechanism. In fact, from Figures 3.5 to 3.12, two flocculation trends can be identified. For the BHMW polymer, the flocs grow progressively until reaching a steady-state, whereas for the A1++ polymer and the E1 and G1 polymer series, the floc size increases with time up to a maximum and decreases, thereafter, due to aggregate restructuring and/or to break up of the flocs formed. The first behaviour is typical of the flocculation induced by polymers of high charge density as it is the case of BHMW. When the polymer charge density is high there is a tendency for the polymer chains to adopt a flatter reconformation on the particle surface. As the charge density decreases, the polymer chain adsorbs at the particle surfaces forming tails and loops that extend far beyond the surface and interact easily with other particles. In this case, flocculation occurs by the bridging mechanism. After aggregation, the polymer chains can rearrange at the particle surface. This reconformation process results in flocs restructuring that is identified by a flocs size decrease during flocculation as in Figures 3.7 to 3.12, and most certainly a compaction of the flocs as will be discussed later. Hence, the E1 and G1 polymers series, which are polymers of medium to low charge density, flocculate the particles by bridging mechanisms. This effect is more pronounced when charge density decreases.

The decrease of the zeta potential values described in Figures 3.13b and 3.13c confirms that reconformation of the polymer chains occurs during flocculation. However, A1++ is a polymer of high charge density with a flocculation trend similar to the one of the medium charge density. This is due to the fact that, in this case, the polymer has got a branched structure that reduces its capability to adopt a flat conformation on the particle surface and, because it has a very high molecular weight, the capacity to form patching bonds is reduced. The intermediate configuration of the polymer in this case, allows the polymer chains to rearrange on the particle surface but to a lower degree, in agreement with the low decrease of the flocs size in Figure 3.5 and the decrease of the zeta potential in Figure 3.13a during the flocculation process.

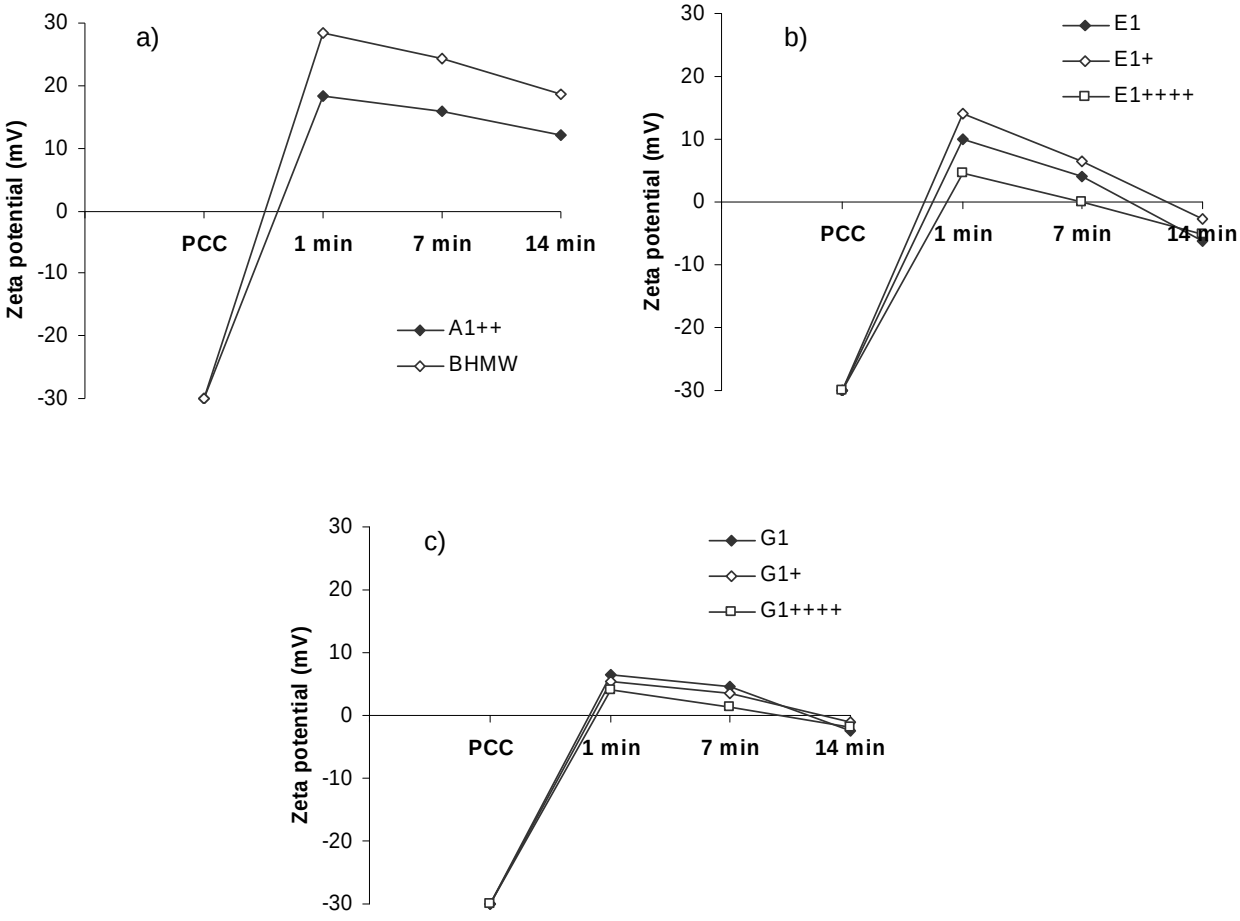

Figure 3. 13. Zeta potential at different stages of the flocculation process for the optimum dosage a) A1++, BHMW, b) E1, E1+, E1++++ and c) G1, G1+, G1++++.

Moreover, the zeta potential values for BHMW polymer also slightly decrease during flocculation (Figure 3.13a) indicating that, despite this polymer having a high

charge density, reconformation does also occur to some extent. Here, the very high molecular weight of the polymer has to be considered in the same manner again as for the A1++ polymer. Indeed, the patching mechanism normally occurs when polymers have both high charge density and a low molecular weight. Hence, for the BHMW polymer, the capacity to form patching bonds can be affected due to the molecular weight but that reduction is small enough so that it does not influence the flocculation kinetics. For the A1++ and BHMW polymers, patching and bridging bonds are probably present simultaneously during flocculation process due to their very high molecular weight.

From Table 3.3, the optimum flocculant dosage is also dependent on the charge density. There is a tendency for the optimum flocculant dosage to increase with the decrease of the polymer charge density. This agrees with the flocculation mechanisms that occur. Indeed, as the charge density increases the polymer chain can adopt a flatter conformation at the particle surface, and thus, each polymer molecule covers a larger area of the particle surface. Consequently, for polymers of high charge density the amount of polymer to reach the optimum surface coverage is lower. This is confirmed by the zeta potential measurements (Figure 3.13) where it can be observed that at the beginning of flocculation (just one minute after flocculant addition), the zeta potential decreases as the charge density of the polymer decreases. In fact, the PCC particles, initially negatively charged (-30 mV), become positively charged with the addition of flocculant due to the cationic character of the polyelectrolytes.

However, for the flocculants studied, this parameter cannot be used to determine the optimum flocculant dosage since it does not allow assessing neither the mechanism nor the kinetics of the flocculation process.

It can be also observed that the polymer charge density not only affects the flocculation kinetics but also the flocs properties, namely the flocs size and the flocs structure. Table 3.4 summarizes the median flocs sizes at the maximum in the kinetic curve (if it exists) and at the end of the flocculation process, for the optimum flocculant dosage and for all the polymers studied.

Table 3. 4. Median flocs size at the maximum and at the end of flocculation kinetics curve for the optimum flocculant dosage.

	d_{p50} (μm)		
Alpine-Floc™	**Max. of kinetic curve**	**End of flocculation**	**Restructuring (%)**
A1++	113	80	29
BHMW	-	55	-
E1	65	47	28
E1+	228	99	57
E1++++	165	83	49
G1	370	147	60
G1+	427	145	66
G1++++	332	129	61

There is a tendency to produce larger flocs as the polymer charge density decreases. In fact, the polymer conformation at the particle surface mainly depends on the charge density. If the polymer adopts a flat configuration at the particle surface, the distance between particles in the aggregate will be smaller than if the polymer adsorbs at the particle surfaces forming tails and loops that extend far beyond the surface. On the other hand, a polymer chain that extends far beyond the particle surface can adsorb more easily at the surface of other particles when collision occurs. As a result, the distance between the particles is higher and, additionally, the aggregates contain a larger number of single particles when polymers of low to medium charge density are used.

Furthermore, mass fractal dimension and scattering exponent were calculated at the maximum and at the end of flocculation kinetics curve from the light scattering patterns for all the experiments. Those values are presented in Table 3.5. The scattering exponents were calculated because, as discussed before, there is restructuring of the flocs due to polymer rearrangement during flocculation, and thus, secondary flocs are formed from the aggregation of primary flocs as described in the examples of Figure 3.14. This implies that the Rayleigh-Gans-Debye theory is no longer valid and, therefore, the scattering exponent rather than the fractal dimension has to be calculated to describe the fractal nature of the aggregates, as discussed in section 1.3.1.2.

The flocs size distribution was determined using the Mie theory and a very good agreement of the fitting of data with the optical model was found, as can be seen in the

example of Figure 3.15. This agreement confirms the accuracy of the LDS technique and of the scattering model used.

Table 3. 5. Mass fractal dimension and scattering exponent of flocs.*

Alpine-Floc™	**Dosage (mg/g)**	**Max. of kinetic curve**		**End of flocculation**	
		d_F	**SE**	**d_F**	**SE**
A1++	4	1.34	2.27	1.32	2.32
	10	-	-	1.60	2.22
BHMW	6	-	-	1.36	2.56
	14	-	-	1.46	2.43
E1	2	1.45	2.19	1.54	2.55
	4	1.33	2.36	1.54	2.47
	8	1.48	2.48	1.51	2.55
E1+	8	1.36	2.05	1.59	2.51
	12	1.13	1.37	1.54	2.56
	16	1.12	1.48	1.49	2.39
E1++++	6	1.53	1.74	1.57	2.45
	8	1.46	1.61	1.52	2.33
	10	1.31	1.97	1.49	2.37
G1	6	1.62	1.72	1.48	2.59
	10	1.52	1.50	1.19	2.44
	14	1.44	2.12	1.21	2.58
G1+	20	1.65	1.67	1.62	2.49
	30	1.57	1.51	1.35	2.43
	40	1.34	1.93	1.21	2.46
G1++++	20	1.62	1.47	1.62	2.49
	30	1.63	1.34	1.42	2.43
	40	1.34	2.06	1.29	2.58

* grey lines refer to the optimum flocculant dosage

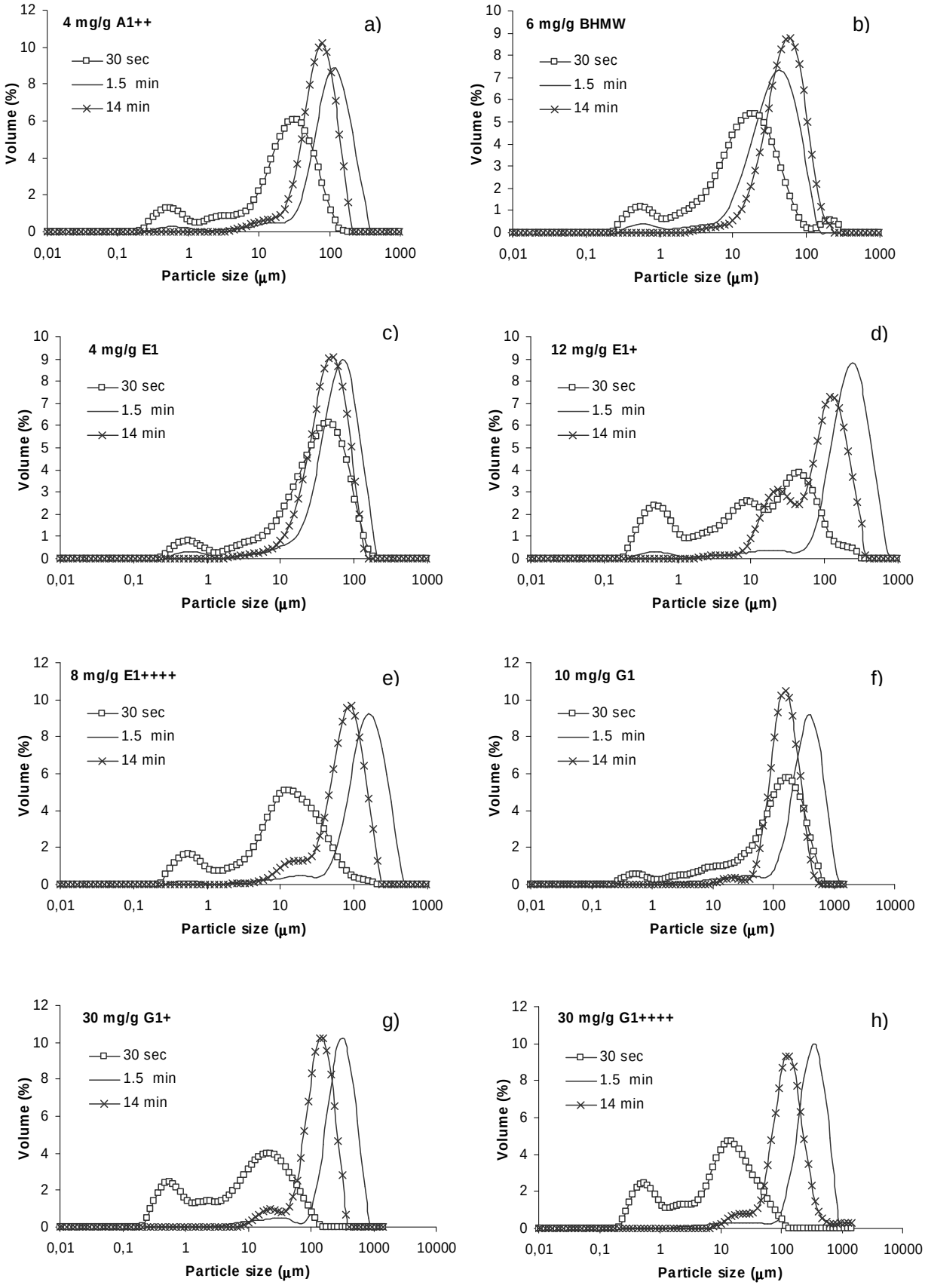

Figure 3. 14. Flocs size distribution evolution during flocculation for the optimum flocculant dosage of a) A1++, b) BHMW, c) E1, d) E1+, e) E1++++, f) G1, g) G1+and h) G1++++.

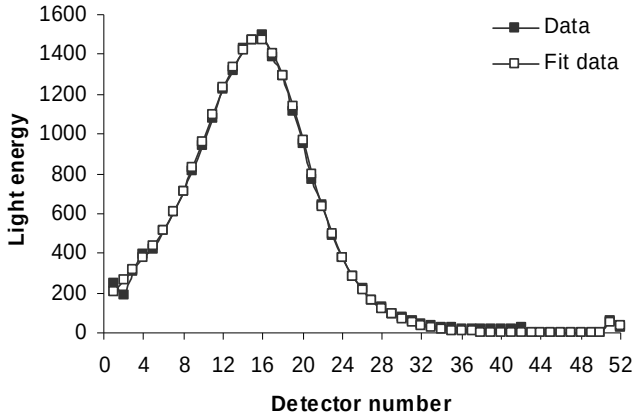

Figure 3. 15. Scattering pattern data and fitting curve based on the Mie theory at the end of flocculation for 4 mg/g of E1.

In addition, Figure 3.14 shows that, effectively, the decrease in the flocs sizes during flocculation is mainly due to the reconformation of the polymer at the particles surface even if a small amount of flocs are broken up during this phase.

In general, both d_F and *SE* values decrease as the flocculant dosage increases, mainly at the end of the flocculation process. This indicates that the flocs become more open with the increase of the flocculant concentration. Indeed, at low concentration, polymers rearrange relatively fast but, on the contrary, rather slowly on crowded surfaces, since neighbouring molecules interfere with the rearrangement (van de Ven and Alince, 1996b; Biggs *et al.*, 2000). Hence, at high flocculant concentrations, the degree of polymer reconformation is lower, the distance between the particles increasing, and thus, producing more porous flocs.

Comparing d_F and *SE* results obtained for the optimum flocculant dosage (indicated by the grey background in the Table 3.5), the E1 polymers series produces, in general, flocs denser than those obtained with the G1 polymers series. Hence, as the flocculant charge density increases the flocs become denser. This agrees with the fact that the distance between particles increases as the charge density decreases as discussed previously. However, for the A1++ polymer, this behaviour is not followed. In this case, despite the polymer having a high charge density, flocs produced are open probably due to the presence of the branches that inhibits the polymer adsorption in a flat configuration.

Moreover, in general, flocs are less compact (*SE* is smaller) at the maximum in the kinetic curve where flocs produced are larger. At the end of flocculation, flocs are more

compact (*SE* is higher) than at the maximum in the kinetic curve due to restructuring of polymer chains. This is more notorious for the secondary aggregates.

3.3.1.4 – Flocculant branching effect

As seen in the previous section, the branches of A1++ polymer affect the flocculation kinetics and the flocs structure. The same happens with the G1 and E1 polymers series where the degree of branches varies from zero to four. Regarding flocculation results obtained only for the E1 and G1 series, several effects of polymer branching can be identified.

Comparing results obtained for the E1 polymer series, reconformation is less evident in the cases of both the linear (E1) and the highly branched polymer (E1++++) (see Table 3.4). In fact, for the linear polymer, flocculation kinetics was faster. Moreover, the amount of polymer necessary to perform flocculation was lower (see Table 3.3). During the first seconds of the flocculation the polymer adsorbed at the particle surface in a flat configuration and, under these conditions, the polymer chain has got less space for reconformation than in the case of the branched polymers. For the highly branched polymer (E1++++), the radius of gyration of the polymer (hydrodynamic size of the polymer chain) is smaller than in the linear ones and reconformation becomes also more difficult (Huang *et al.*, 2000). In fact, for a constant molecular weight, as the number of branches increases, the polymer radius of gyration decreases (Huang *et al.*, 2000).

Furthermore, the polymer structure also affects the flocs size at the maximum in the flocculation curve as described in Table 3.4. The larger flocs were produced by the low branched polymer (E1+). A linear relationship between the flocs size and the polymers branching degree does not exist probably due to the reasons explained before (kinetics and polymer conformation). It is reasonable to assume that flocs size and polymer structure must be related. Therefore, since the linear polymer adsorbs in a flatter configuration at the particle surface, the space between particles is small and smaller flocs are obtained. In the case of the highly branched polymer, the space between particles is also small but now due to the smaller polymer radius of gyration. That is, there are different factors related with the polymer characteristics that condition the flocs size.

The trends detected in Table 3.5 reinforce the conclusion that the degree of branching of the polymer affects the flocculation process and the flocs structure. Indeed, comparing results obtained for the optimum flocculant dosage and for the E1 polymer

series, both the mass fractal dimension and scattering exponent at the maximum in the kinetic curve indicate that flocs produced with E1 and E1++++ have a denser structure. This agrees with what was observed before in relation with flocs size. Moreover, the larger E1++++ flocs have got a more open structure than flocs produced with E1 (d_F and *SE* are lower for E1++++ than for E1).

At the end of flocculation, the differences in the d_F values are small probably due to flocs restructuring. However, comparing results for the optimum flocculant dosage, the scattering exponent value is higher for flocs produced with E1+ and lower for flocs produced with E1++++. Furthermore, the increase in d_F and *SE* during flocculation is small for both E1 and E1++++ confirming that the polymer reconformation is less extensive. Thus, extensive polymer reconformation can lead to denser flocs even if those flocs were, in the initial stages of flocculation, more open due to the type of aggregation mechanism prevailing (mainly bridging). Additionally, in the case of E1++++ the flocs structure is much more open at the maximum in the kinetics curve than for E1 and, thus, the degree of flocculant reconformation was not enough to reach the same degree of compactness at the end of flocculation, as that obtained with E1.

Regarding the different values for the optimal concentration for the three polymers, the larger difference can be found between the linear and the branched polyelectrolytes. In fact, as mentioned before, the linear polymer tends to acquire a flatter configuration on the particles surface, and thus, coverage is obtained with a smaller dosage of polymer. In the case of both E1+ and E1++++ the dosage necessary is higher, being smaller for E1++++ than for E1+. The higher number of branches in the chain of E1++++, though giving rise to a lower radius of gyration, can also lead to a more even distribution of the charges and therefore an easier attachment of the polymer to the particles. This is why the dosage is slightly lower than the one of E1+. Even though bridging being also the predominant mechanism in the case of E1++++, polymer chains do not protrude so much from the particle surface and, because of what was just referred, will tend to have again a flatter configuration on the particle surface than the one occurring with E1+. This agrees with the more open structure of the E1+ aggregates, at the maximum of the kinetics curve as discussed above.

Concerning the results obtained for the G1 polymer series, it is more difficult to identify the same trend observed with the E1 polymer series. In fact, the effect of the branching degree on the flocs structure and size is less notorious as described in Tables 3.4 and 3.5. Since the polymer chain with a low charge density is attached to the particles in

few sites, the space between particles is probably high enough for branching not affecting flocculation kinetics and flocs characteristics. Still, the main difference is on the optimum dosage which is lower for the linear polymer (see Table 3.3).

3.3.1.5 – Validation of the LDS technique using the image analysis technique

As referred before selecting LDS to monitor the flocculation process, a preliminary with optical microscopy was performed. From Table 3.6 it may be concluded that LDS and optical microscopy with image analysis, although being different techniques, give similar results for the median size of the flocs. However, it should be emphasized that, besides being laborious and time consuming image analysis considers just a few particles (between 100 and 120 for the samples analysed) and, thus, the sample is always less representative than the one tested in LDS. Moreover, it does not allow us obtaining kinetics curves.

Table 3. 6. Median flocs size calculated from LDS and image analysis techniques.

Alpine-Floc™	**d_{p50} by LDS (μm)**	**d_{p50} by image analysis (μm)**
A1++	70	68
BHMW	53	51
E1+	103	98
E1++++	76	75

3.3.1.6 – Comparison with the FBRM technique

Figure 3.16 shows, for the E1, E1+ and E1++++ polymers, the weighted mean square diameters of the flocs as a function of the amount of polymer added to the PCC suspension in the FBRM equipment in order to define also the optimal polymer concentration range. The weighted mean square was selected from all the parameters that the FBRM supplies because these values, calculated according to Equation 3.1, are the closest to the values calculated by the LDS technique since, as in LDS, it is the area of the particle or aggregate that is taken in consideration. In Equation 3.1 n_i is the number of counts in the size class *i*, n_T is the total number of counts in all the size ranges and *l* is the mean chord length in the size class *i*. As for LDS, these tests enabled the selection of a range of flocculant concentrations for the subsequent flocculation experiments.

$$Mean\ sqr = \sum_{i=1}^{k} \left(\frac{n_i / n_T \times (l_i)^2}{\sum n_i / n_T \times (l_i)^2} \times l_i \right) \tag{3.1}$$

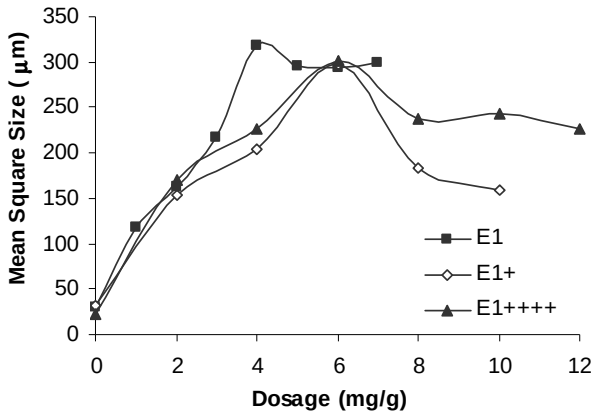

Figure 3. 16. Optimum flocculant dosage for E1, E1+ and E1++++ with the FBRM technique.

FBRM measurements were also performed for G1, G1+ and G1++++ but, unfortunately, they can not be presented. Indeed, with these flocculants many problems appeared, namely problems of result reproducibility. As seen with the LDS results, the polymers of low charge density produce large flocs and require high flocculant concentrations. Since in the FBRM equipment the concentration of the PCC suspension is higher than in the LDS equipment, the adhesion of the flocs to the wall beaker and to the window of the equipment is much more pronounced resulting in a drastic decrease of the signal quality. Moreover, when flocs are submitted to the increase of the stirring speed, flocs break up is very small and flocs size can even increase. This is an indication of the detachment of the flocs from the wall of the beaker, which leads to an increase of the signal quality, and thus, the flocs size measured is larger instead of being smaller during the break up stage.

Figure 3.16 indicates that the optimum flocculant dosage is lower for E1 than for E1+ and E1++++ that exhibit an optimum flocculant dosage very similar. Hence, the optimum flocculant dosage for E1 will be close to 4 mg/g and for E1+ and E1++++ close to 6 mg/g. Then, flocculation tests were performed around these flocculants concentration to define the effective optimum flocculant dosage. In this way, the optimum dosage found for E1 was 4 mg/g, for E1+ was 10 mg/g and for E1++++ was 8 mg/g. These results agree well with the results obtained by LDS (Table 3.3). Indeed, the optimum flocculant dosages found by FBRM are close to the ones found by LDS. This indicates that the concentration

of the PCC suspension has only a minor effect on the optimum flocculant dosage. Moreover, the optimum flocculant dosage was lower for the linear polymer than for the branched polymers On the other hand, despite the results obtained for the G1 polymer series not being represented, the high flocculant concentration necessary to flocculate the suspension confirms that polymers of low charge density flocculate for higher dosages than polymers of medium charge density agreeing with LDS results.

Figure 3.17a shows the comparison of the flocculation kinetics curve obtained for the E1, E1+ and E1++++ polymers in terms of the mean square for the optimum flocculant dosage. As noted by LDS, flocculation kinetics for the linear polymers (E1) is faster than for the branched polymers. However, FBRM measurements did not allow verifying differences on the flocs size between the flocculants used. Hence, FBRM measurements do not allow, in this case, detecting the influence of the polymer structure on the flocculation process. In fact, in the FBRM equipment, the turbulence and the concentration of the suspension is higher than in the LDS equipment. Thus, the collision between particles is very high and reconformation of the polymer is very fast. As a result, aggregation and aggregates reorganization due to polymer reconformation are very fast, and thus, flocs stabilize earlier than in the LDS equipment. In this case, flocs reach a stable structure for times lower than one minute while with LDS this time is higher than two minutes.

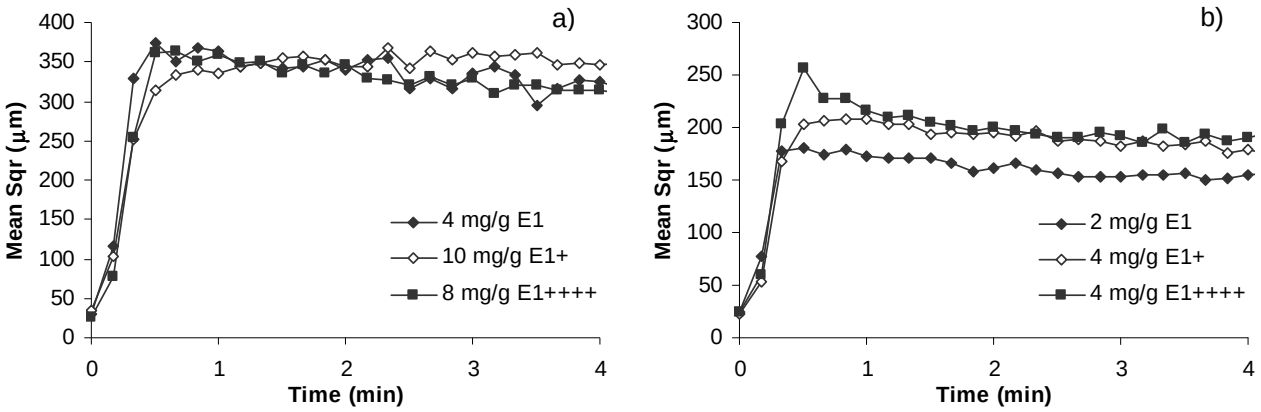

Figure 3. 17. Flocculation process in the FBRM studied for E1, E1+ and E1++++ for a) the optimum flocculant dosage and b) lower flocculant dosage.

Figure 3.17b illustrates the flocculation kinetics for the lowest flocculant concentration studied. Tests were performed for a concentration of 4 mg/g except for E1 for which flocculation was performed for 2 mg/g since the optimum flocculant

concentration for this flocculant is 4 mg/g. As expected the flocs size is smaller when the flocculant concentration is lower than the optimum one and flocculation kinetics is slower.

Figure 3.18 is an example of the evolution of the measured number of counts in the FBRM during the flocculation process. Comparing this curve with the flocculation kinetics observed in Figure 3.17, just after adding the flocculant an increase in the flocs size corresponds to an increase of the number of counts. This is contradictory since an increase in the flocs size indicates the aggregation of the PCC particles, and thus, a decrease of the number of counts. As measured by the LDS technique, the median size of the PCC particles is about 0.5 μm. The FBRM technique is not able to detect the smaller PCC particles because the limit of detection of the equipment is 0.5 μm and, therefore, the number of counts increases, initially, when more particles become visible to the FBRM detector by forming aggregates larger than 0.5 μm. In fact, comparing the particle size distribution of the PCC particles obtained in LDS (Figure 3.1) with that obtained by FBRM (Figure 3.19), the median size of the PCC particles by the FBRM is much larger than that measured by LDS. Consequently, the signal, and thus, the measurements of the first points of the kinetics curve can not be considered representative and accurate.

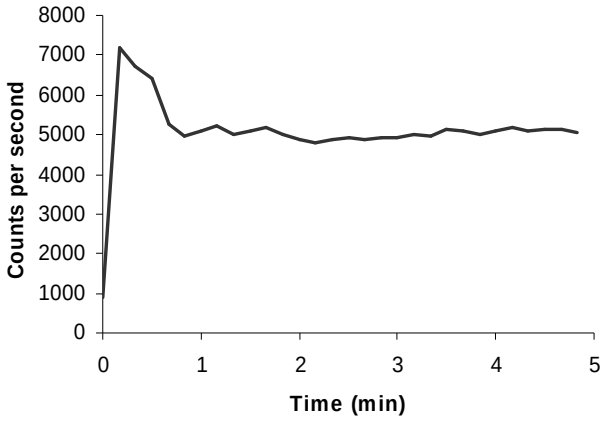

Figure 3. 18. Evolution of the number of counts per seconds during the flocculation process.

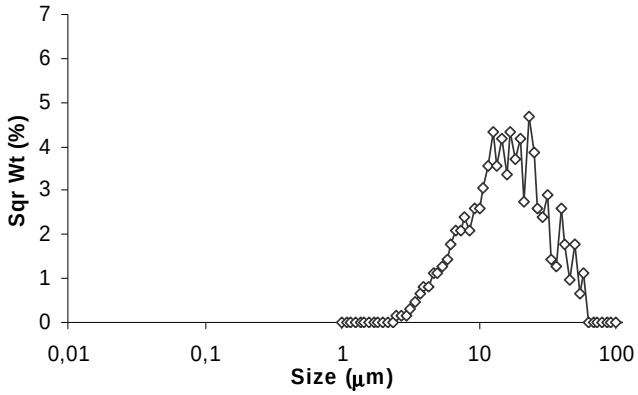

Figure 3. 19. Square weighted size distribution of the PCC particles measured by FBRM.

3.3.2 – FLOCS RESISTANCE

Using the LDS technique, when the flocs are submitted to sonication, their size rapidly decreases as shown in Figures 3.5 to 3.12. Breakage of flocs indicates that the polymer chains detach from the particles surface resulting on rupture of bonds between the particles in the aggregate.

Flocs break-up described in Figures 3.5 to 3.12 are summarized in Table 3.7 for the eight polymers studied and when flocs are submitted to sonication and to an increase of the pump speed. The percentage of flocs break-up were calculated as the ratio of the difference between the initial and final flocs size after shearing and the size of the flocs at the end of flocculation.

Table 3.7 shows that break-up of flocs is higher as the applied sonication frequency increases, since the shear forces increase. Moreover, it is observed that, in general, when the polymer is in excess the flocs break up decreases confirming again that flocs strength can increase if the polymer dosage is higher than the optimum one. As described by Negro and co-workers (2005), in this case, the number of polymer bonds between the particles is higher resulting on particles stronger attached in the aggregate.

With regard to the effect of the polymer charge density, it seems that as the charge density increases the flocs resistance increases (break up percentages decreases). This agrees with the configuration that the polymer adopts at the particle surface. In fact, in this case, as the charge density decreases the flat configuration capability is reduced, and thus, the polymer is more weakly attached to the particles, and thus, flocs break up easier. This

is confirmed by the flocs structure presented in Table 3.5, where it can be seen that flocs have a more open structure as the polymer charge density decreases.

Table 3. 7. Flocs break up percentages for all the flocculants studied.*

Alpine-Floc™	**Dosage (mg/g)**	**Break up (%)**			
		10 kHz	**20 kHz**	**1800 rpm**	**2200 rpm**
A1++	4	-	68	-	18
	10	-	41	-	5
BHMW	6	-	45	-	16
	14	-	46	-	15
E1	2	9	25	9	19
	4	20	39	7	17
	8	26	43	7	17
E1+	8	-	67	-	20
	12	-	78	-	17
	16	-	76	-	17
E1++++	6	44	68	8	19
	8	54	77	9	19
	10	27	65	7	18
G1	6	67	79	9	20
	10	70	82	7	21
	14	37	55	5	10
G1+	20	69	74	8	17
	30	64	78	8	16
	40	43	54	8	15
G1++++	20	66	73	9	15
	30	45	72	9	17
	40	32	47	6	14

* grey lines refer to the optimum flocculant dosage

However, the A1++ polymer continues to be an exception since despite having a high charge density, the flocs are open and are less resistant due to the presence of the two branches. In fact, the branched polymers, in general, impair the flocs resistance. Flocs

produced with the branched polymers (A1++, E1+, E1++++, G1+, G1++++) are less resistant than flocs produced with E1 and BHMW. This fact does not correlate well with the d_F and *SE* values calculated at the end of the flocculation process (Table 3.5). Size seems to be the factor that most affects the resistance to breakage, since the main difference between the flocs produced with the different polymers, at the end of flocculation, is on the flocs sizes (Table 3.4). Consequently, as the flocs size increases, flocs resistance decreases. This is confirmed by Figure 3.20 where the flocs resistance when they are submitted to sonication at 20 kHz as a function of the median flocs size at the end of flocculation and for the optimum flocculant dosage has been presented.

The results of Table 3.7 show also that the resistance of the aggregates submitted to increasing hydrodynamic shearing forces follows the same trend as detected when sonication was applied. Nevertheless, the decrease in the flocs size under hydrodynamic shearing was less notorious than under sonication (Figures 3.5 to 3.12). This is due to the way how the shearing force was applied. When the flocs were submitted to sonication the stresses were applied to the entire floc resulting in rupture by fragmentation, while the increase of the pump speed corresponded to a shear stress applied at the flocs surface only and, thus, flocs rupture occurred by erosion.

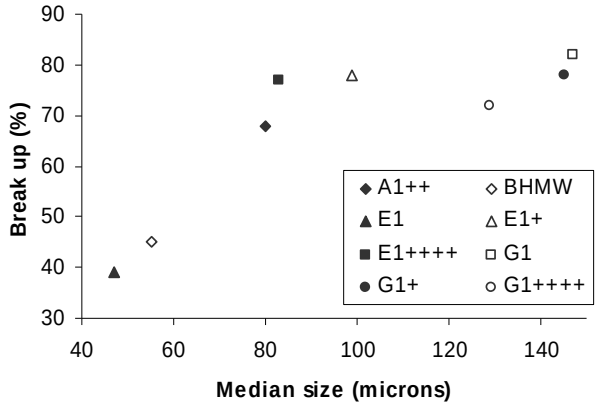

Figure 3. 20. Flocs break up as function of the median flocs size for the optimum flocculant dosage.

Additionally, neither the branching and flocculant dosage nor the flocs size seem to affect flocs resistance when hydrodynamic shearing is applied, since rupture by erosion is not much dependant on the type of bonds established and neither on flocs structure. In reality, what happens is that flocs reach another equilibrium state where aggregation and fragmentation rates are the same.

3.3.3 – REFLOCCULATION CAPACITY

From Figures 3.5 to 3.12 (LDS technique), it is evident that the reflocculation degree of the flocs is very small or practically inexistent for all the polymers studied with the exception of the BHMW polymer. As seen before, BHMW acts mainly by the patching mechanism. This bond type is only partially affected by the shear stress and, thus, these bonds are more easily restored, resulting in a higher reflocculation percentage compared to the other polymers that act mainly by bridging mechanism. If flocs formed by bridging mechanism break up, the polymer degrades and the reflocculation process becomes more difficult (Tanaka *et al.*, 1992; Norell *et al.*, 1999; Alfano *et al.*, 2000; Blanco *et al.*, 2005). As described in the literature, the original polymer bonds are not able to reform to their previous extent, and, moreover, the polymer chains at the particle surface reconform, increasing coverage of the surface and inhibiting reflocculation with fresh polymer (Tanaka *et al.*, 1992; Norell *et al.*, 1999; Alfano *et al.*, 2000; Blanco *et al.*, 2005).

Mass fractal dimension and scattering exponent values of the reflocculated flocs are summarized in Table 3.8. The mass fractal dimension values of the reflocculated flocs are slightly higher than before breakage (compare with Table 3.5). This indicates a more compact structure of the reflocculated flocs since the restructuring of particles due to shear forces originates flocs which are more compact. The structure of the reflocculated flocs produced by the E1 polymers series follows the same trend as described before for flocs structure at the end of flocculation, i.e., flocs produced with the highly branched polymer are less compact. The reflocculated flocs structure when G1, G1+ and G1++++ were used have, in general, a more open structure when comparing with the respective medium charge density polymer (E1, E1+ and E1++++). Moreover, the variation of the reflocculated flocs structure with the degree of branching is not so notorious as in the case of the E1 series, following the trend described and explained previously for flocs at the end of flocculation (see section 3.3.1). Furthermore, when the hydrodynamically sheared flocs are reflocculated the change in d_F (before and after breakage) is not so pronounced as for the sonicated ones. This can be explained by the fact that shearing led only to surface erosion, and thus, restructuring did not occur.

Table 3. 8. Mass fractal dimension and scattering exponent after 5 minutes of reflocculation.*

Alpine-Floc™	Dosage	10 kHz		20 kHz		1800 rpm		2200 rpm	
	(mg/g)	d_F	SE	d_F	SE	d_F	SE	d_F	SE
A1++	4	-	-	1.58	2.57	-	-	1.35	2.32
	10	-	-	1.62	1.89	-	-	1.61	2.23
BHMW	6	-	-	1.53	2.44	-	-	1.44	2.55
	14	-	-	1.45	2.39	-	-	1.42	2.47
E1	2	1.52	2.55	1.54	2.57	1.59	2.51	1.61	2.47
	4	1.63	2.42	1.65	2.48	1.69	2.44	1.61	2.37
	8	1.64	2.45	1.65	2.51	1.58	2.60	1.59	2.51
E1+	8	-	-	1.62	2.43	-	-	1.66	2.53
	12	-	-	1.60	2.55	-	-	1.62	2.56
	16	-	-	1.52	2.58	-	-	1.55	2.54
E1++++	6	1.68	2.34	1.69	2.31	1.60	2.34	1.61	2.43
	8	1.68	2.30	1.75	2.28	1.61	2.32	1.57	2.29
	10	1.59	2.37	1.62	2.26	1.56	2.35	1.59	2.40
G1	6	1.55	2.58	1.54	2.61	1.55	2.57	1.52	2.56
	10	1.60	2.36	1.60	2.46	1.17	2.54	1.27	2.56
	14	1.54	2.35	1.57	2.41	1.27	2.59	1.27	2.65
G1+	20	1.62	2.47	1.60	2.47	1.65	2.51	1.68	2.49
	30	1.58	2.48	1.58	2.49	1.42	2.44	1.45	2.44
	40	1.50	2.34	1.52	2.38	1.26	2.46	1.28	2.43
G1++++	20	1.62	2.44	1.60	2.44	1.63	2.43	1.65	2.43
	30	1.59	2.42	1.60	2.43	1.47	2.33	1.45	2.33
	40	1.56	2.27	1.58	2.28	1.39	2.47	1.41	2.54

* grey lines refer to the optimum flocculant dosage

3.3.4 – Effect of microparticles on the reflocculation process

Reflocculation tests with bentonite addition were conducted using the LDS technique for E1, E1++++, G1 and G1++++ polymers. Reflocculation with bentonite was evaluated for the optimum flocculant dosage obtained and for the lower flocculant dosage studied and presented in the section 3.3.1. The flocs were broken up by sonication (20

kHz) or by increasing the pump speed (2200 rpm) and the bentonite was added after the initial shearing being restored (see section 3.2.5).

Figures 3.21 to 3.24 describe reflocculation results when bentonite is added after breaking up flocs produced with E1, E1++++, G1 and G1++++ polymers respectively. The respective kinetic curves without the addition of bentonite are also represented in the same figures (points filled in black). For G1 and G1++++ some kinetic curves, after break up, are not complete due to the larger flocs obtained that originate sticky problems in the equipment windows and obscuration values below 5%.

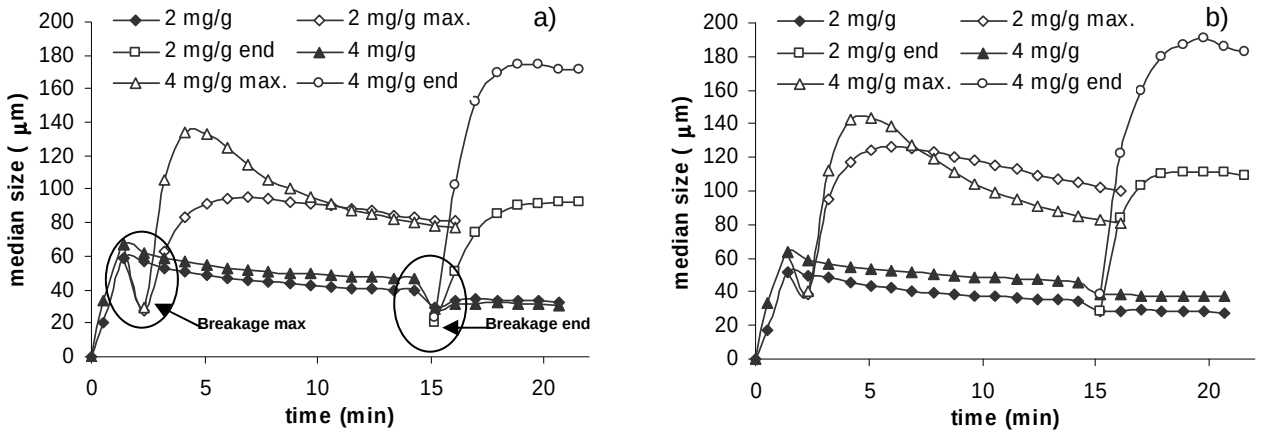

Figure 3. 21. Reflocculation with bentonite after flocs break up at a) 20kHz and b) 2200 rpm for E1.

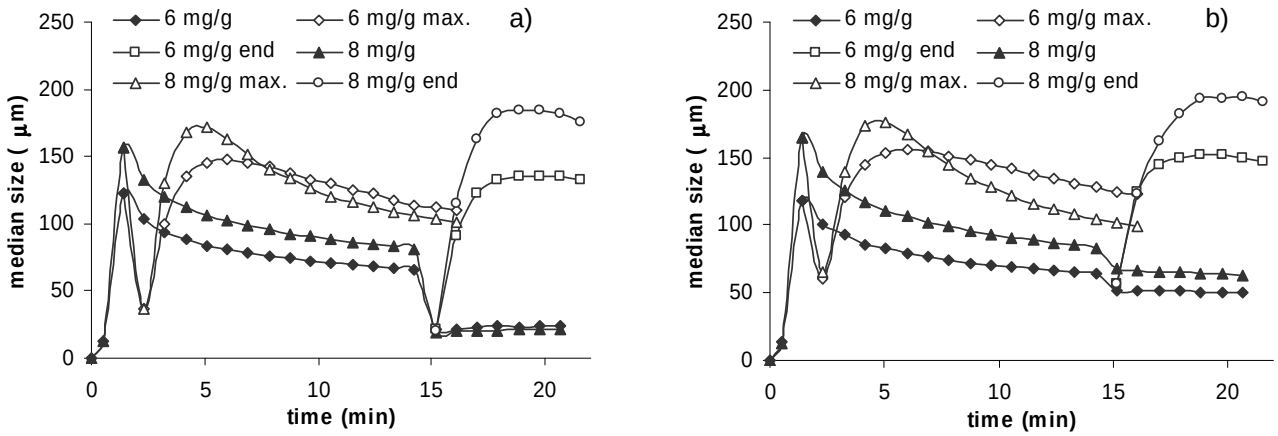

Figure 3. 22. Reflocculation with bentonite after flocs break up at a) 20kHz and b) 2200 rpm for E1++++.

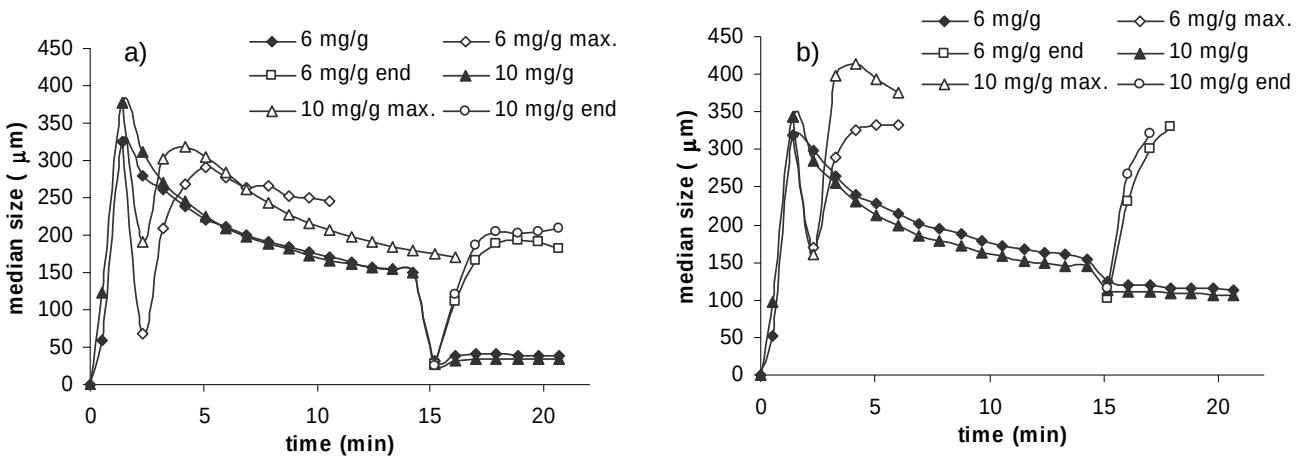

Figure 3. 23. Reflocculation with bentonite after flocs break up at a) 20kHz and b) 2200 rpm for G1.

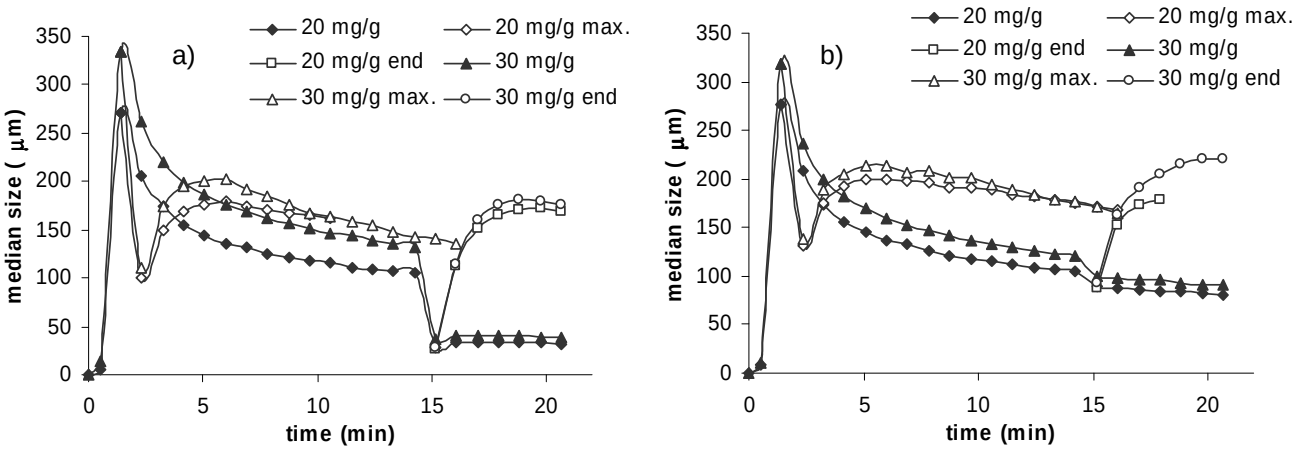

Figure 3. 24. Reflocculation with bentonite after flocs break up at a) 20kHz and b) 2200 rpm for G1++++.

Reflocculation percentages with bentonite obtained by the LDS technique are summarized in Table 3.9. Situation 1 corresponds to the reflocculation percentages of reflocculated flocs with bentonite when flocs are broken up at the maximum in the kinetics curve whereas Situation 2 corresponds to the reflocculation percentages of the reflocculated flocs with bentonite when flocs are broken up at the end of flocculation.

Table 3. 9. Reflocculation percentages with bentonite of flocs broken up in the LDS equipment.*

Alpine-Floc™	Dosage (mg/g)	Reflocculation of flocs for situation 1 (%)		Reflocculation of flocs for situation 2 (%)	
		20 kHz	2200 rpm	20 kHz	2200 rpm
E1	2	192	167	348	288
	4	163	104	631	390
E1++++	6	210	106	531	186
	8	185	57	820	242
G1	6	-	-	500	-
	10	0	-	690	-
G1++++	20	62	31	559	-
	30	26	23	538	138

* grey lines refer to the optimum flocculant dosage

For the four flocculants studied, bentonite addition improves significantly the reflocculation capacity of the flocs after being broken up comparing with results obtained without bentonite addition. When flocs are broken up at the maximum in the kinetic curves, reflocculation occurs with flocs restructuring since flocs size decreases during the reflocculation process. Indeed, at this time flocs structure is not fully stabilized yet. Flocs are weaker (they break up easier) but polymer degradation is lower. As a result, the polymer is able to reconforme and the bentonite action is less effective than when flocs are broken up at the end of the flocculation process. From Figures 3.21 to 3.24 and Table 3.9, it can be seen that reflocculation capacity is more significant when bentonite is added after breaking up the flocs at the end of flocculation. In this case, flocs restructuring does not occur during reflocculation. Moreover, when flocs are broken up at the maximum in the kinetic curve, the bentonite action is more significant when a lower flocculant dosage is used. In this case, flocs produced with less amount of flocculant are weaker than those produced with the optimum dosage. The same does not occur when flocs are broken up at the end of the flocculation process because at this point the flocs structure is more similar to the flocs structure observed for the optimum dosage.

In addition, reflocculation degree is higher when flocs are broken up by sonication. In fact, despite the reflocculated flocs size being similar independently of the applied shear, since flocs break up is higher when flocs are submitted to sonication, the resulted reflocculation degree is higher. The results of the Table 3.7 confirm that the bentonite

action depends mainly on the flocs resistance. Hence, as the flocs break up increases the bentonite effect is more pronounced.

The charge density seems to affect the bentonite action. Indeed, for the polymers of low charge density G1 and G1++++ reflocculation with bentonite is less significant mainly when the flocs are broken up at the maximum in the kinetic curve (Situation 1) than for Situation 2. As seen before, when the flocs break up at the maximum in the kinetic curve the polymer degradation is low. Reflocculation with bentonite becomes more difficult as the polymer charge density decreases because the polymer chains that are not degraded adsorb at the particle surface in a much extended configuration. The reflocculation mechanism with bentonite presented in Figure 1.8 (section 1.2.2.4) is not feasible.

The microparticulate system also affects the structure of the reflocculated flocs. In Tables 3.10 and 3.11, mass fractal dimension and scattering exponent values of the reflocculated flocs with and without bentonite are compared when either flocs are submitted to sonication or to an increase of the pump speed, respectively. Situation 1 corresponds to the structure of reflocculated flocs with bentonite when flocs are broken up at the maximum in the kinetics curve whereas Situation 2 corresponds to the structure of the reflocculated flocs with bentonite when flocs are broken up at the end of flocculation. Data are not available for G1 since for this polymer, at the end of reflocculation, the results are out of the quality range.

Table 3. 10. Mass fractal dimension and scattering exponent of the reflocculated flocs with and without bentonite after breaking up flocs at 20 kHz.*

		without bentonite		**Situation 1**		**Situation 2**	
Alpine-Floc™	**Dosage (mg/g)**	**d_F**	**SE**	**d_F**	**SE**	**d_F**	**SE**
E1	2	1.54	2.57	1.29	2.52	1.23	2.52
	4	1.65	2.48	1.34	2.55	1.20	2.61
E1++++	6	1.69	2.31	1.25	2.45	1.25	2.49
	8	1.75	2.28	1.29	2.48	1.22	2.37
G1	6	1.54	2.61	-	-	-	-
	10	1.60	2.46	-	-	-	-
G1++++	20	1.60	2.44	1.30	2.33	1.48	2.13
	30	1.60	2.43	1.32	2.36	1.48	2.08

* grey lines refer to the optimum flocculant dosage

Table 3. 11. Mass fractal dimension and scattering exponent of the reflocculated flocs with and without bentonite after breaking up flocs at 2200 rpm.*

		without bentonite		**Situation 1**		**Situation 2**	
Alpine-Floc™	**Dosage (mg/g)**	**d_F**	**SE**	**d_F**	**SE**	**d_F**	**SE**
E1	2	1.61	2.47	1.21	2.53	1.21	2.56
	4	1.61	2.37	1.37	2.47	1.17	2.54
E1++++	6	1.61	2.43	1.22	2.47	1.21	2.49
	8	1.57	2.29	1.27	2.49	1.18	2.40
G1	6	1.52	2.56	-	-	-	-
	10	1.27	2.56	-	-	-	-
G1++++	20	1.65	2.43	1.28	2.32	1.30	2.32
	30	1.45	2.33	1.34	2.33	1.37	2.10

* grey lines refer to the optimum flocculant dosage

Reflocculated flocs with bentonite have, in general, a more open structure when comparing with that obtained without bentonite mainly as far as the primary flocs are considered (d_F values). In fact, when bentonite is used, the reflocculation is very high, and thus, the reflocculated flocs with bentonite are larger and more open than those produced without bentonite. Furthermore, the flocs structure becomes much more open when flocs were broken up at the end of flocculation (Situation 2). In this situation, as seen before, the reflocculation capacity is higher since the bentonite action is more significant, and thus, flocs produced are larger and more open than the reflocculated flocs in Situation 1. The flocs produced with E1++++ and with bentonite continue to have a more open structure when comparing with those produced with the linear one E1. The polymer of low charge density (G1++++) used with bentonite produces again, as expected, flocs with a more open structure. There are not significant differences in the structure of the reflocculated flocs with bentonite when flocs are submitted to sonication or to an increase of the pump speed.

Figures 3.25 to 3.27 illustrate the reflocculation processes with bentonite carried out in the FBRM equipment for E1, E1+ and E1++++ flocculants respectively, in terms of the evolution of the floc mean square size with time for the optimum flocculant dosage. Furthermore, reflocculation without bentonite addition (full symbols) as well as the

complete flocculation process without breakage (continuous line) are also described, in order to evaluate the effect of the bentonite addition on the reflocculation process. In the FBRM equipment, the flocs were broken up 30 seconds and one minute after the flocculant addition. As for the LDS experiments, one minute corresponds to the time where the flocs have a stable structure and 30 seconds corresponds, in general, to the maximum of the kinetics curve obtained by FBRM. Bentonite was always added after flocs break up, and two different stirring speeds (450 and 650 rpm) were used for the break up of the flocs. Figures 3.28 to 3.30 present the same results but for the lower flocculation dosage studied.

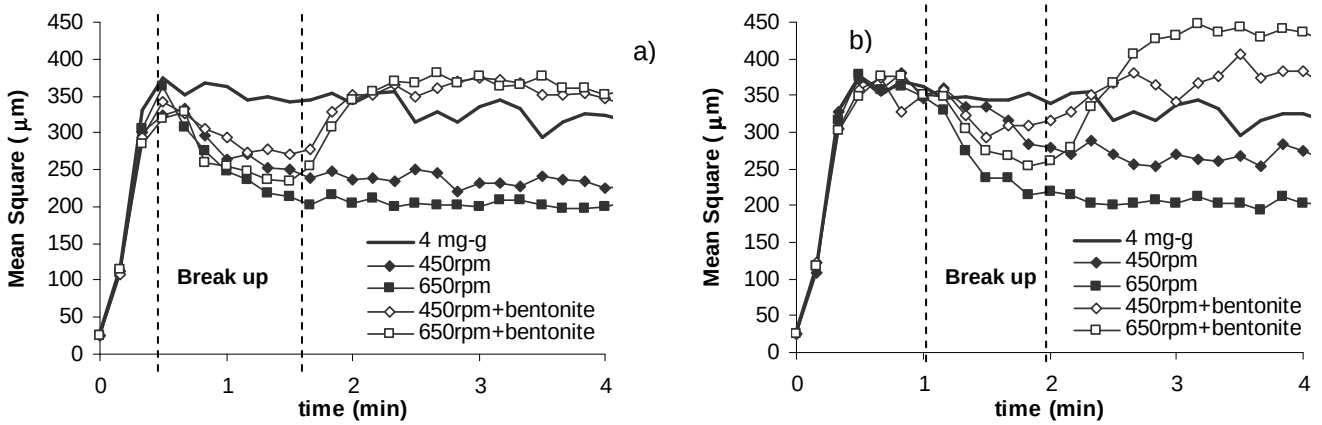

Figure 3. 25. Resistance of flocs produced with 4 mg/g of E1 a) 30s and b) 1 min after the flocculant addition and reflocculation with bentonite.

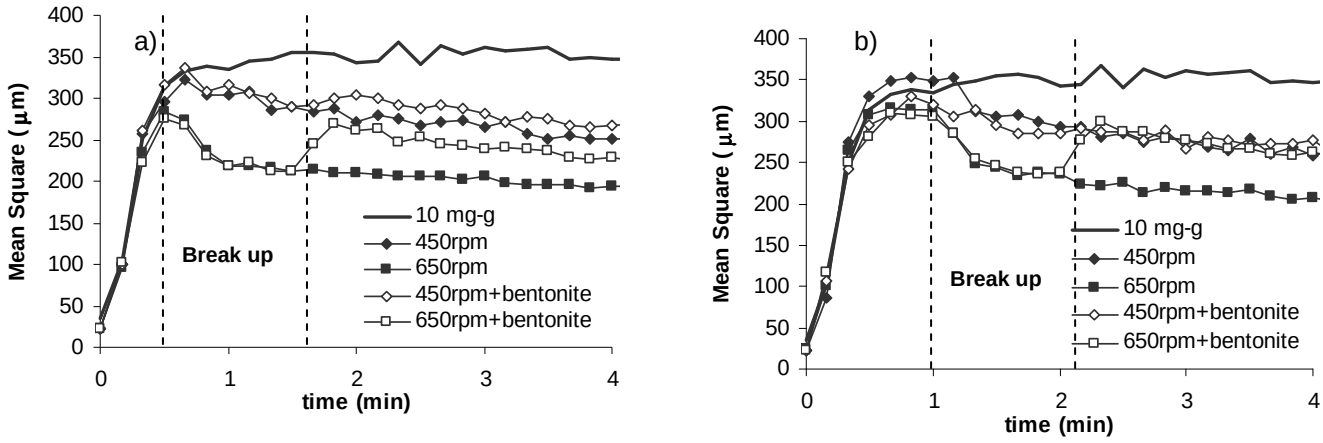

Figure 3. 26. Resistance of flocs produced with 10 mg/g of E1+ a) 30s and b) 1 min after the flocculant addition and reflocculation with bentonite.

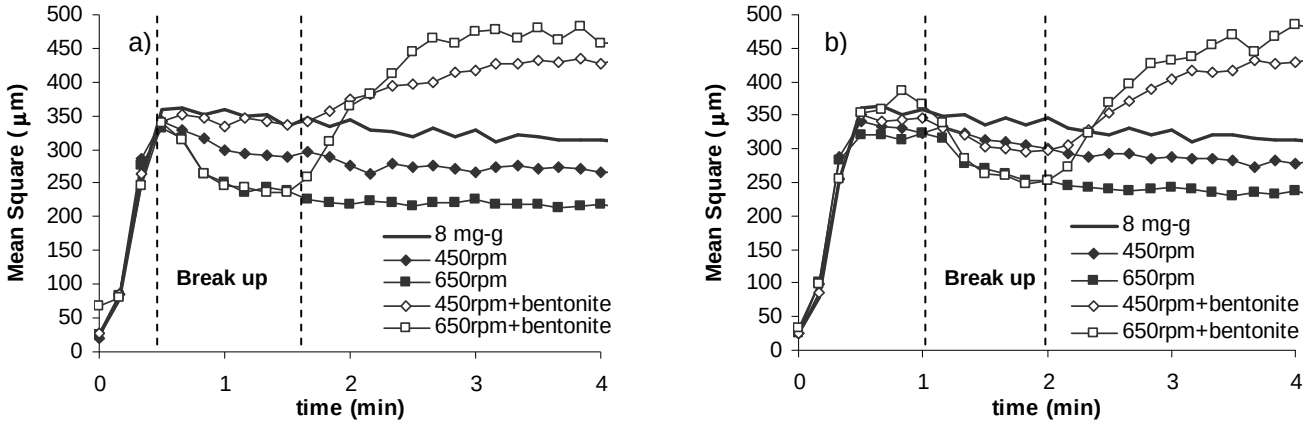

Figure 3. 27. Resistance of flocs produced with 8 mg/g of E1++++ a) 30s and b) 1 min after the flocculant addition and reflocculation with bentonite.

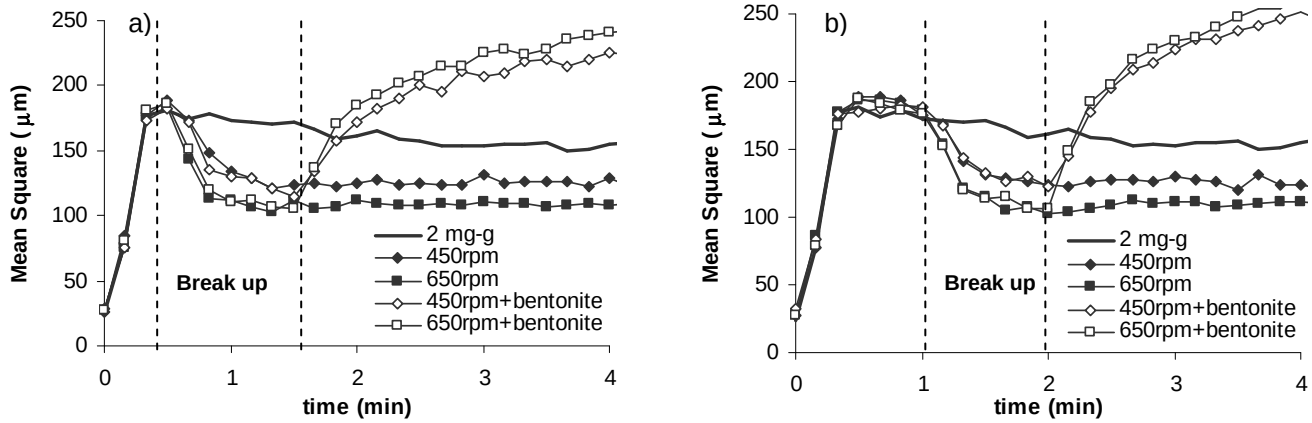

Figure 3. 28. Resistance of flocs produced with 2 mg/g of E1 a) 30s and b) 1 min after the flocculant addition and reflocculation with bentonite.

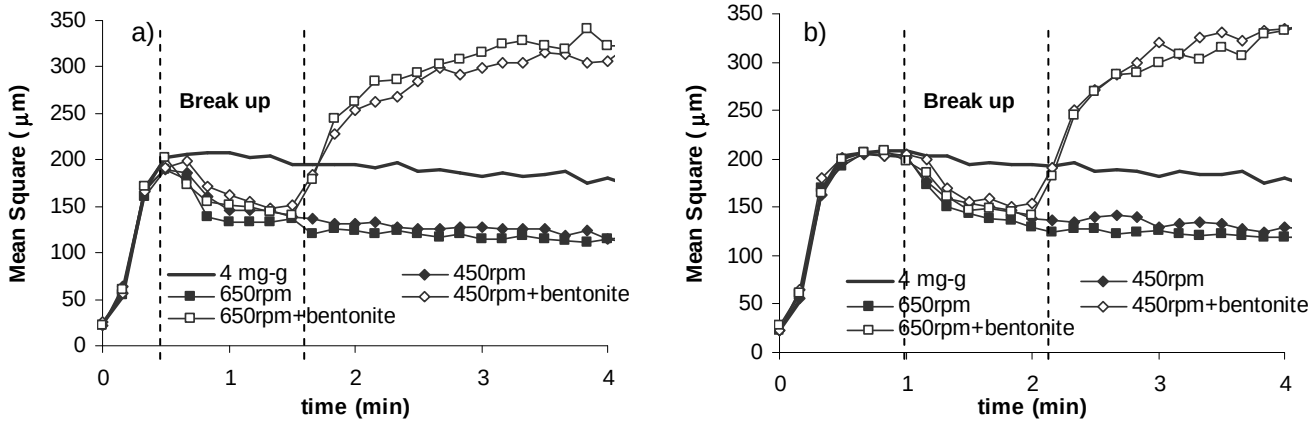

Figure 3. 29. Resistance of flocs produced with 4 mg/g of E1+ a) 30s and b) 1 min after the flocculant addition and reflocculation with bentonite.

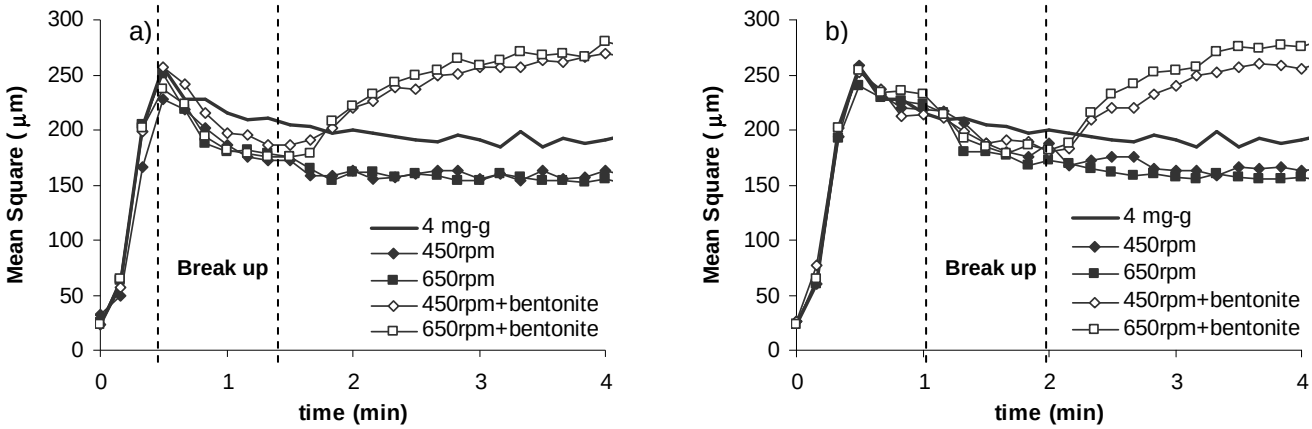

Figure 3. 30. Resistance of flocs produced with 4 mg/g of E1++++ a) 30s and b) 1 min after the flocculant addition and reflocculation with bentonite.

From the results of Figures 3.25 to 3.30, the break up percentages, when flocs are broken up 30 seconds and one minute after flocculant addition, were calculated in the same manner as for the break up percentages presented in Table 3.7 and are summarized in Table 3.12.

Table 3. 12. Flocs break up percentages for E1, E1+ and E1++++ using the FBRM technique.*

Alpine-Floc™	Dosage (mg/g)	Break up after 30s (%)		Break up after 1min (%)	
		450 rpm	650 rpm	450 rpm	650 rpm
E1	2	35	39	29	43
	4	23	41	19	37
E1+	4	27	28	31	36
	10	3	25	16	25
E1++++	4	24	30	14	23
	8	15	28	8	22

* grey lines refer to the optimum flocculant dosage

As verified with LDS measurements, as the shearing forces increase, the flocs break up increases. Moreover, with FBRM measurements and when comparing results obtained for the optimum flocculant dosage, it is possible to conclude that flocs produced after one minute of the flocculant addition are, in general, more resistant than flocs that are produced 30 seconds after flocculant addition. In fact, as for the LDS results, at 30 seconds of the

flocculation process, the flocs structure is not fully stabilized yet, and thus, polymer chains are weakly attached to the particles. Moreover, for the lower shearing rate, flocs resistance is higher for the optimum flocculant dosage. For 650 rpm, no significant differences on the flocs resistance as concentration changes were detected. Additionally, the effect of the shear force intensity is not significant on flocs break up when the amount of the flocculant used is lower than the optimum one. On the other hand, since the flocs size is very similar between the flocculants used, no significant difference on flocs resistance for the different flocculants tested could be detected by FBRM, mainly at 650 rpm. Indeed, the Figure 3.31 that represents the break up percentages as a function of the flocs size before the break up with 650 rpm confirms that the breakage depends mainly on the flocs size. As verified also by the LDS measurements, the flocs break up increases as the flocs size increases.

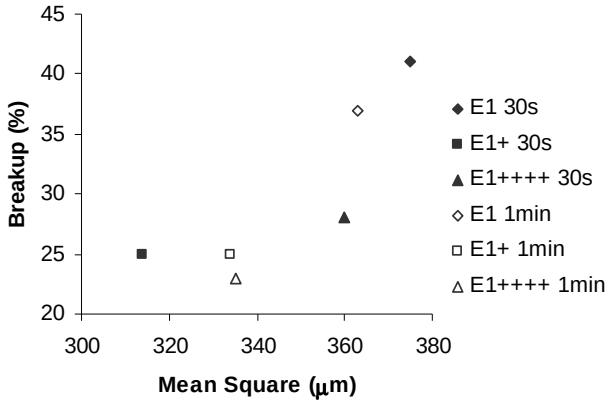

Figure 3. 31. Flocs break up percentages as a function of the size of the flocs before breakage and produced with E1, E1+ and E1++++ for the optimum flocculant dosage.

Reflocculation percentages with bentonite obtained by FBRM measurements (Figures 3.25 to 3.30) are summarized in Table 3.13. The results from Table 3.13 and the observation of the curves in Figures 3.25 to 3.30 indicate that, in general, the bentonite addition improves significantly the reflocculation process. As detected in the LDS measurements, this improvement increases as the flocs break up increases. In fact, reflocculation percentages are higher as the shearing rate used to break the flocs increases. In the same way, since flocs produced with a smaller amount of flocculant are weaker than those produced with the optimum flocculant dosage (Table 3.12), the bentonite action is more significant in that case. For the results obtained with E1+ these effects are quite evident. Indeed, on Table 3.12, for this flocculant, the flocs break up is very low at 450 rpm and in this case, the bentonite does not have any effect on the reflocculation process

(Table 3.13). Furthermore, for the optimum flocculant dosage break up is much lower, and thus, reflocculation with bentonite is also lower. Moreover, comparing the reflocculation degree obtained for the optimum dosage of E1 and E1++++, values are very similar since, as seen before (Figures 3.25 to 3.30), the flocs sizes obtained by FBRM are, in this case, very similar.

The trends detected for the reflocculation with bentonite using the FBRM technique agree well with the results obtained by LDS where bentonite was added after flocs break up at the maximum in the kinetic curve (Table 3.9). However, in the LDS equipment reflocculation was even more intense because break up by sonication is more effective.

Table 3. 13. Reflocculation percentages with bentonite of flocs broken up in the FBRM.*

Alpine-Floc™	**Dosage (mg/g)**	**Reflocculation of flocs broken up after 30s (%)**		**Reflocculation of flocs broken up after 1min (%)**	
		450 rpm	**650 rpm**	**450 rpm**	**650 rpm**
E1	2	67	94	82	118
	4	39	67	35	80
E1+	4	88	109	100	111
	10	0	19	0	16
E1++++	4	27	39	32	40
	8	37	87	36	70

* grey lines refer to the optimum flocculant dosage

3.3.5 – Effect of water cationic content on flocculation process

Similar flocculation tests were conducted in the LDS equipment using industrial water as the suspending medium for the E1, E1+ and E1++++ polymers. Figures 3.32 to 3.34 compare flocculation, deflocculation and reflocculation kinetics obtained in industrial water with those obtained in distilled water for the optimum flocculant dosage in each case and for a lower concentration. The kinetics of the flocculation process in industrial water follow a pattern that is similar to the pattern of the flocculation in distilled water, though slightly faster in the industrial white water. In fact, it is known that the thickness of the double layer surrounding the particle surface depends upon the concentration of ions in solution and can be calculated from the ionic strength of the medium: the higher the ionic strength, the more compressed the double layer becomes. Therefore, the thickness of the

double layer of the PCC particles was reduced due to the high cationic content of the white water and this contributed to the faster flocculation of the PCC particles. Flocculation, though being mainly due to bridging, is facilitated by the decrease of the repulsive forces and this is why velocity is slightly higher.

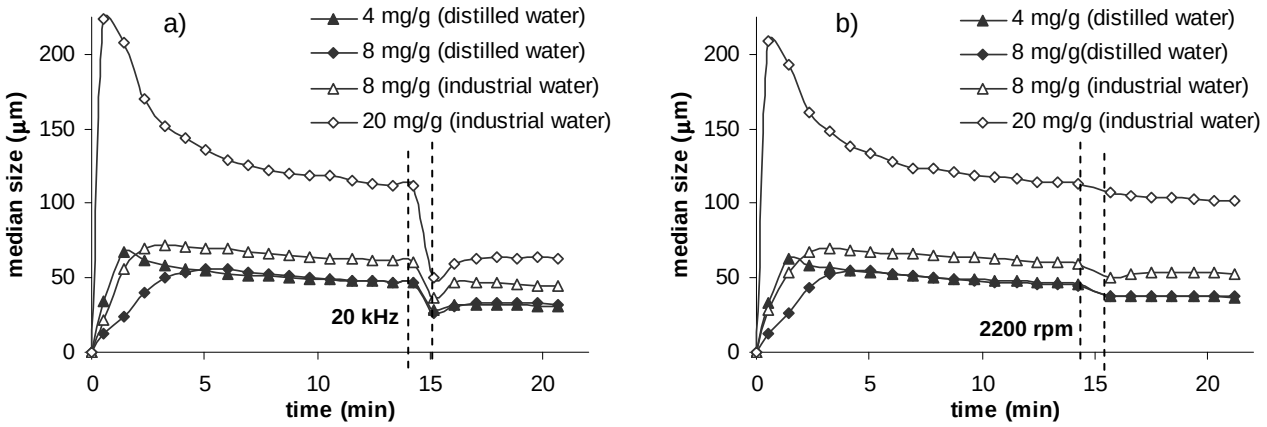

Figure 3. 32. Flocculation, deflocculation and reflocculation with E1 in distilled and industrial water when flocs are submitted to a) sonication at 20 kHz and b) increase of the pump speed to 2200 rpm.

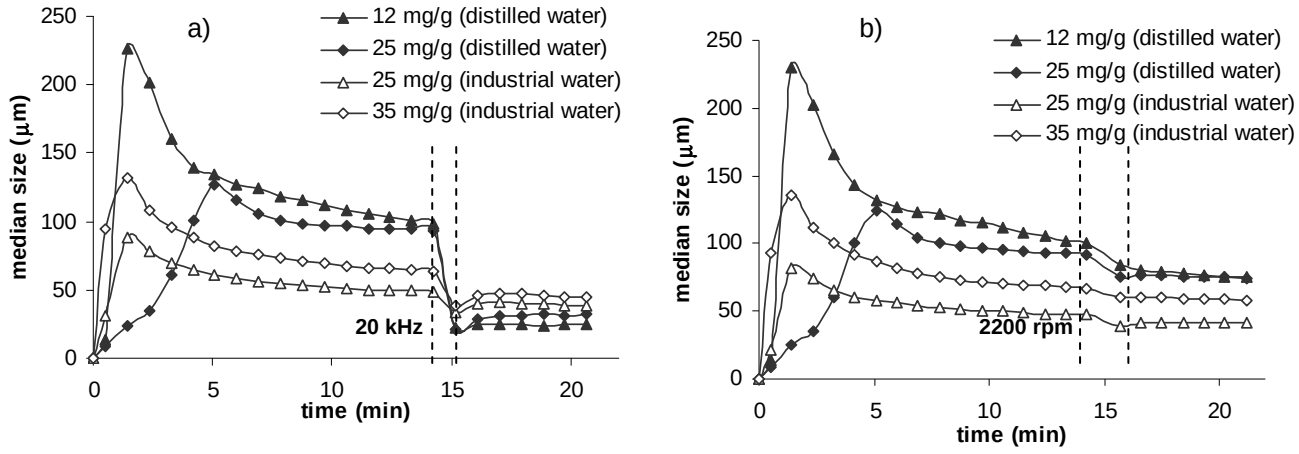

Figure 3. 33. Flocculation, deflocculation and reflocculation with E1+ in distilled and industrial water when flocs are submitted to a) sonication at 20 kHz and b) increase of the pump speed to 2200 rpm.

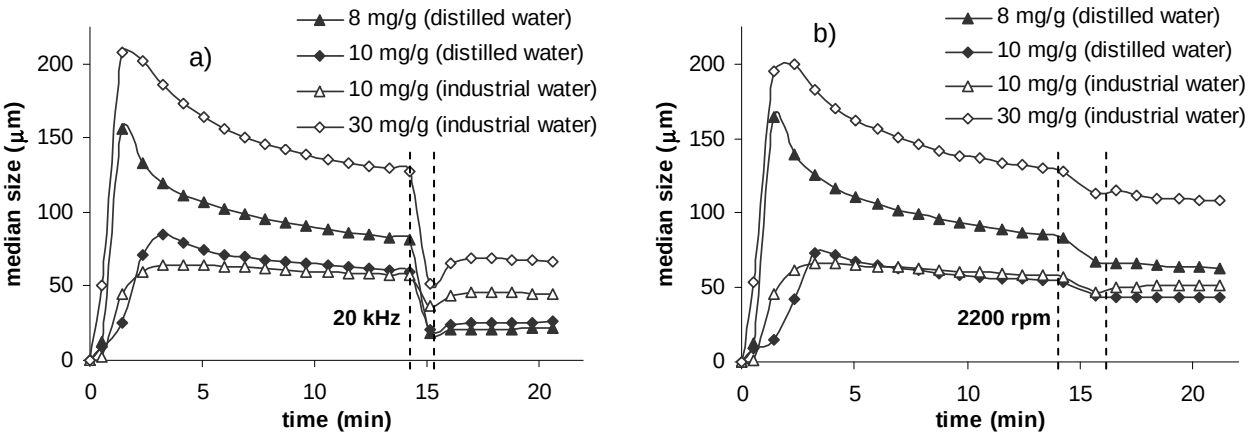

Figure 3. 34. Flocculation, deflocculation and reflocculation with E1++++ in distilled and industrial water when flocs are submitted to a) sonication at 20 kHz and b) increase of the pump speed to 2200 rpm.

Moreover, with industrial water, restructuring was less effective when using E1+ and E1++++ since the flocs size decreased less. This can be explained by a salting-out effect caused by the high cationic content of the industrial water; the polymer adopts a more coiled structure and, thus, the capability for reconformation is reduced (Shubin and Linse, 1997; Hulkko and Deng, 1999; Greenwood and Kendall, 2000). In fact, the zeta potential does not decrease during flocculation as can be observed in Figure 3.35, therefore, the reduction of the polymer reconformation capability is confirmed. The polymer chain of E1 is also affected by the salting-out effect but the flocs size decrease during flocculation is more pronounced than in distilled water (Figure 3.32). Considering that the polymer chain adopts a more coiled structure in the presence of salts, a flat adsorption on the particle surface is no longer possible, and thus, chains of E1 in industrial water have a similar behaviour as E1+ in distilled water, i.e., becomes more flexible.

Moreover, before the maximum in the kinetic curve, due to the very fast adsorption of this polymer at particle surface, particles do not have enough time to reach stable positions. As a result, there is enough space for restructuring of the polymer chain to occur afterwards, with the consequent decrease in flocs size as observed in Figure 3.32. The slight decrease of the zeta potential during flocculation in industrial water is an indication that reconformation of the E1 polymer exists (Figure 3.35).

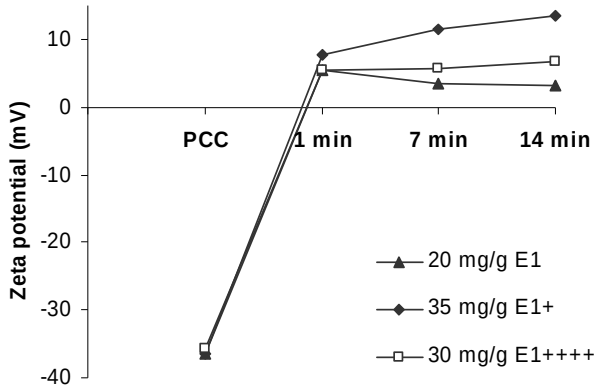

Figure 3. 35. Zeta potential at different stages of the flocculation process in industrial water for the optimum dosage of E1, E1+ and E1++++.

For flocculation in industrial water, higher polymer dosages are, in general, required, in agreement with the lower zeta potential of the initial PCC particles (Figure 3.35). In fact, since the industrial water contains more contaminants, the surface charge of the PCC particles in industrial water is more negative than in distilled water, and thus, a higher amount of polymer is necessary to neutralize those charges. Studies have shown that polymer adsorption is promoted by decreasing the salt concentration (Shubin and Linse, 1997; Stoll and Chodanowski, 2002). Consequently, in industrial water, a larger amount of polyelectrolyte was needed to obtain the same particle surface coverage with the polymer.

Nevertheless, the optimum flocculant dosage for E1+ continued to be higher than for E1++++ and again the lowest value was obtained for E1 (35 mg/g, 30 mg/g and 20 mg/g, respectively). It is interesting to note that some tests conducted with "simulated industrial water" (distilled water to which exactly the same cations as in the industrial water were added) do not show the same trends as with the real industrial water. Therefore, in fact, the higher negative charge of the PCC particles in the white water is a determinant factor for the results.

The high cationic content of the industrial water also alters the effect of the branching of the polymer in flocculation. The flocs obtained in distilled water with E1+ are, in general, larger while in industrial water the opposite happens. E1++++ is less affected by the salting-out effect than E1+ due to its smaller gyration radius (Huang *et al.*, 2000). Concerning E1, the polymer which now has a more coiled structure, flocs where the distance between particles is higher are obtained, resulting in larger flocs than in distilled water, which are more similar to the ones produced with E1++++, also in industrial water.

These effects are also reflected in the fractal dimension and scattering exponent values shown in Table 3.14. For the optimum concentrations, the structure of flocs produced by E1+ and E1++++, at the maximum in the kinetic curve, is denser in industrial water than in distilled water (Table 3.5) as a result of the more coiled structure adopted by the polymers. Furthermore, these differences are again less pronounced for E1++++. For E1, the high decrease of the *SE* value from distilled to industrial water indicates that flocs structure becomes more open in industrial water. Indeed, as explained before, the salting-out effect allows an increase of the polymer chain flexibility, and thus, produces larger flocs with a more open structure than in distilled water. This difference is more evident for the secondary aggregates (by comparison of the *SE* values) since secondary aggregates are still very loose at the maximum in the kinetic curve due to the very fast kinetics in industrial water.

Table 3. 14. Mass fractal dimension and scattering exponent of flocs in industrial water.*

Alpine-Floc™	Dosage (mg/g)	Max. of kinetic curve		End of flocculation	
		d_F	SE	d_F	SE
E1	8	1.51	2.47	1.48	2.66
	20	1.40	1.45	1.37	2.64
	25	1.42	1.66	1.17	2.62
E1+	25	1.47	2.12	1.38	2.61
	35	1.45	1.98	1.27	2.60
	40	1.29	1.84	1.06	2.57
E1++++	10	1.44	2.45	1.43	2.60
	30	1.53	1.75	1.30	2.57
	35	1.33	2.26	1.23	2.58

* grey lines refer to the optimum flocculant dosage

At the end of flocculation, the behaviour is very different from that observed in distilled water. Indeed, in distilled water both primary and secondary flocs have a denser structure at the end of flocculation than at the maximum in the kinetic curve, due to flocs restructuring. In industrial water, the secondary aggregates are effectively denser at the end of flocculation but primary aggregates become slightly less compact. Reconformation occurs mainly at the secondary aggregates level because primary aggregates were already quite compact at the maximum of the kinetic curve.

Despite these differences in the flocs structure, the same trend is observed in distilled and in industrial water, relatively to the flocculant concentration. As the flocculant concentration increases the mass fractal dimension and the scattering exponent, at the end of flocculation, decrease.

The effect of sonication and of pump speed on flocs resistance in industrial water is similar to the one observed in distilled water (Figures 3.7 to 3.9 and Figures 3.32 to 3.34). The results in Tables 3.7 and 3.15 show that the resistance of flocs produced with E1 and E1++++ is similar in both waters when comparing values obtained for the optimum dosages. However, for the optimum dosage, the flocs produced with E1+ are more resistant in industrial water than in distilled water. Here again, the flocculant branching seems to have little effect on flocs resistance because the flocs structure at the end of flocculation is similar. As in distilled water, it is the flocs size that most affects the flocs resistance. This explains the higher resistance of flocs produced with E1+, in industrial water, which are smaller in size.

Flocs produced in industrial water become generally more compact after breakage than those produced in distilled water, mainly when breakage occurs by sonication (Tables 3.9 and 3.16). These differences are more notorious in the secondary flocs (*SE* values). The secondary aggregates are more compact in industrial than in distilled water (Tables 3.9 and 3.16). When the breakage resulted from hydrodynamic shearing (erosion mechanism) the densification is almost negligible.

Table 3. 15. Flocs break up percentages for the flocculants studied in industrial water.*

Alpine-Floc™	**Dosage (mg/g)**	**Break up (%)**	
		20 kHz	**2200 rpm**
E1	8	40	16
	20	55	5
E1+	25	31	17
	35	40	9
E1++++	10	36	18
	30	60	12

* grey lines refer to the optimum flocculant dosage

Table 3. 16. Mass fractal dimension and scattering exponent after 5 min of reflocculation in industrial water.*

Alpine-Floc™	Dosage (mg/g)	20 kHz		2200 rpm	
		d_F	SE	d_F	SE
E1	8	1.50	2.66	1.52	2.66
	20	1.45	2.65	1.37	2.69
E1+	25	1.46	2.62	1.41	2.68
	35	1.45	2.59	1.23	2.65
E1++++	10	1.51	2.63	1.48	2.62
	30	1.49	2.59	1.30	2.64

* grey lines refer to the optimum flocculant dosage

3.4 - CONCLUSIONS

Firstly, the results obtained in this chapter demonstrated the advantage of using the LDS technique to evaluate and understand the flocculation process and to determine the flocs characteristics. The developed experimental methodology allows, in a single integrated test, the acquisition of information on the evolution with time of flocs dimensions and structure and also the evaluation of flocs resistance and flocculation kinetics. This led to the definition of the optimum flocculant dosage and to the understanding of the flocculation mechanisms involved that could be correlated with the mass fractal dimension and the scattering exponent of the flocs. With this method, it was possible to study the influence of polyelectrolyte charge density and degree of branching and polymer concentration on the flocculation process of PCC, used in papermaking, and on flocs properties.

Thus, it is legitimate to conclude that LDS is a valuable tool to assess the performance of polymeric flocculants, being particularly suited to study flocculation in a turbulent environment. The results obtained by image analysis confirmed the validity of the LDS results. Furthermore, it was demonstrated that the LDS technique is a better tool to determine flocs characteristics than other traditional techniques like image analysis.

The comparison of flocculation tests induced by eight polymers with high molecular weight shows that polymer charge density, polymer structure and dosage affect

the flocculation mechanism and the flocs structure. As the flocculant concentration increases, the flocculation rate decreases and flocs structure becomes more open.

Moreover, flocculants of low and medium charge density act by the bridging mechanism whereas flocculants of high charge density flocculate mainly by the patching mechanism. However, the capacity to form patching bonds is reduced due to the very high molecular weight of the polymers of high charge density studied. The optimum flocculant dosage decreases as the polymer charge density increases. As a result, as the polymer charge density decreases flocs produced are larger and have a more open structure.

When flocculation takes place by bridging, flocs restructuring occurs during flocculation. This was confirmed by the zeta potential measurements that indicate the existence of polymer reconformation during the flocculation process. However, these measurements do not allow obtaining information about the optimal dosage, the flocculation mechanism or the flocculation kinetics.

Furthermore, branching of the polymer of high charge density also reduced the capacity to form patching bonds. For the polymers of medium charge density studied, the optimum flocculant dosage increases when going from a linear to a branched structure but, for the very high branched polymer the optimum dosage slightly decreases. Flocculation is faster when linear polymers are used. Moreover, flocs restructuring is less notorious when linear and highly branched polymers are used. In the first case, flocs restructuring is reduced due to the high speed of the flocculation process. In the second case, flocs restructuring is reduced because polymer reconformation becomes more difficult due to the more coiled structure of this polymer. Consequently, these polymers produce smaller and denser flocs when comparing with the low branched polymers, the linear polymer being the one that produces the smallest and densest flocs. Additionally, the effect of the branching degree on the flocs structure and size is less significant when polymers of low charge density are used.

LDS was also successfully applied to study deflocculation and reflocculation processes when flocs were submitted either to sonication or to an increase of the hydrodynamic shearing, in the same test carried out to study the flocculation stage.

Despite the decrease in the flocs size under hydrodynamic shearing being less notorious than under sonication, the same trends are detected. When flocs were submitted to sonication the rupture occurs by fragmentation while it occurs by erosion when flocs are submitted to the increase of the pump speed. It was shown that when the polymer is in

excess, flocs strength can increase. On the other hand, as the polymer charge density increases the flocs resistance increases. However, independently of the charge density, the presence of the polymer branches reduces flocs resistance but this reduction of the flocs strength is mainly due the flocs size. As the flocs size increases the flocs strength decreases.

Reflocculation is very small or practically inexistent for all the polymers studied, with the exception of the linear polymer of high charge density that produces flocs that partially reflocculate. The structure of the reflocculated flocs is always more compact than before flocs break up and continues to be more open as the charge density decreases.

The LDS technique was, in the same way, used to investigate, with success, the effect of the microparticles on the reflocculation process and the influence of the water cationic content on flocculation, deflocculation and reflocculation processes and on flocs properties.

Reflocculation of flocs produced with polymers of low and medium charge density combined with microparticulate systems was significantly improved. As the flocs strength decreases the effect of the microparticles on reflocculation increases. However, the charge density of the polymers affects the action of the microparticles during reflocculation. The action of the microparticles is reduced as the charge density decreases. Reflocculated flocs without microparticles have a denser structure than reflocculated flocs with microparticles.

Additionally, FBRM, a particle size measurement technique that has been reported in the literature as a tool to monitor flocculation in papermaking was also applied in this study. The FBRM measurements performed agree well with those obtained by the LDS for the flocculants of medium charge density, and thus, similar conclusions could be extracted about the effect of the polymer structure on the optimum flocculant dosage, on flocculation kinetics, deflocculation and reflocculation processes. However, this technique does not allow evaluating, for the flocculants studied, the effect of the polymer properties on the flocs characteristics (size and structure) because of the experimental conditions in the FBRM. Indeed, the high concentration of the suspension and the high shear rate needed to perform flocculation tests using FBRM, result in very fast flocculation kinetics (occurring in less than 1 minute) and in similar flocs size independently of the degree of the polymer branching. Moreover, FBRM could not be used when high concentrations of polymer were required, or when very large flocs were obtained, due to adhesion problems, as was the

case with the G1 series. Adhesion made it also difficult to study, in some cases, reflocculation induced by microparticles. Furthermore, due to test limitations to induce flocs break up, it is also more difficult to study flocs resistance if the FBRM technique is used. Another difficulty experienced with the FBRM technique had to do with the uncertainty of the first points in the flocculation kinetics curves, due to the fact that particles smaller than 5 µm can not be detected by FBRM. Hence, to study the effect of the polymer properties on the flocculation, deflocculation and reflocculation processes and on the flocs characteristic, the LDS technique proved to be more adequate. Furthermore, the LDS technique allows estimating the flocs structure by the fractal dimension calculation.

Despite the flocculation processes monitored by FBRM measurements being closer to the industrial scale processes, the LDS technique can be a good tool to screen flocculants performance for these industrial processes. Indeed, it was proved that doubling the particles concentration did not alter the flocculation process. Moreover, the results obtained by LDS can be extrapolated to the industrial scale since the main conclusions obtained with the FBRM measurements are similar to those obtained with the LDS measurements.

Finally, having in mind water closure in industrial plants, flocculation was also performed in industrial water (white water). The high cationic content of the industrial water enhances the flocculation kinetics. Nevertheless, the optimum flocculant dosage becomes higher in industrial water due to the more coiled conformation of the polymer and the presence of contaminants which increases the particle zeta potential. Flocs restructuring is less notorious and this was confirmed by zeta potential measurements. The branched flocculant is less affected by the cationic content of the water. For the linear polymer, the more coiled configuration of the polymer in industrial water results in larger and less compact flocs than in distilled water. The effect of sonication and of pump speed on flocs resistance when industrial water is used is similar to the one observed in distilled water. Moreover, since flocculation occurred by the bridging mechanism, reflocculation capability of the flocs is very low in industrial water and the reflocculated flocs become, generally, more compact than those produced in distilled water.

It can be concluded that highly branched flocculants are less affected by the water cationic content in all the stages, flocculation and break up, thus leading to similar flocs structures independently of the suspending medium.

CHAPTER 4 – RETENTION AND DRAINAGE EVALUATION IN THE DYNAMIC DRAINAGE ANALYSER

4.1 - INTRODUCTION

In papermaking, chemical flocculation is fundamental for achieving both a high retention and a high drainage rate simultaneously (Forsberg and Ström, 1994; Whipple and Maltesh, 2002, Cadotte *et al.*, 2007). However, the choice of the retention aid systems has to be made with caution since retention, drainage and sheet formation depend on several factors for example on flocculants characteristics and dosage or residence time (Norell *et al.*, 1999).

The branched polymers are expected to exhibit better performance than the linear ones on fast paper machine, and thus, have a significant potential as papermaking retention aids (Shin *et al.*, 1997a, 1997b; Brouillette *et al.*, 2004, 2005). However, the few studies presented so far have always been based on retention and drainage performance of these polymers in microparticulate systems. Hence, it is of great interest to study these new polymers in single component system in order to understand better the mechanisms involved.

Therefore, the objective of this study is to evaluate the effect of the degree of polymer branching on retention and drainage performance and, simultaneously, to correlate the results with flocculation kinetics and flocs structure making use of the flocculation tests presented in Chapter 3. Additionally, the effects of flocculant concentration, flocculant charge density and flocculant contact time with the furnish were investigated.

Drainage tests were performed in a Dynamic Drainage Analyser which was kindly provided by the Paper and Forest Research Institute RAIZ (Portugal).

The pulp suspension at 1% of consistency and with 20% of PCC was flocculated with seven of the flocculants used in Chapter 3 (BHMW, E1, E1+, E1++++, G1, G1+ and G1++++). Flocculation was performed varying the flocculant dosage. The optimum flocculant dosage found by LDS technique (Chapter 3) was always tested. Moreover, two different flocculant contact times were tested.

4.2 – EXPERIMENTAL STRATEGY

4.2.1 – MATERIALS

In all experiments a eucalyptus bleached kraft pulp was used. The length weight of the fibres was 0.582 mm. The pulp suspension, refined to 32º SR, was diluted to a consistency of 1% in distilled water.

The PCC suspension and the flocculant solutions were prepared in distilled water in the same manner as described in section 3.2.1.

4.2.2 – DRAINAGE EVALUATION

Drainage tests were carried out using the dynamic drainage analyser (DDA, AB Akribi Kemikonsulter) which is able to come as close to papermaking conditions as possible (see section 1.2.5.1).

The pulp suspension was prepared by mixing 500 mL of the fibre suspension and 100 mL of the PCC suspension (20% (w/w of fibre)). The mixture was added to the DDA vessel equipped with a 350 μm square openings wire. In this way, a solid concentration (fibre + PCC) of 10 g/L was reached. The vacuum was maintained at 30 kPa and the stirring speed in the vessel was 800 rpm. The suspension of fibre and PCC was stirred during 2 minutes before the addition of the flocculant in an adequate concentration. For each experiment, the flocculant contact time varied from 30s to 90s and a drainage test without flocculant (blank) was performed daily.

4.2.3 – RETENTION EVALUATION

The wet sheets obtained from the drainage tests in the DDA were used to determine fines and filler retention. The residues collected were dried at 105ºC to calculate the total solid retention. Afterwards, the samples were burned at 600ºC during 16 hours to determine the PCC retention degree (Ferreira *et al.*, 2005).

4.3 – RESULTS AND DISCUSSION

4.3.1 – RETENTION AND DRAINAGE

4.3.1.1 – Drainage results

Drainage tests were performed for the optimum flocculant dosage found by LDS and for a common flocculant dosage, 6 mg/g (mg of flocculant/g of PCC) for all the flocculant used. Moreover, for G1+ and G1++++, drainage tests were performed for 20 mg/g and for E1 and E1+, flocculant dosages of 2 mg/g and 16 mg/g, respectively, were also tested. For the BHMW polymer, drainage tests were also performed for 2 mg/g. Flocculant dosages tested in the DDA are summarized in Table 4.1 for all the flocculants used. As an example, Figure 4.1 shows the drainage curves obtained for E1 when the flocculant contact time was 90s.

Table 4. 1. Flocculants dosages tested in the DDA.

Alpine-Floc™	**G1**	**G1+**	**G1++++**	**E1**	**E1+**	**E1++++**	**BHMW**
Optimum dosage found by LDS (mg/g)	10	30	30	4	12	8	6
Others dosages (mg/g)	6	6, 20	6, 20	2, 6	6, 16	6	2

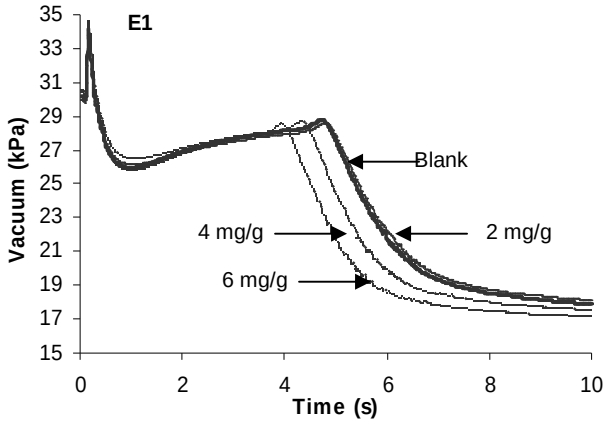

Figure 4. 1. Drainage curves obtained for several E1 dosages and for 90 seconds of contact time.

The main results obtained from the drainage tests (drainage time, sheet permeability, total solid retention and PCC retention) in the DDA are summarized in Tables 4.2 and 4.3.

Table 4. 2. Drainage tests results for 30 seconds of contact time.*

Alpine-Floc™	Dosage (mg/g)	Drainage time (s)	Final vacuum through the sheet (kPa)	Total solid retention (%)	PCC retention (%)
Blank	-	5.10	16.8	84.3	11.5
G1	6	3.81	14.4	94.1	73.1
	10	3.78	14.2	94.7	76.3
G1+	6	4.96	16.7	89.7	41.9
	20	5.14	16.2	94.7	72.2
	30	5.34	16.1	95.8	78.6
G1++++	6	4.82	16.2	86.0	24.9
	20	4.70	16.0	94.0	73.4
	30	4.68	16.0	94.7	77.7
E1	2	4.27	15.8	92.6	59.8
	4	3.73	14.9	95.5	76.9
	6	3.42	14.4	96.6	83.5
E1+	6	4.05	15.2	96.0	78.9
	12	3.48	14.5	96.0	78.8
	16	4.16	14.9	96.0	78.9
E1++++	6	3.78	14.6	95.4	76.5
	8	3.56	14.2	95.4	76.2
BHMW	2	5.91	18.0	93.8	72
	6	4.92	17.0	94.0	73.3

* grey lines refer to the optimum flocculant dosage

Table 4. 3. Drainage tests results for 90 seconds of contact time.*

Alpine-Floc™	Dosage (mg/g)	Drainage time (s)	Final vacuum through the sheet (kPa)	Total solid retention (%)	PCC retention (%)
Blank	-	5.10	16.8	84.3	11.5
G1	6	3.76	14.7	94.6	75.8
	10	3.78	13.7	95.9	83.9
G1+	6	4.93	16.7	89.6	41.5
	20	4.98	16.2	95.0	73.5
	30	4.93	16.2	95.7	77.6
G1++++	6	4.67	16.5	88.4	39.2
	20	4.62	15.9	94.8	78.0
	30	4.45	16.1	96.7	89.4
E1	2	4.89	16.6	94.6	71.7
	4	4.39	16.1	95.6	77.4
	6	4.01	16.0	96.0	79.9
E1+	6	4.02	15.3	96.6	82.1
	12	3.49	14.5	96.5	81.7
	16	3.64	14.7	95.6	76.1
E1++++	6	3.99	15.4	94.8	72.3
	8	3.67	14.8	95.2	75.1
BHMW	2	6.65	18.3	93.9	72.6
	6	5.90	18.4	93.8	72.4

* grey lines refer to the optimum flocculant dosage

In order to compare drainage results, the normalized drainage times were calculated relatively to the drainage time of the blank test. The normalized drainage times for 30 and 90 seconds of contact time are represented in Figures 4.2 and 4.3 as a function of flocculant dosage, for all the flocculants tested. The average drainage time for blank experiments is 5.1 seconds (± 0.5s).

The addition of G1+ and G1++++ does not improve the drainage time relatively to the blank. For the high flocculant concentrations, for which G1+ and G1++++ reach the

optimum flocculant dosage, the amount of flocculant is too high leading to an increase of the suspending medium viscosity, and thus, to an increase of the drainage time. On the contrary, when dosed at a lower level of 6 mg/g, the degree of flocculation is low, far from the optimum flocculant dosage (30 mg/g) resulting in a drainage time close to the one observed for the blank unflocculated suspension. The same occurs when 2 mg/g of the BHMW polymer is used resulting in a higher drainage time when comparing with what is observed for the unflocculated suspension.

For the other polymers, all the flocculated suspensions exhibit a lower drainage time than the unflocculated one. As the flocculant concentration becomes close to the optimum dosage, lower drainage times are observed. Hence, despite the flocculation results being related only with the flocculation of PCC suspension and the operating conditions being different in the DDA and in the LDS, it is possible to observe a good correlation between the flocculation tests (performed in the LDS) and the drainage tests performed in the DDA. In fact, it is observed that a lower drainage time (DDA) corresponds to the optimum flocculant dosage determined by LDS. This can be explained by the fact that in a composite furnish containing refined fibres, fines and filler particles, the polymer adsorbs preferentially on the filler and flocculates it (Whipple and Maltesh, 2002). Thus, LDS and DDA tests can be regarded as complementary techniques to pre-screen flocculants for use in papermaking.

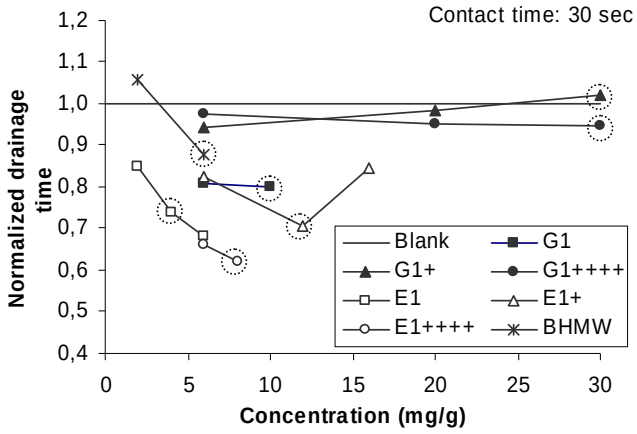

Figure 4. 2. Normalized drainage time as function of flocculant concentration for 30s of contact time (optimum dosage).

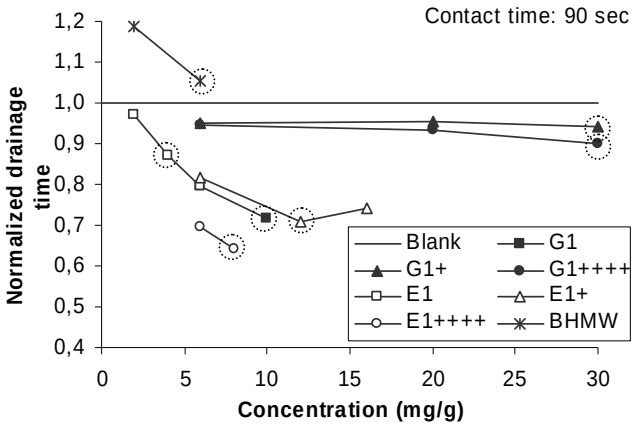

Figure 4. 3. Normalized drainage time as function of flocculant concentration for 90s of contact time (optimum dosage).

In the case of E1+, if the flocculant concentration increases too much, the drainage time increases again. When the flocculant is in excess, the flocculation progresses at a lower rate as shown by LDS and, thus, for the flocculant contact time used in these studies the flocs are still too small (low flocculation) and the sheet structure is relatively close to the blank and so is the drainage time.

The flocculant contact time is also an important parameter. For the E1 series and for the BHMW polymer, the increase in the contact time results in an increase in the drainage time while for the G1 series the increase in the contact time results in a decrease in the drainage time. However, the highest drainage time variations with the contact time are observed for the linear polymers BHMW, E1 and G1. The trend of the drainage time with flocculant contact time observed for the E1 series and the BHMW polymer agrees with the work of Forsberg and Ström (1994). They demonstrated that the increase of the drainage time with the contact time is due to the polymer configuration at the particle surface. At the first stage of the flocculation process the polymer has an extended conformation at the particle surface but as the time increases the flocs become smaller and more compact due to the polymer reconformation and degradation. In this case, it becomes more difficult to remove the interstitial water from this type of flocs, and thus, the drainage time increases. However, when the polymer E1+ is in excess (16 mg/g), the drainage time decreases as the contact time increases: for such dosage the flocculation degree is higher at 90 s than at 30 s resulting in the improvement of the drainage time.

Nevertheless, the G1 series does not follow this behaviour. LDS results have shown that flocs produced with the G1 series is much larger than those produced with the E1

series and the BHMW polymer due to the very low charge density, therefore resulting in overflocculation and producing too large flocs that reduce the drainage performance. In this case, the decrease of the flocs size with flocculation time due to polymer reconformation and degradation reduces the effect of the overflocculation, and thus, results in drainage time decrease with flocculant contact time increase.

Figures 4.4 and 4.5 summarize the final vacuum normalized relatively to the final vacuum obtained in the blank tests, through the formed sheet, as a function of the flocculant concentration. A low final vacuum corresponds to a high sheet permeability, i.e., to high sheet porosity. The final vacuum average through the sheet for the unflocculated suspension is 16.8 kPa (± 0.6 kPa). The same trend observed for the drainage time is verified for the sheet permeability when the flocculant dosage varies. In fact, lower drainage times correspond to higher sheet permeabilities that correspond to lower final vacuums through the sheet (Forsberg and Bengtsson, 1990). Figures 4.6 and 4.7 confirm the linear correlation between the drainage time and the sheet porosity.

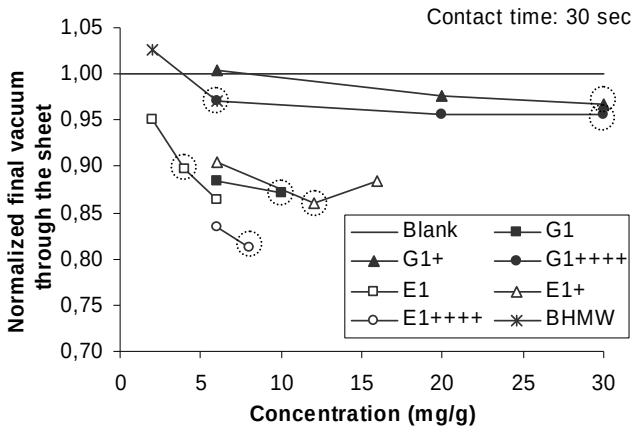

Figure 4. 4. Normalized final vacuum as function of flocculant concentration for 30s of contact time (◌ optimum dosage).

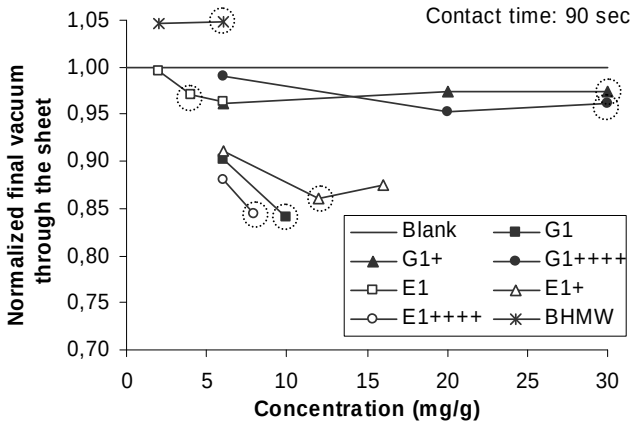

Figure 4. 5. Normalized final vacuum as function of flocculant concentration for 90s of contact time (optimum dosage).

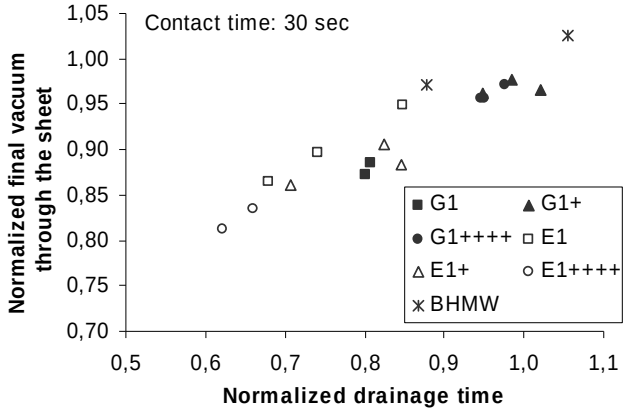

Figure 4. 6. Normalized final vacuum as function of normalized drainage time (contact time: 30s).

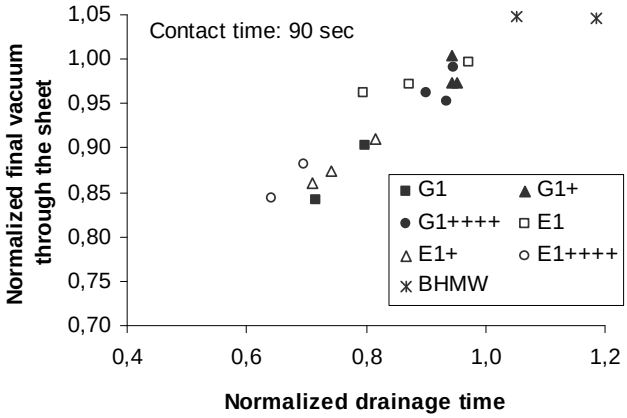

Figure 4. 7. Normalized final vacuum as function of normalized drainage time (contact time: 90s).

From these first results, it is possible to conclude that the behaviour of the E1 polymers series corresponds to the most adequate situation for modern papermaking production, since the fast paper machines require good dewaterability with low contact time. Moreover, for this series of polymers, a significant improvement of the drainage time can be achieved with the low flocculant dosage. The highly branched polymer, E1++++, exhibits the best result in a compromise between the flocculant dosage and the drainage time.

4.3.1.2 – Retention results

The PCC retentions, normalized relatively to the PCC retention obtained for the blank tests, are plotted for the seven polymers against the polymer dosage in Figures 4.8 and 4.9. The total solid retention is not plotted here since the change in total retention is mainly caused by filler retention as referred by Cadotte *et al.* (2007) (see Tables 4.2 and 4.3). This fact confirms also that the polymer flocculates the filler preferentially. The total solid retention and the PCC retention averages of the unflocculated suspension are 84.3% (±0.5%) and 11.5% (±1%) respectively.

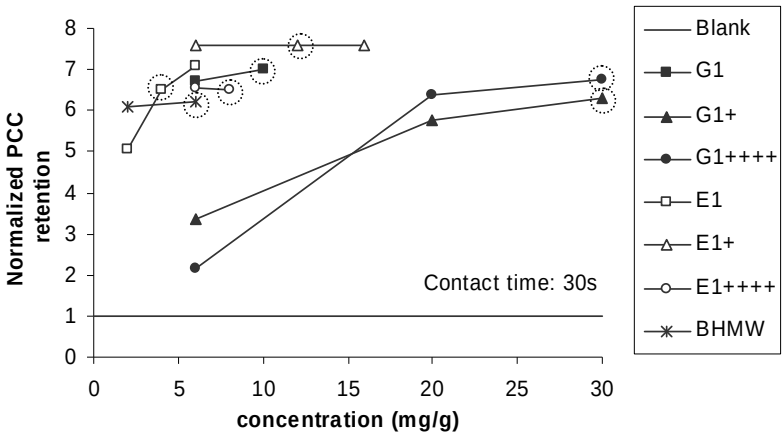

Figure 4. 8. Normalized PCC retention as function of flocculant concentration for 30s of contact time (◌ - optimum dosage).

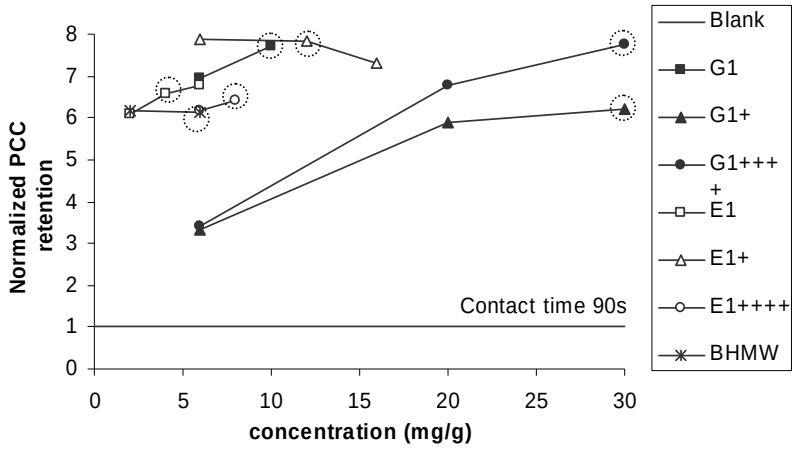

Figure 4. 9. Normalized PCC retention as function of flocculant concentration for 90s of contact time (optimum dosage).

In general, for all the polymers tested, the maximum in the PCC retention corresponds to the optimum flocculant dosage. However, as flocculant dosage increases further, retention tends to reach a plateau. Hence, it is possible to find a flocculant dosage range where a low drainage time and a high PCC retention can be achieved simultaneously. In this study, this range is 5-10 mg/g of PCC for all the polymers, except for the G1+ and G1++++ polymers. At the lowest flocculant concentration, G1+ and G1++++ not only impair drainage but also present the worst results for PCC retention. Low flocculation results in a low drainage rate and in a low PCC retention because the poorly flocculated suspension behaviour is close to the one observed for the unflocculated suspension. At higher dosages of G1+ and G1++++, the PCC retention is similar to the ones observed for the other polymers. In this range, E1+ offers the best PCC retention and BHMW the lowest PCC retention.

As for drainage, the increase in the contact time impairs the PCC retention for the E1 series as opposed to the G1 series that improves retention, though the differences, as far as retention is considered, are small. As a consequence, the E1 series is again more adequate as a retention aid for papermaking.

Drainage and retention results have shown that branched flocculants of medium charge density give the best results as retention and drainage agents. However, it is important to stress that E1++++ is probably the most adequate polymer to improve retention and drainage simultaneously. Indeed, with this polymer the retention degree is high despite of being slightly smaller than with E1+ and, most important, the drainages times are the lowest with a low flocculant dosage. Moreover, in section 3.3.5 of the

Chapter 3, it was shown that this polymer is less affected by the changes in the cationic content of the suspending medium due to its branched configuration.

It can be concluded, based on the results presented, that the advantages of the use of highly branched polymers for improving retention and drainage of pulp fibre suspensions suggest that these types of flocculants have a significant potential as retention aid in papermaking.

4.3.2 – CORRELATION WITH FLOCS PROPERTIES

Since the best results for both retention and drainage are obtained close to or for the optimum flocculant dosage, the effect of flocs size and structure on the drainage time is investigated for the optimum flocculant dosage obtained by LDS (Figures 4.10 and 4.11).

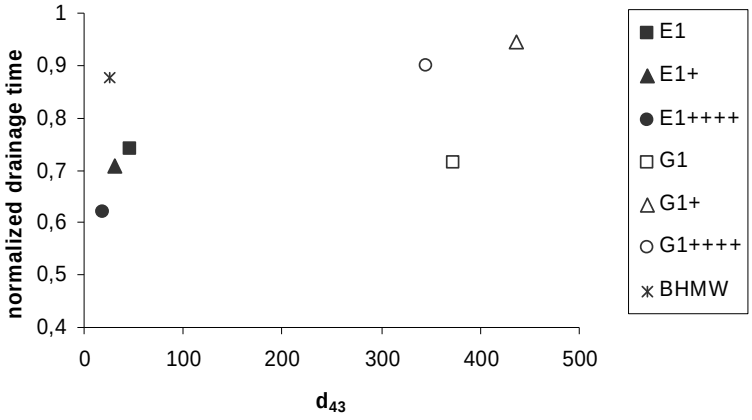

Figure 4. 10. Normalized drainage time as function of mean floc size for the optimum flocculant dosage.

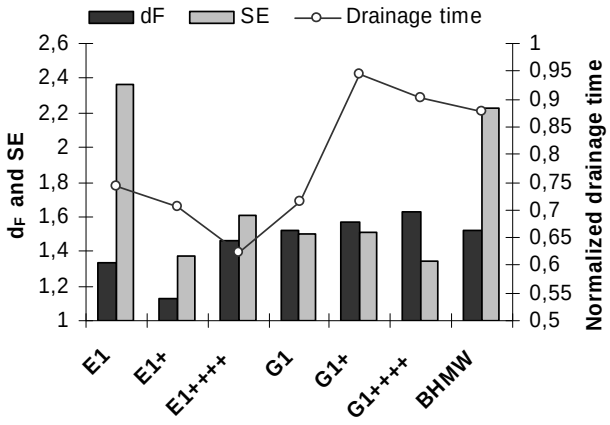

Figure 4. 11. Flocs structure and normalized drainage for optimum flocculant dosage.

The normalized drainage time corresponding to the optimum flocculant dosage is represented in Figure 4.10 as a function of the average flocs size. The results correspond to a flocculation time of 30 and 90 seconds, for the E1s and BHMW polymers and for the G1s polymers respectively, for which both drainage and retention give best results. The drainage time decreases with the decrease in the flocs size. The E1 series produces the smallest flocs. Additionally, E1++++ is the flocculant that produces the smallest flocs and gives the lowest drainage time. Thus, it can be concluded that it is possible to have fast dewatering and high filler retention with small flocs. However, the BHMW polymer produces also smaller flocs but, in this case, this does not correspond to a fast drainage rate. It will next discuss if this behaviour is somehow related with flocs structure.

Larger flocs reduce the drainage rate as confirmed for the G1 series, since they retain much more interstitial water that is difficult to remove. So, overflocculation (very large flocs) results in low drainage despite retention being not significantly affected.

The drainage time is plotted as a function of the flocs structure, quantified by the mass fractal dimension and by the scattering exponent, for the optimum flocculant dosage, in Figure 4.11. The mass fractal dimension, d_F, gives indication about the structure of the primary flocs while the scattering exponent, *SE*, gives information about the structure of secondary flocs that result from the aggregation of the primary ones. The mass fractal dimension and the scattering exponent are represented for the maximum in the flocculation kinetic curve as reported in Chapter 3. Primary flocs produced with E1 are open (small d_F) while the secondary flocs are compact (high *SE*). Both primary and secondary flocs produced with E1+ are open (small d_F and *SE*) when comparing with the E1 flocs. Besides, the configuration of flocs produced with E1++++ seems to be the most adequate to easily remove the water from the flocs, since the primary flocs are slightly more compact than with E1+, while secondary flocs are open comparing with E1 and E1+.

However, the structure of the flocs produced with the G1 series is similar to the structure of the E1++++ flocs. In this case, the drainage time is mainly affected by the larger floc size (overflocculation).

Moreover, despite the flocs produced with the BHMW polymer being small, as observed in Figure 4.10, their structure is quite different from the one produced with the E1+ and E1++++ polymers (d_F is small and *SE* is high). Thus, the drainage time is much higher for flocs produced with the BHMW polymer. In fact, the BHMW polymer has a very high charge density, and thus, it adsorbs at the particle surface in flatter configuration. Consequently, flocs produced with the BHMW polymer are simultaneously smaller and

more compact than flocs produced with the E1 polymers series. The very compact secondary aggregates make drainage more difficult and, therefore, drainage time is higher.

4.4 - CONCLUSIONS

As expected, the polymer characteristics namely the charge density and the number of branches affect the drainage and the retention performance in papermaking.

Flocculants either of low charge density and of too high charge density do not improve drainage time compared to the unflocculated suspension but offer very high filler retention. In the case of polymers of low charge density, an increase of the flocculant contact time can slightly decrease the drainage time and increase filler retention. For polymers of very high charge density, the opposite is verified, due to the very compact structure of the flocs obtained as flocculation proceeds.

Polymers with medium charge density offer simultaneously low drainage times and very high filler retentions at low flocculant dosage and at low flocculant contact time.

The lowest drainage times are obtained for the optimum flocculant dosage determined by the LDS technique. A low flocculation degree also results in a low drainage rate and, mainly, in poor filler retention. Thus, the optimization of the polymer dosage performed using the LDS technique is important when analysing retention and drainage performance.

Polymers of medium charge density and with a branched structure improve significantly the drainage rate and filler retention comparing with the linear ones. In this case, the improvement in the drainage time is due to the formation of small flocs sizes with an open structure, mainly at the secondary aggregates level. The increase of the drainage time for the linear polymers with medium and high charge density is due to the more compact structure of the small flocs formed.

To summarize, it can be stated that polymers of medium charge density are more suitable to be used as retention aid because low drainage time and very high filler retention are obtained simultaneously, with low flocculant contact time and low flocculant dosage. Moreover, highly branched polymers can be considered an adequate choice because the balance between flocculant dosage, drainage time and filler retention is the best. Thus, these polymers represent a promising additive for papermaking.

CHAPTER 5 – RHEOLOGICAL BEHAVIOUR OF FLOCCULATED SUSPENSIONS

5.1 - INTRODUCTION

Since the paper industry relies on the transport of pulp in aqueous media, it is of real interest to evaluate and understand the rheological behaviour of flocculated pulp suspension. In this way, rheological measurements have been performed in the rotational viscometer developed by UCM (Blanco *et al.*, 1995) which were afterwards correlated with flocculation results from Chapter 3.

In all experiments the same eucalyptus bleached kraft pulp used in drainage tests presented in Chapter 4 are used. The pulp suspension with 20% (w/w of fibre) of PCC was flocculated with four of the polyelectrolytes used in Chapter 3 (A1++, BHMW, E1+ and E1++++). Flocculation was performed at 1% of pulp consistency for a common flocculant concentration (6 mg/g) and for the optimum flocculant dosage found by LDS for each flocculant (Chapter 3).

5.2 – EXPERIMENTAL STRATEGY

5.2.1 – MATERIALS

The fibres, the PCC and the flocculants materials are similar and were prepared in the same manner of those used in Chapter 4.

5.2.3 – RHEOLOGICAL TESTS

The pulp suspension was prepared daily at a concentration of 10 grams of fibres per litre and with 20% (w/w of fibre) of PCC. The pulp suspension obtained (6.5 L) was stirred during 2 minutes before adding the flocculant in the adequate dosage. Flocculation takes

place during 5 minutes. After that the flocculated suspension was transferred to the vessel of the viscometer developed by UCM (see section 1.4). The rotational speed of the rotor of the viscometer was increased gradually from 0 to 45 rad/s in steps of 5 rad/s. All experiments were carried out at room temperature approximately 23ºC. A test was carried out in the same way but without flocculant. Rheological tests were repeated at least once.

5.3 – RESULTS AND DISCUSSION

The rheograms for the unflocculated and flocculated pulp suspensions are represented in Figures 5.1 to 5.2 for the optimum flocculant dosage and for 6 mg/g. The optimum dosage for BHMW is 6 mg/g, for A1++ is 4 mg/g, for E1+ is 12 mg/g and for E1++++ is 8 mg/g as presented in Chapter 3.

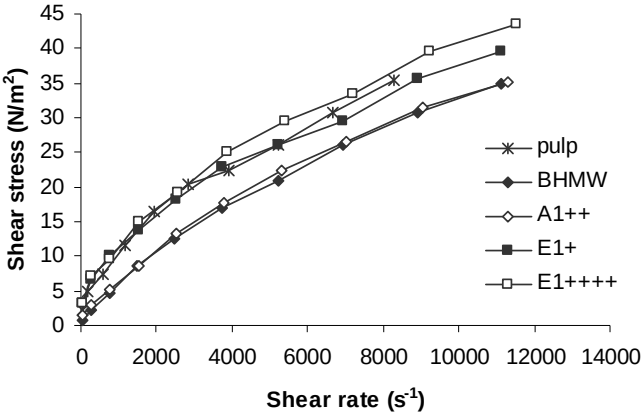

Figure 5. 1. Rheograms for the unflocculated and flocculated pulp suspensions for the optimum flocculant dosage.

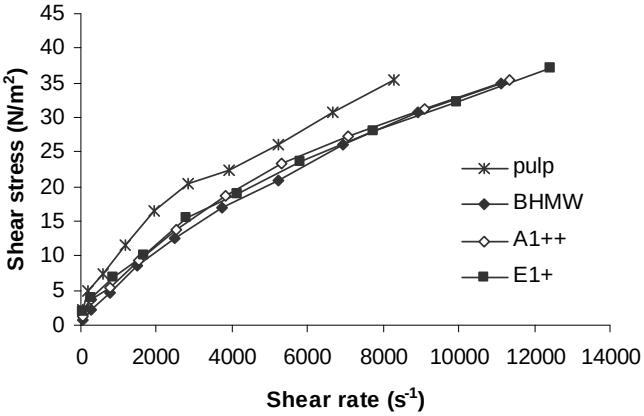

Figure 5. 2. Rheograms for the unflocculated and flocculated pulp suspensions for 6 mg/g of polymer.

For the A1++ and BHMW polymers and for both 6 mg/g and for the optimum flocculant dosage, the flocculant addition decreases the shear stress indicating that the presence of the aggregates decreases the effect of the continuous fibre network. In the case of E1+ and E1++++, at 6 mg/g the flocculant addition effectively decreases the shear stress of the suspension, although, at the optimum flocculant dosage, rheological behaviour is similar to the unflocculated suspension. In order to understand what is happening, the rheograms were fitted to the Herschel-Bulkley model described by Equation 1.11 (Chapter 1). The correlation coefficient obtained by fitting the experimental results to the model are always higher than 0.99 indicating that this model is adequate for describing the flow behaviour of the pulp suspensions. From these fits, the behaviour indexes, n ($\pm$ 0.01), are obtained for all the rheological tests and are correlated with the median flocs size at the end of the flocculation process acquired by LDS (Chapter 3). Figure 5.3 shows results for the optimum flocculant dosage and Figure 5.4 for a flocculant dosage of 6 mg/g.

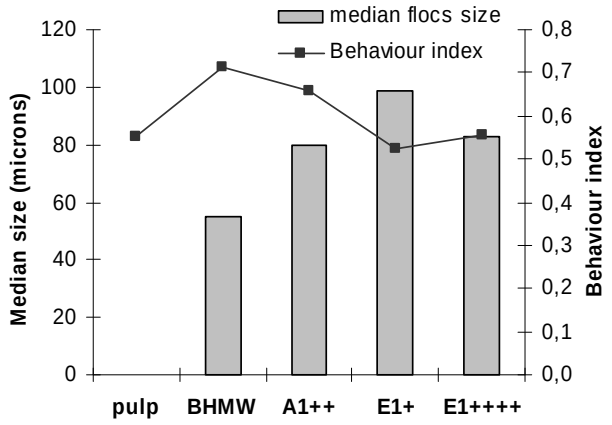

Figure 5. 3. Median flocs size and behaviour index for the optimum flocculant dosage.

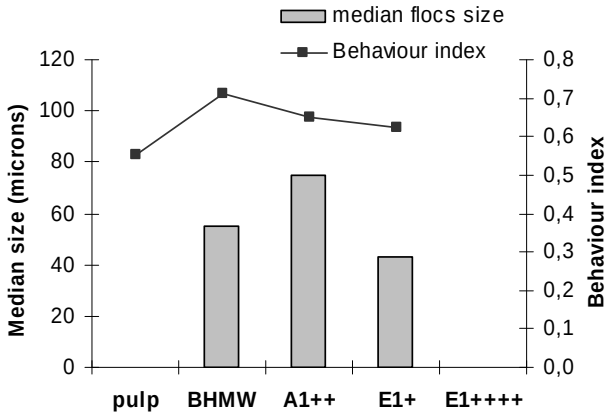

Figure 5. 4. Median flocs size and behaviour index for a flocculant dosage of 6 mg/g.

For each rheological test presented in Figures 5.1 and 5.2, the yield stresses obtained are always lower than 1 N/m^2. Consequently, the flow behaviour of the suspensions can be considered to be pseudoplastic as referred by Negro and co-workers (2006).

The behaviour index, *n*, quantifies the deviation from Newtonian behaviour, and thus, a closer behaviour index to the unity indicates a rheological behaviour closer to Newtonian. From Figures 5.3 and 5.4, the flocs size seems to affect the behaviour index, and consequently, the rheological behaviour. In fact, for the optimum flocculant dosage (Figure 5.3), as the flocs size increases the behaviour index decreases indicating that smaller flocs correspond to a rheological behaviour closer to the Newtonian one. The higher behaviour index obtained for the suspension flocculated with BHMW can be related with the Newtonian flow (n=1). In fact, a behaviour index closer to unity indicates a higher stiffness of the aggregates. In this case, the stiffness of the flocs produced with BHMW is higher than for the other polymers studied and is mainly due to the polymer configuration at the particle surface. On the other hand, comparing the results for E1+ for which the decrease of the flocs size is more notorious with the flocculant dosage (Figures 5.3 and 5.4), the behaviour index increases with the decrease of the flocculant dosage since smaller flocs are obtained with the lower dosage. However, despite the A1++ and E1++++ polymers producing flocs of similar size, the behaviour index is very different (Figure 5.3). This indicates that the behaviour index also depends on the flocculant characteristics that affect namely the flocs size and structure and their resistance as seen in Chapter 3.

Moreover, as referred by Negro and co-workers (2006), when a pulp suspension is submitted to hydrodynamic forces, the break up of the flocs can be by erosion or/and by fragmentation. For a pseudoplastic suspension, the erosion of the aggregates reduces the behaviour index while their fragmentation increases it. In addition, as seen in Chapter 3, the flocs resistance depends essentially on the flocs size and as the flocs size increases the flocs resistance decreases. So, in this case, since the behaviour index decreases with the decrease of the flocs resistance (increase of the flocs size), flocs break up must occur by erosion.

The behaviour index can also be related with the polymer configuration on the particle surface which is known to affect the flocs resistance. In Chapter 3, it was shown that flocs produced with the BHMW polymer are smaller and the flocs are stronger due to the flat configuration that the polymer adopted at the particle surface. This agrees with the rheological results where, for the BHMW polymer the maximum behaviour index is

reached indicating that flocs erosion is less notorious. In the case of A1++ and E1++++, the first one has a higher charge density thus, the polymer chains are more strongly attached to the particles than the polymer chains of E1++++ and erosion of flocs is more difficult with A1++ (higher *n* for A1++) despite the flocs produced with both polymers being similar in size (Figure 5.3). This fact is confirmed by flocs resistance results presented in Chapter 3 where, in Table 3.7, the A1++ polymer produces stronger flocs than E1++++.

Rheological results confirm that polymer branching impairs the flocs resistance, as seen in Chapter 3, since the behaviour index does not increase with the decrease of the flocs size. Indeed, in Figure 5.3, despite the flocs size produced with E1++++ being smaller than flocs produced with E1+, the behaviour index is not significantly improved.

As referred in the work presented by Negro *et al.* (2006), the reflocculation capacity of the flocs is also a factor that affects rheological behaviour. The reflocculation capability of the flocs mitigates the effect of the erosion on the suspension behaviour resulting in an increase of the behaviour index. From results presented in Chapter 3, the BHMW and eventually the A1++ polymers are the polymers that produce flocs that can partially reflocculate after breaking up. This can explain the fact that for these flocculants the behaviour index is higher.

From the rheological study it has been demonstrated that, effectively, flocs resistance and reflocculation capacity are key factors for determining the flocculated pulp suspension behaviour. However, it must be stressed that despite the flocs size being the main factor that affects the flocs resistance, the charge density and the polymer branching have to be taken into account since they also influence the flocs resistance and the reflocculation capability. In fact, it was demonstrated in Chapter 3 that charge density and polymer branching are the key parameters that affect the flocculation mechanism, and thus, the flocs characteristics.

5.4 – CONCLUSIONS

The effect of chemical flocculation on the rheological behaviour of a pulp suspension has been studied correlating flocculation results obtained by the LDS technique with the rheological behaviour measured with the rotational device developed by UCM.

For the consistency tested, both the unflocculated and flocculated pulp suspensions exhibit a pseudoplastic behaviour and, in general, the flocculant addition reduces the resistance of the continuous fibre network to shearing.

The flocs properties, namely the flocs resistance and the reflocculation capacity as measured during the flocculation studies (Chapter 3), are well correlated with the rheological behaviour of the flocculated pulp suspensions. The rheological behaviour can be also related with the charge density and the degree of branching of the flocculants since, as demonstrated in Chapter 3, these parameters affect both the flocculation mechanism and the flocs size, and thus, the flocs resistance and the reflocculation capacity.

The choice of the flocculants is important for reducing the power consumption in papermaking. Flocculants with high charge density and without branches seem to be those that more reduce the resistance of the pulp suspension to shearing. However, this is not enough to optimise the papermaking process. Indeed, as seen in Chapter 4, linear polymers of high charge density do not improve and even impair retention and drainage in the wet-end stage. Furthermore, since the differences between the rheological behaviour of the unflocculated and flocculated pulp suspensions are small, attention has to be focused on the improvements that can be reached on retention and drainage performance as a function of the polymer characteristics. It is this last process that will be crucial for the choice of the flocculant to be used. Combining the rheological and drainage information, the highly branched polymer appears again as a promising possibility as a papermaking additive, since it maximises retention and drainage, without making the pulp suspension highly non-Newtonian.

CHAPTER 6 – FLOCCULATION PROCESS MODELLING

6.1 – INTRODUCTION

As for many other industrial processes, in papermaking the properties of the flocs formed will affect the process efficiency and the final product quality. In fact, as seen in the previous chapters, flocs characteristics influence the fines and filler retention, the water drainage and the sheet formation during the wet-end stage. Moreover, it was observed that the flocs structure and size depend on flocculant concentration and polymer characteristics. Hence, it is necessary to monitor and manipulate adequately these parameters to control flocs size and structure during the flocculation process.

In this way, to understand, predict and control the flocculation process of PCC particles by polyelectrolytes, development of a quantitative model which is able to describe flocculation under various processing conditions is of utmost importance.

In this Chapter, it will be given more attention to the flocculation process induced by the three C-PAMs of medium charge density used in Chapter 3 (E1, E1+ and E1++++). As seen, flocculation induced by these polymers occurs by bridging mechanism and flocs restructuring occurs due to polymer chain reconformation at the particles surfaces. This effect can not be neglected and has to be implemented in the model. In addition, modelization was performed also for G1++++ in order to reinforce the validation of the model proposed.

The common modelling approach is based on population balance equations. Population balance models are of great importance to describe the dynamics of particulate systems. In fact, in many applications, the particle size distribution is considered as the most relevant property that describes the process. Since variations on the particle population originate variations on the system properties, the particles need to be count. So the aim of this study is to implement a population balance model that is able to describe the flocculation process of PCC particles by bridging mechanism using the Matlab® software. In this study, the discretized population balance equation expressed by Equation 1.20 and proposed by Hounslow *et al.* (1988) and Spicer and Pratsinis (1996b) has been used to describe flocculation in terms of aggregation and breakage.

$$\frac{dN_i}{dt} = \sum_{j=1}^{i-2} 2^{j-i+1} \alpha_{i-1,j} \beta_{i-1,j} N_{i-1} N_j + \frac{1}{2} \alpha_{i-1,i-1} \beta_{i-1,i-1} N_{i-1}^2$$

$$- N_i \sum_{j=1}^{i-1} 2^{j-i} \alpha_{i,j} \beta_{i,j} N_j - N_i \sum_{j=i}^{\infty} \alpha_{i,j} \beta_{i,j} N_j - S_i N_i + \sum_{j=i}^{\infty} \Gamma_{i,j} S_j N_j \qquad (1.20)$$

Additionally, model parameters will be correlated with the polymer characteristics (concentration and branching) in order to obtain a model that can predict the aggregates characteristics (size and structure) or the operating conditions that produce aggregates with the characteristics required for a predefined performance.

6.2 – POPULATION BALANCE MODEL DESCRIPTION

6.2.1 – COLLISION EFFICIENCY

The model developed by Kusters (1997) and described by Equation 1.14 was introduced in the model of the Equation 1.20 to take into account the effect of particles size on the collision efficiency factor (see section 1.5).

$$\alpha_{ij} = \left[\frac{\exp\left(-x \left(1 - \frac{i}{j} \right)^2 \right)}{(i \times j)^y} \right] \times \alpha_{\max} \qquad (1.14)$$

In this study, we have considered $x=y=0.1$ as in the work of Selomulya *et al.* (2003) and Soos *et al.* (2006). The maximum collision efficiency value (α_{max}) is an adjustable parameter as in the work of Soos *et al.* (2006).

6.2.2 – COLLISION FREQUENCY

As stated by Smoluchowski (1917), the collision frequency between two particles is the result of the collision frequency due to Brownian motion and the collision frequency due to orthokinetic aggregation as described in Equation 6.1.

$$\beta_{ij} = \beta_{perikinetic} + \beta_{orthokinetic} \tag{6.1}$$

The collision frequency for Brownian motion is given by Equation 6.2 (Smoluchowski, 1917) where k_B is the Boltzmann constant, T is the absolute temperature and μ is the viscosity of the fluid.

$$\beta_{ij,perikinetic} = \left(\frac{2k_B T}{3\mu}\right)\frac{\left(R_{ci} + R_{cj}\right)^2}{R_{ci}R_{cj}} \tag{6.2}$$

The collision frequency for orthokinetic aggregation is given by Equation 6.3 (Saffman and Turner, 1956) where ε is the average energy dissipation rate and ν is the kinematic viscosity of the fluid.

$$\beta_{ij,orthokinetic} = 1.294\left(\frac{\varepsilon}{\nu}\right)^{1/2}\left(R_{ci} + R_{cj}\right)^3 \tag{6.3}$$

In Equations 6.2 and 6.3, R_c is the effective capture radius for the two species *i* and *j* and, for fractal aggregates, is calculated according to Equation 6.4 where r_0 is the primary particle radius, N is the number of primary particles in aggregate, k_c is a constant close to unity and d_F is the mass fractal dimension of the aggregates. The mass fractal dimension is a way of quantifying the aggregate structure, with $1<d_F<3$ (Chakraborti *et al.*, 2003). Small fractal dimension values indicate very extended and tenuous structures while larger values indicate structures mechanically stronger and quite dense (Bushell, 2005).

$$R_{ci} = r_0\left(\frac{N}{k_c}\right)^{1/d_F} \tag{6.4}$$

6.2.3 – FRAGMENTATION RATE

The fragmentation rate, S_i is given by the semi-empirical relation proposed by Kusters (1997) (Equation 6.5). In Equation 6.5, ε_{bi} corresponds to the critical energy dissipation rate that causes break-up of flocs.

$$S_i = \left(\frac{4}{15\pi}\right)^{1/2}\left(\frac{\varepsilon}{\nu}\right)^{1/2}\exp\left(\frac{-\varepsilon_{bi}}{\varepsilon}\right) \tag{6.5}$$

The critical energy dissipation rate can be related with the aggregate size using the relation observed experimentally by François (1987) (Equation 6.6). Equation 6.6 shows that the energy dissipation necessary for breakage to occur is smaller for larger aggregates and, thus, larger flocs break-up easier. Moreover, the fragmentation rate increases as the shear rate ($G = (\varepsilon/\nu)^{0.5}$) increases.

$$\varepsilon_{bi} = \frac{B}{R_{ci}} \tag{6.6}$$

B will be a fitting parameter which allows to define at which size class *i* the flocs starts to break up and with what intensity breakage occurs in this size class *i* for a given shear rate.

6.2.4 – BREAKAGE DISTRIBUTION FUNCTION

There are many ways to define the breakage distribution function. In this study, the binary breakage distribution function is used since it is simple to implement and it gives simultaneously good results (Spicer and Pratsinis, 1996b). In this case, we assume that the floc is divided into two flocs of the same size, as described by Equation 6.7, where V_0 is the volume of the primary particle.

$$\Gamma_{ij} = \frac{V_j}{V_i} \qquad for\ \ j = i+1$$

$$\Gamma_{ij} = 0 \qquad for\ \ j \neq i+1 \qquad \text{where} \quad \begin{matrix} V_i = 2^{i-1}V_0 \\ V_j = 2^{i}V_0 \end{matrix} \tag{6.7}$$

6.2.5 – FLOCS RESTRUCTURING

When restructuring of flocs occurs, the fractal dimension that quantifies the flocs structure varies with flocculation time. Hence, the model proposed by Bonanomi *et al.* (2004) and described in Equation 1.15 (see section 1.5), was introduced into the population balance model to take into account the decrease in the flocs size due to polymer conformation.

$$\frac{dd_F}{dt} = \gamma\left(d_{F,\max} - d_F\right) \tag{1.15}$$

In Equation 1.15, γ is a fitting parameter and $d_{F,max}$ is the maximum fractal dimension value. Fractal dimension values are normally obtained experimentally by using techniques as microscopy or light scattering. However, when light scattering techniques are used and when aggregate restructuring occurs, the mass fractal dimension is replaced by the scattering exponent, *SE* (Lin *et al.*, 1990; Selomulya *et al*., 2002). In fact, when restructuring occurs, we can no longer assume flocs to be primary aggregates. The restructured flocs have to be considered as secondary aggregates which then have to be described by the empirical scattering exponent.

In a second part of this study, since the decrease of the flocs size during the flocculation process is not only due to the flocs restructuring but also to the polymer degradation, we have implemented the equation proposed by Heath and co-workers in their first study (2003). Hence, the breakage irreversibility was introduced into the model by making the particle collision efficiency term decrease during flocculation time by using Equation 1.18 (see section 1.5).

$$\alpha = Ce^{-t/D} \tag{1.18}$$

6.2.6 – FLOCS SIZE DETERMINATION

Flocculation kinetics is normally monitored by the variation of the mean flocs size with flocculation time. Thus, in the population balance equation of the model (Equation 1.20) which describes the evolution of the number of particles in each size class with time, it is necessary to transform the aggregate number concentration in each class *i* to a scale of

size. In this study, the volume mean size, *d[4,3]* was calculated from the aggregate number distribution using Equation 6.8.

$$d[4,3] = \frac{\sum N_i D_i^4}{\sum N_i D_i^3} \tag{6.8}$$

In equation 6.8, N_i is the number of flocs in class i and D_i is the characteristic diameter of the class i calculated from Equation 6.9. In Equation 6.9, d_0 is the characteristics diameter for the class i=0.

$$D_i = \left(2^{\frac{i-1}{d_F}} \right) d_0 \tag{6.9}$$

6.2.7 – SOLUTION OF THE MODEL EQUATIONS

The model proposed was numerically solved using the ordinary differential equation solver in Matlab® (see Appendix A). The maximum number of intervals used was 30 (i_{max}=30) to guarantee that all the aggregates sizes are present and the initial particle diameter was set to 0.1μm which is the smallest size of the primary PCC particles.

The shear rate (G) was constant and equal to 312 s^{-1} whereas the scattering exponent (SE) at time t=0, was assumed equal to 1.65. The shear rate in the Mastersizer 2000 beaker was determined by CFD modelling using the COMSOL Multiphysics® software (Bouanini *et al.*, 2006) (see Appendix B). In fact, it was not possible to use the power curves from Holland and Chapman (1966), to calculate the shear rate from the power number, assuming a normal propeller, because the shape of the shaft is very different from the common ones, and thus, the need to make use of a CFD description of the flow in the beaker.

The maximum scattering exponent comes, in each case, from experimental data for $t = t_{max}$. The parameters (α_{max}, B, γ) estimation was done by minimising the sum of squares errors between the model and the experimental results for the change in the volume mean diameter. The objective function used for parameter estimation is described by Equation 6.10 and it was implemented in the Matlab® simulation.

$$\min_{\alpha_{max},B,\gamma} \psi = \sum_{t=0}^{t=t_{max}} \left(d[4,3]_{exp\,t} - d[4,3]_{mod\,el} \right)^2 \qquad (6.10)$$

The experimental data used refer to flocculation studies presented in Chapter 3 for the four C-PAMs of very high molecular weight and medium charge density (E1, E1+ and E1++++) and low charge density (G1++++). For each flocculation time, the volumetric flocs size distribution and the flocs structure (*SE*) were supplied by the LDS technique as described previously.

Additionally, the total solid volume was monitored for each flocculation time to ensure that the mass is not lost during simulation. Calculations stop if the loss of volume is higher than 1%.

6.3 – RESULTS AND DISCUSSION

6.3.1 – COMPARISON WITH EXPERIMENTAL DATA

For each experiment presented in Figure 6.1, the population balance model proposed was applied. The outputs from the model are the optimized fitting parameters values, the mean flocs size evolution, the scattering exponent evolution and, for each flocculation time, the number flocs size distribution. The simulation time with these three parameters is in average of 12 hours.

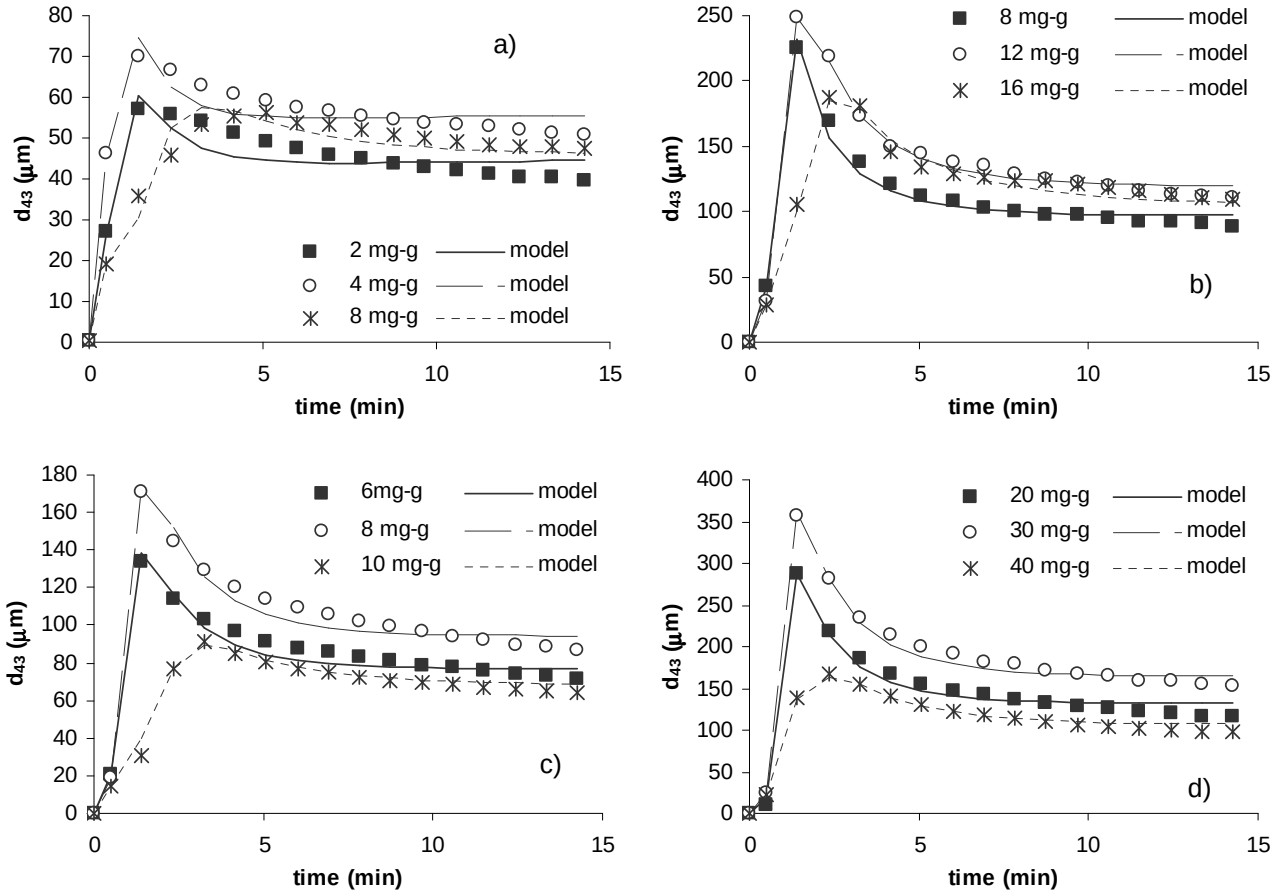

Figure 6. 1. Experimental and modelled flocculation kinetics for different flocculant concentrations: a) E1, b) E1+, c) E1++++ and d) G1++++.

The optimized fitting parameters that have originated the modelled results are resumed in Table 6.1. In order to quantify the degree of the model fit to experimental results, a "goodness of fit" was calculated (Biggs and Lant, 2002). The "goodness of fit" is calculated from Equation 6.11.

$$GoF = \frac{\overline{d[4,3]}_{\exp t} - st_{error}}{\overline{d[4,3]}_{\exp t}} \qquad (6.11)$$

In Equation 6.11, st_{error} is the standard error calculated from Equation 6.12 where n is the number of measured points. In Equation 6.12 st_{error} is divided by $n-3$ that corresponds to the number of degrees of freedom when fitting three model parameters.

$$st_{error} = \sqrt{\frac{\sum_{t=0}^{t=t_{final}} \left(d[4,3]_{\exp t} - d[4,3]_{\mathrm{mod}\,el}\right)^2}{n-3}} \qquad (6.12)$$

The "goodness of fit" calculated in this manner considered that for values higher than 90% the model offers a good approximation. Since in our case all the "goodness of fit" values obtained are higher than 90%, it is confirmed that the model proposed can be used to predict flocculation of the systems studied.

Table 6. 1. Optimum fitting parameters for E1, E1+, E1++++ and G1++++.

	Flocculant dosage (mg/g)	α_{max}	**B**	**γ**	**GoF***
E1	2	0.8897	17.7867	0.6020	91%
	4	0.9830	19.7897	0.7592	93%
	8	0.3596	21.2228	0.2480	92%
E1+	8	0.5237	38.7485	0.4015	94%
	12	0.4164	51.7346	0.3357	96%
	16	0.2616	40.2421	0.2306	95%
E1++++	6	0.5250	29.7027	0.4083	94%
	8	0.4331	31.4321	0.3945	94%
	10	0.3121	26.1265	0.2810	95%
G1++++	20	0.4575	51.6744	0.4054	93%
	30	0.3742	60.7544	0.3799	95%
	40	0.2897	49.1072	0.2897	95%

* GoF – "Goodness of fit"

In Figure 6.2, the experimental variation of the scattering exponent is compared with the scattering exponent variation calculated from Equation 1.15 for the four flocculants and for three different flocculant concentrations. In general, the modelled scattering exponent variations describe quite well the experimental flocs structure variations allowing in this manner, to obtain the flocculation kinetic profiles of Figure 6.1. In Figure 6.1, the experimental flocculation kinetics are compared with the modelled flocculation kinetics for both the four flocculants and for each flocculant concentration.

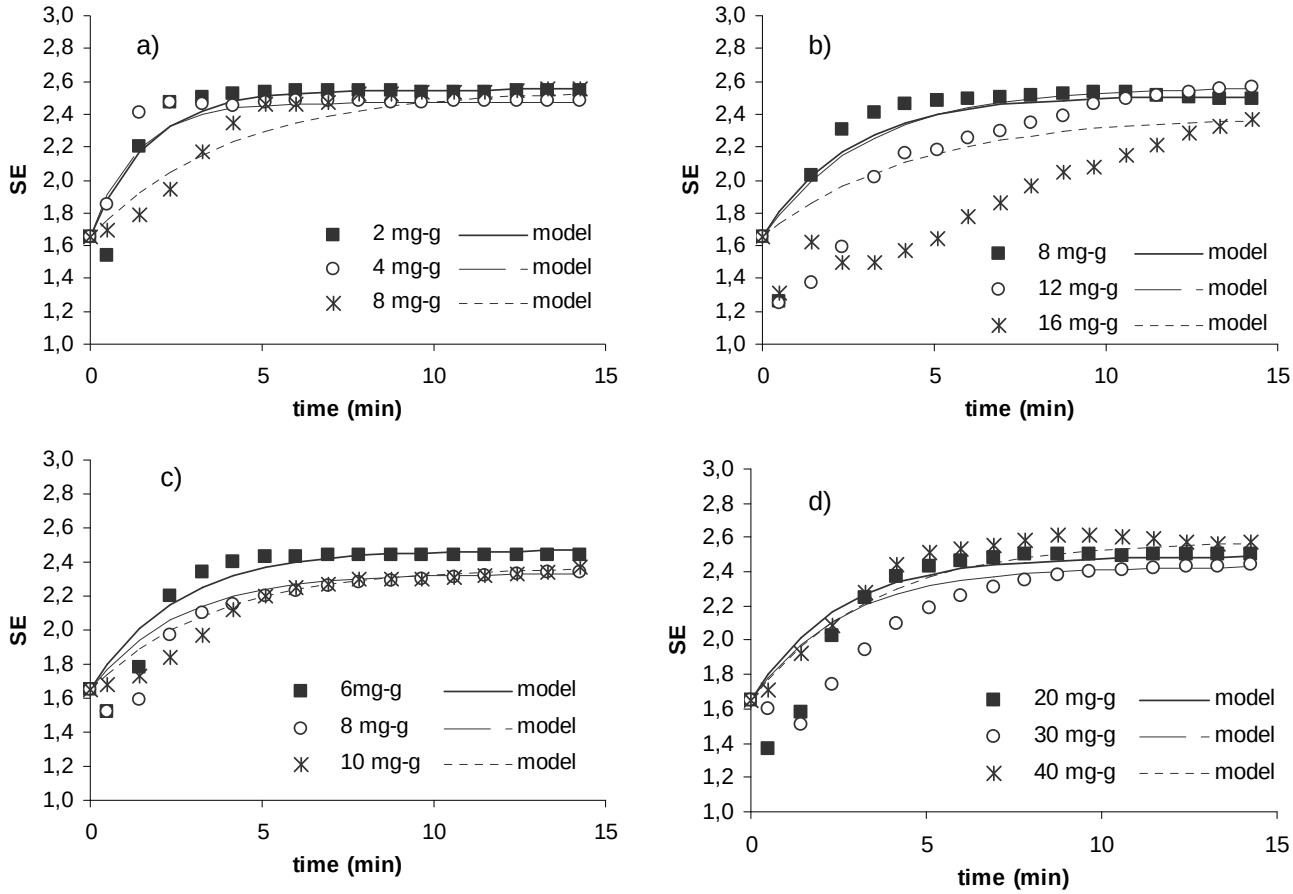

Figure 6. 2. Experimental and modelled structure variation for different flocculant concentrations: a) E1, b) E1+, c) E1++++ and d) G1++++.

The model is capable of simulating the same flocculation trends observed experimentally, i.e., the flocs size reaches rapidly a maximum and then starts to decrease due to flocs restructuring. Hence, these results demonstrate that for these flocculation systems, the flocs structure information can not be neglected.

The number size distributions obtained directly from the model have been converted to volume size distributions, since the LDS technique gives the size distribution based on volume. In Figure 6.3, some examples of the flocs size distributions obtained from the model are represented for two different times: the time corresponding to the maximum of the kinetics curve and for the end of the flocculation process. These results are then compared with the corresponding experimental data. The modelled results show that the modelled particle size distributions appear for the same size range as the experimental distributions, the same trends being observed, i.e., flocs size decreases during

flocculation after reaching a maximum size in the kinetics curve, due to flocs restructuring. Nevertheless, some deviations are clear between the modelled and the experimental distributions, mainly due to the wider nature of the experimental particle size distribution. This must be due to the limitations of the numerical methodology, namely as far as the number and width of the size classes selected, dictated by the computational limitations.

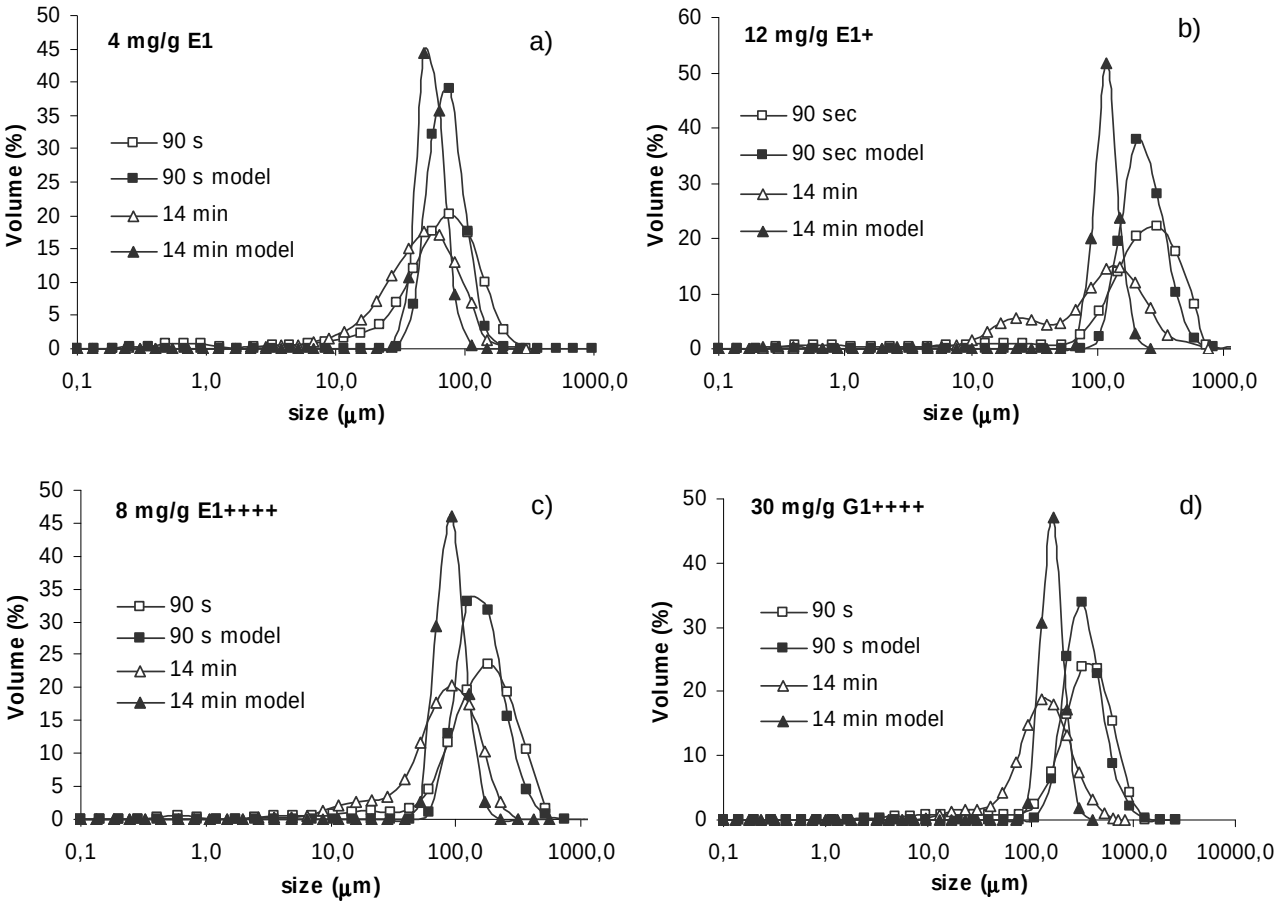

Figure 6. 3. Flocs size distributions from experimental and modelled results for a) 4 mg/g of E1, b) 12 mg/g of E1+, c) 8mg/g of E1++++ and d) 30mg/g of G1++++.

6.3.2 – EFFECT OF POLYMER CHARACTERISTICS

The parameters values of Table 6.1 were correlated with polymer properties and polymer concentration. Figure 6.4 represents the parameters values as a function of polymer concentration for the four polymers studied.

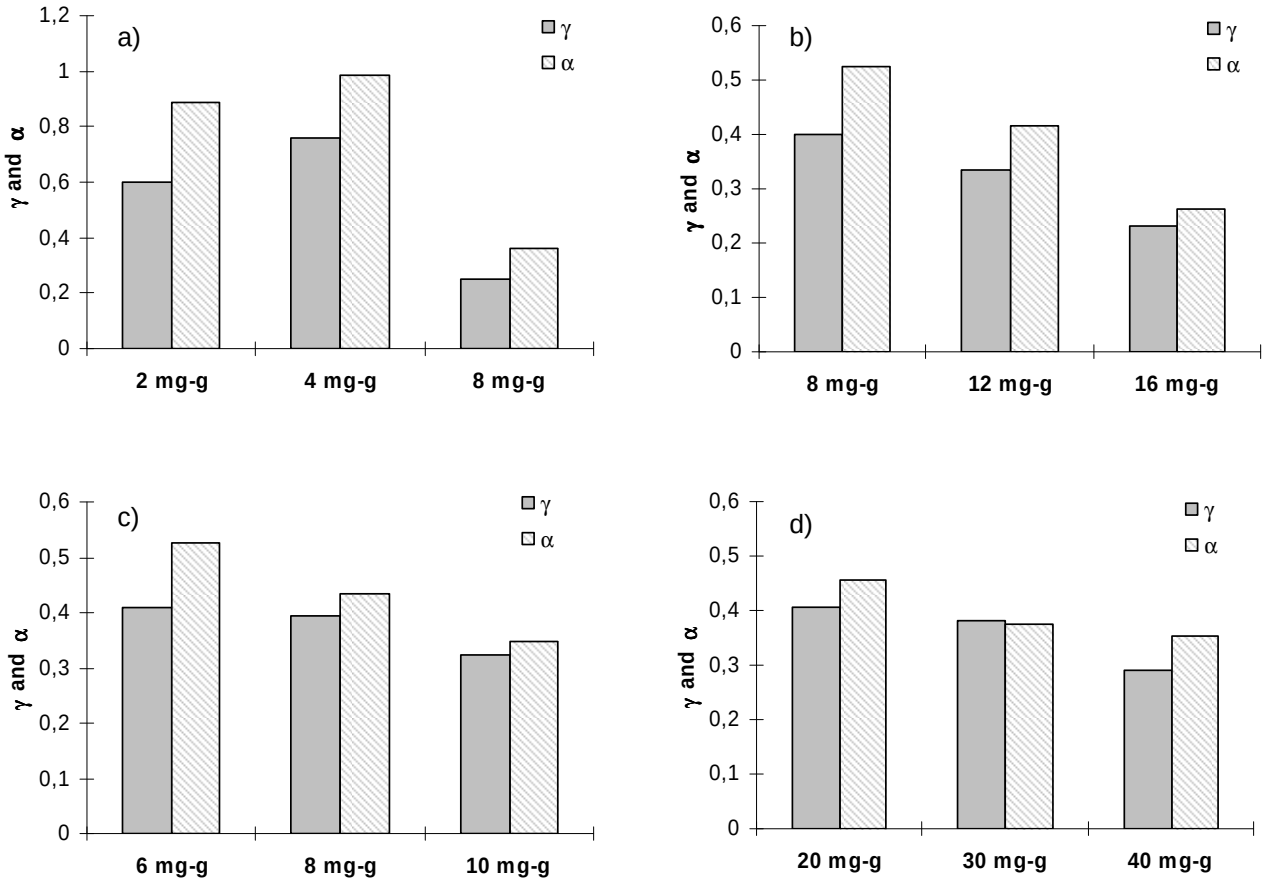

Figure 6. 4. α_{max} and γ as a function of flocculant concentration for a) E1, b) E1+, c) E1++++ and d) G1++++.

Figure 6.4 shows that an increase in the maximum collision efficiency factor (α_{max}) corresponds always to an increase of the kinetic parameter for flocs restructuring (γ). This indicates that the faster the flocculation kinetics, the faster the flocs restructuring rate will be. Since flocculation kinetics becomes slower as the flocculant concentration above the optimum dosage increases (Figure 6.1 and Chapter 3) it was expected that these two parameters would decrease with the flocculant dosage increase, as can be observed in Figure 6.4. In fact, the flocculation kinetics becomes slower as the flocculant dosage increases because there is a higher competition between polymer chains. On the other hand, it will be also more difficult for the adsorbed polymer chains to reconforme resulting in a slow restructuring rate (see Chapter 3).

Figures 6.5 and 6.6 represent the three fitting parameters (α_{max}, γ and B) as a function of flocs sizes and degree of restructuring, respectively, for the four polymers

studied and for the optimum flocculant concentration of each polymer. The optimum flocculant dosage corresponds to the intermediate flocculant concentration modelled.

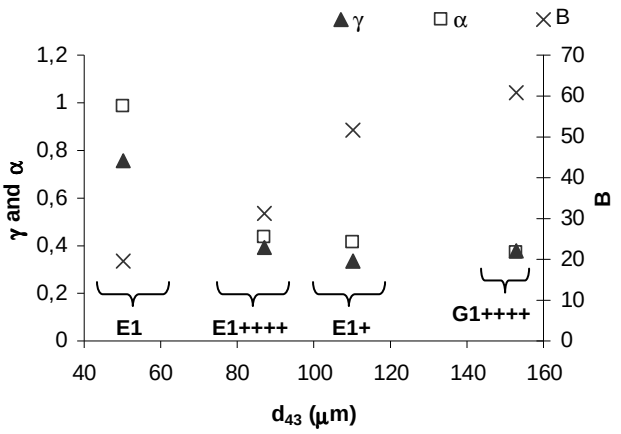

Figure 6. 5. Fitting parameters as a function of mean flocs size at t =14 min and for the optimum flocculant dosage.

In Figure 6.5, the maximum collision efficiency factor and the kinetic parameter for flocs restructuring are higher for the linear polymer (E1). Indeed, as seen in Chapter 3, flocculation kinetics and flocs restructuring rate are the fastest for the linear polymer. The flocs size produced with E1 stabilizes earlier. Hence, the branched polymer structure impairs the velocity of the flocculation process. The influence of charge density on the kinetics and flocs restructuring rate is not very pronounced when the highly branched polymers are compared (E1++++ and G1++++) although the two parameters are slightly lower for the lower charge density, as would be expected.

Moreover, the parameter related with fragmentation rate, *B*, increases with the increase of the flocs size. This was expected since as the parameter *B* increases, flocs break up occurs for higher size classes thus, the flocs produced will be larger. Furthermore, an increase in the parameter *B* corresponds to a decrease in the other parameters. Thus, larger flocs are obtained from lower flocculation rate and lower restructuring rate. This agrees with the parameters variation with the degree of flocs restructuring (Figure 6.6). In fact, flocs restructuring is more notorious when the reconformation of the polymer chains on the particle surface is more difficult. Thus, the flocs take longer to reach the final, stable configuration and restructuring is more visible because it occurs more slowly. In this case, the branched polymer structure impairs again the flocculation process.

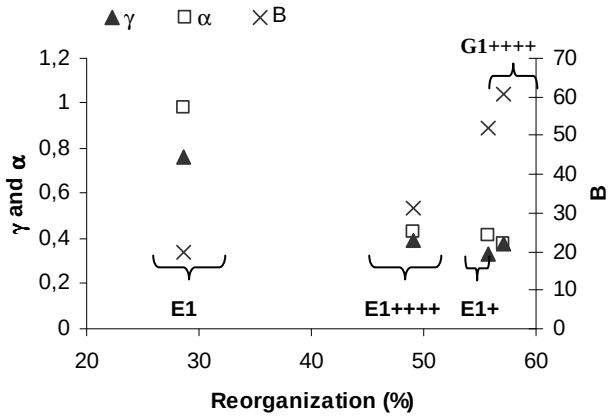

Figure 6. 6. Fitting parameters as a function of degree of flocs restructuring for the optimum flocculant dosage.

From Figures 6.5 and 6.6, it can be also stressed that the parameter *B* varies with the charge density of the polymer (comparison between E1++++ and G1++++). In accordance to results obtained in Chapter 3, *B* increases as the flocs size increases. The flocs produced with G1++++ are larger and thus, the model delivers a higher value for *B*. Moreover, the larger *B* value for G1++++ corresponds also to a higher degree of flocs reorganization (Figure 6.6) because as the polymer charge density decreases the polymer adopts a more extended configuration at the particle surface, and thus, polymer reconformation becomes more significant.

Furthermore, Figure 6.7 shows that as the parameter *B* increases the scattering exponent at the maximum in the kinetics curve decreases, i.e., that the flocs structure becomes more open, as expected. This agrees with the fact that *B* increases as the flocs size increases. Indeed, it was shown in Chapter 3 that larger flocs exhibit a more open structure.

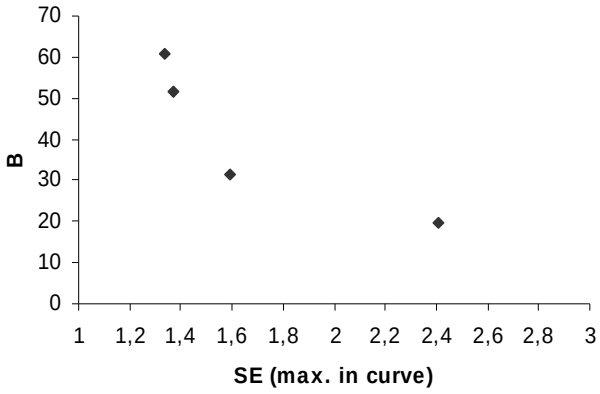

Figure 6. 7. Fitting parameter *B* as a function of the scattering exponent at the maximum in the kinetics curve.

It is known that the radius of gyration, R_g, is influenced by the number of polymer branches. In fact, for a constant molecular weight, as the number of branches increases, the polymer radius of gyration must decrease (Huang *et al.*, 2000). It is expected that as R_g decreases both the restructuring and the flocculation rates decrease. This is confirmed by Figure 6.8 where the fitting parameters are represented as a function of the polymers branching, the variation observed in these parameters follows the trend expected for R_g. Indeed, the polymer layer thickness at the particles surface decreases when the polymer radius of gyration decreases. Consequently, collision between particles is more difficult (lower α). On the other hand, the configuration that the polymer adopts when branches exist makes the polymer reconformation at the particles surface more difficult as referred previously (lower γ).

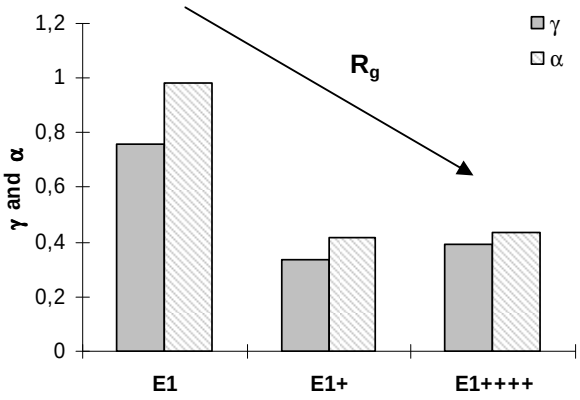

Figure 6. 8. α_{max} and γ as a function of polymer branching and R_g for the optimum flocculant dosage.

6.3.3 – EFFECT OF POLYMER DEGRADATION

In addition to the study already presented, the decrease with time of the collision efficiency factor given by Equation 1.18, was implemented in the model. This decrease in the collision efficiency factor will take into account the decrease on the flocs size during flocculation due to polymer degradation. In this case, the model had four fitting parameters: the parameter related with the fragmentation rate (*B*), the kinetic parameter of restructuring rate (γ), the maximum collision efficiency factor at t=0 (*C*) and the parameter for the rate of decrease of the collision efficiency with time (*D*).

Simulations were only performed for E1 and E1++++ polymers. Table 6.2 summarises the optimum fitting parameters obtained for all experiments. Comparing with

the results of Table 6.1, we can say that the small improvement of adjustment between experimental and model data does not justify using this more elaborated model to simulate the flocculation process for the system studied. In fact, the "goodness of fit" just slightly increases if the decrease of the collision efficiency factor during flocculation is considered. The difference between the computational time to perform simulations with three and four parameters is also a reason not to have proceeded with this last model. For one more parameter, the simulation time was multiplied by more than four.

Table 6. 2. Optimum fitting parameters for E1 and E1++++.

	Flocculant dosage (mg/g)	**C**	**B**	**γ**	**D**	**GoF***
E1	2	0.8813	19.8017	0.6220	12.7836	93%
	4	1.0674	21.3172	0.7764	17.0668	96%
	8	0.6362	22.0567	0.2447	43.3737	92%
E1++++	6	0.4552	31.4000	0.4266	25.3086	96%
	8	0.9782	31.7630	0.3935	97.3123	98%
	10	0.3312	26.0433	0.2798	91.1589	96%

* GoF – "Goodness of fit"

It is nevertheless, interesting to represent the maximum collision efficiency factor decrease during the flocculation process (Figure 6.9). Indeed, the collision efficiency factor slightly decreases for the higher flocculant dosage indicating that polymer degradation is insignificant but also that an excess of flocculant allows producing stronger flocs as verified by Blanco and co-workers (2005) and in Chapter 3. When comparing the two flocculants, the decrease of the collision efficiency factor is much more notorious for the linear polymer. This indicates that the polymer degradation is more important for flocs produced with the linear polymer. As seen before, for the linear polymer the restructuring rate is fast, and thus, the flocs size reaches quickly a steady-state. Consequently, the decrease of the flocs size during flocculation is mainly due to flocs break up which leads to polymer degradation, while for the branched polymer the decrease is mainly due to flocs restructuring (collision efficiency remains more or less constant).

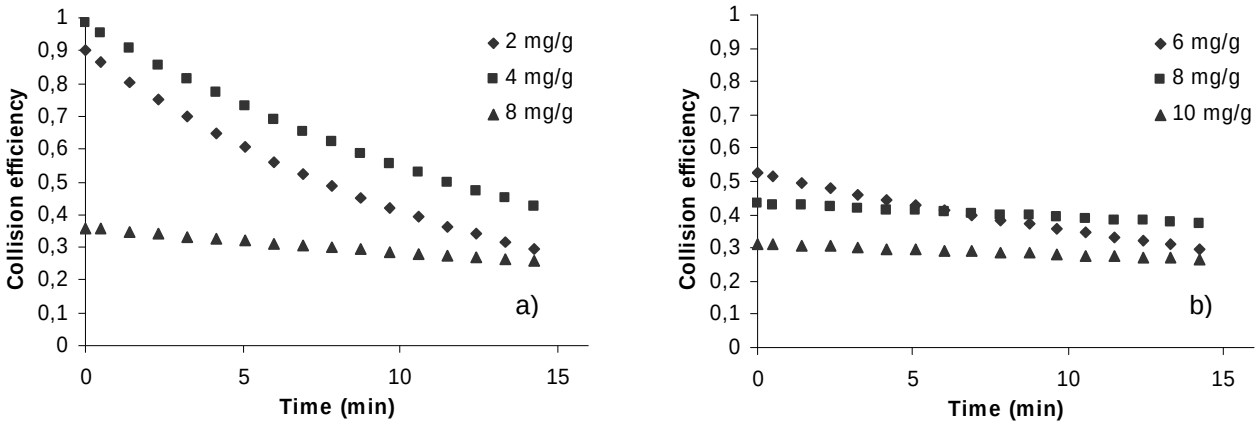

Figure 6. 9. Variation of the modelled maximum collision efficiency factor with flocculation time for a) E1 and b) E1++++.

6.4 – CONCLUSIONS

Flocculation of precipitated calcium carbonate with C-PAMs of very high molecular weight and low and medium charge density was successfully described using the population balance model proposed by Hounslow (1988) and Spicer and Pratsinis (1996b) where the flocs' restructuring was taken into account. It was demonstrated that for the flocculation system presented in this work, the flocs structure information can not be neglected.

The fitting parameters correlate well with the effect of the flocculant concentration, charge density and the degree of polymer branches on flocculation kinetics and on flocs characteristics (size and structure).

The possibility of using a model with four fitting parameters was abandoned since only minor improvements in the fitting were obtained while the computation time increased dramatically.

It is important to stress that the model proposed not only predicts in advance the flocs characteristics and the flocculation kinetics for a given process, but it will also allow to chose operating conditions and the flocculant that originate aggregates with given characteristics and consequently a given performance. In the case of the papermaking process, this capacity of the model is of great importance to define the conditions that lead to a balance between additives retention and drainage of the water during sheet formation.

CHAPTER 7 – FINAL CONCLUSIONS AND RECOMMENDATIONS FOR FUTURE WORK

The present study demonstrates the capacity of the light diffraction scattering technique (LDS) to evaluate and understand the flocculation process and to determine the flocs characteristics. The developed experimental methodology allows, in a single integrated test, the acquisition of information on the evolution, with time, of flocs dimensions and structure and also the evaluation of flocs resistance and flocculation kinetics which represent a clear advantage of this technique compared to traditional techniques to evaluate flocculation processes such as titration, image analysis, hindered settling or turbidity measurements. This development led to the assessment of the optimum flocculant dosage and to the understanding of the flocculation mechanisms involved which could be correlated with the mass fractal dimensions of the flocs. Moreover, the LDS technique allows one to study the flocculation process in a turbulent environment, in conditions similar to the ones prevailing in several industrial processes, as for instance in papermaking.

Accordingly, in this work, the LDS technique has been successfully applied to study, in the same single test, the flocculation, deflocculation and reflocculation processes of a precipitated calcium carbonate (PCC) suspension, when flocs were submitted either to sonication or to an increase of the hydrodynamic shearing. These two tests supply information on flocs resistance in two different situations that can be found in process equipment: (i) sonication gives information on intrinsic flocs resistance, important when the flocs are submitted to highly turbulent environments, and (ii) the hydrodynamic shearing evaluates superficial flocs resistance, important when flocs are conveyed in pipes and ducts. Both tests can be very useful to evaluate flocs resistance. The first one is important, for instance, to predict flocs behaviour in highly turbulent environments like mixing tanks or the headbox of a paper machine. The second one supplies information on flocs resistance in conditions similar to those prevailing when a flocculated suspension is conveyed in a pipe.

Dual retention aids have also been evaluated with the LDS technique. The flocculants performance in combination with microparticles has been studied successfully using the methodology developed in this dissertation.

Thus, it is legitimate to conclude that LDS is a valuable tool to assess the performance of polymeric flocculants on flocculation processes, in single or complex systems. Furthermore, it was demonstrated that the LDS technique is a better tool to determine flocs characteristics than other traditional techniques like image analysis or hindered settling.

As a final comment about the methodology presented in this dissertation, it is important to refer that this methodology can be easily applied to other flocculation systems to evaluate and predict flocculants performance. The main limitation of this methodology lies in the maximum solids concentration that can be used. This maximum particles concentration can be far from the solids concentrations encountered at the industrial scale. Nevertheless, in the present case, comparison between the LDS and the FBRM techniques results has shown that the information obtained by LDS could be extrapolated to the industrial scale.

The same methodology was adopted to study the influence of the water cationic content on flocculation, deflocculation and reflocculation processes and on the flocs properties. The results obtained allow one to stress that when screening flocculants performance and optimizing flocculant dosage for industrial purposes, it is essential to take into account the characteristics of the suspending medium. So, the common practice of using distilled water for the screening tests may lead to erroneous conclusions.

The overall study of the flocculation process of PCC, performed using the LDS technique, confirms that the flocculant characteristics are an important parameter to take into account when flocs with a given size, structure and resistance are needed to increase the performance of a process. In this study, the flocculants tested were cationic polyacrylamides of very high molecular weight. The flocculants studied can be divided into three categories: low charge density, medium charge density and high charge density. In each level of charge density, the polymer structure also varies from linear to highly branched. From all the flocculants studied, the branched polymers, presented, so far, only in few studies in the literature, either in distilled or industrial water, have shown a distinct behaviour compared to the linear ones that can be an advantage for some industrial processes. For example, in the case of the highly branched polymer of medium charge density, the flocs produced are larger but have a more open structure than the flocs

produced with the linear one. Moreover, highly branched flocculants are less affected by the water cationic content in all the stages, flocculation and break up, thus, leading to similar flocs structures independently of the suspending medium.

In the second part of the dissertation, the polyelectrolytes performance on retention and drainage of a pulp suspension with PCC is investigated. The drainage tests performed in the Dynamic Drainage Analyser (DDA) allow studying the effect of the polymer characteristics on retention and drainage. In addition, it was demonstrated that the flocculation tests help to understand the drainage results, and thus, that the LDS is a useful tool to be used in combination with the DDA. The same applies to the interpretation of the rheological tests performed in the viscometer developed by UCM. Indeed, results from both techniques confirm that the flocculants' properties influence the retention and the drainage performance and the flow behaviour of the pulp suspension, since they affect the flocculation process. Thus, in the case of the papermaking process, the combinations of these techniques (LDS, DDA and viscometery) can be useful to optimise the flocculation process.

Furthermore, correlations made between flocculation and drainage tests have shown that polymers of medium charge density are more suitable to be used as retention aid because low drainage time and very high filler retention are obtained simultaneously, with low flocculant contact time and low flocculant dosage. Moreover, the branched polymers of medium charge density have a significant potential as retention aids in papermaking, since they significantly improve simultaneously retention and drainage with low flocculant dosage and relatively fast flocculation kinetics, due to the formation of small flocs with an open structure, mainly at the secondary aggregates level. Additionally these polymers are less affected by the changes in the cationic content of the suspending medium.

Finally, the model presented in this dissertation can be a good starting point to describe the flocculation processes induced by polyelectrolytes. A population balance model was developed to describe the flocculation of PCC particles with polyelectrolytes of very high molecular weight and low and medium charge density. The model proposed describes successfully and simultaneously aggregation, breakage and flocs restructuring as well as the flocs size distribution. The flocs restructuring process has to be taken into account since flocs restructuring is normally found in these flocculation systems where flocculation occurs by the bridging mechanism. The maximum collision efficiency factor,

a parameter related with the fragmentation rate and a time constant for flocs restructuring have been taken as fitting parameters. The optimized parameters were then correlated with flocculant concentration, charge density and the degree of polymer branches which influence flocculation kinetics and the flocs characteristics (size and structure). The correlations obtained show well the effects of the flocculants' characteristics and of the flocs' properties on the flocculation kinetics and flocs restructuring as described by the model.

Nevertheless, the system modelled is still too simple in comparison with the complex systems found in industry. In fact, the polymer configuration at the particle surface not only depends on the polymer characteristics (molecular weight, charge density, structure) but also on the suspending medium characteristics (pH, conductivity, temperature…). Thus, these effects have to be implemented in the model in order to better describe the industrial processes.

For future work, it could be interesting to study the effect of the temperature on the flocculant performance since many industrial processes occur for temperatures different from the room temperature. In fact, studies have shown that the polymer adsorption is influenced by the temperature (Nedelcheva and Stoilkov, 1978; Jönsson *et al.*, 1998; Nyström *et al.*, 2003).

On the other hand, the retention and drainage information presented here should be complemented with retention and drainage tests of flocculated pulp suspensions in industrial water or, still, using as retention aids a microparticles system. Furthermore, it is necessary to investigate the effect of these flocculants on paper sheet formation to complement the retention and drainage information since good paper sheet formation is also essential to achieve product quality and process efficiency. It is also important to extend this study to other systems, that is to different types of furnish and fibres; namely considering the differences in the anionic charge level. Regarding the rheological measurements, it is necessary to deepen the study with other flocculants. In fact, little time has been spent with these measurements, and thus, more rheological tests are needed to generalize the conclusions. Moreover, for both drainage and rheological measurements, it could be interesting to study, in more detail, the effect of the flocculant contact time with the suspension, since it is an important parameter to consider for the optimisation of flocculation processes in papermaking.

Finally, it would be important to start implementing in the model, in a quantitative way, the influence of the polymer concentration and of the polymer structure, in order to obtain a predictive model that will be able to predict the performance, on flocculation, of a polymer with pre-defined characteristics. One possibility is to use Equation 1.17 that takes into account the configuration and the thickness of the polymer layer at the particle surface. In fact, the configuration and the thickness of the polymer layer at the particle surface depend on the flocculant concentration and on the polymer characteristics (molecular weight, charge density and branching), and thus, they influence the flocculation kinetics and the flocs properties. Moreover, if the polymer is characterized by its radius of gyration or by the hydrodynamic radius, this parameter should be easily correlated with the degree of coverage included in the collision efficiency parameter and also with the polymer layer thickness, referred above, enabling the explicit introduction of the polymer characteristics in the model. Moreover, introduction of the polymer degradative function in the breakage kernel, when bridging is the prevailing mechanism, would be another important step.

REFERENCES

Alfano, C.J., Carter, P.W., Whitten, J.E., "Use of scanning laser microscopy to investigate microparticle flocculation performance", *J. Pulp Paper Sci.* 25(6), 189-195, **1999**.

Alfano, J.C., Carter, P.W., Duham, A.J., Nowak, M.J., Tubergen, K., "Polyelectrolyte-induced aggregation of microcrystalline cellulose: reversibility and shear effects", *J. Colloid Interf. Sci.* 223, 244-254, **2000**.

Allen, L.H., "Particle size distributions of fines in mechanical pulps and some aspects of their retention in papermaking", *Tappi J.* 68(2), 91-94, **1985**.

Allen, T., "Particle size measurement", Chapman & Hall, 4th Ed., London, **1990**.

Antunes, E., Garcia, F.A.P., Ferreira, P., Rasteiro, M.G., "Flocculation of PCC filler in papermaking: influence of the particle characteristics", *Chem. Eng. Res. Des.* 86, 1155-1160, **2008**.

Asselman, T., Garnier, G., "The flocculation mechanism of microparticulate retention aid systems", *J. Pulp Paper Sci.* 27(8), 273-278, **2001**.

Bennington, C.P.J., Kerekes, R.J., Grace, J.R., "The yield stress of fibre suspensions", *Can. J. Chem. Eng.* 68, 748-757, **1990**.

Bennington, C.P.J., Kerekes, R.J., Grace, J.R., "Motion of pulp fiber suspensions in rotary devices", *Can. J. Chem. Eng.* 69(1), 251-258, **1991**.

Berlin, Ad.A., Kislenko, V.N., "Kinetic model of suspension flocculation by polymers", *Colloid Surf.* 104, 67-72, **1995**.

Berlin, Ad.A., Solomentseva, I.M., Kislenko, V.N., "Suspension flocculation by polyelectrolytes: Experimental verification of a developed mathematical model", *J. Colloid Interf. Sci.* 191, 273-276, **1997**.

Biggs, C.A., Lant, P.A., "Modelling activated sludge flocculation using population balances", *Powder tech.* 124, 201-211, **2002**.

Biggs, S., Habgood, M., Jameson, G.J., Yao-de-Yan, "Aggregate structures formed via a bridging flocculation mechanism", *Chem. Eng. J.* 80, 13-22, **2000**.

Blanco, A., "Estudio de la floculación en la fabricación de papel", PhD. Thesis, Universidad Complutense, Madrid, Spain, **1994**.

Blanco, A., Tijero, J., Hooimeijer, A., "Study of flocculation process in papermaking", Papermakers Conference, TAPPI Proceedings, 455-463, **1995**.

Blanco, A., Negro, C., Hooimeijer, A., Tijero, J., “Polymer optimization in paper mills by means of a particle size analyser: an alternative to zeta potential measurements”, *Appita J.* 49, 113-116, **1996**.

Blanco, A., Fuente, E., Negro, C., Tijero, J., “Flocculation monitoring: focused beam reflectance measurement as a measurement tool”, *Can. J. Chem. Eng.* 80, 734-740, **2002**.

Blanco, A., Negro, C., Fuente, E., Tijero, J., “Effect of shearing forces and flocculant overdose on filler flocculation mechanisms and flocs properties”, *Ind. Eng. Chem. Res.* 44, 9105-9112, **2005**.

Bonanomi, E., Morari, M., Sefcik, J., Morbidelli, M., “Analysis and control of turbulent coagulator”, *Ind. Eng. Chem. Res.* 43, 6112-6124, **2004**.

Bouanini, M., Bascoul, A., Mouret, M., Sellier, A., “Hydrodynamic simulation of non Newtonian fluid in an agitated vessel”, in Proceedings of the Comsol Users Conference, Paris, **2006**.

Bremmell, K.E., Jameson, G.J., Biggs, S., “Kinetic Polyelectrolyte adsorption at the solid/liquid interface interaction forces and stability”, *Colloid Surf.* 139, 199-211, **1998**.

Britt, K.W., Unbehend, J.E., Shridharan, R., “Observations on water removed in papermaking”, *Tappi J.* 69(7), 76-79, **1986**.

Brouillette, F., Morneau, D., Chabot, B., Daneault, C., “Paper formation improvement through the use of new structured polymers and microparticle technology”, *Pulp Paper Can.* 105(5), 108-112, **2004**.

Brouillette, F., Morneau, D., Chabot, B., Daneault, C., “A new microparticulate system to improve retention/drainage in fine paper manufacturing”, *Appita J.* 58(1), 47-51, **2005**.

Bushell, G.C., Yan, Y.D., Woodfield, D., Raper, J., Amal, R., “On techniques for the measurement of the mass fractal dimension of aggregates”, *Ad. Colloid Interf. Sci.* 95, 1-50, **2002**.

Bushell, G., “Forward light scattering to characterise structure of flocs composed of large particles”, *Chem. Eng. J.* 111, 145-149, **2005**.

Cadotte, M., Tellier, M.E., Blanco, A., Fuente, E., van de Ven, T.G.M., Paris, J., “Flocculation, retention and drainage in papermaking: a comparative study of polymeric additives”, *Can. J. Chem. Eng.* 85, 240-248, **2007**.

Chakraborti, R.K., Gardner, K., Atkinson, J., Van Benschoten, J., “Changes in fractal dimension during aggregation”, *Water. Res.* 37, 873-883, **2003**.

Chase, W.C., Donatelli, A.A., Walkinshaw, J.W., “Effects of freeness and consistency on the viscosity of hardwood and softwood pulp suspensions”, *Tappi J.* 72(5), 199-204, **1989**.

Cheng, D.C-H, Heywood, N.I., "Flow in pipes: Part 1: Flow of homogeneous fluids", Phys. Technol. Vol. 15, Ireland, **1984**.

Claesson, P.M., Poptoshev, E., Blomberg, E., Dedinaite, A., "Polyelectrolyte-mediated surface interactions", *Adv. Colloid Interf. Sci.* 114-115, 173-187, **2005**.

Cohen, R.D., "Self-similar cluster size distribution in random coagulation and breakup", *J. Colloid Interf. Sci.* 149, 261-270, **1992**.

COMSOL Multiphysics User's Guide, Version 3.3 by COMSOL AB, **2006**.

De Boer, G.B.J., de Weerd, C., Thoenes, D., Goossens, H.W.J., "Laser diffraction spectroscopy: Fraunhofer diffraction versus Mie scattering", *Part. Charact.* 4, 14-19, **1987**.

Duffy, G.G., Titchener, A.L., "The disruptive shear stress of pulp networks", *Svensk Papperstidning* 78(13), 474-479, **1975**.

Dunham, A.J., Sherman, L.M., Alfano, J.C., "Effect of dissolved and colloidal substances on drainage properties of mechanical suspensions", *J. Pulp Paper Sci.* 28(9), 298-304, **2002**.

Eklund, D., Lindström, T., "Paper Chemistry: an introduction", DT Paper Science Publications, Finland, **1991**.

Fair, G., Gemmell, R.S., "A mathematical model of coagulation", *J. Colloid Interf. Sci.* 19, 360-372, **1964**.

Fan, A., Turro, N.J., Somasundaran, P., A study of dual polymer flocculation", *Colloid Surf.* 162, 141-148, **2000**.

Fardim, P., "Papel e Química de Superfície – Parte I – A superfície da fibra e a química da parte Úmida", *O Papel*, 97-102, Abril **2002**.

Farias, T.L., Koylu, U.O., Carvalho, M.G., "Range of validity of the Rayleigh-Gans-Debye theory for optics of fractal aggregates", *Appl. Optics* 35(33), 6560-6567, **1996**.

Ferreira, P., Velho, J., Figueiredo, M., Mendes, A. "Effect of thermal treatment on the structure of PCC particles", *Tappi J.* 4(11), 18-22, **2005**.

Flesch, J.C., Spicer, P.T., Pratsinis, S.E., "Laminar and turbulent shear-induced flocculation of fractal aggregates", *AIChE J.* 45, 1114-1124, **1999**.

Forsberg, S., Bengtsson, M., "The dynamic drainage analyzer (DDA)", Tappi 1990 Papermakers Conference Proceedings, Tappi Press, Atlanta, **1990**.

Forsberg, S., Ström, G., "The effect of contact time between cationic polymers and furnish on retention and drainage", *J. Pulp Paper Sci.* 20(3), 71-76, **1994**.

François, R.J., "Strength of aluminium hydroxide flocs", *Water Res.* 21(9), 1023-1030, **1987**.

Fuente, E., Blanco, A., Negro, C., San Pio, I., Tijero, J., "Monitoring flocculation fillers in papermaking", *Paper Tech.* 44(8), 41-50, **2003**.

Glover, S.M., Yao-de-Yan, Jameson, G.J., Biggs, S., Bridging flocculation studied by light scattering and settling", *Chem. Eng. J.* 80, 3-12, **2000**.

Gray, S.R., Ritchie, C.B., "Effect of organic polyelectrolyte characteristics on floc strength", *Colloid Surf.* 273, 184-188, **2006**.

Greenwood, R., Kendall, K., "Effect of ionic strength on the adsorption of cationic polyelectrolytes onto alumina studied using electroacoustic measurements", *Powder Tech.*, 148-157, **2000**.

Gregory, J., "The action of polymeric flocculants", Flocculation, in Proceedings of Sedimentation and Consolidation, Engineering foundation Conference, Georgia, USA, **1985**.

Gullichsen, J., Härkönen, E., "Medium consistency technology: I. Fundamental data", *Tappi J.* 64(6), 69-72, **1981**.

Hammarström, D., "A model for simulation flows", Technical reports from KTH Mechanics, Royal Institute of Technology, Stockholm, Sweden, **2004**.

Heath, A.R., Koh, P.T.L., "Combined population balance and CFD modelling of particle aggregation by polymeric flocculant", 3rd International Conference on CFD in the Minerals and Process Industries, Melbourne, Australia, **2003**.

Heath, A.R., Parisa, A.B., Fawell, P.D., Farrow, J.B., "Polymer flocculation of calcite: relating the aggregate size to the settling rate", *AIChE J.* 52(6), 1987-1993, **2006a**.

Heath, A.R., Bahri, P.A., Fawell, P.D., Farrow, J.B, "Polymer flocculation of calcite: population balance model", *AIChE J.* 52(5), 1641-1653, **2006b**.

Hermawan, M., Yang, T., Bushell, G., Amal, R., Bickert, G., "A new approach in determining floc strength", Part. Syst. Analysis, Harrogate, UK, **2003**.

Hiemenz, P.C., Rajagopalan, R., "Principles of colloids and surface science", Marcel Dekker, Inc., New York, **1997**.

Holland, F.A., Chapman, F.S., "Liquid mixing and processing in stirred tanks", Reinhold Publishing, New York, **1966**.

Hounslow, M.J., Ryall, R.L., Marshall, V.R., "A discretized population balance for nucleation, growth and aggregation", *AIChE J.* 34, 1821-1832, **1988**.

Huang, Y.; Bu, L.W.; Zhang, D.Z.; SU, C.W., Xu, Z.D.; Bu, L.J.; Mays, J.W. Characterization of star-block copolymers having PS-b-PI arms via SEC/RT/RALLS/DV. *Polym. Bulletin* 44, 301-307, **2000**.

Hubbe, M.A., “Fines management for increases paper machine productivity”, Proc. Sci. Tech. Advan. Wet End Chem., PIRA, Vienna, Paper 3, **2002**.

Hubbe, M.A., “Selecting laboratory tests to predict effectiveness of retention and drainage aid programmes”, Filler & Pigments for Papermakers, Pira Conference, Barcelona, **2003**.

Hubbe, M.A., “Charge-related measurements, A reappraisal. Part 2: Fibre-pad streaming potential”, *Paper Tech.* 45(8), 27-34, **2004**.

Hubbe, M.A., Heitmann, J.A., “Review of factors affecting the release of water from cellulosic fibers during paper manufacture”, Water release, papermaking, *BioResources* 2(3), 500-533, **2007**.

Hulkko V.M., Deng, Y., “Effects of water-soluble inorganic salts and organic materials on the performance of different polymer retention aids”, *J. Pulp Paper Sci.* 25(11), 378-389, **1999**.

ISO 13320-1, “Particle Size Analysis-Laser Diffraction Methods. Part 1: General Principle”, International Organization of Standardization, Genève, **1999**.

Jarvis, P., Jefferson, B., Gregory, J., Parsons, S.A., “A review of floc strength and breakage”, *Water Res.* 39, 3121-3137, **2005**.

Jönsson, B., Lindman, B., Holmberg, K., Kronberg, B., “Surfactants and polymers in aqueous solution”, John Wiley & Sons, England, **1998**.

Kerekes, R.J., Soszynski, R.M., Tam Doo, P.A., “The flocculation of pulp fibres”, Papermaking Raw Materials, Transactions 8th Fundamental Research Symposium, Mech. Eng. Publ. Ltd., Oxford, **1985**.

Kippax, P., “Measuring particle size using modern laser diffraction techniques”, Paint & Coatings Industry, **2005**.

Kirk, R.E., Othmer, D.F., Kroschwitz, J.I., Howe-Grant, M., “Papermaking additives”, in Kirk-Othmer encyclopedia of chemical technology, Vol. 18, 4th ed. Wiley, New York, **1998**.

Koethe, J., Scott, W., “Polyelectrolyte interactions with papermaking fibers: mechanism of surface charge decay”, *Tappi Papermakers Conference Proceedings*, Tappi Press, **1993**.

Kostoglou, M.S., Dovas, S., Karabelas, A.J., “On the steady-state size distribution of dispersion in breakage processes”, *Chem. Eng. Sci.* 52(8), 1285-1299, **1997**.

Krogerus, B., “Laboratory testing of retention and drainage”, Book 4: Papermaking Chemistry, Papermaking Science and Technology, TAPPI PRESS, Finland, **1999**.

Kusters, K.A., Wijers, J.G., Thoenes, D., “Aggregation kinetics of small particles in agitated vessels”, *Chem. Eng. Sci.* 52, 107-121, **1997**.

La Mer, V.K., Healy, T.W., “Adsorption-flocculation reactions of macromolecules at the solid-liquid interface”, *Rev. Pure Appl. Chem.* 13, 112-133, **1963**.

Lee, C.H., Liu, J.C., “Sludge dewaterability and floc structure in dual polymer conditioning”, *Ad. Env. Res.* 5, 129-136, **2001**.

Li, T.Q., Ödberg, L., “Flow properties of cellulose fiber suspensions flocculated by cationic polyacrylamide”, *Colloid Surf.* 115, 127-135, **1996**.

Liao, J.Y.H., Selomulya, C., Bushell, G., Bickert, G., Amal, R., “On different approaches to estimate the mass fractal dimension of coal aggregates”, *Part. Part. Syst. Charact.* 22, 299-309, **2005**.

Lin, M.Y., Klein, R., Lindsay, H.M., Weitz, D.A., Ball, R.C., Meakin, P., “The structure of fractal colloidal aggregates of finite extent”, *J. Colloid Interf. Sci.* 137,263-280, **1990**.

Lindström, T., Glad-Nordmark, G., “Network flocculation and fractionation of latex particles by means of a polyethyleoxide-phenolformaldehyde resin complex”, *J.Colloid Interf. Sci.* 97(1), 62-67, **1984**.

Lindström, T, Hallgren, H., Hedborg, F., “Aluminium based microparticle retention aid systems”, *Nord. Pulp Paper Res. J.* 4(2), 99-103, **1989**.

Litchfield, E., “Dewatering aids for paper applications”, *Appita J.* 47(1), 62-65, **1994**.

Lumpe, C., Joore L., Homburg, K., Verstraeten, E., “Focused beam reflectance measurement (FBRM) a promising tool for wet-end optimisation and web break prediction”, *Paper Tech.* 42(4), 39-44, **2001**.

Luukko, K., Paulapuro, H., “Mechanical pulp fines: Effect of particle size and shape”, *Tappi J.* 82(2), 95-101, **1999**.

Miyanishi, T., “Effects of zeta potential on flocculation measurement in microparticle systems”, *Tappi J.* 78(11), 135-141, **1995**.

Miyanishi, T., Shigeru, M., “Optimizing flocculation and drainage for microparticle systems by controlling zeta potential”, *Tappi J.* 80(1), 262-270, **1997**.

Negro, C., Fuente, E., Blanco, A., Tijero, J., “Flocculation mechanism induced by phenolic resin/PEO and floc properties”, *AIChE J.* 51(3), 1022-1031, **2005**.

Negro, C., Fuente, E., Blanco, A., Tijero, J., “Effect of chemical flocculation mechanisms on rheology of fibre pulp suspensions”, *Nord. Pulp Paper Res. J.* 21(3), 336-341, **2006**.

Nicke, R., Pensold, S., Hartmann, H-J, Tappe, M., “Polydiallyldimethylammonium chloride as a flocculating agent”, *Wochenbl. Papierfabr.* 120(14), 559-564, **1992**.

Norell, M., Johansson, K., Persson, M., “Retention and Drainage”, Book 4: Papermaking Chemistry, Papermaking Science and Technology, TAPPI PRESS, Finland, **1999**.

Nurmi, M., Westerholm, M., Eklund, D., “Factors influencing flocculation of dissolved and colloidal substances in a thermomechanical pulp water”, *J. Pulp Paper Sci.* 30(2), 41-44, **2004**.

Nyström, R., Backfolk, K., Rosenholm, J.B., Nurmi, K., “Flocculation of calcite dispersions induced by the adsorption of highly cationic starch”, *Colloid Surf.* 219, 55-66, **2003**.

Nyström, R., Hedström, G., Gustafsson, J., Rosenholm, J.B., “Mixtures of cationic starch and anionic polyacrylate used for flocculation of calcium carbonate – influence of electrolytes”, *Colloid Surf.* 234, 85-93, **2004**.

Paradis, M.A., Genco, J.M., Bousfield, D.W., Hassler, J.C.,Wildfong, V, “Determination of drainage resistance coefficients under known shear rate”, *Tappi J.* 1(8), 12-18, **2002**.

Parker, D.S., Kaufman, W.J., Jenkins, D., “Floc breakup in turbulent flocculation processes”, J. Sanit. Eng. Div.: Proc. Am. Soc. Civ. Eng., SA1, 79-99, **1972**.

Parker, J., “The sheet forming process”, STAP Nº 9, Tappi, Atlanta, **1972**.

Nedelcheva, M.P., Stoilkov, G.V., “Cationic starch adsorption by cellulose: Part I”, *J. Colloid Interf. Sci.* 66 (3), 475-482, **1978**.

Pruden, B., “The effect of fines on paper properties”, *Paper Tech.* 46(4), 19-26, **2005**.

Räisänen, K.O., Paulapuro, H., Karrila, J., “The effects of retention aids, drainage conditions and pretreatment of slurry on high-vacuum dewatering: a laboratory study”, *Tappi J.* 78(4), 140-147, **1995**.

Rasteiro, M.G., Garcia, F.A.P., del Mar Peréz, M., “Applying LDS to monitor flocculation in papermaking”, *Part. Sci. Tech.* 25(3), 303-308, **2007**.

Rasteiro, M.G., Garcia, F.A.P., Ferreira, P., Blanco, A., Negro, C., Antunes, E., “The use of LDS as a tool to evaluate flocculation mechanisms”, *Chem. Eng. Proc.* 47, 1329-1338, **2008a**.

Rasteiro, M.G., Garcia, F.A.P., Ferreira, P., Blanco, A., Negro, C., Antunes, E., “Evaluation of flocs resistance and reflocculation capacity using the LDS technique”, *Powder Tech.* 183, 231-238, **2008b**.

Rawle, A., “Basic principles of particle size analysis”, Technical Paper from Malvern Instruments Limited, **2000**.

Roberts, J.C., “Paper Chemistry”, Chapman & Hall, New York, **1991**.

Saffman, P.G., Turner, J.S., “On the collision of drops in turbulent clouds”, *J. Fluid Mech.* 1(16), 16-30, **1956**.

Schuster, J., Friedrich, K., “Modeling of the mechanical properties of discontinuous-aligned-fiber composites after thermoforming”, *Comp. Sci. Tech.* 57(4), 405-413, **1997**.

Scott, W.E., “Principles of wet-end chemistry”, Tappi press, Atlanta, **1996**.

Selomulya, C., Bushell, G., Amal, R., Waite, T.D., “Aggregation mechanisms of latex of different particle sizes in a controlled shear environment”, *Langmuir* 18, 1974-1984, **2002**.

Selomulya, C., Bushell, G., Amal, R., Waite, T.D., “Understanding the role of restructuring in flocculation: the application of a population balance model”, *Chem. Eng. Sci.* 58, 327-338, **2003**.

Serra, T., Casamitjana, X., “Modelling the aggregation and break-up of fractal aggregates in a shear flow”, *Appl. Sci. Res.* 59, 255-268, **1998**.

Servais, C, Manson, J.A.E., “The relationship between steady-state and oscillatory shear viscosity in planar randomly oriented concentrated fiber suspensions”, *J. Rheology* 43(4), 1019-1031, **1999**.

Servais, C., Luciani, A., Manson, J.A.E., “Squeeze flow of concentrated long fibre suspensions: experiments and model”, *J. Non-Newtonian Fluid Mech.* 104, 165-184, **2002**.

Shin., J-H., Han, S.H., Sohn, C., Ow, S.K., Mah, S., “Highly branched cationic polyelectrolytes: filler flocculation”, *Tappi J.* 80(11), 179-185, **1997a**.

Shin., J-H., Han, S.H., Sohn, C., Ow, S.K., Mah, S., “Highly branched cationic polyelectrolytes: fines retention”, *Tappi J.* 80(10), 185-189, **1997b**.

Shubin, V., Linse, P., “Self-consistent-field modelling of polelectrolyte adsorption on charge-regulating surfaces”, *Macromolecules* 30, 5944-5952, **1997**.

Smoluchowski, M.v., “Versuch einer mathematischen theorie der koagulations-kinetic kolloider lösungen”, *Z. Phys. Chem.* 92, 124-168, **1917**.

Smook, G.A., “Hanbook for Pulp & Paper Technologists”, 2nd ed. TAPPI, New York, **1992**.

Solberg, D., Wågberg, L., “Adsorption and flocculation behavior of cationic polyacrylamide and colloidal silica”, *Colloid Surf.* 219, 161-172, **2003**.

Soos, M, Sefcik, J., Morbidelli, M., “Investigation of aggregation, breakage and restructuring kinetics of colloidal dispersions in turbulent flows by population balance modelling and static light scattering”, *Chem. Eng. Sci.* 61, 2349-2363, **2006**.

Spicer, P.T., Pratsinis, S.E., “Shear-induced flocculation: the evolution of floc structure and the shape of the size distribution at steady state”, *Water Res.* 30, 1049-1056, **1996a**.

Spicer, P.T., Pratsinis, S.E., “Coagulation and fragmentation: universal steady-state particle-size distribution”, *AIChE J.* 42(6), 1612-1620, **1996b**.

Spicer, P.T., Pratsinis, S.E., Raper, J., Amal, R., Bushell, G., Meesters, G., "Effect of shear schedule on particle size, density and structure during flocculation in stirred tanks", *Powder Tech.* 97, 26-34, **1998**.

Stemme, S., Ödberg, L., Malmeten, M., "Effect of colloidal silica and electrolyte on the structure of an adsorbed cationic polyelectrolyte layer", *Colloid Surf.* 155, 145-154, **1999**.

Stén, M., "Importance of papermaking chemistry", Book 4: Papermaking Chemistry, Papermaking Science and Technology, TAPPI PRESS, Finland, **1999**.

Stoll, S., Chodanowski, P., "Polyelectrolyte Adsorption on an oppositely charged spherical particle: Chain rigidity effects", *Macromolecules* 35, 9556-9562, **2002**.

Stone, S., Bushell, G., Amal, R., Ma, Z., Merkus, H.G., Scarlett, B., "Characterization of large fractal aggregates by small-angle light scattering", *Meas. Sci. Tech.* 13, 357-364, **2002**.

Swerin, A., Powell, R.L., Ödberg, L., "Linear and nonlinear dynamic viscoelasticity of pulp fibre suspensions", *Nordic Pulp Paper Res.* J. 3, 126-132, **1992**.

Swerin., A., Sjödin, U., Ödberg, L., "Flocculation of cellulosic fibre suspensions by model microparticulate retention systems", *Nordic Pulp Paper J.* 4, 159-166, **1993**.

Swerin, A., Ödberg, L., "Flocculation of cellulosic fibre suspensions by a microparticulate retention aid system consisting of cationic polyacrylamide and anionic montmorillonite", *Nordic Pulp Paper J.* 1, 22-29, **1996a**.

Swerin, A., Ödberg, L., Wågberg, L., "An extended model for the estimation of flocculation efficiency factors in multicomponent flocculant systems", *Colloid Surf.* 113, 25-38, **1996b**.

Swerin, A., Risinger, L., Ödberg, L., "Flocculation in suspensions of microcrystalline cellulose by microparticle retention aid systems", *J. Pulp Paper Sci.* 23(8), 374-381, **1997**.

Swerin, A., "Rheological properties of cellulosic fibre suspensions flocculated by cationic polyacrylamides", *Colloid Surf.* 133, 279-294, **1998**.

Tadros, T., "Applied Surfactants: principles and applications", Wiley-VCH, Weinheim, **2005**.

Tanaka, H., Swerin, A., Ödberg, L., "Cleavage of polymer chain during transfer of cationic polyacrylamide from cellulose fibers to polystyrene latex", *J. Colloid Interf. Sci.* 153, 13-22, **1992**.

Tang, S., Ma, Y., Shiu, C., "Modelling the mechanical strength of fractal aggregates", *Colloid Surf.* 180, 7-16, **2001**.

Teixeira, J., "Small-angle scattering by fractal systems", *J. Appl. Cryst.* 21, 781-785, **1988**.

"The Dynamic Drainage Analyser Manual", operating manual, AB Akribi Kemikonsulter, Sweden, **2001**.

Thomas, D.N., Judd, S.J., Fawcett, N., "Flocculation modelling: a review", *Water Res.* 33(7), 1579-1592, **1999**.

Trepanier, R.J., "The G/W drainage-retention tester", *Tappi J.* 75(5), 139-142, **1992**.

U.S. EPA (Environmental Protection Agency), "Profile of the Pulp and Paper Industry, 2nd ed.", Pulp and Paper Industry: sector notebook project, Washington, November **2002**.

Unbehend, J.E., "Wet end chemistry of retention, drainage and formation aids", Pulp and Paper Manufacture, Vol. 6, R.V. Hagemeyer, Ed., 3rd ed., TAPPI PRESS, Atlanta, **1992**.

van de Ven, T.G.M., Alince, B., "Association-induced polymer bridging: new insights into the retention of fillers with PEO", *J. Pulp Paper Sci.* 22(7), 257-263, **1996a**.

van de Ven, T.G.M., Alince, B., "Heteroflocculation by asymmetric polymer bridging", *J. Colloid Interf. Sci.* 181, 73-78, **1996b**.

Vanerek, A., Alince, B., Van de Ven, T.G.M., "Colloidal behaviour of ground and precipitated calcium carbonate fillers: effects of cationic polyelectrolytes and water quality", *J. Pulp Paper Sci.* 26(4), 135-139, **2000**.

Ventura, C, Blanco, A, Negro, C, Ferreira, P, Garcia, F, Rasteiro, M.G, "Modeling pulp fiber suspension rheology", *Tappi J.* 6(7), 17-23, **2007**.

Wahren, D., "On three-dimensional fibre networks", Doctoral Thesis, KTH, Stockholm, **1964**.

Whipple, W.L., Maltesh, C. "Adsorption of cationic flocculants to paper slurries", *J. Colloid Interf. Sci.* 256, 33-40, **2002**.

Wilcox, D.C. "Turbulence Modeling for CFD", DWC Industries Inc., **1998**.

Wildfong, V.J., Genco, J.M., Shands, J.A., Bousfield, D.W., "Filtration mechanics of sheet forming. Part I: Apparatus for determination of constant-pressure filtration resistance", *J. Pulp Paper Sci.* 26(7), 250-254, **2000a**.

Wildfong, V.J., Genco, J.M., Shands, J.A., Bousfield, D.W., "Filtration mechanics of sheet forming. Part II: Influence of fine material and compression", *J. Pulp Paper Sci.* 26(8), 280-283, **2000b**.

Xiao, H.N., Pelton, R., Hamielec, A., "Novel retention aids for mechanical pulps", *Tappi J.* 79(4), 129-135, **1996**.

Yan, Z., Deng, Y., "Cationic microparticle based flocculation and retention systems", *Chem. Eng. J.* 80, 31-36, **2000**.

Yeung, A.K.C., Pelton, R., “Micromechanics: a new approach to studying the strength and breakup of flocs”, *J. Colloid Interf. Sci.* 184, 579-585, **1996**.

Yoon, Se-Y., Deng, Y., “Flocculation and reflocculation of clay suspension by different polymer systems under turbulent conditions”, *J. Colloid Int. Sci.* 278, 139-145, **2004**.

Yu, X., Somasundaran, P., “Enhanced flocculation with double flocculants”, *Colloid Surf.* 81, 17-23, **1993**.

Yukselen, M.A., Gregory, J., “The reversibility of floc breakage”, *Int. J. Miner. Process* 73, 251-259, **2004**.

APPENDIX A

MATLAB® PROGRAM FOR SOLVING THE POPULATION BALANCE MODEL

```
%script file for commands to call FMINSEARCH optimizer

%%%%%%%%%%%%%%%%%%%%%%%%%%%%%%%%%%%%%%%%%%%%%%%%%%%%%%%%%%%%%%%%%%%%%%%%%%%%%%%%

%Input
    %imax - number of size class i
    %tmax - maximum flocculation time
    %no - number distribution of primary particles for t=0
    %do - particles size in size class i=1
    %G - shear rate
    %dFo - mass fractal dimension for t=0
    %dFmax - maximum mass fractal dimension for t=tmax
    %x,y - fitting parameters for alpha estimation =0.1

%Fitting parameters
    %amax - maximum collision efficiency factor
    %B - fitting parameter for fragmentation rate
    %gama - fitting parameter for restructuring rate

%Output
    %time - time vector of size(tmax,1)
    %number - matrix with particles number in each size class i of
size(tmax,imax)
    %VMD - volume mean diameter vector calculated at each t of
size(tmax,1)
    %dF - fractal dimension vector at each time t of size(tmax,1)

%Resolution using ode23 of dY/dt=[dNdt ddFdt] where N=Ncurrent+dN/dt*dt,
%dF=dFcurrent+ddF/dt*dt


%initial guesses of the unknown parameters for optimizer just collect in
1 vector

B=25.8;
amax=0.315;
gama=0.28;
teta=[amax B gama];

%the sampling instants data for the fitting: sampling instants t and
measured d43
texp=[0 0.5 1.4 2.3 3.3 4.2 5.1 6 6.9 7.8 8.8 9.7 10.6 11.5 12.4 13.3
14.3];
dexp=[0.38 14.61 31.132 76.621 91.602 84.82 80.225 77.021 74.752 72.567
70.869 69.561 68.673 67.33 66.225 65.062 64.155];
data=[texp' dexp'];
```

```
%initial value for ODE solver
G=312;%s-1
imax=30;%maximum size interval
dFo=1.65;
dFmax=2.37;
do=100;%nm
x=0.1;
y=0.1;

%Original number distribution, #/cm3
a=[4.60e8 6.31e9 1.24e9 2.89e6 4.24e7 8.77e6 5.79e5 1.34e5 2.32e4
1.89e3];
sizea=size(a,2);
sizeb=imax-sizea;
b=zeros(1,sizeb);
no=[a,b];%size(no)=1ximax

%Time span
t=0;
tmax=14;%min

Totalvol1=solvol(no,do);%Reference for total volume of solid

dcurrent=convertVMD(no,dFo,do);
%output printout
time(1)=t;
number(1,:)=no;
VMD(1)=dcurrent*1e-3;%VMDin microns
dF(1)=dFo;

%normalization of no
nref=zeros(1,imax);
for i=1:imax
    if no(1,i)==0;
       nref(1,i)=1;
    else
       nref(1,i)=no(1,i);
    end
end
nonorm=no./nref;%size 1ximax
dFref=dFo;
dFnorm=dFo./dFref;

%call the optimizer:
teta_opt=fminsearch(@mylsq,teta,[],nonorm,dFnorm,G,dcurrent,dFmax,do,nref
,dFref,imax,x,y,data);

%ODE solver called once more, to get the optimized solution
amax=teta_opt(1);
B=teta_opt(2);
gama=teta_opt(3);

%estimate Alpha based on alpha(i,j)=exp(-x*(1-i/j)^2)/(i*j^y for i>=j
[Alpha]=alphaest(x,y,imax,amax);

i=1;
while t<tmax,
    if i==1
        ti=t+0.5;
        tspan=t:0.5:ti;
```

```
    else
        ti=t+0.92;
        tspan=t:0.92:ti;
    end

    Yo=[nonorm dFnorm];%size(Yo)=1x(imax+1)
    options=odeset('AbsTol',1e-4,'OutputFcn','odeprint');


[tf,Yf]=ode23(@aggregationdF,tspan,Yo,options,Alpha,B,G,dcurrent,dFmax,do
,nref,dFref,constant,imax);
    tfrow=size(tf,1);
    [Yfrow,Yfcol]=size(Yf);%Yfrow=tfrow,Yfcol=imax+1
    j=1;
    while j<=(Yfcol-1),
        if Yf(Yfrow,j)<0
            Yf(Yfrow,j)=0;
        else
            Yf(Yfrow,j)=Yf(Yfrow,j);
        end
        j=j+1;
    end
    nonorm=Yf(Yfrow,1:(Yfcol-1));
    no=nonorm.*nref;
    Totalvol2=solvol(no,do);
    dTotalvol=((abs(Totalvol2-Totalvol1))/(Totalvol1))*100;
    if dTotalvol>1
        error('calculation terminated');
    else
        nonorm=Yf(Yfrow,1:(Yfcol-1));
        dFnorm=Yf(Yfrow,Yfcol);
        no=nonorm.*nref;
        t=tf(tfrow);
        i=i+1;
        dFo=dFnorm.*dFref;
        dcurrent=convertVMD(no,dFo,do);%dcurrent in nm
        time(i)=t;
        number(i,:)=no;
        dF(i)=dFo;
        VMD(i)=dcurrent*1e-3;%VMD in micron
        dFref=dFo;
        dFnorm=dFo./dFref;
        for k=1:imax
            if number(i,k)==0;
                nref(1,k)=1;
            else
                nref(1,k)=number(i,k);
            end
        end
        nonorm=no./nref;
    end
end

timeprint=time';
VMDprint=VMD';
dFprint=dF';

%plot the data vs solution
plot(texp,dexp,'o',time,VMD)
```

%calculate total solid volume of aggregates

%%

```
function [TotalVol]=solvol(Y,do)
%calculate total solid volume for lumped discrete population balance
%lower limit,ie. 4 for i=3, 8 for i=4 etc
%vi=2^(i-1)*vo

ro=(do/2)*1e-9;%in m
u1=4/3*pi*ro^3;%in m3
[m,jmax]=size(Y);
for j=1:jmax,
    u=u1*(2^(j-1));%m3
    vo(j,1)=u;
    j=j+1;
end
vi(:,1)=vo;
Vol=vi;

Y=Y';
Totalvoli=zeros(jmax,m);

for i=1:m;
    Totalvoli(:,i)=Y(:,i).*Vol;
    Sumvoli(i,1)=sum(Totalvoli(:,i));
    i=i+1;
end
TotalVol=Sumvoli;
```

%Calculate volume mean diameter of aggregates

%%

```
function [VMDm]=convertVMD(N,dF,do)

%Calculating volume mean diameter (VMD) from number concentration of
flocs of size i (Ni) and characteristic floc diameter (Di)

d1=do*1e-7; %primary particle diameter,cm
n=length(N);

%Di: characteristic floc diameter
%Di=2^((i-1)/dF)*d1
%VMD)sum(Ni*Di^4)/sum(Ni*Di^3)
Di=0;
for i=1:n,
    Di(i)=(2^((i-1)/dF))*d1;
    i=i+1;
end
D=Di;

%col=n (section i)
TopVMDi=0;
BotVMDi=0;
for col=1:n,
    TopVMDi(col)=N(1,col)*D(col)^4;
    BotVMDi(col)=N(1,col)*D(col)^3;
```

```
    col=col+1;
end
TopVMD=sum(TopVMDi);
BotVMD=sum(BotVMDi);
VMD=TopVMD/BotVMD;
VMDm=VMD*1e7; %in nm
```

%file that describe the objective function used in optimizer.m

```
%%%%%%%%%%%%%%%%%%%%%%%%%%%%%%%%%%%%%%%%%%%%%%%%%%%%%%%%%%%%%%%%%%%%%%%%%%%

Function[lsq]=mylsq(teta,nonorm,dFnorm,G,dcurrent,dFmax,do,nref,dFref,ima
x,x,y,data);

t=0;
tmax=9;
y_obs=data(:,2)';
y_cal(1)=dcurrent*1e-3;%VMDin microns

amax=teta(1);
B=teta(2);
gama=teta(3);

%no concentration, no/cm3
a=[4.60e8 6.31e9 1.24e9 2.89e6 4.24e7 8.77e6 5.79e5 1.34e5 2.32e4
1.89e3];
sizea=size(a,2);
sizeb=imax-sizea;
b=zeros(1,sizeb);
no=[a,b];%size(no)=1ximax
Totalvol1=solvol(no,do);%Reference for total volume of solid

%estimate Alpha based on alpha(i,j)=exp(-x*(1-i/j)^2)/(i*j^y for i>=j
[Alpha]=alphaest(x,y,imax,amax);

%call the ODE solver to get the states VMD

i=1;
while t<tmax,
    if i==1
        ti=t+0.5;
        tspan=t:0.5:ti;
    else
        ti=t+0.92;
        tspan=t:0.92:ti;
    end

    Yo=[nonorm dFnorm];%size(Yo)=1x(imax+1)
    options=odeset('AbsTol',1e-4,'OutputFcn','odeprint');


[tf,Yf]=ode23(@aggregationdF,tspan,Yo,options,Alpha,B,G,dcurrent,dFmax,do
,nref,dFref,constant,imax);
    tfrow=size(tf,1);
    [Yfrow,Yfcol]=size(Yf);%Yfrow=tfrow,Yfcol=imax+1
    j=1;
    while j<=(Yfcol-1),
        if Yf(Yfrow,j)<0
```

```
            Yf(Yfrow,j)=0;
        else
            Yf(Yfrow,j)=Yf(Yfrow,j);
        end
        j=j+1;
    end
    nonorm=Yf(Yfrow,1:(Yfcol-1));
    no=nonorm.*nref;
    dFnorm=Yf(Yfrow,Yfcol);
    t=tf(tfrow);
    i=i+1;
    dFo=dFnorm.*dFref;
    dcurrent=convertVMD(no,dFo,do);%dcurrent in nm
    time(i)=t;
    number(i,:)=no;
    dF(i)=dFo;
    y_cal(i)=dcurrent*1e-3;%VMD in micron
    dFref=dFo;
    dFnorm=dFo./dFref;
    for k=1:imax
        if number(i,k)==0;
            nref(1,k)=1;
        else
            nref(1,k)=number(i,k);
        end
    end
    nonorm=no./nref;
end

%compute the expression to be minimized:

lsq=sum((y_obs-y_cal).^2);
```

%calculate collision efficiency between aggregates

```
%%%%%%%%%%%%%%%%%%%%%%%%%%%%%%%%%%%%%%%%%%%%%%%%%%%%%%%%%%%%%%%%%%%%%%%%%%%%%%%%

function [alpha]=alphaest(x,y,imax,amax)
%estimate alpha from alpha(i,j)=[exp(-x*[1-(i/j)]^2]/[(i*j)^y]
%x,y are constants
%i>=j

alpha=zeros(imax,imax);
for i=1:imax,
    for j=1:imax;
        h=[i,j];
        hmin=min(h); %pick smaller from i and j
        hmax=max(h); %pick larger from i and j
        alpha(i,j)=(exp(-x*(1-(hmax/hmin))^2)/(hmax*hmin)^y)*amax;
        j=j+1;
    end
    i=i+1;
end
```

```
%Calculate dN/dt

%%%%%%%%%%%%%%%%%%%%%%%%%%%%%%%%%%%%%%%%%%%%%%%%%%%%%%%%%%%%%%%%%%%%%%%%%%%%

Function[dYdt]=aggregationdF(t,Y,Alpha,B,G,dcurrent,dFmax,do,nref,dFref,g
ama,imax)

%Y=[N dF]is a row vector
%dYdt=[dNdt;ddFdt] return a column vector

dYdt=zeros(imax+1,1);%a column vector of size (imax+1)x1

%dNdt
v=1e-2;%kinematic viscosity,cm2/s
e=G^2*v; %energy dissipation rate,cm2/s3
temp=296;%absolute temperature,K
kb=1.380622e-23; %Boltzman's constant,J/K
miu=1e-3;%viscosity of surrounding medium,Pa.s
Nref=nref';
N=Y(1:imax,1).*Nref;%size(N)=imax x1
dFcurrent=Y(imax+1,1).*dFref;

%Calculate collision radius for classe i
[Rc]=radius(do,imax,dFcurrent);

dNdt=zeros(imax,1);
dNnormdt=zeros(imax,1);
for i=1:imax,

    %first term: birth in interval i due to collision between particles
in
    %intervales i-1 and 1 to i-2
    %j=1 to j=i-2:2^(j-1+1)*Alpha*Beta[i-1,j]*N[i-1]*N[j]
    if (i-2)>=1
        first=zeros(i,1);
        for j=1:(i-2);
            Beta1a=1.294*G*(Rc(i-1)+Rc(j))^3;%shear kernel,cm3/s
            Beta1b=((2*kb*temp)/(3*miu)*((1/(Rc(i-1)*1e-2))+(1/(Rc(j)*1e-
2)))*((Rc(i-1)*1e-2)+(Rc(j)*1e-2)))*1e6;%Brownian kernel,cm3/s
            Beta1=Beta1a+Beta1b;
            first(j)=2^(j-i+1)*Alpha(i-1,j)*Beta1*N(i-1)*N(j);
            j=j+1;
        end
        sumfirst=sum(first);
    else
        sumfirst=0;
    end

    %2nd term: birth in interval i due to collisions between particles in
    %intervales i-1 and i-1 (the no of particles available is Ni-1)
    %1/2*Alpha*Beta[i-1,i-1]*N[i-1]^2
    if (i-1)==0;
        second=0;
    else
        Beta2a=1.294*G*(Rc(i-1)+Rc(i-1))^3;%shear kernel,cm3/s
        Beta2b=((2*kb*temp)/(3*miu)*((1/(Rc(i-1)*1e-2))+(1/(Rc(i-1)*1e-
2)))*((Rc(i-1)*1e-2)+(Rc(i-1)*1e-2)))*1e6;%Brownian kernel,cm3/s
        Beta2=Beta2a+Beta2b;
        second=(1/2)*Alpha(i-1,i-1)*Beta2*((N(i-1))^2);
    end
```

```
    %3rd term: death by aggregation in intervale i due to collision of
    %particles in intervales i and 1 to i-1
    %j=1 to j=i-1:Ni*sum(Alpha*Beta[i,j]*N[j])
    if (i-1)>=1
        third=zeros(i,1);
        for j=1:(i-1),
            Beta3a=1.294*G*(Rc(i)+Rc(j))^3;%shear kernel,cm3/s
            Beta3b=((2*kb*temp)/(3*miu)*((1/(Rc(i)*1e-2))+(1/(Rc(j)*1e-
2)))*((Rc(i)*1e-2)+(Rc(j)*1e-2)))*1e6;%Brownian kernel,cm3/s
            Beta3=Beta3a+Beta3b;
            third(j)=2^(j-i)*Alpha(i,j)*Beta3*N(j);
            j=j+1;
        end
        sumthird=(sum(third))*N(i);
    else
        sumthird=0;
    end

    %fourth term: death by aggregation of particles in intervals i and i
to
    %imax
    %j=i to j=imax: Ni*sum(Alpha*Beta[i,j]*N[j])
    fourth=zeros(imax,1);
    j=i;
    p=1;
    if j<imax
        for j=i:imax,
           Beta4a=1.294*G*(Rc(i)+Rc(j))^3;%shear kernel,cm3/s
           Beta4b=((2*kb*temp)/(3*miu)*((1/(Rc(i)*1e-2))+(1/(Rc(j)*1e-
2)))*((Rc(i)*1e-2)+(Rc(j)*1e-2)))*1e6;%Brownian kernel,cm3/s
           Beta4=Beta4a+Beta4b;
           fourth(p)=Alpha(i,j)*Beta4*N(j);
           j=j+1;
           p=p+1;
        end
        sumfourth=sum(fourth)*N(i);
    else
        sumfourth=0;
    end

    %5th term: death by fragmentation of flocs in interval i
    %Si*Ni
    if i>1
        ebi=B/(Rc(i));
        Si=(4/(15*(22/7)))^(1/2)*G*exp(-ebi/e);
        fifth=Si*N(i);
    else
        fifth=0;
    end

    %6th term: breakage of flocs greater than i into flocs of size i
    %binary breakage: R(i,j)=V(i) for j=i+1, and R(i,j)=0 otherwise
    if i<imax
        R=2; %V(i+1)/V(i)
        ebi=B/(Rc(i+1));
        Si=(4/(15*(22/7)))^(1/2)*G*exp(-ebi/e);
        sixth=R*Si*N(i+1);
    else
        sixth=0;
    end
```

```
    agg(i,1)=sumfirst+second-sumthird-sumfourth;
    frag(i,1)=-fifth+sixth;
    dNdt(i,1)=(agg(i,1)+frag(i,1))*60;
    dNnormdt(i,1)=dNdt(i,1)./Nref(i,1);
    i=i+1;
end
dYdt(1:imax,1)=dNnormdt;

ddFdt=gama*(dFmax-dFcurrent);
ddFnormdt=ddFdt./dFref;

dYdt(imax+1,1)=ddFnormdt;
```

%Calculate collision radius of aggregates

```
%%%%%%%%%%%%%%%%%%%%%%%%%%%%%%%%%%%%%%%%%%%%%%%%%%%%%%%%%%%%%%%%%%%%%%%%%%%%

function [Rc]=radius(do,jmax,dF)

%do:diameter of primary particles,nm
%u:characteristic solid volume =u1*2^(i-1),cm3
%rm=characteristic solid floc radius=(u/((4/3*pi))^(1/3),cm
%ro: primary particle radius,cm
%u1: primary particle volume,cm3
%Npo: number of primary particle comprising a floc of size i=2^(i-1)
%Rc: maximum collision radius=ro*(Np/k)^(1/dF)
%dF= fractal dimension

ro=do/2*1e-7;%in cm
u1=4/3*pi*ro^3;%in cm3
kc=1;
rco=zeros(jmax,1);
for j=1:jmax,
    u=u1*2^(j-1);%in cm3
    rm=((u/(4/3*pi))^(1/3))*1e4; %radius of i in micron
    npo=(2^(j-1)); %Characteristic number of particles in section i
    if j<=2
        rco(j,1)=rm/1e4;
    else
        rco(j,1)=ro*((npo/kc)^(1/dF));
    end
    j=j+1;
end

%print Rc (maximum collision radius,cm)
Rc=rco(:,1);
```

```
% Plot size distribution for a given flocculation time

%%%%%%%%%%%%%%%%%%%%%%%%%%%%%%%%%%%%%%%%%%%%%%%%%%%%%%%%%%%%%%%%%%%%%%%%%%%%%%%

Ntest=load('number.m');
dotest=380;
dFtest=load('dF.m');
timeplot=1;
[Dres,Vol,Numcalc]=convnumberdF(dotest,Ntest,dFtest,timeplot);


%Plot number distribution of aggregates

%%%%%%%%%%%%%%%%%%%%%%%%%%%%%%%%%%%%%%%%%%%%%%%%%%%%%%%%%%%%%%%%%%%%%%%%%%%%%%%

function [D,Vol,Numcalc]=convnumberdF(do,N,dF,timeplot);

[m,n]=size(N);
d1=do*1e-7; %diameter of primary particle,cm

Di=zeros(m,n);
%Di: characteristic floc collision diameter
%Di=(2^((i-1)/dF))*d1
%row=m (time)
%col=n (section i)
TotalN=zeros(m,1);
Nest=zeros(m,n);
for row=1:m,
    for col=1:n,
        Nest(row,col)=N(row,col)*2^(col-1);
        col=col+1;
    end
    TotalN(row)=sum(Nest(row,:));
    row=row+1;
end
Ni=zeros(m,n);
Vi=zeros(m,n);
vi=zeros(m,n);
TotalV=zeros(m,1);
for row=1:m,
    dFrow=dF(row);
    for col=1:n,
        Ni(row,col)=Nest(row,col)./TotalN(row);
        Di(row,col)=(2^((col-1)/dFrow))*d1;
        vi(row,col)=(4*3.14/3)*((Di(row,col)/2)^3);
        Vi(row,col)=N(row,col)*vi(row,col);
        col=col+1;
    end
    TotalV(row)=sum(Vi(row,:));
    row=row+1;
end
for row=1:m,
    for col=1:n,
        Volume(row,col)=Vi(row,col)./TotalV(row);
        col=col+1;
    end
    row=row+1;
end

Numcalc=Ni*100;
```

```
Vol=Volume*100; %volumetrica
D=[Di].*1e4; %in micron

Dplot=D(timeplot,:);
Numplot=Vol(timeplot,:);
semilogx(Dplot,Numplot,'k.-');
xlabel('Aggregate collision diameter, micron');
ylabel('%Volume');
hold;
```

APPENDIX B

ESTIMATION OF THE SHEAR RATE IN THE MASTERSIZER 2000 BEAKER WITH COMSOL MULTIPHYSICS®

COMSOL Multiphysics is a powerful interactive environment for modelling and solving all kinds of scientific and engineering problems based on partial differential equations (PDEs). To solve the PDEs, COMSOL Multiphysics uses the finite element method (FEM). The software runs the finite element analysis together with adaptive meshing and error control using a variety of numerical solvers (COMSOL Multiphysics 3.3 User's Guide, 2006).

With COMSOL Multiphysics it is possible to extend conventional models for one type of physics into multiphysics models that solve coupled physics phenomena, and do so simultaneously. On the other hand, it is possible to build models by defining the relevant physical quantities, such as material properties, loads, constraints, sources and fluxes rather than by defining the underlying equations. Moreover, the COMSOL Multiphysics can be used standalone through a flexible graphical user interface, or by script programming in the COMSOL Script language or in the MATLAB language (COMSOL Multiphysics 3.3 User's Guide, 2006).

The modelling procedure consists of five basic steps: to draw the device, to define the physics where the material properties and boundary conditions are specified, to create a mesh, to select and run a solver and finally, to postprocess the results.

The COMSOL Multiphysics contains an easy-to-use CAD tool to draw the device.

3D GEOMETRY OF THE IMPELLER AND SHAFT OF THE MASTERSIZER 2000

In this study, to estimate the shear rate in the Mastersizer 2000 beaker, the impeller and the shaft of the equipment was drawn in 3D using the CAD tool of the COMSOL Multiphysics (Figure B.1). The geometry of Figure B.1 was firstly created in 2D work planes in which projections were drawn, then extruded and revolved to create a 3D object.

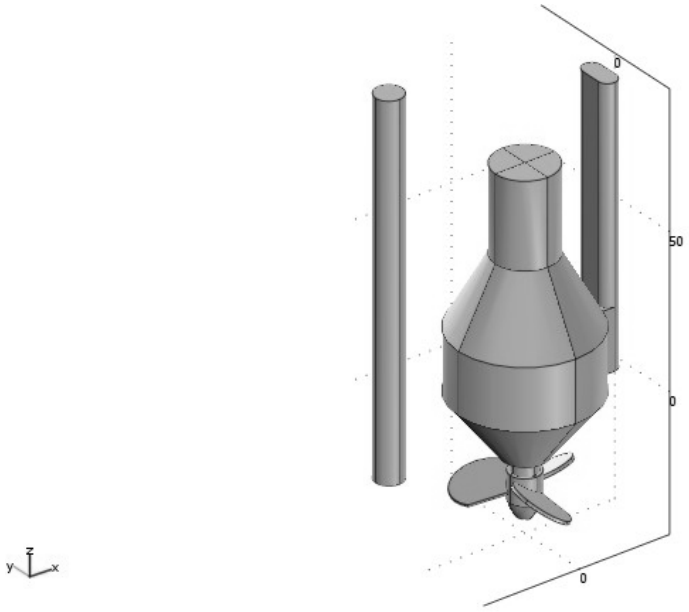

Figure B.1. 3D geometry of the mastersizer 2000 stirrer.

MODEL DEFINITON

The Swirl Flow application mode is an extension of the Incompressible Navier-Stokes application mode for axially symmetric geometries. The basic Navier-Stokes application mode assumes that the radial velocity u_φ in a 2D axisymmetric model is zero, while the Swirl Flow application mode only assumes that flow in the radial direction is constant.

For a system in cylindrical coordinates, under the assumption that $\partial/\partial\varphi = 0$, the flow is described by:

$$\frac{\partial u_r}{\partial r} + \frac{u_r}{r} + \frac{\partial u_z}{\partial z} = 0 \qquad \text{(B-1)}$$

$$\rho\left(\frac{\partial u_r}{\partial t} + u_r\frac{\partial u_r}{\partial r} + u_z\frac{\partial u_r}{\partial z} - \frac{u_\varphi^2}{r}\right) = -\frac{\partial p}{\partial r} + \frac{1}{r}\frac{\partial}{\partial r}\left(r\tau_{rr}\right) + \frac{\partial \tau_{zr}}{\partial z} - \frac{\tau_{\varphi\varphi}}{r} + F_r \qquad \text{(B-2)}$$

$$\rho\left(\frac{\partial u_z}{\partial t} + u_r\frac{\partial u_z}{\partial r} + u_z\frac{\partial u_z}{\partial z}\right) = -\frac{\partial p}{\partial z} + \frac{1}{r}\frac{\partial}{\partial r}\left(r\tau_{rz}\right) + \frac{\partial \tau_{zz}}{\partial z} + F_z \qquad \text{(B-3)}$$

$$\rho\left(\frac{\partial u_\varphi}{\partial t} + u_r\frac{\partial u_\varphi}{\partial r} + \frac{u_r u_\varphi}{r} + u_r\frac{\partial u_\varphi}{\partial z}\right) = \frac{1}{r^2}\frac{\partial}{\partial r}\left(r^2\tau_{r\varphi}\right) + \frac{\partial \tau_{z\varphi}}{\partial z} + F_\varphi \qquad \text{(B-4)}$$

In an axisymmetric geometry, COMSOL Multiphysics assumes the symmetry axis to be at $r = 0$.

The swirl flow application was combined with the k-ε turbulence model. This model introduces two additional transport equations and two dependent variables: the turbulence kinetic energy, k, and the dissipation rate of turbulence energy, ε. Turbulent viscosity is modelled by:

$$\eta_T = \rho C_\mu \frac{k^2}{\varepsilon} \tag{B-5}$$

where C_μ is a model constant.

The transport equation for k can be derived by analogy with the equations for the Reynolds stresses:

$$\rho \frac{\partial k}{\partial t} - \nabla \cdot \left[\left(\eta + \frac{\eta_T}{\sigma_k} \right) \nabla k \right] + \rho U \cdot \nabla k = \frac{1}{2} \eta_T \left(\nabla U + (\nabla U)^T \right)^2 - \rho \varepsilon \tag{B-6}$$

An equation for ε can be derived in a similar manner. That equation is, however, impossible to model on a term-by-term basis. Instead, all terms that do not have an equivalent term in the k equation are discarded. The resulting equation reads:

$$\rho \frac{\partial \varepsilon}{\partial t} - \nabla \cdot \left[\left(\eta + \frac{\eta_T}{\sigma_\varepsilon} \right) \nabla \varepsilon \right] + \rho U \cdot \nabla \varepsilon = \frac{1}{2} C_{\varepsilon 1} \frac{\varepsilon}{k} \eta_T \left(\nabla U + (\nabla U)^T \right)^2 - \rho C_{\varepsilon 2} \frac{\varepsilon^2}{k} \tag{B-7}$$

The model constants in the above equations are determined from experimental data (Wilcox, 1998); their values are listed in the following Table B.1.

Table B.1. Model constants in Equations B-5, B-6 and B-7.

Constant	Value
C_{μ}	0.09
$C_{\varepsilon 1}$	1.44
$C_{\varepsilon 2}$	1.92
σ_k	1.0
σ_{ε}	1.3

2D GEOMETRY WITH AXIAL SYMMETRY

The 3D geometry of the Mastersizer 2000 stirrer was approximated to the following 2D geometry, assuming axial symmetry, in order to simplify the simulation, and thus, to get an approximated value for the shear rate in the Mastersizer 2000 beaker when water is used.

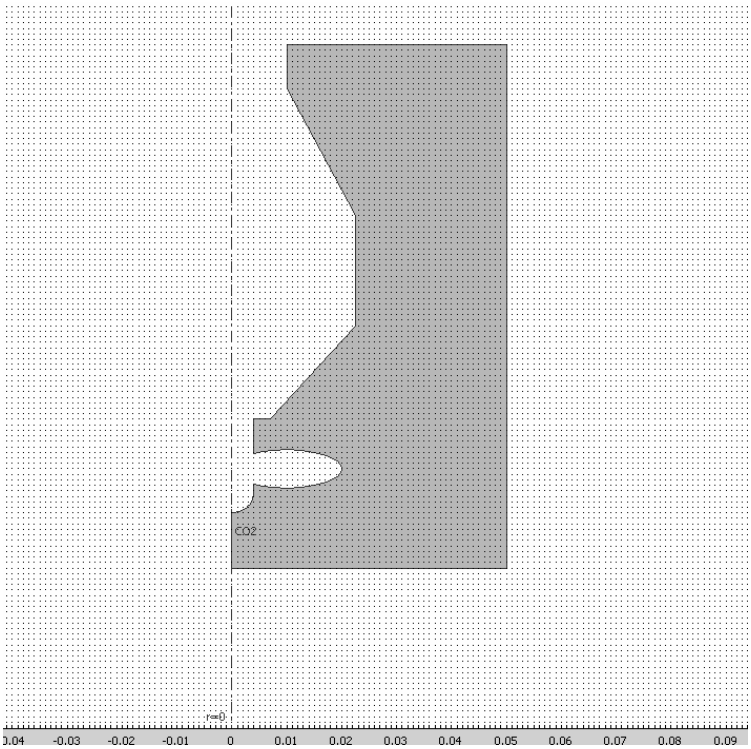

Figure B.2. 2D geometry of the mastersizer 2000 stirrer with axial symmetry.

RESULTS

The solution was computed for three different rotational speeds of the impeller: 1400 rpm, 1800 rpm and 2200 rpm. The average shear rates obtained from the calculations are summarized in Table B.2. We assumed the shear rates that describe the flow in the equipment beaker as the average shear rate because as seen in Figures B.3 to B.5, that show the velocity field in the fluid for the three stirring speeds used, the magnitude of the shear rate in the beaker only differs in a small region very close to the stirrer baffles. In this region the shear rate reaches the highest values but comparing to the extension of the region in blue, it is adequate to assume the shear rate for the flocculation process as the average shear rate in the beaker.

Table B.2. Average shear rates computed for stirring speeds of the impeller of 1400, 1800 and 2200 rpm .

Stirring speed	**1400 rpm**	**1800 rpm**	**2200 rpm**
γ (s^{-1})	312	488	708

-1400 rpm

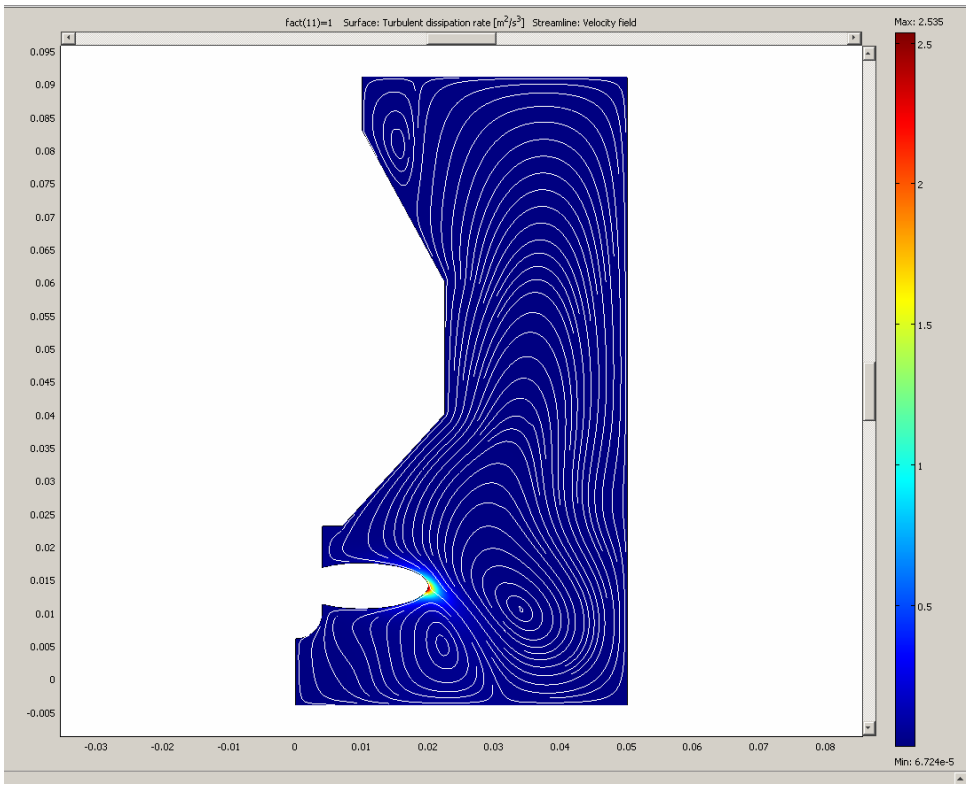

Figure B.3. Results for 1400 rpm.

- 1800 rpm

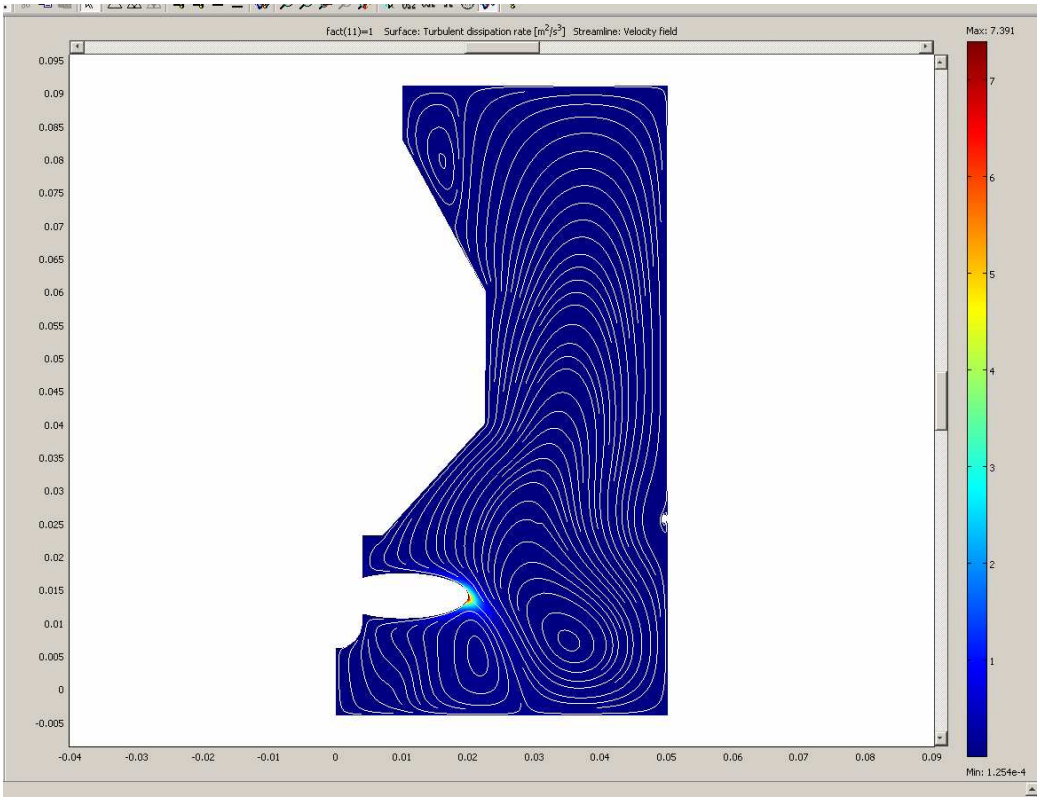

Figure B.4. Results for 1800 rpm.

- 2200 rpm

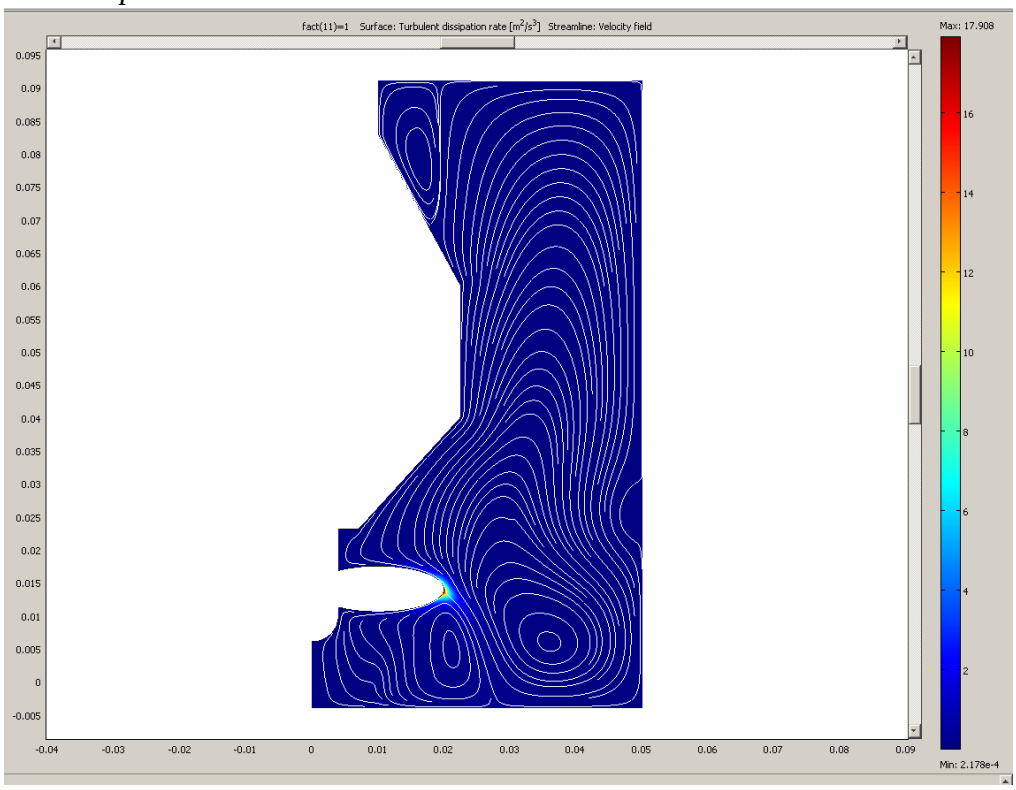

Figure B.5. Results for 2200 rpm.

APPENDIX C

LIST OF PUBLICATIONS

Paper 1: Rasteiro, M.G., Garcia, F.A.P., Ferreira, P., Blanco, A., Negro, C., Antunes, E., "The use of LDS as a tool to evaluate flocculation mechanisms", *Chem. Eng. Proc.* 47, 1329-1338, 2008.

Paper 2: Rasteiro, M.G., Garcia, F.A.P., Ferreira, P., Blanco, A., Negro, C., Antunes, E., "Evaluation of flocs resistance and reflocculation capacity using the LDS technique", *Powder Tech.* 183, 231-238, 2008.

Paper 3: Antunes, E., Garcia, F.A.P., Ferreira, P., Rasteiro, M.G., "Flocculation of PCC filler in papermaking: influence of the particle characteristics", *Chem. Eng. Res. Des.* 86, 1155-1160, 2008.

Paper 4: Antunes, E., Garcia, F.A.P., Ferreira, P., Blanco, A., Negro, C., Rasteiro, M.G., "Effect of water cationic content on flocculation, flocs resistance and reflocculation capacity of PCC induced by polyelectrolytes", *Ind. Eng. Chem. Res.* 47, 6006-6013, 2008.

Paper 5: Antunes, E., Garcia, F.A.P., Ferreira, P., Blanco, A., Negro, C., Rasteiro, M.G., "Use of new branched CPAMs to improve retention and drainage in papermaking", *Ind. Eng. Chem. Res*, 47, 9370-9375, 2008.

Paper 6: Rasteiro, M.G., Garcia, F.A.P., Ferreira, P., Antunes, E., Wandrey, C., Hunkeler, D., "Flocculation by cationic polyelectrolytes: relating efficiency with polymer characteristics", submitted to J. Applied Polym. Sci.

Paper 7: Antunes, E., Garcia, F.A.P., Ferreira, P., Rasteiro, M.G., "Evaluation of polyelectrolytes performance on PCC flocculation using the LDS technique", submitted to special issue of Particulate Science and Technology.

Paper 8: Antunes, E., Garcia, F.A.P., Ferreira, P., Blanco, A., Negro, C., Rasteiro, M.G., "Modelling PCC flocculation by bridging mechanism using population balances to understand the effect of polymer characteristics on flocculation", In preparation.

Paper 9: Antunes, E., Garcia, F.A.P., Ferreira, P., Blanco, A., Negro, C., Rasteiro, M.G., "Evaluation of a microparticulate system based on new C-PAMs on flocculation performance", In preparation.

LIST OF COMMUNICATIONS

- Rasteiro, M.G, Garcia, F.A.P., Ferreira, P., Antunes, E., "The use of LDS to assess flocculation dynamics"PARTEC, 2007, Germany.

- Antunes, E., Garcia, F.A.P., Ferreira, P., Rasteiro, M.G., "Effect of water cationic content on PCC flocculation induced by CPAM", XX Encontro Nacional da Tecnicelpa, 2007, Tomar.

- Antunes, E., "Simulação numérica da reorganização dos agregados em processos de floculação por formação de pontes poliméricas", 6º Workshop anual de engenharia de processos e sistemas, 2008, FCTUC, Coimbra.

- Rasteiro, M.G., Antunes, E., Garcia, F., Ferreira, P., Wandrey, C., Hunkeler, D., "Flocculation by Polyelectrolytes: Correlating the Flocculation Process with Polymer Characteristics", Polyelectrolytes 2008, FCTUC, Coimbra.

- Antunes, E., Garcia, F.A.P., Ferreira, P., Rasteiro, M.G., "Monitoring Flocculation of Precipitated Calcium Carbonate Using LDS: study of the influence of polyelectrolyte branching" Particle Systems Analysis 2008, UK.

- Antunes, E., Garcia, F.A.P., Ferreira, P., Rasteiro, M.G., "Correlating retention and drainage in papermaking with flocculation: effect of polyelectrolyte branching", AIChE Annual Meeting 2008, Philadelphia.

- Antunes, E., Garcia, F.A.P., Ferreira, P., Rasteiro, M.G., "Flocculation process modelling: correlating model parameters with retention and drainage in papermaking", 8th World Congress of Chemical Engineering, 2009, Montreal.

The flocculation process induced by polymeric additives has been studied extensively and is well reported in the literature. However, from the point of view of the papermaking process, still few studies relate flocculation behaviour and flocs characteristics with retention, drainage and sheet formation under various process conditions and for different retention aid systems. This correlation is of great importance in order to understand, predict and optimize retention and drainage performance and thus, sheet formation and quality.

In this study, a strategy that allows obtaining information about flocculation kinetics, flocs characteristics, flocs resistance and reflocculation capacity in a single test and in turbulent conditions was developed. The light diffraction scattering technique (LDS) was used to monitor the flocculation process due to its advanced capabilities that allow one to extract information on both the particle size distribution and the fractal dimension of the flocs.

Monitorization of the flocculation of precipitated calcium carbonate (PCC) particles with new cationic polyacrylamides allowed assessing how the polymer characteristics, namely the charge density and the degree of branching affect flocculation, flocs characteristics, flocs resistance and reflocculation capacity in distilled and in industrial water.

Furthermore, the effect of the degree of polymer branching on retention and drainage performance of flocculated kraft pulp fibre suspensions containing PCC was investigated in the dynamic drainage analyser (DDA) and the results have been correlated with flocs properties obtained by LDS.

Moreover, the effects of the chemical flocculation on the rheological behaviour of the pulp suspension have been studied correlating flocculation data obtained by LDS with the rheological behaviour obtained with the rotational viscometer developed by the Universidad Complutense of Madrid.

Finally, a population balance model for the flocculation of PCC particles with the polyelectrolytes used is presented. Model parameters were correlated with the polymer characteristics in order to obtain a model that can predict the aggregates characteristics (size and structure) or the operating conditions that produce aggregates with the characteristics required for a predefined performance.